ISSN 0132-1447

BULLETIN
OF THE GEORGIAN ACADEMY OF SCIENCES

საქართველოს მეცნიერებათა აკადემიის
მოამბე

VOLUME 159, NUMBER 3
MAY–JUNE
1999

TBILISI
თბილისი

The Journal is founded in 1940

BULLETIN

OF THE GEORGIAN ACADEMY OF SCIENCES

is a scientific journal, issued bimonthly in
Georgian and English languages

Editorial Office:

Georgian Academy of Sciences
52, Rustaveli Avenue,
Tbilisi, 380008,
Republic of Georgia

Telephone : + 995 32 99.75.93
Fax : + 995 32 99.88.23
E-mail : **BULLETIN@PRESID.ACNET.GE**

CONTENTS

MATHEMATICS

PHYSICS

GEOPHYSICS

ZOOLOGY

ENTOMOLOGY

EXPERIMENTAL MEDICINE

ECOLOGY

LINGUISTICS

LAW

საქართველოს მეცნიერებათა აკადემიის მოამბე, 159, №3, 1999
BULLETIN OF THE GEORGIAN ACADEMY OF SCIENCES, 159, №3, 1999

MATHEMATICS

Sh. Makharadze

Maximal Idempotent Semigroups in the Binary Relation Semigroup

Presented by Corr. Member of the Academy D. Baladze, December 30, 1998

ABSTRACT. **In the present work we consider a class of subsemigroups from the binary relation semigroup B_X whose every semigroup has as its right unit on the set X the maximal quasiorder relation, which is different from the universal relation. All maximal idempotent semigroups are described for that class of semigroups.**

Key words: Binary relation, idempotent, semigroup.

It is known that every semigroup is isomorphic to a subsemigroup of a semigroup of all binary relations on the non-empty set X [1]. Therefore separation and investigation of a class of subsemigroup from the semigroup B_X is always of a great interest. There is a vast number of works devoted to that semigroup [1-4].

Let X be an arbitrary non-empty set. Under a binary relation on the set X is understood a subset α of the direct product $X\times X$. If $(x, y) \in \alpha$, where x, y are elements of the set X, then we shall write $x\alpha y$.

If α and β are relations on X, then their composition $\alpha\circ\beta$ will be defined as follows: $x(\alpha\circ\beta)y$, if there exists an element $z \in X$, such that $x\alpha z\beta y$. Obviously, the set B_X of all binary relations on X is the semigroup with respect to the operation $(\circ)$.

In what follows, by $\varnothing$ and $\Delta_x = \{(x, x) / x \in X\}$ will be denoted respectively an empty and a diagonal binary relation on the set X;

$\omega_{X_1X_2} = (X_1\times X) \cup (X_2\times X_2)$, where X_1 and X_2 are non-empty subsets from X,

$$X_2 = X\setminus X_1 \text{ and } \alpha^{rt} = \bigcup_{n=1}^{\infty}(\alpha \cup \Delta_X)^n .$$

Let $Y\subseteq X$ and $\alpha \in B_X$. Then $Y_\alpha = \{x \in X / y\alpha x \text{ for some } y\in Y\}$, and $V(\alpha) = \{Y_\alpha / Y\subseteq X\}$.

Recall that the binary relation $\alpha \in B_X$ is called reflexive if $\Delta_X\subseteq \alpha$, transitive, if $\alpha\circ\alpha \subseteq\alpha$ and idempotent if $\alpha\circ\alpha = \alpha$.

The reflexive and transitive binary relations are called quasi-order relations. A semigroup is called idempotent, if its every element is idempotent.

Let α be an arbitrary fixed element from B_X and let

$$\Theta_X^{(r)}(\alpha) = \{\beta \in B_X / \beta\circ\alpha \subseteq \beta\}$$

and

$$E_X^{(r)}(\alpha) = \{\beta \in \Theta_X^{(r)}(\alpha)/\gamma\circ\beta = \gamma \text{ for all } \gamma \in \Theta_X^{(r)}(\alpha)\}.$$

Obviously, $\Theta_X^{(r)}(\alpha)$ is a subsemigroup B_x, and $E_X^{(r)}(\alpha)$ is a subsemigroup of idempotent elements from $\Theta_X^{(r)}(\alpha)$.

Propositions below, which will be used in the sequel are proved in [4].

1. Relation β from B_X belongs to the semigroup $\Theta_X^{(r)}(\alpha)$, if and only if $V(\beta) \subseteq V(\alpha^{rr})$ (Theorem 1.3).

2. Relation β from B_X belongs to the semigroup $\Theta_X^{(r)}(\alpha)$, if and only if $\beta = \bigcup_{y \in Y} (X_y \times Z_y)$ for some different $Z_y \in V(\alpha^{rr})$ and for pairwise non-intersecting subsets X_y of the set X (Theorem 1.3).

3. Relation ε is the right unit of the semigroup $\Theta_X^{(r)}(\omega_{X_1X_2})$, if and only if $\varepsilon = (Y_1 \times X) \cup (Y_2 \times X_2) \cup (Z \times X_2)$ for some $\varnothing \neq Y_1 \subseteq X_1$, $\varnothing \neq Y_2 \subseteq X_2$ and $Z = X_1 \setminus Y_1$ (Theorem 2.3).

Now we find all maximal idempotent subsemigroups of the semigroups $\Theta_X^{(r)}(\omega_{X_1X_2})$.

Let I' denote a set of all idempotents of the semigroup $\Theta_X^{(r)}(\omega_{X_1X_2})$. Then $I' = E_X^{(r)}(\omega_{X_1X_2}) \cup K(X) \cup K(X_2) \cup \{\varnothing\}$, where $K(X) = \{Y \times X / \varnothing \neq Y \subseteq X\}$, $K(X_2) = \{Y \times X_2 / Y \subseteq X;\ Y \cap X_2 \neq \varnothing\}$, and $E_X^{(r)}(\omega_{X_1X_2})$ is a set of all right units of the semigroup $\Theta_X^{(r)}(\omega_{X_1X_2})$. It is evident that $E_X^{(r)}(\omega_{X_1X_2})$, $K(X)$ and $K(X_2)$ are semigroups of right zeros. Further, we denote by $<B>$ a subsemigroup of the semigroup $\Theta_X^{(r)}(\omega_{X_1X_2})$, which is generated by the non-empty set B from $\Theta_X^{(r)}(\omega_{X_1X_2})$.

Lemma. *Let* $|X| \geq 2$. *Then the following assertions are valid*:

(1) $$<E_X^{(r)}(\omega_{X_1X_2}) \cup K(X)> = E_X^{(r)}(\omega_{X_1X_2}) \cup K(X);$$

(2) $$<E_X^{(r)}(\omega_{X_1X_2}) \cup K(X_2)> = E_X^{(r)}(\omega_{X_1X_2}) \cup K(X_2);$$

(3) $$<E_X^{(r)}(\omega_{X_1X_2}) \cup K_1(X) K(X_2)> = E_X^{(r)}(\omega_{X_1X_2}) \cup K_1(X) \cup K(X_2),$$ where

$$K_1(X) = \{Y \times X / Y \subseteq X;\ Y \cap X_2 \neq \varnothing\}.$$

Proof. Let us prove equation (1). Indeed, let $\beta \in E_X^{(r)}(\omega_{X_1X_2}) \cup K(X)$. Then $\beta = \beta_1 \circ \beta_2 \circ \ldots \circ \beta_k$ for some $\beta_1, \beta_2, \ldots, \beta_k \in E_X^{(r)}(\omega_{X_1X_2}) \cup K(X)$. If $\beta_1, \beta_2, \ldots, \beta_k \in E_X^{(r)}(\omega_{X_1X_2})$ or $\beta_1, \beta_2, \ldots, \beta_k \in \cup K(X)$, then we obtain $\beta \in E_X^{(r)}(\omega_{X_1X_2})$ or $\beta \in K(X)$, respectively. Suppose that among $\beta_i (1 \leq i \leq k)$ there are elements belonging to both semigroups $E_X^{(r)}(\omega_{X_1X_2})$ and $K(X)$.

If $\beta_1 \in K(X)$, then taking into account the fact that $K(X)$ is the semigroup of left zeros and $E_X^{(r)}(\omega_{X_1X_2})$ is a set of all units of the semigroup $\Theta_X^{(r)}(\omega_{X_1X_2})$, we obtain $\beta = \beta_1 \in K(X)$.

If now $\beta_i \in E_X^{(r)}(\omega_{X_1X_2})$ and i $(1 \leq i \leq k)$ is a natural number, such that $\beta_1, \beta_2, \ldots, \beta_{i-1} \in E_X^{(r)}(\omega_{X_1X_2})$ and $\beta_i \in K(X)$, then $\beta = (\beta_1 \circ \beta_2 \circ \ldots \circ \beta_{i-1}) \circ (\beta_i \circ \ldots \circ \beta_k) = \beta_1 \circ \beta_i$.

By assertion 3 from item 1.6, $\beta_1 = (Y_1 \times X) \cup (Y_2 \times X_2) \cup (Z \times X_2)$ for some $\varnothing \neq Y_1 \subseteq X_1$, $\varnothing \neq Y_2 \subseteq X_2$, and $Z \subseteq X_1 \setminus Y_1$. This for $\beta_i = Y \times X$, where $\varnothing \neq Y \subseteq X$, implies

$$\beta = \beta_1 \circ \beta_i = \begin{cases} Y_1 \times X, & \text{if } X_2 \cap Y = \varnothing, \\ (Y_i \cup Y_2 \cup Z) \times X, & \text{if } X_2 \cap Y \neq \varnothing, \end{cases}$$

i.e., $\beta \in K(X)$.

Hence $<E_X^{(r)}(\omega_{X_1X_2}) \cup K(X)> \subseteq E_X^{(r)}(\omega_{X_1X_2}) \cup K(X)$. The inverse inclusion is obvious. Equation (2) is proved analogously. Let us prove equation (3). Let

$$\beta \in <E_X^{(r)}(\omega_{X_1X_2}) \cup K_1(X)> \cup K(X_2)>.$$

Then $\beta = \beta_1 \circ \ldots \circ \beta_k$ for some $\beta = \beta_1, \beta_2, \ldots, \beta_k \in E_X^{(r)}(\omega_{X_1X_2}) \cup K_1(X) \cup K(X_2)$.

If $\beta_1, \beta_2, \ldots, \beta_k \in E_X^{(r)}(\omega_{X_1X_2})$, or $\beta_1, \beta_2, \ldots, \beta_k \in K_1(X)$, or $\beta_1, \beta_2, \ldots, \beta_k \in K(X_2)$, then we obtain $\beta \in E_X^{(r)}(\omega_{X_1X_2})$, or $\beta \in K_1(X)$, $\beta \in K(X_2)$, respectively. Suppose that the decomposition of the element β involves elements from all semigroups $E_X^{(r)}(\omega_{X_1X_2})$, $K_1(X)$ and $K(X_2)$.

If $\beta_1 \in K_1(X) \cup K(X_2)$, then the product $\beta_1 \circ \beta_2 \circ \ldots \circ \beta_k$ can be reduced to the form $\beta_1 \circ \beta'_2 \circ \ldots \circ \beta'_p$ so that $\beta = \beta_1 \circ \beta'_2 \circ \ldots \circ \beta'_p$ and $\beta'_2 \circ \beta'_3 \circ \ldots \circ \beta'_p \in K_1(X) \cup K(X_2)$. But this product, by definition of $K_1(X)$, is equal to $\beta_1 X \times X \beta'_p$, i.e.,

$$\beta = \beta_1 X \times X \beta'_p \in K_1(X) \cup K(X_2).$$

If $\beta_1 \in E_X^{(r)}(\omega_{X_1X_2})$, then the product $\beta_1 \circ \beta_2 \circ \ldots \circ \beta_k$ can be reduced to the form $\beta = \beta_1 \circ \delta$, where $\delta \in K_1(X) \cup K(X_2)$. Thus, by assertion 3 implies that $\beta = \beta_1 \circ \delta \in K_1(X) \cup K(X_2)$.

Hence $\langle E_X^{(r)}(\omega_{X_1X_2}) \cup K_1(X) \cup K(X_2) \rangle \subseteq E_X^{(r)}(\omega_{X_1X_2}) \cup K_1(X) \cup K(X_2)$.

The inverse inclusion is obvious.

Theorem 1. *Let $|X| \geq 2$. Then all maximal subsemigroups of idempotent elements from $\Theta_X^{(r)}(\omega_{X_1X_2})$ are exhausted by semigroups of the type*

$$E_X^{(r)}(\omega_{X_1X_2}) \cup K(X) \cup \{\varnothing\}, E_X^{(r)}(\omega_{X_1X_2}) \cup K_1(X) \cup K(X_2) \cup \{\varnothing\}.$$

Proof. By Lemma, it is evident that all sets mentioned in the theorem are the subgroups of idempotent elements from $\Theta_X^{(r)}(\omega_{X_1X_2})$ with zero $\varnothing$.

Let now S be an arbitrary subsemigroup of idempotent elements from $\Theta_X^{(r)}(\omega_{X_1X_2})$.

Then
$$S \subseteq I' = E_X^{(r)}(\omega_{X_1X_2}) \cup K_1(X) \cup K(X_2) \cup \{\varnothing\}.$$

If $S \cap K(X) = S \cap K(X_2) \neq \varnothing$ or $S \cap K(X) \neq \varnothing$ and $S \cap K(X_2) = \varnothing$ or $S \cap K(X) = \varnothing$ and $S \cap K(X_2) \neq \varnothing$, then we respectively obtain $S \subseteq E_X^{(r)}(\omega_{X_1X_2}) \cup \{\varnothing\}$ or $S \subseteq E_X^{(r)}(\omega_{X_1X_2}) \cup K(X) \cup \{\varnothing\}$, or $S \subseteq E_X^{(r)}(\omega_{X_1X_2}) \cup K(X_2) \cup \{\varnothing\}$.

Suppose that $S \cap K(X) = K_1 \neq \varnothing$ and $S \cap K(X_2) = K_2 \neq \varnothing$ and prove that $K_1 \subseteq K_1(X)$. Indeed, if $Y \times X \in K_1$ and $Y_1 \times X_2 \in K_1$, where $\varnothing \neq Y \subseteq X$, $\varnothing \neq Y_1 \subseteq X$, then

$$(Y \times X) \circ (Y_1 \times X_2) = Y \times X_2 \in S.$$

The condition $Y \times X_2 \in S$ is fulfilled, if and only, if $Y \cap X_2 \neq \varnothing$. From this we obtain $Y \times X \in K_1(X)$ and $K_1 \subseteq K_1(X)$. Hence $S \subseteq E_X^{(r)}(\omega_{X_1X_2}) \cup K_1(X) \cup K(X_2) \cup \{\varnothing\}$.

Thus the theorem is proved.

Batumi Sh. Rustaveli State University

REFERENCES

1. *A. Clifford, G. Preston.* Algebraic theory of semigroups., M., **1**, 1972.
2. *K. A. Zaretski.* Matem. sbornik, **61**, 3, 1970 (Russian).
3. *E. S. Lyapin.* Semigroups. M., 1960 (Russian).
4. *Ya. I. Diasamidze, Sh. I. Makharadze.* Irreducible generating sets of some idempotently generated subsemigroups of all binary relations, Batumi, 1966 (Russian).

საქართველოს მეცნიერებათა აკადემიის მოამბე, 159, №3, 1999
BULLETIN OF THE GEORGIAN ACADEMY OF SCIENCES, 159, №3, 1999

MATHEMATICS

Ya. Diasamidze, Sh. Makharadze

Right Zeros of Complete Semigroups of Binary Relations

Presented by Corr. Member of the Academy D.Baladze, December 30, 1998

ABSTRACT. **In the present paper we consider right zeros of complete semigroups of binary relation.**

Key words: semigroup, binary relation, right zero.

Let X be an arbitrary non-empty set. Under a binary relation on the set X is understood a subset α of the cartesian product $X\times X$ of the set X by itself. If $(x, y) \in \alpha$, where x, y are the elements of X, then we shall write $x\alpha y$. There is a vast number of papers devoted the semigroup of binary relation (see [1-3] and references in these).

If α and β are the relations on $\alpha\circ\beta$, then their composition $\alpha\circ\beta$ is defined as follows: $x(\alpha\circ\beta)y$, if there exists an element $z \in X$ such that $x\alpha z\beta y$. obviously, the set B_X of all binary relations on X is a semigroup with respect to the operation $(\circ)$.

Let $Y \subseteq X$ and $\alpha \in B_X$. Then

$$\alpha^{-1} = \{(x, y)/y\alpha x\};\ Y\alpha = \{x \in X/y\alpha x \text{ for some } y \in Y\};\ \alpha Y = Y\alpha^{-1}.$$

Denote by $\varnothing$ an empty set or the empty binary relation.

Let now D be a non empty set of subsets from X, which are closed with respect to the operations of set-theoretic union of elements from D, i.e. $\cup D' \in D$ for any non-empty subset D' from D. In this case, the set D will be called a complete X-semilattice of unions.

Further, let f be an arbitrary mapping of X into D. To every such a mapping f we put in correspondence the binary relation α_f on the set X, satisfying the condition

$$\alpha_f = \bigcup_{x\in X}(\{x\}\times f(x)). \tag{1}$$

We denote a set of such α_f ($f\colon X \to D$) by $B_X(D)$. Obviously, $B_X(D)$ is a subset of the semigroup B_X of all binary relations on X. Let us prove that $B_X(D)$ is a sub-semigroup of the semigroup B_X. Indeed, let $\alpha_f, \alpha_g \in B_X(D)$. We define the mapping ψ of the set X into a set of all subsets of the set X as follows:

$$\psi(x) = \bigcup_{z\in x\alpha_f} z\alpha_g$$

for all $x \in X$. It is evident that $\psi(x) \in D$ for every $x \in X$, since $z\alpha_g \in D$ for any $z \in X$, and D is closed with respect to the operations of the set-theoretic union. Next, by virtue of equation (1) and by the definition of multiplication of binary relations, the equality

$$x(\alpha_f\circ\alpha_g) = x(\alpha_f)\alpha_g = \bigcup_{z\in x\alpha_f} z\alpha_g = x\alpha_\psi;$$

i. e., $\alpha_f \circ \alpha_g = \alpha_w \in B_X(D)$, is valid for any $B_X(D)$. Hence $B_X(D)$ is the subsemigroup of the semigroup B_X.

The semigroup $B_X(D)$ will be called a complete semigroup of binary relations defined by the complete X-semilattice of unions D.

Note that if $D = 2^X$, i.e. D is a set of all subsets of the set X, then $B_X(2^X) = B_X$.

Let Z be an arbitrary element of the complete X-semilattice of unions D. Denote by $k(z)$ a set of all non-empty elements from d, different from z; F is an arbitrary mapping of the set X into the set $D\backslash K(Z)$. To every such mapping f put into correspondence the binary relation α_f on the set X, satisfying the condition

$$\alpha_f = \bigcup_{x \in X} (\{x\} \times f(x)).$$

Denote a set of all such $\alpha_f (f: X \to D\backslash K(Z))$ by $L_X(Z)$. It can be easily verified that the set

$$K_X(D) = \bigcup_{z \in D} K_X(Z)$$

is a subsemigroup of the semigroup $B_X(D)$. This semigroup will be called a complete semigroup of rectangular binary relations defined by the semilattice D.

Theorem. *Let $\varnothing \notin D$ and $|D| \geq 1$. Then the right zeros of the semigroup $B_X(D)$ are barely the elements from $K_X(D)$.*

Proof. Recall that under the condition $\varnothing \notin D$ the semigroup $K_X(D)$ contains only those binary relations which are of the form $X \times Z$, where $Z \in D$. Let now

$$\alpha \circ \beta = \beta$$

for any $\alpha \in B_X(D)$ and for some $\beta \in B_X(D)$.

Let us prove that $x\beta = y\beta$ for all $x, y \in X$. Indeed, suppose first that $x, y \in \mathbf{X} = \cup D$. Hence there exist binary relations α_1 and α_2 from $B_X(D)$, such that $x\alpha_1 = y\alpha_2 = \mathbf{X}$. By the assumption, the relations

$$\alpha_1 \circ \beta = \alpha_2 \circ \beta = \beta$$

hold, and therefore

$$x\beta = x(\alpha_1 \circ \beta) = \bigcup_{z \in x\alpha_1} z\beta \supseteq y\beta,$$

$$y\beta = y(\alpha_2 \circ \beta) = \bigcup_{t \in y\alpha_2} t\beta \supseteq x\beta,$$

since $x, y \in x\alpha_1 = y\alpha_2$. Consequently, the equality

$$x\beta = y\beta \tag{2}$$

is valid for all $x, y \in \mathbf{X}$.

Suppose $x \notin \mathbf{X}$. By the assumption, $x\alpha \in D$ for any $x \in X$ and $\alpha \in B_X(D)$, whence by equation (1) we obtain

$$x\beta = x(\alpha \circ \beta) = \bigcup_{z \in x\alpha} z\beta = z\beta,$$

Thus $x\beta = y\beta$ for all $x, y \in X$. This results in

$$\beta = X \times x\beta \in K_X(D).$$

Conversely, if $\beta \in K_X(D)$ and $\alpha \in B_X(D)$, then

$$x(\alpha\circ\beta) = \bigcup_{z\in x\alpha} z\beta = z\beta = x\beta,$$

since $x\beta = z\beta$ for all $x, z \in X$.

Thus the theorem is proved.

Corollary. *Let* $\varnothing \notin D$ *and* $|D| \geq 2$. *Then the semigroup* $B_X(D)$ *has no left zeros.*

Finally we note that if $\varnothing \in D$, then the binary relation is zero of the semigroup $B_X(D)$.

Batumi State University

REFERENCES

1. *A. Clifford, G. Preston.* Algebraic theory of semigroups. **1**, M., 1972 (Russian).
2. *K. A. Zaretskii.* Matem. sbornik. **61**, 3, 1970 (Russian).
3. *E. S. Lyapin.* Semigroups. M., 1960. (Russian).

საქართველოს მეცნიერებათა აკადემიის მოამბე, 159, №3, 1999
BULLETIN OF THE GEORGIAN ACADEMY OF SCIENCES, 159, №3, 1999

MATHEMATICS

A. Liparteliani

Additional Properties for Large Inductive Dimension in the Classes of Normal Spaces

Presented by Corr. Member of the Academy N. Berikashvili, May 25, 1998

ABSTRACT. In the present paper there are given inequalities for large inductive dimension in the classes of normal spaces, which are similar to Menger-Urison's inequalities.

Key words: Menger-Urison's inequalities, addition theorems, normal spaces.

In this paper all encountered spaces are assumed to be Hausdorff and completely regular (≡Tychonoff).

$IndX$ denotes large inductive dimension [1] (≡ $IndX = -1$ iff $X = \varnothing$; for $n > -1$ inequality $IndX \le n$ means that for each closed set E and each open set G of X such that $E \subseteq G$ there exists an open set U of X, such that $E \subseteq U \subseteq G$ and $IndFr_X U \le n - 1$, where $Fr_X U$ denotes boundary of U in X).

Remark 1. It is obvious that definition of $IndX$ is suitable for general spaces.

Definition 1. Let X be a topological space. We say that the space X satisfies finite sum theorem for Ind (abbreviated X is FST –space) if for each finite family $F_1, \dots, F_m$ of closed subsets of X we have:

$$Ind(\bigcup_{i=1}^{m} F_i) \le \max_{1 \le i \le m} \{IndF_i\}.$$

All results obtained in the present paper are essentially based on the following theorem proved in [2].

Theorem 1. [2] *Suppose X is a normal space and Y is a dense subspace of X, such that $IndY \le n$. Then for every closed set F of X and every open set OF of X such that $F \subseteq OF$, there exists an open set VF in X such that $F \subseteq VF \subseteq OF$ and $Ind(Fr_X VF \cap Y) \le n - 1$.*

Remark 2. Theorem 1 does not hold when the space X is not normal. Really, in [3] there is constructed space X which is locally bicompact, weakly paracompact and non normal (see [3] example 2.2). The subset $Y = (\alpha \backslash \Phi) \cup (\beta F)$ of space X is σ-compact (consequently paracompact), everywhere dense in X and $IndY = 0$. Let us consider a closed in X subset $F = E\{(x; y; z) \in \beta: x \in C, y = 1, z = 0\}$ and its open neighbourhood β. It can be proved that for each open subset G of X, where $F \subseteq G \subseteq \beta$, we have $Ind(Fr_X G \cap Y) = 0 > -1$.

Remark 3. Theorem 1 does not hold even in that case when X is a normal space, but Y is not a dense subset of X. Really, in [4] such space X is constructed in the following way: by ω_0 is denoted the first infinite ordinal, by ω_1 the first uncountable ordinal, $N \equiv \{k: k$ is an ordinal, $0 \le k \le \omega_0\}$, $P \equiv \{a: a$ is an ordinal, $0 \le a \le \omega_1$, $I \equiv [0;1]$, $Z \equiv P \times I \times N$. By D

is denoted a decomposition of Z with following classes of equivalence: $\{z\} \equiv \{(a; t; k)\}$, where $a \neq \omega_1$, and $E_t \equiv \{(a; t; k): a = \omega_1, 0 \leq k \leq \omega_0\}$.

By π is denoted the natural quotient mapping $\pi: Z \to Z/D$. Let $X = Z/D$. By $r_0 = 0$, $r_1 = 1, r_2, \ldots, r_n, \ldots$ is denoted an enumeration of the rational numbers in I.

Let $A_k \equiv \{(a; r_k; k): a \in P, a < \omega_1\}$ for every $k \in N$. It is clear that $A_k \subseteq X$.

Let $C \equiv \pi(C')$, $Y \equiv \bigcup_{k=0}^{\infty} A_k \cup C$ and $H \equiv \pi(H')$, where $C' = \{(a; t; k): a = \omega_1 t$ is irrational, $0 < t < 1\}$ and $H' = \{(a; t; k): t = 0, a \in P, k \in N\}$. It is clear that $Y \subseteq X$ and H is closed in X.

It is easy to show that Y is not a dense in X. Indeed, suppose $k_0 \in N$ and $0 < k < \omega_0$. Let $B'_{k_0} \equiv \{(a; t; k_0): a \neq \omega_1, a \in P, t \in I\}$ and $A'_{k_0} \equiv \{(a; r_{k_0}; k_0): a \in P\}$. It is obvious that the set $B = \pi(B'_{k_0}) \setminus \pi(A'_{k_0})$ is open in X and $B \cap Y = \varnothing$.

In [4] it is shown that X is a normal space, $\dim Y = 0$ and thus $IndY = 0$. Besides, there exists an open neighbourhood G of H in X such that for every open set W in X, for which $H \subseteq W \subseteq G$, we have $FrW \cap Y \neq \varnothing$.

In [5] based on theorem 1 there are obtained inequalities, which are similar to Menger-Urison's inequalities. The theorems mentioned below represent the strengthening of the results obtained in [2,5]. With this point of view we can assume the present paper to be the extension of mentioned works.

The following theorem is true.

Theorem 2. *Suppose X is a normal FST-space. If $X = \bigcup_{i=1}^{k} A_i$, where $1 \leq k < \infty$, $IndA_i \leq n_i$ and $n_i \geq -1$, then $IndX \leq \sum_{i=1}^{k} n_i + k - 1$.*

Remark 4. From theorem 2 it follows that if X is normal FST-space then for X the Menger-Urison's inequality is fulfilled even in that case when subspaces of X are arbitrary topological spaces.

When X is not the FST-space, then there is obtained weaker estimation than in theorem 2.

Theorem 3. *Suppose X is a normal space $X = \bigcup_{i=1}^{n} A_i$, $X \neq \varnothing$ and $A_i \neq \varnothing$, $i = \overline{1,n}$. If $IndA_i \leq n_i$, $i = \overline{1,n}$, then*

$$IndX \leq \begin{cases} n_1, & \text{when } n = 1; \\ A_s^{s-1} + A_s^{s-2} + \ldots + A_s^1, & \text{when } n > 1; \end{cases}$$

where $s = \sum_{i=1}^{k} n_i + n$ *and* $A_m^n = \frac{m!}{(m-n)!}$.

When a space X is represented as the union of its two subsets, then more explicit estimations are obtained. Namely, the following theorems are fulfilled.

Theorem 4. *Suppose X is a normal space and $X = A \cup B$. If $IndA \le m$, $IndB \le n$ and B is normal space, $m, n \ge -1$, then $IndX \le 2(m+n) + mn + 2$.*

Theorem 5. *Suppose X is a normal space and $X = A \cup B$, where A or B is not empty. If $IndA \le m$, $IndB \le n$, then $IndX \le \frac{(m+n+3)!}{2} - 1$.*

Tbilisi I. Javakhishvili State University

REFERENCES

1. *A. R. Pears.* Dimension Theory of General Spaces. London-New York-Melbourn, 1975.
2. *L. G. Zambakhidze.* Bull. Acad. Sci. GSSR. **89**, 1, 1978, 41-44.
3. *L. G. Zambakhidze.* Dokl.Akad.Nauk. SSSR. **191**, 2, 1970, (Russian).
4. *T. H. Walton.* Fund. Math. 61, 1968, 309-311.
5. *L. G. Zambakhidze.* Bull. Georgian Acad. Sci. **149**, 3, 1994, 365-368.

საქართველოს მეცნიერებათა აკადემიის მოამბე, 159, №3, 1999
BULLETIN OF THE GEORGIAN ACADEMY OF SCIENCES, 159, №3, 1999

MATHEMATICS

I. Khazhalia

Shift Operator with Respect to Wavelet Bases

Presented by Member of the Academy L.Zhizhiashvili, April 6, 1998

ABSTRACT. **The boundedness of shift operator in $L^p(\mathbf{R})$, $1 < p < +\infty$, with respect to wavelet bases is investigated.**

Key words: $L^p(1 < p < \infty)$ spaces, multiresolution analysis, wavelet bases.

1. Z. Ciesielski and S. Kwapin [1] proved that in $L^p(0,1)$, $1 < p < \infty$, the shift operator with respect to Haar and Franklin bases is bounded. In $L^1(0,1)$ this fact is not true [1,2]. The purpose of the present article is to study the shift operator with respect to wavelet bases.

2. The notion of the multiresolution analysis was introduced by Y. Meyer [3] and S. Mallat [4]. We use definition of multiresolution of the following form [5].

A pair $(\{V_m\}_{m\in Z}, \varphi)$ is an orthonormal multiresolution of $L^2(R,C)$ if the four following properties are satisfied.

(1) $\varphi \in L^2(R,C)$ and V_m is the closed subspace of $L^2(R,C)$ spanned by $\{\varphi(2^{-m}\bullet - k)\}_{k\in Z}$ for each $m \in Z$;

(2) $V_m \subset V_{m-1}$, $m \in Z$;

(3) $\lim_{m\to-\infty} P_m(f) = f$ for every $f \in L^2(R,C)$, where $P_m: L^2(R,C) \to V_m$ is the orthogonal projection operator;

(4) $\{\varphi(\bullet - k)\}_{k\in Z}$ is an orthonormal set in $L^2(R,C)$.

The function φ is called the father wavelet or scaling function. With its help the function ψ, the so-called mother wavelet, such that the set $\{\psi(\bullet - k)\}_{k\in Z}$ constitute an orthonormal basis for the orthogonal complement W_0 of V_0 inside V_{-1}, may be constructed.

Since $V_0 \subset V_{-1}$ and the set $\{\sqrt{2}\varphi(2\bullet - k)\}_{k\in Z}$ is an orthonormal basis for V_{-1}, we may write

$$\varphi \overset{L^2}{=} \sqrt{2}\sum_{k\in Z} h_k \varphi(2\bullet - k),$$

where the sequence $\{h_k\}_{k\in Z} \in l^2(Z)$,

$$h_k = \sqrt{2}\int_{-\infty}^{+\infty} \varphi(x)\overline{\varphi(2x-k)}dx$$

is named the filter.

If the filter coefficients h_k has been chosen it completely determines φ and ψ wavelets and therefore the multiresolution analysis. The mother wavelet ψ is defined by

$$\overset{L^2}{\psi} = \sqrt{2}\sum_{k\in Z}(-1)^k \overline{h_{1-k}}\varphi(2\bullet - k).$$

For every $m \in Z$ we define W_m to be the orthogonal complement of V_m in V_{m-1}. We have

$$V_{m-1} = V_m \oplus W_m$$

and

$$W_m \perp W_{m'} \text{ if } m \neq m'.$$

From (3) it follows that for every $n \in Z$

$$L^2(R,C) = V_n \oplus \bigoplus_{m=-\infty}^{n} W_m \tag{5}$$

and

$$L^2(R;C) = \bigoplus_{m\in Z} W_m \tag{6}$$

(5) and (6) immediately yields that the sets

$$\{2^{-n/2}\varphi(2^{-n}\bullet - k),\ 2^{-m/2}\psi(2^{-m}\bullet - k)\}_{m,k\in Z, m\le n}\ (n \in Z)$$

and $\{2^{-m/2}\psi(2^{-m}\bullet - k)\}_{m,k\in Z}$ are the orthonormal bases in $L^2(R, C)$ [6].

3. In [5] G. Gripenberg has shown that if the father wavelet $\varphi \in L^\infty(R, C)$ and there holds the condition

$$\int_0^{+\infty} x \operatorname*{ess\,sup}_{|y|\ge x} |\varphi(y)|\, dx < +\infty, \tag{7}$$

then the orthonormal bases $\{\varphi_{n,k}\ \psi_{m,k}\}_{m,k\in Z,\ m\le n}\ (n \in Z)$, $\{\psi_{m,k}\}_{m,k\in Z}$, where $\psi_{m,k} = 2^{-m/2}\psi(2^{-m}\bullet - k)$ and $\varphi_{m,k} = 2^{-m/2}\varphi(2^{-m}\bullet - k)(m,\ k \in Z)$, are unconditional bases in $L^p(R;\ C)(1 < p < +\infty)$ spaces.

For fixed $k, l \in Z$ let us consider the operator $T^{(k,l)}: L^2(R;\ C) \to L^2(R;\ C)$ defined by

$$T^{(k,l)}(f) = \sum_{m,j\in Z}\langle f, \psi_{m,j}\rangle \psi_{m+k,\,j+l} \tag{8}$$

or

$$T^{(k,l)}(f) = \sum_{j\in Z}\langle f, \varphi_{n,j}\rangle \varphi_{n+k,\,j+1} + \sum_{\substack{m,j\in Z\\ m\le n}}\langle f, \psi_{m,j}\rangle \psi_{m+k,\,j+l}\ (n \in Z)$$

We have the following theorems

Theorem 1. *Let* $(\{V_m\}_{m\in Z},\ \varphi)$ *be an orthonormal multiresolution of* $L^2(R;\ C)$, ψ *be the associated mother wavelet and* $m,\ k \in Z$:

$$\psi_{m,k} = 2^{-m/2}\psi(2^{-m}\bullet - k) \wedge \varphi_{m,k} = 2^{-m/2}\varphi(2^{-m}\bullet - k).$$

Suppose that $\varphi \in L^{\infty}(R;C)$ *and the Gripenberg condition* (7) *holds. Let for fixed* $k, l \in Z$ $T^{(k,l)}:L^2(R;C) \to L^2(R;C)$ *be the operator defined by* (8). *Then operator* $T^{(k,l)}$ *is of weak type* (1, 1).

Theorem 2. *Let* $(\{V_m\}_{m\in Z}, \varphi)$ *be an orthonormal multiresolution of* $L^2(R;C)$, ψ *be the associated mother wavelet and* $n,m, k \in Z$:

$$\psi_{m,k} = 2^{-m/2}\psi(2^{-m}\bullet - k), \quad \varphi_{m,k} = 2^{-m/2}\varphi(2^{-m}\bullet - k).$$

Suppose that $\varphi \in L^{\infty}(R;C)$ *and* (7) *holds.*

Then $T^{(k,l)}:L^2(R;C) \to L^2(R;C)$ *operator defined by* (8) *extended to a continuous operator from* $L^p(R;C)$ *in* $L^p(R;C)$, *where* $1 < p < +\infty$, *and the following inequalities hold*

$$\frac{1}{c_p}\| f \|_{L^p(R)} \le \| T^{(k,l)}(f) \|_{L^p(R)} \le c_p \| f \|_{L^p(R)} \tag{9}$$

for some constant c_p.

Remark. The similar theorems is true for the regular wavelet basis [6].

Corollary. *Shift operator with respect to the compactly supported wavelets - Daubechies wavelets* [7] *is bounded in* $L^p(R)$, $1 < p < +\infty$.

Tbilisi I. Javakhishvili State University

REFERENCES

1. *Z. Ciesielski, S. Kwapin.* Comment Mathematica, Tomus special in honoren Ladislaw Orlicz, Part 2, Warczawa.
2. *G. Gevorkyan.* Mathematicheskie zametki. **38**, 4, 523-433 (Russian).
3. *Y. Meyer.* Ondelettes et fonctions splines. Technical report, seminaire edp, Ecole Polytechnique, Paris, 1986.
4. *S. Mallat.* Trans. Am. Math. Soc. 315, 1989, 69-88.
5. *G. Gripenberg.* Studia mathematica, 108(2), 1993, 175-187.
6. *Y. Meyer.* Ondelettes et Operateurs, Hermann. Paris, 1990.
7. *I. Daubechies.* Comm. Pure and appl. Math. 41, 1988, 909-996.

საქართველოს მეცნიერებათა აკადემიის მოამბე, 159, №3, 1999
BULLETIN OF THE GEORGIAN ACADEMY OF SCIENCES, 159, №3, 1999

MATHEMATICS

G. Khimshiashvili, A. Ushveridze

On the Average Topological Degree of Random Polynomials

Presented by Corr. Member of the Academy N.Vakhania, April 27, 1998

ABSTRACT. **We investigate the average topological degree of random polynomial mappings defined by pairs of random polynomials in two variables. We fix the algebraic degree n of both polynomials and investigate its relation to the average absolute value of topological degree. For certain normal distribution of coefficients, it is established that this average asymptotically grows as $n^{1/2}$. Some corollaries and related results are also presented.**

Key words: random polynomial, multivariate normal distribution, topological mapping degree.

Since the seminal work of M.Kac [1], distribution of roots of random polynomials became a topic of permanent interest in mathematics and physics [2-4]. For real polynomials of one variable, several important numerical characteristics, especially the average real roots number, have been investigated in great detail [2].

Much less is known about common real roots of random polynomials of several variables. An important breakthrough was recently made by M.Shub and S.Smale, who were able to find a suitable probabilistic setting in higher dimensions [5]. For certain special distributions of coefficients, they computed the average number of common real roots, which may be considered as a far-reaching generalization of classical results due to M.Kac [1]. These and other recent developments in the spirit of [5] are summarized in [6].

Despite those important contributions many natural problems for random polynomials in several variables still remain completely uninvestigated. In particular, no numerical invariants specific for higher dimensions seem to be considered in the literature. The present note grew out from our attempt to start investigation in this direction by considering the average topological degree of mappings defined by random polynomials. As is well known, many other topological invariants are expressible via topological mapping degree [7], so our contribution may be considered as a first step towards "statistical topology of real polynomials". In this note we present but two typical results of such kind leaving their development and applications for future publications.

We only deal with random polynomials in two variables with certain special multivariate normal distributions of coefficients first introduced in [5]. At the moment we are unable to manage neither higher dimensional mappings nor other natural distributions of coefficients, but it is our hope that the approach developed below may appear useful in wider context.

We consider the ring $\mathbf{R}_2$ of real polynomials in two indeterminates. For any $P \in \mathbf{R}_2$ denote by deg P its algebraic degree (highest order of monomials entering in P with non-

zero coefficients). Any P with deg $P = n$ has the form $P(x, y) = \sum a_{kl} x^k y^l$, where $a_{kl} \in \mathbf{R}$, $k, l \in \mathbf{Z}_+$, and the sum is taken over the range $0 \le k + l \le n$. Also, there exists a nonzero a_{kl} with $k + l = n$. Thus the so-called leader P^* (sum of terms of highest degree) of P is a non-trivial binary n-form.

Suppose now that a_{kl} are random variables. Then we will say that a random polynomial is given. We will only consider the coefficients a_{kl} having multivariate normal distribution so the words "random polynomial" will always refer to this case. One can now take a pair of such random polynomials and consider it as a mapping $F = (P, Q) : \mathbf{R}^2 \to \mathbf{R}^2$. This will be expressed by saying that we deal with a random planar polynomial endomorphism.

As is well known, if mapping F is proper (full preimage of every compact remains compact) then its topological degree Deg F is well defined as the sum of signs of Jacobian of F taken over all preimages of any regular value of F (sometimes it is also called the global index Ind F of the vector field defined by F, see e.g. [8]). The condition that $F = (P, Q)$ is proper, is "generic" so it holds almost surely and it is reasonable to make Deg F always defined by putting it equal to zero if F is not proper. Of course these concepts make sense in all dimensions but we restrict ourselves to planar endomorphisms.

Our main concern in this note is to obtain statistical information about the topological degree of random polynomial endomorphisms. Thus we would like to compute averages of some entities related to Deg F. In our setting the average of Deg F itself will always vanish for simple symmetry reasons, but the average of its modulus $E(|\text{Deg } F|)$ is a quite meaningful entity and it is just the invariant (average absolute degree) which we will study in the sequel.

In order to be able to obtain reasonable results we have to further restrict admissible distributions of coefficients a_{kl} of random polynomials in question. It turns out that appropriate is the setting of [5]. Thus we will always suppose that coefficients a_{kl} are independent central (zero mean) normal variables with variances equal to "trinomial coefficients": $Da_{kl} = n!(k!1!(n-k-1)!)^{-1}$.

For such special distributions, we will estimate $E(|\text{Deg } F|)$ over polynomials of fixed algebraic degree n and determine its rate of growth when n tends to infinity (asymptotic properties of such averages are important in some physical problems [3]). As will be explained, it is sufficient to study the case of homogeneous polynomials (binary forms) of degree n with the same distribution of coefficients. They will emerge as leaders P^*, Q^* of random polynomials P, Q.

It appears useful to look first at so-called hyperbolic binary forms. Those are defined as homogeneous n-forms having all their roots on the real axis. In other words, hyperbolic binary n-forms are products of n linear factors of the form $c_j x - d_j y$ with $c_j, d_j \in \mathbf{R}$. Zeroes of such a form constitute a collection of straight lines in $\mathbf{R}^2$. Thus one may consider pairs of points of their intersections with unit circle S^1 and think of them as a point of the projective space $\mathbf{R}P^1 \cong S^1$.

Suppose that zeroes are uniformly distributed on S^1 considered as $\mathbf{R}P^1$. In this case it is possible to indicate a simple combinatorial expression for the average we are interested in, which enables one to find its asymptotics for large n.

Proposition 1. *The average absolute value of topological degree of a random hyperbolic binary n-form with uniformly distributed zeroes is equal to*

$$(\Sigma_{k=0}^{n} (C_k^n)^2 \mid 2k-n \mid)/C_n^{2n}.$$

Proposition 2. *For n large, the average above is asymptotically equivalent to* $(n/\pi)^{1/2}$.

This may be proved using the saddle-point method. The fact that all this is directly related to our main problem follows from an important observation which may be derived from the results of M.Shub and S.Smale concerning the density of real zeroes [5] (cf. [6]).

Proposition 3. *If coefficients of random polynomials P, Q have the aforementioned special multivariate normal distribution, then real roots of their leaders are uniformly distributed on the unit circle considered as projective line.*

After these preparations it becomes possible to determine the rate of growth of the average absolute topological degree.

Theorem 1. *For random polynomials of algebraic degree n with aforementioned distribution of coefficients, the average absolute value of topological degree of induced random planar endomorphism grows as* $n^{1/2}$ *when n tends to infinity.*

This result may be easily generalized in the setting of so-called quasihomogeneous binary forms and polynomials [7]. Also, using the fundamental relation between Euler characteristic and topological degree it is possible to obtain another typical result which is even more in the spirit of the temptative "statistical topology of real polynomials".

Theorem 2. *For random real polynomial of algebraic degree n as above, the average number of components of its level curves grows as* $(n-1)^{1/2}$ *when n tends to the infinity.*

Similar results should hold in a seemingly simpler "discrete" setting when a_{kl} are discrete random variables taking values in a symmetric grid with the step 1/m on the segment [–1, 1] and having variances indicated above. Notice that in such a setting we only have a finite number of polynomials for every fixed value n of the algebraic degree. In this case it becomes possible to make computer modelling by applying a computer program for calculating topological degree developed in Gdansk University by A.Lecki and Z.Szafraniec. We performed several computer experiments for small values of m and analyzed the growth of average absolute degree when n was increasing. The numerical results we obtained support the conjecture that an analogy of Theorem 1 also holds for such discretized random polynomials.

Now we want to say several words about the proofs of main results. Theorem 1 is proved using several reductions. First, we observe that degree of a "typical" planar endomorphism is equal to the degree of mapping defined by pair of leaders (this is an easy consequence of Rouchet's theorem [8]). Then we recall that the topological degree of a homogeneous planar endomorphism may be computed by looking at intersections of its zero lines with the unit circle. More precisely, one only needs to count the number of so-called alternances between zero lines of different components of the endomorphism [8].

Now observe that in the case of random hyperbolic *n*-forms, this number of alternances may be interpreted as the deviation of a symmetric random walk on the line [9]. The possibility of such interpretation follows directly from Proposition 3. This shows that we can simply borrow some well known combinatorics from random walk theory [9], which eventually leads to Proposition 1.

The fact that asymptotics of this average should be such as indicated in Proposition 2, is again in accordance with random walk theory [9] and may be verified by a standard application of the saddle point method.

In order to manage general random polynomials we also need to compute similar averages for pairs of binary n-forms each of which may have an arbitrary amount of real roots on S^1. This may be done in the same combinatorial framework and leads to similar formulas. The average we are interested in, is representable as a weighted sum of such averages for binary forms and by a careful analysis of weights one comes to the rate of growth stated in Theorem 1.

Finally, Theorem 2 follows by applying a general formula from [7] which relates Euler characteristics of level sets of a real polynomial with the topological degree of its gradient [7].

Of course there are many possible modifications of main results. For example, one might consider random polynomials of fixed but different degrees and verify that the average absolute topological degree grows as square root of the least algebraic degree. It should be also possible to manage the case when the coefficients a_{kl} are i.i.d. (independent identically distributed) normal random variables, say standard normal variables. In this case there is a good heuristic evidence that the average absolute degree should grow as $(\log n)^{1/2}$ but we still have no proof of this fact.

There are also some interesting problems concerned with distribution of signs of the Jacobian at common real roots of a pair of random polynomials. Our results suggest that these signs should be i.i.d. Bernoulli random variables (1 and –1 with probabilities one half). It would be interesting to perform a statistical verification of this conjecture.

Acknowledgements. Results of this note were obtained during the period when the both authors were visiting Professors at the Department of Theoretical Physics of the University of Lodz. It is our pleasure to gratefully acknowledge hospitality and assistance of the whole staff of the Department.

Georgian Academy of Sciences
A.Razmadze Mathematical Institute

Department of Theoretical Physics, University of Lodz, Poland

REFERENCES

1. *M.Kac*. Bull. Amer. Math. Soc. 32, 1943, 314-320.
2. *A.Bharucha-Reid, M.Sambandham*. Random Polynomials. Acad. Press., N.Y., 1980.
3. *O.Bogomolny, O.Bohias, P.Leboeuf*. Phys. Rev. Lett. 68, 1992, 2726-2729.
4. *L.Shepp, R.Vanderbei*. Trans. Amer. Math. Soc. 347, 1995, 4365-4384.
5. *M.Shub, S.Smale*. Progress in Math. 109, 1993, 267-288.
6. *A.Edelman, E.Kostlan*. Bull. Amer. Math. Soc. 32, 1995, 1-37.
7. *G.Khimshiashvili*. Trudy Tbilisskogo matem. instituta. 64, 1980, 105-124.
8. *M.Krasnoselsky*. Vector fields on the plane. Moscow, 1963.
9. *W.Feller*. An introduction to probability theory and its applications. N.Y., 1970.

საქართველოს მეცნიერებათა აკადემიის მოამბე, 159, №3, 1999
BULLETIN OF THE GEORGIAN ACADEMY OF SCIENCES, 159, №3, 1999

MATHEMATICS

O. Chkadua, R. Duduchava

Asymptotics of Solutions to the Crack Problem

Presented by Member of the Academy T. Burchuladze, June 22, 1998

ABSTRACT. **A complete asymptotics of solutions of the crack problem for an anisotropic elastic body is investigated, when displacement vectors are given on the crack boundary.**

Key words: Potential-type operators, pseudodifferential equations, asymptotic expansion, crack problem.

In the present paper we have investigated complete asymptotics of solutions to the crack problem.

Let us consider the crack problem for anisotropic elastic body

$$\mathbf{A}(D_x)u(x) = 0,\ x \in \mathbb{R}^3 \setminus S, \tag{1}$$

$$u^{\pm}(t) = f_{\pm}(t),\ t \in S \tag{2}$$

with prescribed displacement vector field $u^{\pm}$ on both faces of the crack surface S, where S is a smooth manifold with the smooth boundary ∂S and

$$\mathbf{A}(D_x) := \left\| \sum_{k,m=1}^{3} a_{jklm}\partial_k\partial_m \right\|_{3\times 3},\ a_{jklm} \in \mathbb{R},\ a_{jklm} = a_{lmjk} = a_{kjlm},$$

$$\sum_{j,k,l,m=1}^{3} a_{jklm}\xi_{jk}\xi_{lm} \geq C_0 \sum_{j,k}^{3} \xi_{jk}^2 \quad \text{for arbitrary } \xi_{jk} \in \mathbb{R},\ \xi_{jk} = \xi_{kj}.$$

A solution to the elliptic equation (1) is represented in the form

$$u(x) = \mathbf{W}_S f_0(x) - \mathbf{V}_S \varphi(x),\quad x \in \mathbb{R}^n \tag{3}$$

where $\mathbf{W}_S$ and $\mathbf{V}_S$ are the double and the single layer potentials for (1), while the densities

$$f_0(t) := f_+(t) - f_-(t),\quad \varphi(t) := \{T(D_t, n(t))u\}^+(t) - \{T(D_t, n(t))u\}^-(t)$$

represent jumps of the displacement and stress fields across the chack surface S.

Thus, we have to found $\varphi(t)$ from the boundary PsDE

$$\mathbf{V}_{-1}\varphi(t) = \mathbf{W}_0 f_0(t) - 1/2\ [f_+(t) + f_-(t)], \tag{4}$$

where $\mathbf{V}_{-1}$ and $\mathbf{W}_0$ are the direct values of potentials $\mathbf{V}_S$ and $\mathbf{W}_S$ on S; they represent pseudodifferential operators of the orders –1 and 0, respectively (see [1-3]).

Let

$$t = (s, \rho) \in \mathbf{Col}_{\varepsilon}^2 := \partial S \times]0, \varepsilon[$$

be the so-called local "plain collar" coordinate system, where $\rho = \rho(t) := \mathbf{dist}(t, \partial S)$ denotes the distance while $s \in \partial S$ is an arc abscissa.

As a solution to elliptic PsDE (4) $\varphi \in C^\infty(S)$ provided S is infinitely smooth.

Moreover, if the data are smooth $f_\pm \in C^\infty(S)$, the complete asymptotic expansion of $\varphi(t)$ in the neighbourhood of the boundary ∂S reads (see [4]).

$$\varphi(\rho, s) = c_0(s)\rho^{-1/2} + \sum_{k=1}^{M}\sum_{m=0}^{k} c_{kj}(s)\rho^{k-\frac{1}{2}} \log^m \rho + \varphi_{M+1}(\rho, s), \tag{5}$$

$$(\rho, s) \in \mathbf{Col}_\varepsilon^2,\ c_0,\ c_{1,0},\ \ldots,\ c_{M,M} \in C^\infty(\partial S),$$
$$\varphi_{M+1} \in C^M(\overline{S}),$$

for arbitrary $M = 1,2,\ldots$ (see also [5], [6]).

Next important step is to establish an asymptotics of $u(x)$ in (3) using asymptotics of density from (5). This is done in rather general setting in [7]. Similar results for canonical half-space case and particular potentials see in [5].

To formulate the main result of the present paper for BVP(1)-(2) let S_0 be some smooth closed manifold without boundary, containing S and introduce a local " thin collar" coordinate system in the neighbourhood of $\partial S \subset \mathbf{R}^3$

$$x = (s, \rho, r) \in \mathbf{Col}_\varepsilon^3 := \partial S \times]-\varepsilon,\ \varepsilon[\times]-\varepsilon,\ \varepsilon[,\ \mathbf{Col}_\varepsilon^3 \cap S = \mathbf{Col}_\varepsilon^2.$$

Here $\rho = \mathrm{dist}(\widetilde{x}, \partial S)$ denotes the distance to ∂S from the projection $\widetilde{x} \in S_0$ of a point $x \in \mathbf{R}^3 \backslash S_0$ along the outer normal to S_0 and takes negative values for $\widetilde{x} \in S_0 \backslash S$. $r = \mathbf{dist}(x, S)$ takes positive (respectively, negative) values for x inside (outside) of S_0.

As a solution to elliptic BVP (1)-(2) $u \in C^\infty(\mathbf{R}^3 \backslash S)$ provided S is infinitely smooth. Moreover, if the data are smooth $f_\pm \in C^\infty(S)$, complete asymptotic expansion of $u(x)$ in the neighbourhood of the boundary ∂S reads

$$u(s, \rho, r) = \sum_{m=1}^{\ell} \mathrm{Re}\Bigg\{ \sum_{j=0}^{n_m - 1} [d_{mj}(s, +1) r^j z_{m,+1}^{2^{-1}-j} - d_{mj}(s, -1) r^j z_{m,-1}^{2^{-1}-j}] +$$

$$+ \mathrm{Re} \sum_{\vartheta=\pm 1} \sum_{l=0}^{M+1} \sum_{k=0}^{M+2-l} \sum_{\substack{j+p=1 \\ l+k+j+p\neq 1}} \rho^l r^j z_{m,\vartheta}^{-\frac{1}{2}+p+k} B_{mlkjp}(s, \log z_{m,\vartheta}) \Bigg\} + \tag{6}$$

$$+ u_{M+1}(s, \rho, r), \quad u_{M+1} \in C^{M+1}(\mathbf{Col}_\varepsilon^3),$$
$$(s, \rho, r) \in (\mathbf{Col}_\varepsilon^3),\ d_{mj}(\cdot, \pm 1) \in C^\infty(\partial S),$$

Here

$$z_{m,\pm 1} := \rho \pm r\tau_{m,\pm 1}, \quad -\pi < \mathrm{Arg} z_{m,\pm 1} < \pi$$

and $\{\tau_{m,\pm 1}\}_{m=1}^{\ell}$ are all different roots of the polynomial $\det \mathbf{A}(J_{\mathfrak{x}}^T(s, 0)\cdot(0, \pm 1, \tau))$ of multiplicity n_m, $m = 1, 2, \ldots, \ell$ in the complex lower half plane $\mathrm{Re}\,\tau < 0$; $\mathbf{A}(\xi)$, $\xi \in \mathbf{R}^3$ is the symbol of elliptic differential operator $\mathbf{A}(D_x)$ in (1), and $J_{\mathfrak{x}}^T(s, \rho)$ is the transposed matrix to the Jacobian of the coordinate diffeomorphism $\mathfrak{x}$ from $\mathbf{R}^3$ to the surface S. $B_{mlkjp}(s, \lambda)$

is a polynomial of the order $\nu_{kjp} = k + \rho + j - 1$ with respect to λ with vector coefficients depending on the arc abscissa s.

All roots $\tau_{m,\pm1}(s)$ depend on the parameter $s \in \partial S$ smoothly $\tau_{m,\pm1} \in C^{\infty}(\partial S)(m=1,\ldots,l)$.

Moreover, the explicit relations between coefficients of expansions (5) and (6) are found. In particular, the leading coefficients $d_{mj}(s, \pm1)$ and $c_0(s)$ of these expansions are related as follows

$$d_{mj}(s, \pm1) = \frac{1}{2\sqrt{\pi}}(\mp i)^{j+1}\Gamma\left(j-\frac{1}{2}\right)\mathcal{G}_{æ}(s, 0)V_{-1,j}^{(m)}(s, 0, 0, \pm1)c_0(s),$$

where $\mathcal{G}_{æ}(s, 0)$ is the GRAMM determinant of the coordinate differomorphism æ and

$$V_{-1,j}^{(m)}(s, 0, 0, \pm1) = -\frac{i^{j+1}}{j!(n_m-1-j)!}\frac{d^{n_m-1-j}}{d\tau^{n_m-1-j}}\left(\tau-\tau_{m,\pm1}\right)^{n_m}\left(A(\mathcal{J}_{æ}^{T}(s,0)\cdot(0,\pm1,\tau))\right)^{-1}\Big|_{\tau=\tau_{m,\pm1}}$$

For isotropic case we have the LAMÉ operator

$$\mathbf{A}(D_x) = \mu\Delta + (\lambda+\mu)\mathbf{grad\ div}$$

and for it $l = 1$, $\tau_{m,\pm1} = \mp i$, $n_1 = 3$, $d_{12}(s, \pm1) = 0$; asymptotic expansion of the corresponding solution takes simpler form

$$u(s, \rho, r) = d_1(s)\mathrm{Im}\, z_{+1}^{\frac{1}{2}} + \mathrm{Re}\, d_2(s)r\left(z_{+1}^{-\frac{1}{2}} - z_{-1}^{-\frac{1}{2}}\right) +$$

$$+\mathrm{Re}\sum_{\vartheta=\pm1}\sum_{\substack{l,k=0\\ l+k+j+p\neq1}}^{M+1M+2-l}\sum_{j+p=1}\rho^{l}r^{j}z_{m,\vartheta}^{-\frac{1}{2}+p+k}B_{1lkjp}\left(s, \log z_{m,\vartheta}\right) + u_{M+1}(s, \rho, r), \tag{7}$$

$$(s, \rho, r) \in \mathbf{Col}_{\varepsilon}^{3},\ z_{\pm1} := \rho \mp ir.$$

Here $d_1(s) = \mathbf{diag}\left\{\frac{1}{\mu}, \frac{\lambda+3\mu}{2\mu(\lambda+2\mu)}, \frac{\lambda+3\mu}{2\mu(\lambda+2\mu)}\right\}\mathcal{G}_{æ}(s, 0)c_0(s)$

and the coefficient $d_2(s) = d_{11}(s, +1)$ calculated analogously.

Georgian Academy of Sciences
A. Razmadze Mathematical Institute

REFERENCES

1. *M. Costabel, E. Stephan.* Integral Equations and Operator Theory 10, 1987, 467-504.
2. *R. Duduchava, D. Natroshvili, E. Shargorodsky.* Trudy inst. pricl. mat. I. N. Vekua, 1990, 63-84.
3. *R. Duduchava, D. Natroshvili, E. Shargorodsky.* Georgian Mathematical Journal 2, 1995.
4. *O. Chkadua, R. Duduchava.* Bull. Georg. Acad. Sci. 158.2, 1998, 207-210.
5. *G. Eskin.* Translations of Mathematical Monograps. AMS, Providence, Rhode Island 1981.
6. *J. Bennish.* Journal for Mathematical Analysis and Applications 179, 1993.
7. *O. Chkadua, R. Dundua.* Bull.Georg. Acad. Sci., 159, 1, 1999, 23-27.

საქართველოს მეცნიერებათა აკადემიის მოამბე, 159, №3, 1999
BULLETIN OF THE GEORGIAN ACADEMY OF SCIENCES, 159, №3, 1999

MATHEMATICS

U. Goginava

On the Uniform Convergence of Multiple Fourier Series with Respect to the Trigonometric System

Presented by Member of the Academy L. Zhizhiashvili, April 27, 1998

ABSTRACT. **In 1976 Z.A. Chanturia considered the question of uniform convergence of one dimensional Fourier series in a trigonometric system in terms of continuity and variation of moduli. In this paper we study the problems of uniform convergence of multiple Fourier trigonometric series in terms of partial continuity and partial variation of moduli. As special cases, from this theorem follows L.V. Zhizhiashvili's theorem and generalization of the Hardy theorem.**

Key words: Multiple trigonometric Fourier series, uniform convergence, modulus of variation.

Below we shall use the following definitions and notations adopted in [1].

Let $T^N = [0, 2\pi]^N$ denote a cube in the N-dimensional Euclidean space R^N. The elements of R^N are denoted by $x = (x_1, \dots, x_N)$.

Let $M = \{1, \dots, N\}$, $B = \{l_1, \dots, l_r\}$, $B \subset M$, $l_k < l_{k+1}$, $k = 1, \dots, r-1$, $B' = M \setminus B$. For the integer n the vector $(n, \dots, n)$ of the space R^N we denote by $\bar{n}$. Let $\bar{k}(B)$ be a number of elements in B. For any $x = (x_1, \dots, x_N)$ and any $B \subset M$, let x_B denote a vector of the R^N space, whose coordinates with indices from the set B coincide with coordinate of the vector x and the coordinates with indices from the set B' are zero.

Below we shall identify the symbols $\sum_{i_B=P_B}^{m_B}$ and $\sum_{i_{l_1}=P_{l_1}}^{m_{l_1}} \cdots \sum_{i_{l_r}=P_{l_r}}^{m_{l_r}}$.

Denote by $C(T^N)$ the space of continuous on T^N, 2π periodic relative to each variable functions with the norm $\|f\|_C = \max_{x \in T^N} |f(x)|$.

Let $\Delta_{h_{\{l_i\}}}^{\{l_i\}}(f, x, h_{\{l_i\}}) = f(x + h_{\{l_i\}}) - f(x)$, $i = 1, \dots, r$. The expression we get by successive application of operations $\Delta_{h_{\{l_1\}}}^{\{l_1\}}(f, x, h_{\{l_1\}}), \dots, \Delta_{h_{\{l_r\}}}^{\{l_r\}}(f, x, h_{\{l_r\}})$ will be denoted by $\Delta_{h_B}^{B}(f, x, h_B)$.

Let $f \in C(T^N)$. The expression $\omega_B(\delta, f) = \sup_{\substack{|h_i| \le \delta_i \\ i \in B}} \|\Delta_{h_B}^{B}(f, \cdot, h_B)\|_C$, $\delta_i \in (0, \pi]$, $i \in B$, is called a mixed or a particular modulus of continuity, when $\bar{k}(B) \in [2, N]$ or $\bar{k}(B) = 1$ respectively.

Let the function f be bounded on T^N and 2π periodic relative to each variable. The partial modulus of variation for $\bar{k}(B) = 1$ and mixed modulus of variation for $\bar{k}(B) \in [2, N]$ of the function f are defined by $\nu_B(n, f) = \sup_{x \in T^N} \sup_{\Pi_{x_j}^{(j)},\, j \in B} \sum_{k_B=1_B}^{n_B} \left| \Delta_{\bar{2}\pi/k_B - \bar{1}_B}^{B}\left(f, x + \bar{t}_{2k_B - \bar{1}_B}^{(B)}, \bar{t}_{2k_B}^{(B)} - \bar{t}_{2k_B - \bar{1}_B}^{(B)}\right) \right|$,

where $\Pi_{n_{t_i}}^{(t_i)}$, $(i=1,\ldots,r)$ are an arbitrary system of n_{t_i} disjoint intervals $\left(t_{2k_{t_i}-1}^{(t_i)}, t_{2k_{t_i}}^{(t_i)}\right)$,

$k_{t_i}=1,\ldots,n_{t_i}$ i.e. $0\le t_1^{(t_i)}<t_2^{(t_i)}\le t_3^{(t_i)}<\cdots\le t_{2n_{t_i}-1}^{(t_i)}<t_{2n_{t_i}}^{(t_i)}\le 2\pi$ and $\tilde{t}_{2k_B}^{(B)}=\sum_{i=1}^{r}\tilde{l}_{|t_i|}t_{2k_{t_i}}^{(t_i)}$.

For $N=1$, see [2].

We say that f is of bounded variation [3] in Hardy's sense, if each of the numbers $\sup_{m_i\ge 1,\, i\in B} v_B(m,f)$, $\forall B: B\subset M,\ B\ne\{\varnothing\}$, is finite. Given a function f, integrable in Lebesgue sense on T^N, 2π periodic in each variable, its Fourier series is defined by

$$\sum_{i_M=0_M}^{\infty}2^{-\lambda(i_M)}\sum_{B\subset M}a_{i_M}^{(B)}\prod_{j\in B}\cos i_j x\prod_{k\in B'}\sin i_k x\ ,$$

where $a_{i_M}^{(B)}=\frac{1}{\pi^N}\int_{T^N}f(x)\prod_{j\in B}\cos i_j x\prod_{k\in B'}\sin i_k x\ dx_1\ldots dx_N$ is the Fourier coefficient of f and $\lambda(i_M)$ is the number of those coordinates of the vector i_M, which are equal to zero.

L.V.Zhizhiashvili ([1], pp.331-347) has considered the question of uniform convergence of multiple Fourier series in the trigonometric system in terms of continuity modulus. The following Theorem is proved.

Theorem A. *a) Let $f\in C(T^N)$ and for any $B\subset M$, $B\ne\{\varnothing\}$*

$$\omega_B(\delta,f)\prod_{i\in B}\log\frac{2\pi}{\delta_i}\to 0,\ \delta_i\to 0+\ ,\ i\in B\ .$$

Then the N-dimensional Fourier series of the function f with respect to the trigonometric system convergence uniformly in the sense of Pringsheim;

b) for any $B_0\subset M$, $\bar{k}(B_0)\in[1,N]$ there exists a function $f\in C(T^N)$ such that

$$\omega_{B_0}(\delta,f)\prod_{i\in B_0}\log\frac{2\pi}{\delta_i}<\infty,\ \delta_i\in]0,\pi],\quad i\in B_0$$

and for any $B\subset M$, $B\ne B_0$, $B\ne\{\varnothing\}$, $\omega_B(\delta,f)\prod_{i\in B}\log\frac{2\pi}{\delta_i}\to 0$, $\delta_i\to 0+$, $i\in B$.

However, the N-dimentional Fourier series of the function f with respect to the trigonometric system λ-diverges (for $\lambda=1$) in the metric of C.

From Theorem A we can conclude that, in general, the fulfilment of the conditions

$$\omega_{\{i\}}(\delta,f)\log\frac{2\pi}{\delta_i}\to 0,\ (\delta_i\to 0+)\ ,\ i=\overline{1,N},\ N\ge 2\ ,$$

does not guarantee the uniform convergence of the N-dimensional Fourier series of the function f with respect to the trigonometric system. On the basis of the above-said argu-

ments P.L.Uljanov has formulated the following problem: *let* $f \in C(T^N)$. *What conditions the partial moduli of continuity must satisfy in order to provide uniform convergence in Pringsheim's sense of the N-dimentional Fourier series of the function* f *with respect to the trigonometric system.* L.V. Zhizhiashvili ([1], pp.331-347) has solved this problem.

Theorem B. *a) Let* $f \in C(T^N)$ *and* $N \geq 2$. *If there exists* i_0 *such that*

$$\omega_{i_0}(\delta, f)\left(\log\frac{2\pi}{\delta_{i_0}}\right)^N \to 0,\ \left(\delta_{i_0} \to 0+\right) \text{ and } \omega_{\{i\}}(\delta, f)\left(\log\frac{2\pi}{\delta_i}\right)^N < \infty,\ \delta_i \in]0,\pi],\ \left(i = \overline{1,N},\ i \neq i_0\right).$$

Then the N-dimensional Fourier series of the function f *with respect to the trigonometric system converges in Pringsheim's sense in* C.

b) For every $N \geq 2$, *there exists a function* $f \in C(T^N)$ *such that*

$$\omega_{\{i\}}(\delta, f)\left(\log\frac{2\pi}{\delta_i}\right)^N < \infty,\ \delta_i \in]0,\pi],\ \left(i = \overline{1,N}\right)$$

and the N-dimensional Fourier series of the function f *with respect to the trigonometric system* λ *-diverges (for* $\lambda = 1$*) in the metric of* C.

Z. Chanturia [4] investigated the problem of uniform convergence of one-dimensional Fourier series in the trigonometric system in terms of the continuity and variation moduli.

Theorem C. *Let* $f \in C(T^N)$ *and* $\nu_{\{1\}}(n, f)$, $\omega_{\{1\}}(\delta, f)$ *be moduli of variation and continuity, respectively. If the condition*

$$\lim_{n_1 \to \infty} \min_{1 \leq p \leq \left[\frac{n_1-1}{2}\right]-1} \left\{ \omega_{\{1\}}\left(\frac{1}{n}, f\right) \log p + \sum_{k=p+1}^{\left[\frac{n_1-1}{2}\right]} \frac{\nu_{\{1\}}(k, f)}{k^2} \right\} = 0$$

is fulfilled, then the one-dimensional Fourier series of the function f *with respect to the trigonometric system converges in* C.

From Theorem A we can conclude that, in general, the fulfillment of the conditions

$$\lim_{n_i \to \infty} \min_{1 \leq p \leq \left[\frac{n_i-1}{2}\right]-1} \left\{ \omega_{\{i\}}\left(\frac{1}{n}, f\right) \log p + \sum_{k=p+1}^{\left[\frac{n_i-1}{2}\right]} \frac{\nu_{\{i\}}(k, f)}{k^2} \right\} = 0,\ \left(i = \overline{1,N}\right)$$

does not provide the uniform convergence of the N-dimensional Fourier series of the function f with respect to the trigonometric system.

Hardy [3] proved

Theorem D. *If* $f \in C(T^N)$ *and if it has bounded variation in Hardy's sense, then multiple trigonometrical Fourier series of this function is converge uniformly.*

On the basis of the above facts we can formulate the following problems:

Problem 1. *Let* $f \in C(T^N)$. *What conditions the partial moduli of continuity and the partial moduli of variation must satisfy in order to provide uniform convergence in Pringsheim's sense of the N-dimentional Fourier series of* f *with respect to the trigono-*

metric system. The solution of this problem is given by Theorem 1.

Problem 2. *It is necessary to require in Hardy's Theorem D for the mixed variation*

$$\left(\sup_{m_j,\ i\in B} v_B(m,f)<\infty,\ \overline{k}(B)\in[2,N]\right)\ \textit{be bounded.}$$

The solution of this problem is given in Corollary 2. We prove the following Theorems:

Theorem 1. *Let* $f\in C(T^N)$ *and* $N\geq 2$. *If there exists* j_0 *such that*

$$\min_{1\leq p\leq \frac{n_{j_0}-3}{2}}\left\{\sqrt[N]{\omega_{\{j_0\}}\left(\tfrac{1}{n},f\right)}\log p+\sum_{i=p+1}^{\frac{n_{j_0}-1}{2}}\frac{\sqrt[N]{\nu_{\{j_0\}}(i,f)}}{i^{1+\frac{1}{N}}}\right\}=o(1),\ \left(n_{j_0}\to\infty\right)\ \textit{and}\ \min_{1\leq p\leq \frac{n_j-3}{2}}\left\{\sqrt[N]{\omega_{\{j\}}\left(\tfrac{1}{n},f\right)}\log p+\right.$$

$$\left.+\sum_{i=p+1}^{\frac{n_j-1}{2}}\frac{\sqrt[N]{\nu_{\{j\}}(i,f)}}{i^{1+\frac{1}{N}}}\right\}=O(1),\ \left(n_j\to\infty\right),\ \left(j\neq j_0,\ j=\overline{1,N}\right),\ \textit{then the N-dimensional Fourier series of}$$

f with respect to the trigonometric system converges in C in Pringsheim's sense.

Theorem 2. *For every* $N\geq 2$ *there exists a function* $f\in C(T^N)$ *such that* $\left(j\neq j_0,\ j=\overline{1,N}\right)$

$$\min_{1\leq p\leq \frac{n_j-3}{2}}\left\{\sqrt[N]{\omega_{\{j\}}\left(\tfrac{1}{n},f\right)}\log p+\sum_{i=p+1}^{\frac{n_j-1}{2}}\frac{\sqrt[N]{\nu_{\{j\}}(i,f)}}{i^{1+\frac{1}{N}}}\right\}=O(1),\ \left(n_j\to\infty\right)\ \textit{and the N-dimentional Fou-}$$

rier series of f with respect to the trigonometric system λ *-diverges (for* $\lambda=1$*) in* C.

Corollary 1. *Let* $f\in C(T^N)$ *and* $(\forall j:\ j\in M)\ \sum_{k=1}^{\infty}\frac{\sqrt[N]{\nu_{\{j\}}(k,f)}}{k^{1+\frac{1}{N}}}<\infty$.

Then the N-dimensional Fourier series of the function f with respect to the trigonometric system converges uniformly in Pringsheim's sense.

Corollary 2. *Let* $f\in C(T^N)$ *and* $\sup_{m_j\geq 1}\nu_{\{j\}}(m,f)<\infty,\ j=1,2,\ldots,N$.

Then the N-dimensional Fourier series of the function f with respect to the trigonometric system converges uniformly in Pringsheim's sense.

Example. Obviously, the fulfilment of the condition of Theorem B implies that the condition of Theorem 1, but not *vice versa*; i.e., there exists $f\in C(T^N)$ for which the condition of Theorem1 is fulfilled and the condition of Theorem B does not.

Tbilisi I. Javakhishvili State University

REFERENCES

1. *L.V. Zhizhiashvili.* Trigonometric Fourier series and their conjugates. 1993 (Russian).
2. *Z.A. Chanturia.* Dokl. AN SSSR, **214**, 1, 1974, 63-66 (Russian).
3. *G.H. Hardy.* Quart. J. Math. 37, 1906, 53-79.
4. *Z.A. Chanturia.* Math. Sbornik, 100(142), 4(8) , 1976, 534-554 (Russian).

საქართველოს მეცნიერებათა აკადემიის მოამბე, 159, №3, 1999
BULLETIN OF THE GEORGIAN ACADEMY OF SCIENCES, 159, №3, 1999

MATHEMATICS

A.Tikaradze

Subdivision of the Simplicial and Semisimplicial Objects

Presented by Corr.Member of the Academy Kh.Inassaridze, November 3, 1998

ABSTRACT. **A new proof is given that any simplicial Abelian group or its any subdivision are of the same homotopic type. The relations between the homotopies of subdivision of semisimplicial Abelian groups and corresponding Tor groups are also investigated.**

Key words: homotopy groups, subdivision, simplicial objects, Tor groups.

In the work of Bokstedt, Hsiang, Madsen [1] the idea of subdivision of a simplicial set is introduced and there proved that a simplicial set and its subdivision have the same homotopic type. The algebraic version of this construction played the important role in the work of R.McCarthy [2]. The aim of the given work is, on the one hand a simple proof of this statement, and on the other hand, the relation investigation of the homologies of the semisimplicial objects' subdivisions with corresponding Tor functors.

We denote by Δ the category, objects of which are $[n] = (0, 1, \dots, n)$ sets, the morphisms between them are nondecreasing functions. Let us denote by Δ_i subcategory of Δ, objects set of which coincides with the objects set of Δ and the morphisms in it are increasing functions. A simplicial (semisimplicial) Abelian group is defined as contravariant functor from Δ (from Δ_i) to the category of Abelian groups.

In [1] there is defined the functor sd_r from Δ in Δ (for any natural r) which sends $[n]$ to $\underbrace{[n]\amalg\cdots\amalg[n]}_{r-\text{times}} = [(n+1)r-1]$ and $sd_r(f)(a(m+1)+b) = a(n+1)+f(b)$ when $f:[m]\to[n]$ and $0 \le b \le m$. It is obvious, the restriction of sd_r to Δ_i is the functor to Δ_i. If X is a simplicial (semisimplicial) Abelian group and, if we consider its composition with sd_r we shall obtain the simplicial (semisimplicial) Abelian group denoted by $sd_r(X)$. The following theorem is correct

Theorem 1. *For any X simplicial Abelian group there existed the natural isomorphism between the groups of X and $sd_r(X)$ homotopies.*

Proof. The idea of our proof is based on fact [3] that the groups of homotopy of X simplicial Abelian group are isomorphic with respect to the following Tor groups

$$\pi_*(X) \approx \mathrm{Tor}_*^{\Delta}(X, Z), \tag{1}$$

where Z is the constant cosimplicial object the value of which is Z. In order to prove the theorem using isomorphism (1) it is sufficient to show, that

$$\pi_*(X) \approx \mathrm{Tor}_*\ \pi_*(sd_r(X)) \approx \mathrm{Tor}_*^{\Delta}(X, Z) \tag{2}$$

The proof of formula (2) uses the known axiomatics of Tor-groups. By this axiomatics everything is reduced to the demonstration that $\pi_i(sd_r(X)) = 0$, when $i > 0$ and $\pi_0(sd_r(X)) = Z$, where $X = Z[\Delta^n]$ is the free Abelian simplicial group produced by the standard n-dimensional Δ^n simplex. We use here the commonly known fact that the indicated simplicial Abelian groups are the projective generators in [3] category of the simplicial Abelian groups. Let us consider the case, when $r = 2$; the proof is identical when $r \neq 2$.

Let us consider the bisimplicial Abelian group Y, where Y_{pq} ($p \geq 0$, $q \geq 0$) is the free Abelian group the basis of which is the subset of $\mathrm{Hom}\Delta([p], [n])\times\mathrm{Hom}\Delta([q], [n])$ elements of which $\eta\times\eta'$, $\eta \in \mathrm{Hom}\Delta([p], [n])$, $\eta' = \mathrm{Hom}\Delta([q], [n])$ are such that for any $0 \leq i \leq p$, $0 \leq i \leq q$ the bisimplicial structure $\eta(i) \leq \eta'(i)$ naturally enters for Y. It is obvious that the diagonalization of the Y bisimplicial Abelian group is $sd_r(Z[\Delta^n])$. In accordance with the Eilenberg-Zilber theorem [4]

$$\pi_*(sd_r(Z[\Delta^n])) = \pi_*(\mathrm{diag}(Y)) \approx H_*\mathrm{Tot}(Y)) \tag{3}$$

Let us denote the m-column of Y by Y^*_m. If $\eta' \in \mathrm{Hom}\Delta([p], [n])$ and $\eta \in \mathrm{Hom}\Delta([m],[n])$ then $\eta'\times\eta$ belongs to Y_{pm} if and only if $\eta'(i) \leq \eta(0)$ for all $0 \leq i \leq p$ i.e. $\eta' \in \mathrm{Hom}\Delta([p],[\eta(0)])$. Therefore Y^*_m is the direct sum of $Z[\Delta^{\eta(0)}]$ simplicial groups where η runs $\mathrm{Hom}\Delta([m], [n])$ product. Because the homotopies groups of $Z[\Delta^n]$ are nonzero in the zero dimension only where it is equal to Z, in accordance with the known properties of the bicomplex

$$H_0(\mathrm{Tot}(Y)) = Z \text{ and } H_i(\mathrm{Tot}(Y)) = 0$$

when $i > 0$. Therefore taking into account (3) the theorem is proved.

Because for the proof we have used the Eilenberg-Zilber theorem it is hopeless to expect the correctness of the theorem in the case of semisimplicial objects. Moreover the results mentioned below will show that for the semisimplicial Abelian groups not only the theorem 1 is not correct but again $\pi_*(X)$ is isomorphic to $\mathrm{Tor}^{\Delta_i}_*(X, Z)$ group, where as $\pi_*(sd_r(X))$ is no longer isomorphic with respect to Tor groups, as soon as $r > 1$.

Theorem 2. *For any semisimplicial Abelian group X we have the natural isomorphism*

$$\pi_*(X) \approx \mathrm{Tor}^{\Delta_i}_*(X, Z) \tag{4}$$

Proof. Starting from the properties of Tor groups it is sufficient to show that $\mathrm{Tor}^{\Delta_i}_o(X, Z) \approx 0$ and $\pi_i(X) = 0$, when $i > 0$, where $X = Z[\Delta^n_i]$. We have the exact sequence:

$$X_i \xrightarrow{d} X_0 \to \pi_0(X) \to 0.$$

Because $X_1 \approx \underset{\Delta_i}{X} \otimes Z[Hom_{\Delta_i}([1],-)]$ and $X_0 \approx \underset{\Delta_i}{X} \otimes Z[Hom_{\Delta_i}([0],-)]$, and because the tensor product is right exact, we obtain

$$\pi_0(X) \approx \underset{\Delta_i}{X} \otimes Co\ker(d : Z[Hom_{\Delta_i}([1],-) - Z[Hom_{\Delta_i}([0],-)] \approx \underset{\Delta_i}{X} \otimes Z = Tor^{\Delta_i}_0(X, Z).$$

It is obvious that $Z[\Delta_i^n]$ is the subsemisimplicial object of $Z[\Delta^n]$. Because $Z[\Delta^n]$ elements, which are not a part of $Z[\Delta_i^n]$, represent the singular part of the simplicial Abelian group $Z[\Delta^n]$, therefore $\pi_i(Z[\Delta_i^n]) = \pi_i(Z[\Delta^n]) = 0$, when $i > 0$.

Let us show that $\pi_*(sd_r(X))$ is not isomorphic with respect to Tor groups. In fact if it would not be so, for any $n \geq 0$ we should have $\pi_i(sd_r(Z[\Delta_i^n])) = 0$ for all $i > 0$. Let us take $r = 2$, $n = 4$, $i = 1$. Because the third member is equal to zero, therefore, d: $Z[Hom_{\Delta_i}([2],[4])] \rightarrow Z[Hom_{\Delta_i}([1],[4])]$ must be monomorphism. But $d(\varepsilon_0 - \varepsilon_1 + \varepsilon_2 - \varepsilon_3 + \varepsilon_4) = 0$, where $\varepsilon_j \in Hom_{\Delta_i}([2],[4])$, $\varepsilon_j(1) = i$ if $i < j$ and is equal to $i+1$ if $i \geq j$, $0 \leq i \leq 3$. We obtain the contradiction i.e. $\pi_*(sd_r(X))$ is not isomorphic with respect to Tor groups, when $r > 1$.

Tbilisi I. Javakhishvili State University

REFERENCES

1. *M.Bokstedt, W.C.Hsiang, I.Madsen.* Invent. Math. **111,** 1993, 465-540.
2. *R.McCarthy.* On operation for Hochschild, Preprint, 1996.
3. *J.L.Loday.* Cyclic Homology. Grundlehren der Mathematischen Wissenschaften, 301, Springer Verlag, 1992.
4. *C.Weibel.* An Introduction to Homological Algebra, Cambridge, 1994.

საქართველოს მეცნიერებათა აკადემიის მოამბე, 159, №3, 1999
BULLETIN OF THE GEORGIAN ACADEMY OF SCIENCES, 159, №3, 1999

MATHEMATICS

Sh. Tetunashvili

On some Properties of Double Function Series

Presented by Member of the Academy L. Zhizhiashvili, May 11, 1998

ABSTRACT. **In the paper we present theorems for some double function series, from which in particular follows that, if double trigonometric series with coefficients a_{ij} is convergent on $[0,1]^2$ to a finite function $F(t,\tau) = f(t)\cdot g(\tau)$ then $a_{ij} = \alpha_i \cdot \beta_j$ for each $i \geq 0$ and $j \geq 0$.**

Key words: double function series, convergence in Pringsheim sense, multiple trigonometric series, Cantor's property.

Let $A \subset [0,1]$ and $B \subset [0,1]$. The set $A \times B$ is Cartesian product of the sets A and B. Let μA be Lebesgue measure of A; i and j are non-negative integer numbers. The symbol $(i, j) \geq (0, 0)$ means that $i \geq 0$ and $j \geq 0$, and $(i, j) \geq (1, 1)$ means that $i \geq 1$ and $j \geq 1$.

Suppose that systems $\Phi = \{\varphi_i(t)\}_{i=0}^{\infty}$ and $\Psi = \{\psi_i(t)\}_{i=0}^{\infty}$ are orthonormal systems of finite functions defined on $[0,1]$.

Consider a series in the system Φ

$$\sum_{i=0}^{\infty} a_i \varphi_i(t) . \tag{1}$$

Definition 1. *We say that the system Φ has Cantor's property if there exists a set $E \subset [0,1]$ such that the only series* (1) *that converges to zero on E is the series all of whose coefficients are zero.*

Definition 2. *A measurable set E belongs to the class $U(\Phi)$ if the only series* (1) *that converges to zero on E is the series all of whose coefficients are zero.*

Definition 3. *Let $\delta \in (0,1]$ be a number. We say that the system Φ is a system of δ linearly independence system if every finite part of the system Φ is linearly independent on each set E, with $\mu E > 1 - \delta$.*

Consider a double series in the system $\Phi \times \Psi = \{\varphi_i(x)\cdot\psi_j(y)\}_{(i,j)\geq(0,0)}$

$$\sum_{i=0}^{\infty}\sum_{j=0}^{\infty} a_{ij}\varphi_i(x)\psi_j(y) . \tag{2}$$

The convergence of the series (2) will be understood as Pringsheim convergence. The equality

$$\sum_{i=0}^{\infty}\sum_{j=0}^{\infty} a_{ij}\varphi_i(x)\psi_j(y) = S$$

means, that the series (2) is convergent to the number S in the point (x, y) in Pringsheim sense.

In the future we shall assume that systems Φ and Ψ has Cantor's property, Φ is δ linearly independence system, the set $A \in U(\Phi)$, $\mu A > 1 - \delta$ and the set $B \in U(\Psi)$. $f(t)$ and $g(t)$ are finite functions defined on $[0,1]$.

We have the following results.

Theorem 1. *Let*

$$\sum_{i=0}^{\infty}\sum_{j=0}^{\infty} a_{ij}\varphi_i(x)\psi_j(y) = f(x)\cdot g(y), \quad \text{when } (x, y) \in A \times B.$$

Then there exist sequences of numbers $\{\alpha_i\}_{i=0}^{\infty}$ *and* $\{\beta_j\}_{j=0}^{\infty}$ *such that* $a_{ij} = \alpha_i \cdot \beta_j$ *for each* $(i, j) \geq (0,0)$.

Theorem 2. *Let* $\varphi_0(x) \equiv \psi_0(y) \equiv 1$ *and*

$$\sum_{i=0}^{\infty}\sum_{j=0}^{\infty} a_{ij}\varphi_i(x)\psi_j(y) = f(x)+g(y), \text{ when } (x, y) \in A \times B.$$

Then $a_{ij} = 0$ *for each* $(i, j) \geq (1,1)$.

Consider a double series in the system $\Phi \times \Phi = \{\varphi_i(x)\cdot\varphi_j(y)\}_{(i,j)\geq(0,0)}$

$$\sum_{i=0}^{\infty}\sum_{j=0}^{\infty} a_{ij}\varphi_i(x)\varphi_j(y). \tag{3}$$

Thus, we have

Theorem 3. *Let the series* (3) *converges on* $A \times A$ *to a finite function* $F(x, y)$, *for which*

$$F(x, y) = F(y, x) \text{ when } (x, y) \in A \times A.$$

Then $a_{ij} = a_{ji}$ *for each* $(i, j) \geq (0,0)$.

Remark 1. The analogous theorems of Theorems 1, 2 and 3 are also valid for d-fold multiple ($d \geq 3$) function series.

Remark 2. As it is well known, the trigonometric system $T = \{1, \sqrt{2}\cos 2\pi it, \sqrt{2}\sin 2\pi it\}_{i=1}^{\infty}$ has Cantor's property (*see* [1], *chapter* IX, #3). At the same time the system T is $\delta = 1$ linearly independence system. i.e. the system T satisfies all conditions of Theorems 1, 2 and 3. So, these theorems are valid for double trigonometric series. Analogous propositions of these theorems are valid also for d-fold multiple ($d \geq 3$) function series.

Georgian Technical University

REFERENCES

1. *A. Zygmund.* Trigonometric series, I, Cambridge 1959.

საქართველოს მეცნიერებათა აკადემიის მოამბე, 159, №3, 1999
BULLETIN OF THE GEORGIAN ACADEMY OF SCIENCES, 159, №3, 1999

MATHEMATICS

A.Danelia

On the Deformation of Zygmund's Classes $Z(\omega^{(2)}; L(T^m))$

Presented by Member of the Academy L. Zhizhiashvili, October 12, 1998

ABSTRACT. **The problem of deformation of the classes $Z(\omega^{(2)}; L(T^m))$ with respect to the operator $\widetilde{f}_B$ has been studied.**

Key words: conjugate functions of multiple variables, modulus of second-order continuity.

Let $\mathbf{R}^m (m = 1, 2, \dots, \mathbf{R}^1 \equiv \mathbf{R})$ be m-dimensional Euclidean space. Let's consider $M = \{1, \dots, m\}$ and assume that B is a nonempty subset of M. We shall denote the number of elements of B set by the symbol $|B|$ and by x_B a point in the space $\mathbf{R}^m$, for which all the coordinates with the indices $M \setminus B$ are zeros.

If $T = [-\pi, \pi]$, then $\mathbf{C}(T^m)$ is a set of continuous functions defined on T^m, with period 2π in each variable and with the norm

$$\|f\|_{\mathbf{C}(T^m)} = \max_{x \in T^m} |f(x)|,$$

and $L^P(T^m)$ $(1 \le P \le \infty)$ is the set of functions, defined on T^m, Lebesgue integrable in P-th power, with period 2π in each variable and with the norm

$$\|f\|_{L^P(T^m)}^P = (2\pi)^{-m} \int_{T^m} |f(x)|^P \, dx.$$

It implies that $L^\infty(T^m) = \mathbf{C}(T^m)$ and $L^1(T^m) = L(T^m)$.

Let $f \in L^P(T^m)$ $(1 \le P \le \infty)$. We consider the difference

$$\Delta_i^2(h) f(x) = f(x_1, \dots, x_i + 2h, \dots, x_m) - 2f(x_1, \dots, x_i + h, \dots, x_m) + f(x_1, \dots, x_m)$$

and define modulus of the second-order continuity for i–th variables by the following equality

$$\omega_i^{(2)}(f; \delta)_{L^P(T^m)} = \sup_{|h| \le \delta_i} \left\| \Delta_i^2(h) f \right\|_{L^P(T^m)} \quad (0 < \delta \le \pi, \ i = 1, \dots, m).$$

The function $\omega^{(2)}: [0, \pi] \to \mathbf{R}$ is called the modulus of the second order continuity, if it satisfies the following four conditions

1) $\omega^{(2)}(0) = 0$;
2) $\omega^{(2)}$ is increasing;
3) $\omega^{(2)}$ is continuous;

4) if $0 < \delta < t \le \pi$, then $\dfrac{\omega^{(2)}(t)}{t^2} \le A \dfrac{\omega^{(2)}(\delta)}{\delta^2}$ $(A = \text{const})$.

We say that the modulus of the second-order continuity $\omega^{(2)}$ satisfies Zygmund's condition if

$$\int_0^{\delta} \frac{\omega^{(2)}(t)}{t}dt + \delta^2 \int_{\delta}^{\pi} \frac{\omega^{(2)}(t)}{t^3} = 0(\omega^{(2)}(\delta)).$$

Let us consider the following classes of functions:

$$Z_i(\omega^{(2)}; L^P(T^m)) = \{f: f \in L^P(T^m);\ \omega_i^{(2)}(f;\delta)_{L^P(T^m)} = O(\omega^{(2)}(\delta)),\ 0 < \delta_i \le \pi,\ i = 1, \dots, m\},$$

$$Z(\omega^{(2)}; L^P(T^m)) = \bigcap_{i=1}^{m} Z_i\ (\omega^{(2)}; L^P(T^m)).$$

We call the expression

$$\widetilde{f}_B(x) = \left(-\frac{1}{2\pi}\right)^{|B|} \int_{T^{|B|}} f(x+S_B) \prod_{i \in B} ctg\frac{S_i}{2} dS_i$$

the conjugate function of f with respect to the variables, the indices of which make the set B [1,p.182].

In the theory of functions of real variables there are many works related to various properties of conjugated functions of multivariables (integrability, continuity, etc.).

The problem of deformation of the class $Z(\delta; C(T^2))$ with respect to conjugated function of two variables affecting this class was studied by J.Zhak [2], and the problem of deformation of the classes $Z(\delta; C(T^m))$ $(m \ge 2)$ was considered by M.Lekishvili [3].

In the present work the problem of deformation of the classes $Z(\omega^{(2)}; L(T^m))$ $(m \ge 2)$ with respect to the $\widetilde{f}_B$ conjugate operator of multivariables affecting these classes is completely solved. The following statement is valid.

Theorem. *If* $f \in Z(\omega^{(2)}; L(T^m))$ $(m \ge 2)$, *and the modulus of second-order continuity* $\omega^{(2)}$ *satisfies Zygmund's condition, then*

$$\widetilde{f}_B \in \left[\bigcap_{i \in B} Z_i\left(\omega^{(2)}|\ln|^{|B|-1}; L(T^m)\right)\right] \bigcap \left[\bigcap_{i \in M \setminus B} Z_i\left(\omega^{(2)}|\ln|^{|B|}; L(T^m)\right)\right];$$

There exists a function such that $F \in Z(\omega^{(2)}; L(T^m))$

$$\omega_i^{(2)}(\widetilde{F}_B;\delta)_{L(T^m)} \ge C(\omega^{(2)}(\delta)|\ln\delta|^{|B|-1}) \quad (i \in B;\ \delta \to 0+),$$

$$\omega_j^{(2)}(\widetilde{F}_B;\delta) \ge C(\omega^{(2)}(\delta)|\ln\delta|^{|B|-1}) \quad (j \in M \setminus B;\ \delta \to 0+)$$

$$C = \text{const}.$$

Tbilisi I. Javakhishvili State University

REFERENCES

1. *L.V. Zhizhiashvili.* Some Problems of the Theory of Trigonometric Fourier Series and their Conjugates. Tbilisi, 1993 (Russian).
2. *I.E.Zhak.* DAN SSSR, **97**, 3, 1954, 387-389 (Russian).
3. *M.M.Lekishvili.* Bull. AN GSSR, **94**, 1, 1979 (Russian).

საქართველოს მეცნიერებათა აკადემიის მოამბე, 159, №3, 1999
BULLETIN OF THE GEORGIAN ACADEMY OF SCIENCES, 159, №3, 1999

MATHEMATICS

D.Kighuradze

On Product of Separable Metric Spaces

Presented by Corr. Member of the Academy N.Berikashvili, June 15, 1998

ABSTRACT. **In this paper some properties of the dimension function dim on the class of separable metric spaces are studied by means of geometric construction which may be realized in Euclidean spaces.**

Key words: Irrational compactum, stable intersection of maps, essential maps, dimension of the product.

We denote: by R^n - n dimensional Euclidean space, by Q^k - k-dimensional cube, by dim and μdim - covering and metric dimension functions, by $\bar{X}$ - the closure of X into R^n and by ∂X - the boundary X in R^n.

A map $f: X \to Q^n$ of a space X into the closed n-cube Q^n is said to be essential if there is no map $g: X \to \partial Q^n$ with the property that $g|_{f^{-1}(\partial Q^n)} = f|_{f^{-1}(\partial Q^n)}$.

Next, a point $x \in \text{int}Q^n$ is called a stable value of a surjective map, if there exists $\varepsilon > 0$ such that for every map $g: X \to Q^n$ such that $\rho(f, g) < \varepsilon$, it follows that $x \in g(X)$ [1]. Clearly, if $f: X \to Q^n$ is an essential map, then every point $x \in \text{int}Q^n$ is a stable value of f. Conversely, if some point $x \in Q^n$ is a stable value of an onto map $f: X \to Q^n$ then there exists a small n-ball $C^n \subset \text{int}Q^n$ such that $x \in \text{int}C^n$ and $f|_{f^{-1}(C^n)} f^{-1}(C^n) \to C^n$ is essential.

A pair of maps $f: X \to R^n$ and $g: X \to Q^n$ of metric spaces X and Y into the Euclidean n-space is said to have a stable intersection if there exists $\varepsilon > 0$ such that for any other pair of maps $f': X \to R^n$ and $g': Y \to R^n$, satistfying the conditions that $\rho(f, f') < \varepsilon$ and $\rho(g, g') < \varepsilon$, it follows that $f'(X) \cap g'(Y) \neq \varnothing$ [2].

For every point $x \in R^n$ let $r(x)$ be the number of rational coordinates of x. For every subset $X \subset R^n$ let $r(X) = \max\{r(x) | x \in X\}$. A subspace $X \subset R^n$, is said to be irrational, if $r(X) = \dim X$.

Theorem 1. *Let $X \subset R^n$, $\dim X = \dim \bar{X} = k$ $(k \leq n)$ and be an irrational compact. Then there exists a k-dimensional plane $L \subset R^n$ and a closed k-dimensional cube $Q^k \subset L$, such that $P|_{(p^{-1}(Q^k) \cap X)}: P^{-1}(Q^k) \cap X \to Q^k$ is an essential map, where $P: R^n \to L$ is the orthogonal projection of R^n onto L.*

Theorem 2. *For every pair of separable metric spaces X and Y, where $\dim X = n$, $\dim Y = m$, we have $\dim(X \times Y) = n + m$, if and only if, when there exist essential maps $f: X \to Q^n$ and $g: Y \to Q^n$, so that $f \times g: X \times Y \to Q^{n+m}$* is essential too.

Theorem 3. *For every pair of separable metric spaces X and Y, where $\dim X = n$, $\dim Y = m$, and $\dim(X \times Y) = n + m$, there exists a pair of maps $f: X \to R^{n+m}$ and*

$g : Y \to R^{n+m}$ *with stable intersection.*

Note: I proved the so-called "irrational compact" theorem in 1990 and based on this theorem, A.N.Dranishnikov, D.Repovs and E.V.Scepin show [2], that if compacts X and Y satisfy condition $\dim(X \times Y) = \dim(X \times Y)$, then there exists a pair of maps $f : X \to R^n$ and $g : Y \to R^n$ with stable intersection, where $n = \dim X + \dim Y$.

Theorem 1 generalizes the "irrational compact" theorem in the class of separable metric spaces. Theorem 3 also generalizes A.N.Dranishnikov, D.Repovs and E.V.Scepin above mentioned statement in the class of separable metric spaces.

This work is made possible by the Grant from the Georgian Academy of Sciences.

Tbilisi I.Javakhishvili State University

REFERENCES

1. *P.S.Aleksandrov, B.A.Pasynkov.* Introduction to Dimension Theory. M., 1973 (Russian).
2. *A.N.Dranishnikov, D.Repovs, E.V.Scepin.* Topology and its Applications. **38** , 1991, 237-253.

საქართველოს მეცნიერებათა აკადემიის მოამბე, 159, №3, 1999
BULLETIN OF THE GEORGIAN ACADEMY OF SCIENCES, 159, №3, 1999

PHYSICS

N. Kekelidze, V. Gogiashvili, Z. Kvinikadze, Z. Davitaya, L. Milovanova, G. Chikhradze, Z. Chubinishvili

The Optical Absorption Processes in the Infrared Region and the Determination of the Impurity Concentration in n-Type Gallium Arsenide

Presented by Corr. Member of the Academy T. Sanadze, January 29, 1998

ABSTRACT. **In the present work the method of determination of electrically active impurity concentration in n-type gallium arsenide is given. The method is based on the investigation of free carrier absorption processes in the infrared region. The corresponding practical recommendations are worked out on the basis of the obtained results.**

Key words: semiconductor, concentration, absorption coefficient, compensation ratio.

The determination of the impurity concentration is one of the main problems in the investigation of electrophysical properties of semiconductor compounds involving GaAs, InP, Si and others, which are widely used in the production of photoelectrical structures. Therefore, for the solution of various scientific or technical problems connected with semiconductors it is necessary to know the impurity concentration in them with high precision.

Proceeding from the theoretical and experimental data one of the best methods of the determination of impurity concentration is the research of electrophysical properties of semiconductor materials [1-5]. Among them the most practically convenient methods are the analysis of free carrier mobility and the method based on the investigation of optical absorption processes in the infrared region [5,6].

As for the infrared absorption caused by intraband transitions, it is observed only if there are defects in the crystal. Therefore the infrared absorption is closely connected with scattering mechanisms in transfer processes. Here the absorption theory does not involve the relaxation time [6] and, besides that, the total absorption coefficient may be represented as a sum of absorption coefficients, defined by separate kinds of defects. It enables one to determine the impurity concentration from absorption coefficient measurements if the free carrier concentration in the crystal is known. The quantum-mechanical theory of infrared absorption for III-V semiconductors has been worked out by Haga and Kimura in the case, when the thermal lattice vibrations and impurity ions play the main role in the scattering processes [2,6]. These authors obtained the analytical form of absorption coefficient dependence for the separate mechanisms on particle concentration, impurity atom number, temperature and, essentially, the dependence on the wavelength of the light, incident onto the crystal.

Therefore the investigation of infrared absorption processes along with the analysis of the Hall effect and the electron mobility may be considered as one of the best and practi-

cally easily realizable methods of determination of impurity concentration in semiconductors.

As has been mentioned above, the correction of the results obtained from the study of electrical properties may be verified by investigation of the free carrier absorption processes in infrared region. As also noted above, the total absorption coefficient is represented as a sum of absorption coefficients caused by separate kinds of defects:

$$\alpha_t = \alpha_{op} + \alpha_{ac} + \alpha_{imp},$$

where α_{op}, α_{ac} and α_{imp} are the absorption coefficients corresponding to the electron interactions with optical phonons, acoustic phonons and impurity ions, respectively. Using the computer, these coefficients have been calculated for room temperature at a wavelength of 10 μm for GaAs with electron concentration within $(10^{16} - 10^{18})$cm^{-3}. The results are represented in Table 1, which makes it possible to determine the compensation ratio in GaAs crystals by measuring the electron concentration and the absorption coefficient and to compare the values of the compensation ratios with those, obtained from the experimental values of electron mobility and electron concentration similar to Table III from [5]. For GaAs samples given in this table the compensation ratios have also been computed on the

Table 1

The theoretical values of the ir absorption coefficient at a wavelength of 10 μm and at room temperature in GaAs

$n \setminus \theta$	0.0	0.1	0.2	0.3	0.4	0.5	0.6	0.7	0.8	0.9
1x10^{16}	0.3696	0.3704	0.3714	0.3727	0.3724	0.3768	0.3804	0.3864	0.3984	0.4344
1.5	0.5560	0.5578	0.5600	0.5629	0.5667	0.5720	0.5800	0.5933	0.6200	0.7000
2	0.7432	0.7464	0.7503	0.7544	0.7621	0.7716	0.7858	0.8269	0.8568	0.9988
3	1.2070	1.2141	1.2230	1.2344	1.2497	1.2710	1.3030	1.3563	1.4630	1.7830
4	1.5060	1.5184	1.5340	1.5539	1.5807	1.6180	1.6740	1.7673	1.9540	2.5140
5	1.8930	1.9123	1.9365	1.9675	2.0090	2.0670	2.1540	2.2990	2.5890	3.4590
6	2.2770	2.3048	2.3395	2.3842	2.4437	2.5270	2.6520	2.8603	3.2770	4.5270
7	2.6670	2.7046	2.7516	2.8119	2.8923	3.0050	3.2820	3.6087	4.0190	5.7090
8	3.0730	3.1219	3.1830	3.2616	3.3663	3.5130	3.7330	4.0997	4.8330	7.0330
9	3.4760	3.5376	3.6146	3.7135	3.7287	4.0300	4.3070	4.8610	5.2420	8.4620
1x10^{17}	3.8750	3.9506	4.0451	4.1665	4.3283	4.5550	4.8950	5.4617	6.5930	9.9950
1.5	5.9730	6.1388	6.3460	6.6125	6.9677	7.4650	8.2110	9.4543	11.941	19.401
2	8.4360	8.4477	8.8060	9.2668	9.8810	10.747	12.031	14.181	18.481	31.381
3	12.846	13.466	14.241	15.237	16.566	18.426	21.216	25.866	35.166	63.066
4	18.000	19.071	20.410	22.131	24.427	27.640	32.440	40.493	56.560	104.76
5	28.400	25.013	27.030	29.623	33.080	37.920	44.560	57.280	81.480	154.08
6	29.380	31.647	34.481	38.123	42.980	49.780	59.980	76.980	110.98	212.98
7	35.590	38.590	42.340	47.161	53.590	62.590	76.090	98.590	143.59	278.59
8	42.220	46.042	50.820	56.963	65.153	76.620	93.820	122.49	179.82	351.82
9	49.250	53.983	59.900	67.507	77.650	97.850	113.15	148.65	219.65	432.65
1x10^{18}	56.700	62.433	78.814	78.814	91.100	108.30	134.10	177.10	263.10	521.10
1.5	98.750	110.62	125.45	144.53	169.95	205.55	258.95	347.95	525.95	1060.0
2	148.50	168.24	192.91	224.64	266.91	326.11	414.91	562.91	858.91	1746.9
3	266.20	305.76	355.20	418.77	503.53	622.20	800.20	1096.9	1690.2	3470.2
4	399.50	462.61	541.50	642.93	778.17	967.50	1251.2	1724.8	2671.5	5511.5
5	542.80	631.69	742.80	885.66	1076.1	1342.8	1742.8	2409.5	3742.8	7742.8

basis of our theoretical calculations and then have been compared with the results of [5] (Table 2).

The analysis of Table 2 confirms the validity of our calculations, because the numerical values of compensation ratio are in good agreement with the results of [5] (except sample 10).

Proceeding from the above, another significant conclusion can be made. Since the values of compensation ratios, obtained from the optical and electrical measurements agree closely with each other, one can determine theoretically the electron mobility by means of the experimental values of absorption coefficient and the electron concentration (but not from the Hall effect), using Table 1 or Fig.1 of [7].

Table 2

N	n. cm^{-3} [5]	$u_{exp.}$ cm^2/Vs [5]	θ Hall [5]	θ absorpt. [5]	α_{exp} cm^{-1} [5]	θ Hall fig. N1 our	α_t = cm^{-1} table N2 our
1	$3.00x10^{16}$	$2.70x10^3$	0.83	0.89	1.51	0.89	1.75
2	$1.10x10^{17}$	$1.80x10^3$	0.83	0.85	8.32	0.85	8.3
3	$5.50x10^{17}$	$3.30x10^3$	0.25	0.23	30.8	0.3	33.87
4	$8.50x10^{17}$	$1.35x10^3$	0.67	0.65	128	0.7	135.6
5	$1.50x10^{18}$	$8.00x10^2$	0.76	0.77	438.2	0.75	437
6	$2.00x10^{18}$	$2.10x10^3$	0.37	0.29	234.3	0.35	245.8
7	$2.60x10^{18}$	$1.65x10^3$	0.4	0.3	326.5	0.3	322
8	$6.00x10^{17}$	$3.60x10^3$	0.18	0.18	29.5	0.2	34.5
9	$1.15x10^{18}$	$2.60x10^3$	0.31	0.25	92.6	0.35	85
10	$1.20x10^{18}$	$3.10x10^3$	0.22	0.22	82.34	0.2	97.5

On the other hand, if the electron concentration (from the Hall effect) and the experimental value of mobility are known, the value of absorption coefficient may also be defined theoretically from corresponding Tables 1 [7] and 1 (present work).

Therefore, on the basis of our study a simple practical method of determination of impurity concentration in gallium arsenide crystals has been developed. It is also shown, that for definition of electrophysical parameters of semiconductors it is sufficient to carry out only electrical or optical investigations. The data of one kind of experiments are enough for determining some parameters of the second kind: electrical-optical and optical-electrical.

Table 1 computed by us is published for the first time.

The investigation has been carried out in the framework of the State Target Programs of the Department of Science and Technology of Georgia.

Tbilisi I. Javakhishvili State University

REFERENCES

1. *D.J. Andrianov et al.* Zavodskaya laboratoria, 7, 1972, 818.
2. *E. Haga, H. Kimura.* J. Phys. Soc. Japan, **19**, 1964, 658.
3. *H. Ehrenreich.* Phys.Rev., 120, 1960, 1951.
4. *V.A. Gogiashvili, N.P. Kekelidze et al.* Collective works of TSU, **135**, 1970, 135.
5. *W.Walukiewicz, L.Lagowski, L.Jastrzebski, M.Lichtensteiger, C.Gatos.* J. Appl. Phys., **50**(2), 1979, 899.
6. *E.Haga, H.Kimura.* J. Phys. Soc. Japan, **18**, 1963, 777.
7. *N.P.Kekelidze, V.A. Gogiashvili et al.* Bull. Georg. Acad. Sci. 159, 1, 1999, 45-48.

საქართველოს მეცნიერებათა აკადემიის მოამბე, 159, №3, 1999
BULLETIN OF THE GEORGIAN ACADEMY OF SCIENCES, 159, №3, 1999

PHYSICS

M.Kaviladze, N.Gubadze, M.Kviriya, G.Natsvlishvili, E.Gamtsemlidze

K-Capcher of ^{41}Ca and δ^{41}K as the Possible Cosmochronometer

Presented by Member of the Academy R.Salukvadze, March 30, 1998

ABSTRACT. **Potassium isotopic determinations was carried out using the Mattauch-Herzog-type mass spectrometer with laser-ion source in which a renium double-filament source is also placed. As a detector, a micro-channeled plate is used. The investigation shows that in the 55 microvolumes of three stony metheorites (Saratov, Orlovka, Elenovka), significant variations of the isotopic ratio $^{41}K/^{39}K$ exceeding 1% are not observed.**

Key words: isotopic analysis, cosmochronometer, nuclear astrophysics, lazer ion source, potassium isotopes ratio.

Radioactive nuclei together with the stable ones are created in the process of nucleosynthesis (the chain of nuclear reactions directed towards the increase of heavy nuclei concentration in the galaxy). Therefore, they might be used as the cosmochronometers for the galactic processes.

Nucleosynthesis has been almost finished in the space around the solar system by the time of its creation. Considering that with the creation of galaxy started the process of nucleosynthesis, it can by written as:

$$\theta_G = \Delta + \theta_s,$$

where θ_G is the age of galaxy; Δ is the length of nucleosynthesis; θ_S is the age of the solar system.

If we denote with the $a_A(t)$ the rate of creation of the A-mass nuclei in the process of nucleosynthesis (the number of nuclei in the unit of time), then the change of the number of these nuclei N_A may be described with the following equation:

$$\frac{dNa(t)}{dt} = a_A(t) - \lambda_A N_A, \tag{1}$$

where λ is the rate of the radioactive disintegration of the given A nuclei, and t is changing from $t = 0$ (the beginning of nucleosynthesis) to $t = \Delta$. The integration of the equation (1) gives us:

$$N_A(t) = \exp(-\lambda_A t)\int_0 a_A(t)\exp(\lambda_A t)dt\,. \tag{2}$$

The function $a(t)$ determines the chosen model.

The determination of the galaxy and solar system age occurs on the basis of the quantitative determination of the radioactive isotopes ^{238}U, ^{235}U, ^{232}Th, ^{146}Sm, ^{87}Rb and their

radiogenic nuclei. At the same time the new age concerning the solar system creation appeared in cosmochronology, namely, a period from the pro-tosun substance coming out of the nucleosynthesis zone, to the formation of the first hard substance and soon the planets consequently. The mentioned period of time - τ is known in the literature as "the creation interval". To determine the time τ are used the radionuclides, the half-life period of which is in the 10^5-10^7 years range.

The mentioned radionuclides were "alive" at the initial stage of the solar system, but nowadays, being "degenerated" - already disintegrated, they appear as radioactive "clock", which is rather sensitive for the estimation of the periods of time between the great phenomena. Such already "degenerated" isotopes are: 1) ^{129}I (T = 17 mln. years); 2) ^{244}Pu (T = 82 mln. years); 3) ^{107}Pd (T = 6.5mln.years); 4) ^{26}Al (T = 0.71 mln.years), etc.

At the initial stage of the development of methods especially wide-spread were ^{129}I and ^{244}Pu, because as a result of the β^--disintegration for ^{129}I

$$^{129}I \Rightarrow {}^{129}Xe + \beta^- + \bar{\nu}_e$$

so for spontaneous fission of ^{244}Pu

$$^{244}_{94}Pu \Rightarrow {}^{136}_{54}Xe + {}_{40}Zr$$

Xe, was obtained which is an inert gas and its isolation from the meteorite is comparatively easy (by heating in vacuum).

The main-point of the method is the following: in the protoplanet substance as a result of the crystallization of I and Pu containing minerals, the process of accumulation of the radiogenic Xe is starting inside them. Nowadays the quantity of the radiogenic ^{129}Xe and ^{126}Xe in the mineral consequently equals the amount of ^{129}I and ^{244}Pu at the moment of its crystallization. Thus, ^{129}I/^{127}I = ^{129}Xe/^{127}I. For the ratio ^{129}I/ ^{127}I J.Reinolds obtained 10^{-4}, to disintegrate such amount to atoms ^{129}I would need approximately $\tau = 200 \times 10^6$ years. The mentioned result was obtained by Reinolds for Richardson meteorite. Afterwards the same results were obtained for other meteorites by the other authors. It means the result is global for the solar system. Approximately the same result for 200mln. years is obtained by Pu cosmochronometer.

The serious difficulties for the model were caused further by the new cosmochronometer.

$$^{26}Al \Rightarrow {}^{26}Mg + \beta^+ + \nu_e$$

for $T = 0.7 \times 10^6$ years.

In the Al minerals there was found excess of the ^{24}Mg atoms. Indeed, if in the protosun fogginess we deal with the "alive" ^{26}Al, it means that from the stopping of the nucleosynthesis to the formation of the hard particles in the protosun system only several million years passed. In this case the amount of ^{129}Xe and ^{136}Xe must be much bigger, than the experiment shows. In other words, if the formation interval is big enough (~200 million years), then by the moment when the particles are formed there must not exist the "alive" ^{26}Al, which was created at the moment when the supernew exploded.

In the 1980s for determination the creation interval D. Kleiton used ^{41}K/^{39}K ratio and he was the first, who found the excess of ^{41}K in the meteorites, which he referred to ^{41}Ca radionuclides.

Therefore, if in the meteorites $\delta^{41}K>0$, it means, that it is formed from the extinct ^{41}Ca and it makes possible to estimate the interval of creation.

The mentioned process was counted as a perspective one by D.Kleiton as in this case the necessary for the method condition, that the amount of Ca must be much bigger than that for K (Ca>>K), is very well accomplished.

And actually Ca and K have sharply different hardness temperatures. Therefore, in the cooling process of the hot substance of the protosun system at first the minerals of Ca, having high temperature are formed and only then begins the condensation of K minerals and thus happens their separation into fractions. Ca is accumulated in the first condensate of substance and K-In the low temperature having phases much later.

In the first condensates to the account of the Ca disintigration would be formed radiogenic ^{41}K which increases the $^{41}K/^{39}K$ ratio in comparison with the cosmic one, which gives the possibility to measure the creation interval. In literature nowadays, in spite of D.Kleiton's big authority, there is not quite definite attitude towards the radiogenic ^{41}K.

Some authors consider that Its amount Is really accumulated, in the high temperature having substance but there are also very serious experimental data of the opposite character. Therefore, it was necessary to carry out such measurements, which would more authentically show if abundance of radiogenic ^{41}K atoms are really formed in meteorite from ^{41}Ca.

Our method [2,3] has got especially considerable actuality exactly for such measurements. We have carried out the number of measurements of meteorite substance on the fragmentation level of 10^{-3} gr [3]. Lately we have created the new method [4] and carried out the measurements of the meteorite substance on the fragmentation level of 10^{-7}-10^{-8}gr.

The measurements showed that even in the case of such high sensitivity with 1% preciseness in solar system the $^{41}K/^{39}K$ ratio in minerals of 3 meteorites (Saratov, Orlovka, Elenovka) is homogeneous. On the basis of our data we consider that at the moment of the Earth and meteorites formation "alive" ^{41}Ca globally did not exist. If there is $\delta^{41}K>0$ in the minerals having high temperature then other reasons are necessary to be suggested.

Obviously, to make the problem more clear, in future it will be necessary to increase statistics as by increasing the meteorite collection, or the number of mineral microvolumes (our method [4] makes it easy).

Tbilisi I. Javakhishvili State University

REFERENCES

1. *D.D.Cleyton.* Astrophys.J. 199, 1975, 765-769.
2. *M.Sh.Kaviladze, T.A.Melashvili.* Avt. svid. S71170, po zayavke N2112318 s prioritetom of 10 marta 1975, (Russian).
3. *M.Sh.Kaviladze, T.A.Melashvili, M.V.Kviriya.* Exp.Tech. USSR, 20, 1977, 512. Translated from Prib. Tekh. Eksp., N2, 1977,166.
4. *M.Sh.Kaviladze, N.V.Gubadze.* International Journal of Mass-Spectrometry and Ion Process, 161, 1997, 87-89.

საქართველოს მეცნიერებათა აკადემიის მოამბე, 159, №3, 1999
BULLETIN OF THE GEORGIAN ACADEMY OF SCIENCES, 159, №3, 1999

PHYSICS

S. Gotoshia

Lazer Raman Spectroscopy Study of Vibrational Dynamics of GaP Crystal Lattice Modified by Boron and Argon Ion Implantation

Presented by Member of the Academy N. Amaglobeli, June 26, 1998

ABSTRACT. **Crystalline GaP surfaces modified by boron and argon ion implantation have been studied by lazer Raman spectroscopy. It has been established that change of full width at half maximum of LO phonon is related with defect-induced stress in the GaP crystal lattice. We have determined amorphization crytical doses for 110keV boron and argon ions by Raman scattering.**

Key words: lazer Raman spectroscopy, ion implantation, full width at half maximum of LO phonon, crytical dose of amorphization.

In the process of ion implantation in a crystal lattice radiation defects are formed, concentration of which increases with radiation dose. After a certain critical dose the crystal transforms in an amorphous state. Crystals with more expressed covalent bond suffer amorphization more easily. The aim of the work is to study the structure change caused by argon and boron ion implantation in GaP with the lazer Raman spectroscopy.

As it is known there is the near as well as the far order in crystals and in the first order Raman scattering (RS) Brillouin zone central phonons $K \approx 0$ participate. The crystal RS spectrum represents a narrow band of spectral lines. Because of nonexistence of the far order in amorphous semiconductors selection rules are broken and therefore interaction of emission with crystal nonactive modes is possible. Thus, all vibrations in amorphous phase become active. But this leads to erasing of RS spectra structure.

We took monocrystal plates of GaP of one mm thickness, electron concentration being $n=5\text{x}10^{17}$ cm^{-3}. The both surfaces of the plates were polished optically and (111) oriented. The degree of polishing was monitored with RS spectrum recording and we chose the samples for which spectral bond half widths at the intensity maximum at LO and TO phonon frequences were no more than $\Delta\nu_{LO} = 5\text{cm}^{-1}$ and $\Delta\nu_{TO} = 6.5\text{cm}^{-1}$ respectively. We covered all halves of the polished samples' surfaces with foils and placed such plates fixed in the aluminum disks in the implantator High Voltage Europa vacuum chamber, where their implantation occured with 110keV boron and argon ions the doses being in the range of 10^{12}-10^{16} ion/cm^2. In all cases we tried the accelerator current to be minimal to avoid the samples' recrystallization through annealing. The current did not exceed 0.05mka/cm^2. After implantation the plates' halves were departed from the foil and they served as etalons for Raman spectra recording. Raman spectra were recorded on home Raman spectrometer. We used argon lazer wavelengths 5145, 4579A and He-Cd lazer wavelength 4416A for excitation of samples for Raman spectra recording. The exciting light angle of incidence was strictly fixed and its value almost always corresponded to Bruster angle.

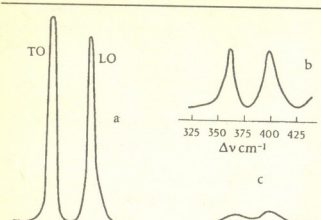

Fig.1 Raman-spectra of standard GaP with (111) orientation (a) and GaP implanted by 110keV argon ions with dose $9x10^{12}$ ion/cm^2 (b) and $3x10^{13}$ ion/cm^2 (c).

GaP is of cubic symmetry. At lazer excitation of (111) surface LO phonon as well as TO phonon appears in RS according to the selection rules. LO=402cm^{-1}, TO=366cm^{-1} in the spectrum of GaP recorded by us.

Fig.1 represents RS spectra for standard GaP as well as for GaP implanted by 110keV argon ion with doses $9x10^{12}$ and $3x10^{13}$ ion/cm^2. According to the spectra intensities of sharp LO and TO spectral bands for crystalline GaP strictly decrease after implantation with rather less doses; as for their half widths, they broaden with dose. Besides, spectral peak shifting to the low frequences takes place within 2.5cm^{-1}. Further increase of dose causes such broadening of LO and TO phonon halfwidths that after joining they give a wide band without structure. The above mentioned spectra have been recorded by argon laser emission l_L=4579A.

Fig. 2 shows the dependence of LO phonon spectral band half width upon argon and boron ion implantation dose. Little shift of spectral band, intensity decrease and halfwidth broadening in a semiconductor may be caused by increasing of free electron number when longitudinal electric field caused by electron plasma vibration interacts with LO phonon (by the way owing to this effect Raman spectroscopy gives an opportunity of noncontact determination free electron concentration in a semiconductor) and instead of LO phonon peak we have spectral band of plasmon-LO phonon interaction; besides, semiconductor disordering and mechanic strains cause change in spectral band shape, intensity and energy. As argon ion implantation does not cause electron enrichment of GaP, Raman-spectra in Fig.1 and the dependence for argon ions in Fig. 2 show that crystalline GaP lattice gradually transfers into disordered state and internal stress increases with implantation dose.

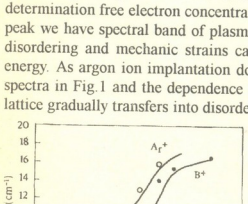

Fig.2. Dependence of full width on half maximum of LO phonon of GaP upon argon and boron ion implantation dose.

In the case of boron ion implantation we have annealed the implanted samples isochronically at 400, 500, 600, 700, 800, 900 ^{0}C during one hour. Before annealing all the samples were covered with protecting SiO_2 and annealing proceeded in argon gas flow. After each annealing stage the sample was installed in Raman spectrometer and Raman spectrum of He-Cd laser excitation l_L=4416A was recorded. Raman spectrum showed that D=$1x10^{15}$ ion/cm^2, 110kev boron ion implanted GaP at 700^{0}C annealing during one hour transfered from disordered into crystal state. It should be noted that electron

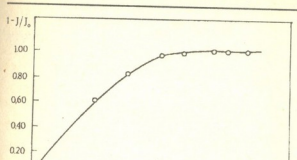

Fig. 3. Normalized intensity of Raman scattering versus dose of argon ions in GaP.

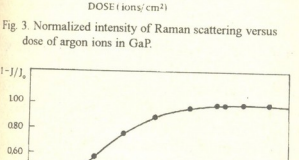

Fig. 4. Normalized intensity of Raman scattering versus dose of boron ions in GaP.

number in GaP did not increase at boron ion implantation as Raman spectrum of annealed sample was characterized by the same halfwidth of spectral band as that of the standard GaP. Thus there is no LO phonon-plasmon interaction due to boron implantation and as in the case of argon spectral band halfwidth broadening is caused by defects produced during implantation, by crystal lattice disorder and by mechanical stresses rather than by activation of boron as impurity. With further increase of implantation dose disorder of crystal lattice achieves the critical threshold and GaP crystal fully transfers into amorphous state. To determine the critical dose of amorphization we have drawn the dependence of dose upon RS normalized intensity:

$$I_n = 1 - I/I_0,$$

where I_0 is RS intensity of standard GaP, and I is RS intensity of different dose doped GaP. Figures 3 and 4 show these dependences in the case of Ga:B and GaP:Ar. When the curve goes to the saturation state, we suggest the dose critical for amorphization [1]. Critical dose of amorphization defined by the above method is $8x10^{13}$ ion/cm^2 for argon ion and $6x10^{14}$ ion/cm^2 in the boron ion case. The energy of either ion is 110keV. Probably GaP crystalline lattice transformation into amorphous state occurs at lower doses of implantation with Ar^+ heavy ions than with (B^+) light ions. We would like to notice that amorphization crytical dose by RS first was defined for silicon [1] and diamond [2]; as for A^3B^5 semiconductors especially GaP and GaAs, evaluation of crytical dose of amorphization due to ion implantation by Raman spectroscopy has been done by us [3].

Thus lazer Raman spectroscopy turns to be a very useful and informative method for diagnozes of physico-chemical properties of semiconductors modified by ion implantation.

Georgian Academy of Sciences
R. Agladze Institute of Inorganic Chemistry
and Electrochemistry

REFERENCES

1. *J. F. Morhange, R. Beserman, M. Balkanski.* Phys. Stat. sol. (a) **23**, 1974, 383.
2. *J. F. Morhange, R. Beserman, J. C. Bourgoin.* Jap. J. Appl. Phys. **14,** 1975, 544.
3. *V. S. Vavilov, L. K. Vodopianov, S. V. Gotoshia.* International Conf. on Ion Implantation in Semiconductors. Reinhardsbrum, (GDR), 37, 1977.

საქართველოს მეცნიერებათა აკადემიის მოამბე, 159, №3, 1999
BULLETIN OF THE GEORGIAN ACADEMY OF SCIENCES, 159, №3, 1999

PHYSICS

L. Mosulishvili, N. Shonia, V. Dundua

Analytical Parameters of X-ray Fluorescence and Neutron Activation Analysis Methods for Determination of Gold Content in Ores and Concentrates

Presented by Member of theAcademy G. Kharadze, April 27, 1998

ABSTRACT. **Among the physical methods of determination of gold content, X ray fluorescence (XFA) and neutron activation analysis (NAA) methods are of particular importance. These two methods make it possible to carry out gold analysis without chemical or mechanical treatment and decomposition of the samples under investigation. On the basis of evaluation of the advantages and disadvantages of these methods, we conclude that with their combined application the analytical possibilities of gold content determination should be increased significantly.**

Key words: X-ray fluorescence; neutron activation.

Materials and Procedures. The XFA method was developed using a ^{109}Cd isotopic source. Two sources each having an activity of $2 \cdot 10^8$ Bq were used. The detection of X-rays was carried out by means of a Si(Li) semiconductor detector with a resolution of 300 eV for 5.9 keV energy. The width of Be-window was 100 μm. Spectrometry of X-lines was carried out by means of a 1024 channel analyzer and computer programs.

The NAA method is based on ^{197}Au (n,γ) ^{198}Au nuclear reaction, that proceeds with a high probability at thermal neutron irradiation (activation cross-section 98 barn). In the present work as a source of thermal neutrons the subcritical assembly of SA-1 type is used piled up by powder of uranium dioxide enriched with ^{235}U isotope dispersed in polyethylene plates as described in [1]. The system provides stable fluxes of thermal neutrons of the order of 10^7 neutron/cm^{2}s. Below we describe high-selectivity method of gold determination developed using fluxes of thermal neutrons of such intensity.

The samples under study and that of a standard containing gold were of tablet form and of the same geometrical shape. The diameter of the samples is 20 mm with a thickness of 2 mm. The standard tablets containing gold are made on the basis of phenolformaldehyde resin according to the technology described in [2]. In standard tablets of this type the gold content is changed discretely in the range of $2 \cdot 10^{-4}$ - $2 \cdot 10^{-1}$ %. In total, gold containing standard tablets of 12 different concentrations were made.

XFA-method of gold determination. The average values of K_α and K_β line energies of the ^{109}Cd source are 23.07 and 26.45 keV, respectively, as presented in IAEA-Tecdoc-619 [3]. At these energies in gold atoms the exitation of only L_α, L_β and L_γ -lines of the L-series is possible with an average value of 9.668; 11.483; 13.380 keV, respectively. On the spectrograms in Figure 1 the photopeaks corresponding to these lines are clearly

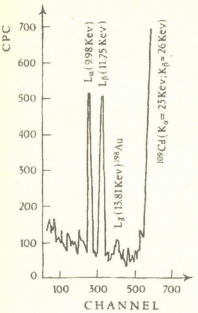

Fig. 1. X-ray fluorescent spectrum of gold. The content of gold in the target is 100 ppm.

observed. L_α and L_β lines are well resolved and are also rather intense and thus these two lines are of equal analytical significance. The intensity of the L_γ line is low, therefore its use for analysis is limited. The sensitivity in the given regime is 5 μg, while the precision varies in the 5-25 % interval. The exposure duration on the detector of sample sources for gold content determination by this method is of the order of 100-600 s. Actually this is a rapid method of gold analysis suitable for studying ores and concentrates containing gold and gold alloys. For illustration of our statement we present gold content determination in samples of quarzite type in Table.

We note that the precision of determination is reduced as the content of gold in the sample is reduced and thus the results of analysis for concentrations below 5 μg have only qualitatitive value. For low concentrations, a modified alternative instrumental version of the method of neutron activation analysis (INAA) was developed.

Table

Samlpe Code	Content of gold in ppm
331	20 ± 5
332	18 ± 6
333	6.5 ± 2.6
334	1.0 ± 0.7

INAA method of gold determination. By using the known equation of activation for gold analysis, we obtain, a simplified expression of the following form:

$$S = 3.029\ \varepsilon_\gamma \Phi_n M,$$

where S is the quantity of γ-quants with 411.8 keV energy; ε_γ is the efficiency of detection of irradiation of such energy for the given detector; M is the mass of gold in grams. The numerical coefficient is obtained for the case when the time of irradiation and delay is 1 hour and the duration of sample exposure on the detector is 1000 s. The absolute efficiency of the Ge(Li) detector used in the present work is 7 % and $\Phi_n = 10^7$ neutron/cm^{2}s. A radionuclide with the intensity of the order of 2 Bq is obtained by activation of 1 μg gold. After this estimation to ascertain the real value of the sensitivity of gold determination, it is necessary to estimate the effective value of background for the sample selected in 400-420 keV interval of the γ-spectrum. Consider the case when the detection of 411.8 keV energy photopeak is carried out against the background of ^{64}Cu, ^{69}Zn, ^{76}As and other radionuclide intensive radiation. At the same time the intensity of the 511 keV energy photopeak caused by ^{64}Cu nuclide is 2-3 orders of higher magnitude compared to that of the ^{198}Au 411.8 keV energy photopeak in the sample under investigation. This is shown

in Figure 2, where the gold peak is clearly seen against the compton background induced by the high intensity of the ^{64}Cu isotope. In spite of this, the value of peak areas 600 ± 40 pulse corresponding to gold agrees well with the value of ^{198}Au photopeak of the same intensity equal to the 570 ± 20 pulse presented in B-fragment of the spectrum.

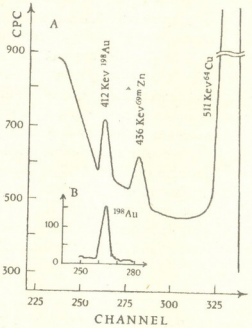

Fig. 2. Data illustrating the possibility of identification of gold 411.8 keV photopeak in multicomponent samples with high background.

Another very crucial point should be noted. The determination carried out by neutron methods is possible for samples of sufficiently high weight, on average 50-100 g,so the sensitivity of the method reaches 10^{-6} %. That is quite enough for carrying out analyses of both experimental and examination types.

Georgian Academy of Sciences
Institute of Physics

REFERENCES

1. *Yu.N.Burmistenko, V.A.Gurkov, R.T.Gambarion.* Radiatsionnaya Tekhnika, **11**, 1975, 206 (Russian).
2. *L.M.Mosulishvili, V.Yu.Dundua, N.E.Kharabadze et al.* J. Radioanalytical and Nuclear Chemistry, **83**, 1984, 13.
3. X-ray and gamma-ray standards for detection calibration, IAEA-TECDOC-619,1991, 86.

საქართველოს მეცნიერებათა აკადემიის მოამბე, 159, №3, 1999
BULLETIN OF THE GEORGIAN ACADEMY OF SCIENCES, 159, №3, 1999

PHYSICS

A. Gerasimov, A. Bibilashvili, Z. Bokhochadze, R. Kazarov, M. Vepkhvadze, G. Chiradze, N. Kutivadze, Z. Samadashvili

Influence of Photostimulated Diffusion-Motive Force on Impurity Redistribution

Presented by Member of the Academy R. Salukvadze, June 2, 1998

ABSTRACT. **On the example of photostimulated diffusion of Al in Si we have shown experimentally that the distribution of impurity atoms depends on the value and direction of diffusion forces arisen as a result of light influence upon the samples, what in its way is defined by volume distribution of the concentration of antibalancing free carriers.**

Key words: diffusion-motive force, photostimulated diffusion of impurity.

For the experiment we have used n-type silicon substrates Si (КЭФ) with orientation (100) that were implanted by phosphore ($N_d = 10^{15}$cm^{-3}). Before Al-deposition the substrates were cleaned with 14th class of purity [1]. The Al was deposed on one of the surfaces (Fig.1 at the left side) with the help of thermo-vacuum evaporation.

The experiment was accomplished by means of low-temperature photonic influence on the unit of impulsing photonic treatment (УИФО) [2]. Irradiation took place in two different modes: I – the sample was placed onto well-thermal conductivity layer in order to remove the heat; II – the sample was hung in the air (Fig.2). Irradiation is done with the light of the power $P_1 = 87$Wt/cm^2; $P_2 = 120$Wt/cm^2 from the side of the surface that wasn't covered with Al, from the right side (Fig.1). The duration of the impulse was changed from 1sec up to 10 sec. After the irradiation Al was etched.

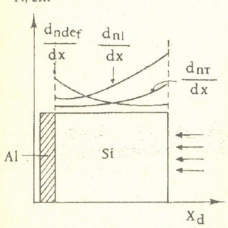

Fig.1. Distribution according to the depth of aquases formed in different ways in Si sample after the irradiation.

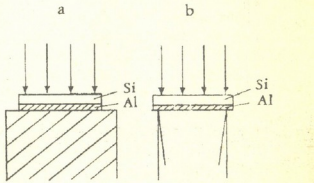

Fig.2. Schematic image of geometry of Al-coated Si-sample emanation. The sample is placed: a – onto special thermoconductor, b – without thermoconductor in the air.

Concentration of the impurity (Al) in the samples was measured using the methods of volt-faradic (C-V) and differential conductivity; (R_s surfacial resistance was measured by the method of 4 probes); depth of impurity diffusion was ascertained according to the location of p-n junction that was determined with the help of spherical lap. Estimating operation for diffusion coefficient was fulfilled using experimental profiles, with the assumption that impurity distribution is described by the law erfc [3] – ($N=N_s$erfc(-x/2√Dt), where N_s is the surfacial concentration, N – the initial concentration of impurities in the sample, t – the time of photonic influence, x – the depth of p-n junction).

Profiles of impurity concentration obtained after the irradiation in the 1st mode are shown in the Fig.3 from which we can see, that the more light intensity and impulse duration are, the more concentration of diffunded Al near the surface is, and the depth of impurity-penetration into Si is small, i.e. the diffusion coefficient (D), correspondingly, is less (Table 1).

Table 1

№	Irradiation power, P, Wt/cm^2	Irradiation time, t, sec	Coefficient of photostimulated diffusion of Al, D, cm^2/sec	Coefficient of Thermal Diffusion, $D(T)$, cm^2/sec	Temperature of sample, T, ^{0}C
1	87	1	$8{,}4\cdot10^{-9}$	$6\cdot10^{-59}$	37
2	87	6	$2.7\cdot10^{-10}$	$1.5\cdot10^{-33}$	255
3	87	10	$3.3\cdot10^{-11}$	$1.3\cdot10^{-26}$	380
4	122	1	$4.4\cdot10^{-10}$	$6.4\cdot10^{-46}$	120
5	122	6	$1\cdot10^{-11}$	$1.9\cdot10^{-15}$	780
6	122	10	$8\cdot10^{-11}$	$4.5\cdot10^{-13}$	780
7	122	50	$6.5\cdot10^{-11}$	$4.5\cdot10^{-13}$	780

In the 2nd mode, while the small, P_1 – intensity, the same picture is observed as for the irradiation in the 1st mode. During the P_2 – intensity D is also reduced by means of the impulse increase (Table 1), in spite of the fact that the profile of impurity-distribution is moved to right, to the depth of Si-sample (Fig.5).

From the obtained results we can see that, if the intensity and the impulse duration are increased (what causes the temperature heightening), D is reduced, e.g., in the same way, as it was in case of surfacial diffusion of the impurity [4], the temperature impedes photostimulated diffusion of the impurity in the volume. Besides that, as it is clear from the Fig.3, the smallest depth of Al penetration we have obtained in case of influence of 10-sec impulse. Because of it we can make a logical assumption that the inverse diffusion has happened (the border of p-n junction is moved to the surface), since during the influence of 10-sec impulse the sample had passed as 1-sec, also – 6-sec influence stages.

It's impossible to explain the obtained results using the existing mechanisms even qualitatively, instead they are explained well by the new conception [5], which informs us that transition of the atom in semiconductor is defined by the means of the change of its chemical connections, what may be accomplished not only by the temperature, but also – by the light and injection. For this purpose let's find out that diffusion-motive forces be-

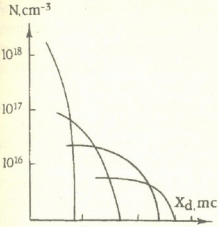

Fig. 3. Profiles of distribution in Si of impurity Al-atoms, after irradiation in the 1st mode by impulses of different parameters: 1) 1imp., t = 1sec., P = 57Wt/cm^2; 2) 1imp., t = 6sec., P = 57Wt/cm^2; 3) 1imp., t = 10sec., P = 57 Wt/cm^2; 4) 1imp., t = 1sec., P = 90 Wt/cm^2; 5) 1imp., t = 6sec., P = 90 Wt/cm^2.

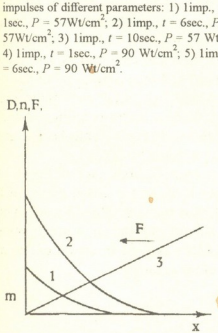

Fig.4. Schematic distribution of aquase concentration $n(1)$, diffusion coefficient $D(2)$ and diffusion-motive force $F(3)$ in accordance with the depth.

sides the concentration gradient (dN/dx) condition the diffusion of Al into Si in our experiments [6]. Concentration of anticonnecting quasiparticles (free electrons and holes – aquases) that arise in Si as a result of light absorption – isn't uniform in the direction of light spreading, and because of it the value of D is also non-uniform, as the dependence of D on n is the exponential function $D \sim n^{\alpha}$ [5]. The non-uniformity of D in the direction of diffusion causes diffusion-motive force that is directed to the high values of diffusion coefficient (Fig.4).

Let's consider the causes of rise of aquases and the distribution of their concentrations in Si sample. While irradiation in the 1st mode, because of light influence, the aquases arise in Si: 1) by temperature; 2) as a result of light absorption: a) with the energy of quants $h\nu > E_g$ on the surface of sample, and b) with the energy of quants $h\nu < E_g$ in the volume of sample on the defects.

1) In the first mode the concentration of aquases that are arisen by temperature – n_T – has a gradient because of the temperature gradient. Correspondingly, there arises the gradient of $D\, dD_T/dx$, what causes the diffusion-motive force, directed from left to right (Fig.1).

2) a) As a result of diffusion in the depth n_L of aquases created by absorption of quants with the energy $h\nu > E_g$ on the surface of sample arises their dn_L/dx, and, accordingly, the gradients of $D \cdot dD_L/dx$. Thus, there will appear the diffusion-motive force, directed from left to right also (Fig.1).

b) Aquases are arisen because of absorption of quants with the energy $h\nu < E_g$ on those defects that have energetic levels in band gap of semiconductor. Such levels have stechiometric defects [7] and defects arisen because of diffusion of Al atoms [8], and their quantity near the left surface is much greater, than in the other regions of crystal. We must mention separately that the increase of the value of D as a result of light absorption on the defects is caused not only by the increase of aquase concentration, but also – by ionization of defects containing Al atoms, e.g., removing one of those electrons that were accomplishing the connection between the atoms of defects. Because of it, in spite of the possibility of $n_{def} \leq n_L$, n_T in the given area of sample, for the reason of the above-mentioned event

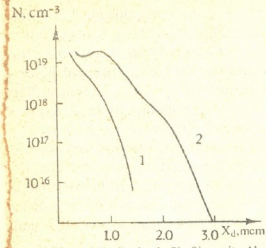

Fig.5. Profiles of distribution in Si of impurity Al-atoms, after irradiation in the 2nd mode by impulses of $P = 90$Wt/cm^2 power and of different duration: 1) 1imp., $t = 10$sec., 2) 5imp., $t = 10$sec.

$D_{def} \geq D_L$ and D_T. The diffusion-motive force caused by these aquases will have the direction from right to left, e.g., the opposite direction in comparison with the diffusion-motive force considered above (Fig.1 and Fig.4).

Thus, upon the atoms of Al four diffusion-motive forces are acting. One of them – the force directed from right to help, in the initial period is small, because of small quantity of defects, and the other three forces, directed to right, ensure the faster transition of impurity into the depth of Si plate, in comparison with the equivalent temperatural mode (Table 1). It's necessary to mention that the first force increases together with the increase of defect concentration, e.g., with the increase of impulse duration and intensity. Besides that, because of the increase of impulse duration the temperatural field in the sample becomes uniform, what means that the gradient of temperature is reduced and then disappears at last. The dn_i/dx is also reduced. Because of it the force directed from right to left puts up the greater and greater resistance to the forces directed from left to right, correspondingly there are reduced the depth of impurity penetration and the value of D (Fig.3, Table 1). The gradients of aquases n_L, n_T and n_{def} will be done in the next article.

During the irradiation in the 2nd mode the temperature is high, and $dT/dx = 0$. The uniform value of D in the whole sample is conditioned by n_i that is arisen thermally and because of dN/dx the travel of Al atoms is accomplished to right. The diffusion-motive force created by dD_L/dx is added to this stream, the stream with the opposite direction is created by dD_{def}/dx diffusion-motive force. So, the value and the direction of the total stream of Al atoms is determined by the correlation of these forces.

Tbilisi I. Javakhishvili State University

REFERENCES

1. Foundations of Technology of Si Integral Schemes. Oxidization, Diffusion, Epitaxy. Ed. by R.Burger and R.Donowan, M., 1969.
2. *M.A. Kuprava.* Candidate thesis, 1993.
3. *B.I. Boltax.* Diffusion in Semiconductors, M., 1961.
4. *T.E. Melkadze.* Candidate thesis, 1992.
5. *A.B. Gerasimov.* Proc. 4th Int. Conf. Materials Science Forum Vols. N.Y. 65-66, 1990, 47.
6. *G. Munning.* Kinetics of Atom Diffusion in Crystals, M., 1971;
7. *I.G. Gverdtsitely, A.B. Gerasimov et al.* Bull. Acad. Sci. GSSR, 127, 3, 1987.
8. *V.V. Emtsev, T.V. Mashovets.* Alloys and Point Defects in Semiconductors. M., 1981.

საქართველოს მეცნიერებათა აკადემიის მოამბე, 159, №3, 1999
BULLETIN OF THE GEORGIAN ACADEMY OF SCIENCES, 159, №3, 1999

GEOPHYSICS

Z. Khvedelidze, N. Ramishvili

The Nature of Changes of Meteorologic Values in the Earth Surface Layer of Atmosphere for Georgian Region

Presented by Member of the Academy B.Balavadze, November 30, 1998

ABSTRACT. **The results of our study show a great role of microrelief peculiarities in Earth surface layer in space time distribution of meteorological values.**

Key words: micro-circulation, atmosphere, flow, exposition, convection.

Republic of Georgia is a country with mountainous relief. Only 12.8% of its territory is situated on altitude of 200 m BSL but on altitude of 1000 m ASL is 53.8% of the territory. Besides the Greater and Lesser Caucasian range, Colchids and Kartli lowland zones, the territory of Georgia is crossed by numerous canyons, ranges and cavities which surface is of varied volume.

It is natural that such a complicated physico-geographical position causes the peculiarities of vertical changes of meteorological values. These peculiarities are specific of the earth surface layer which height is 50-100 m. The processes taking place in this layer mainly determine daily motion of air temperature, night frosts, heat and moisture balance, impurities distribution, turbulent flow, etc. Therefore, the study of peculiarities of atmosphere Earth surface layer for separate microregions is of great theoretical and practical significance.

First of all, let's take the determination of heat turbulent flow, because according to physical content earth surface is that layer of atmosphere in which turbulent flow

$$\vartheta_0 = -C_p \rho K \partial\theta/\partial z \qquad (1)$$

practically remains unchangeable according to the height. Here C_p is a specific heat capacity during constant pressure; ρ is air density; K is a turbulent coefficient; z is vertical coordinate; θ is potential temperature. If we use logarithmic law of temperature distribution [1-3] according to height in the mentioned layer the formula (1) can be expressed as

$$\vartheta_0 = -B_T(T_2 - T_1), \qquad (2)$$

where $B_T = C_p S$, α_T, C_3 is a coefficient of heat transfer; C_3 is wind velocity between Z_1 and Z_2 levels where T_1 and T_2 temperature is measured correspondingly on the height of Z_3; α is a heat exchange coefficient.

Our aim is to take into account the action of microrelief from exposition angle ψ. Suppose $Z = S\sin\psi$ and $K_0 = aS_0\sin\psi_0$. S is a distance along measured earth surface; a is constant. Similar to [2,4] for α_T we obtain the dependence:

$$\alpha = \frac{\chi^2}{\ln\dfrac{S_3\sin\psi_3 + S_0\sin\psi_0}{S_0\sin\psi_0} \cdot \ln\dfrac{S_2\sin\psi_2 + S_0\sin\psi_0}{S_1\sin\psi_1 + S_0\sin\psi_0}} \qquad (3)$$

Determination of α_T in such a way is obtained for the first time. Here χ is Carman's constant. From the formulae (2) and (3) it follows that θ_0 flow is proportional to temperature difference in the layer, wind velocity on Z_1 level and depends on relief exposition. The measurement of meteorologic values should be realized by gradient observations using standard equipments. For this the territory is divided into micro polygons (taking into consideration which polygon is studied), direction of dominant wind is determined and two meteorologic stations or two observation posts are chosen. Sacking values are measured on them in comparatively small interval of time (time - mean 10-20 sec.). As an example, let's regard Tbilisi polygon with the data from six meteorologic stations (Fig.1), which are dislocated at different height and different physico-geographical conditions. Between meteorologic stations the posts have been chosen on the route where gradient observations took place and the angle of relief exposition was measured (theoretically). At the same time many years (1980-1990) data of average values for winter and summer extremal months (January, July) from the stations (Fig.1) have been used. The average values of θ_0 were also calculated. From the analysis of corresponding calculations it is seen that vertical changes of meteorologic values in Earth surface layer for Tbilisi have complicated character. Changes marked up to $h < 50$ m height bear the character of qualitative law, then logarithmic law is valid, but above $h <$ 200 m have linear nature. Wind velocity makes turn at $h = 30$-40 m height (Fig.2). These results basically correspond with those known in literature [4-8].

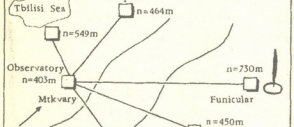

Fig.1

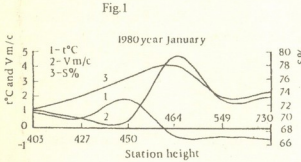

Fig.2

Peculiarities are observed in [4-8]; change of exposition angle strongly acts only in $h < 50$m height layer; temperature, moisture, wind velocity values on the height over 100-150 m in various districts of Tbilisi in summer months (July-August) remain constant (with 2% of error) but in winter the difference according to the place is observed. Such peculiarity is observed for the first time.

From the analysis of experimental materials [5,7] it appears that temperature contrast on the Earth surface layer might reach the heights more than several hundreds. In such case we deal with the formation of pressure gradient which cause small scale air flows [2]. These flows are called micro circulations or local winds

which make on wide scale synoptic forecast, i.e. strengthen horizontal and vertical change in Earth surface and boundary layer of heat flow and motive amount on weather and climate. Almost the whole territory of Georgia promotes the formation and development of the mentioned micro circulation processes.

Natural barriers create the so-called protective orographic waves [6]. Their existence is observed from the satellite pictures of cloudiness and also visually. The existence of orographic waves for the whole Caucasia and the possibilities of their parameters determination are proved in [6].

It is possible to determine the period of micro orographic waves, velocity, power etc. by choosing corresponding parameters (the lengths of waves along meridian and parallel) for different polygons of Georgia. For example, in Rioni canyon in cold period of year from November to May there was observed in average 75 stable waves of orographic (phionic) zones, with increasing wave velocity 20 m/sec and vertical power about 1.25-2 km.

Such waves in Western Georgia are mainly marked in the Black Sea during formation of cyclonic area, when air flow is "absorbed" from the land and flow of warm air is formed [5] in Earth surface layer under the influence of relief. A distinct example of microcirculation motion existence is the influence of Surami Range from the west or from the east on the moving air flow. Such processes are mainly conditioned in regard to some obstacles at speed 10 m/sec (perpendicularly to the mountain) in flow motion, after passing the mountain, transfer of laminar motion into hurricane. The existence of arisen waves is proved by the forming of multilayered clouds whose wave length is 4≈6 km, height 2≈2.5 km.

Let's imagine Surami range as trihedral angle piramide, which length along earth X-axis of earth parallel is 10 km, and along Y-axis meridian is 50 km, then using [6] theory for mountain characteristic parameters we correspondingly obtain:

$$a = -\partial/\partial x(\ln P_z/P_0) = 11\cdot10^{-5}\ 1/m;\ b = -\partial/\partial y(\ln P_z/P_0) = 2\cdot10^{-5}\ 1/m$$

Here P_z is the value of pressure on the mountain height Z and P_0 = 1000m.bar.

Table 1

Station, h(m)	1980 Year					
	January			July		
	Temperature t°C	Relative humidity S%	Wind velocity V(m/sec)	Temperature t°C	Relative humidity S%	Wind velocity V(m/sec)
Observatory 403	1.0	71	1.1	26.9	57	1.4
Vashlijvari 427	0.6	73	0.6	26.4	56	1.7
TSU	1.9	76	0.5	25.1	57	0.7
Aerport 464	-0.5	78	4.7	25.9	58	6.9
Tbilisi Sea 549	-0.5	73	1.8	25.0	61	1.9
Funikular 730	-0.6	74	2.1	24.8	60	2.5

Correlation of corresponding wave lengths of a and b is back proportional and therefore we obtain $Lg = 5Lx$; daily period of fion wave is obtained 16.7h.

This theoretical results are in good agreement with the observed data in Surami, Khashuri and Gori meteorologic stations [2,5]. One important problem is also connected with the local atmospheric processes i.e. the level of air pollution on the territory of Georgia. It should be noted that daily changes of air pollution are basically caused by the complicated nature of turbulent flow in convection and Earth surface layer. The change of average yearly levels of air pollution in Western and East Georgia is quite different [9].

But the essence of the matter is that in both regions many years oscillations of pollution are intensive. This fact proves once more the significance of circulation processes caused by Surami range not only in the process of climate formation, but in the course of the level of air pollution and indicates directly to the more detailed study of the level of micro-local atmosphere processes.

Tbilisi I.Javakhishvili State University

REFERENCES

1. *L.Matveev.* Zogadi meteorologiis kursi – atmosperos fizika. Ed. Z.Khvedelidze. Tbilisi, 1987, 701 (Georgian).
2. *D.Laikhtman.* Fizika pogranichnogo sloya atmosfery, 1970, 340 (Russian).
3. *L.Gandi, L.Laikhtman, L.Matveev, M.Yudin.* Osnovy dinamicheskoi meteorologii. Leningrad, 1955, 701 (Russian).
4. *Z.Khvedelidze, R.Chelidze.* Collective work of TSU A.6-7 (149-159), 1973, 150-155 (Georgian).
5. *A.Khrgian.* Fizika atmosfery. 1975, 701 (Russian).
6. *Z.Khvedelidze.* Meteorologiya i Gidrologia, 10, 1982, 110-115 (Russian).
7. *M.Gurgenidze, Z.Khvedelidze.* Bull.Georg. Acad. Sci., 152, 3, 1995, 516-521.
8. *K.Tavartkiladze et al.* Collective works dedicated to the 150 Aniversary of Tbilisi Geophysical Observatory. Tbilisi, 1997.

საქართველოს მეცნიერებათა აკადემიის მოამბე, 159, №3, 1999
BULLETIN OF THE GEORGIAN ACADEMY OF SCIENCES, 159, №3, 1999

GENERAL AND INORGANIC CHEMISTRY

V. Rukhadze, Z. Vatsadze, M. Gegeshidze, M.Gumberidze

Chemical Processes during Zinc Sulphide Synthesis and their Influence on the Pigmented Characteristics of Zinc Sulphide

Presented by Corr. Member of the Academy J.Japaridze, April 8, 1998

ABSTRACT. **Zinc sulphide synthesis process from zinc chloride solution was investigated. Anomalous fall of solution pH was outlined in that process. It was theoretically explained and confirmed by experimental data that this phenomenon was caused by the formation of base zinc sulphide. Mentioned assertion was proved by derivatographic investigations of the final product. It is recommended to make synthesis in pH 1-3 interval.**

Key words: zinc sulphide, zinc chloride, pH synthesis, base zinc sulphide, thermalgravimetrical analysis.

It is known that during zinc sulphide synthesis process the composition and the structure of sediment are formed. But concrete accessory chemical processes, which considerably affect characteristics of the final product are not explained. Zinc sulphide synthesis pH is the main factor that influences on correlation of forming solid phase and rate of crystal growth.

Fig.1 represents synthesis of ZnS and as a result the reagents are mixed in different correlation. Formation of ZnS sediment is attended by the formation of hydrogen ions which is caused by following processes: water solutions of barium sulphide and zinc chloride salts undergo hydrolysis:

$$Zn^{2+} + HOH \rightleftarrows (ZnOH)^{+} + H^{+} \quad (1)$$

$$S^{2-} + HOH \rightleftarrows HS^{-} + H^{-} \quad (2)$$

We must take into account that along with ZnS precipitation of $(ZnOH)_2S$ takes place and we can explain anomalous pH decrease in the following way. By the reaction (3):

$$2(ZnOH)^{+} + S^{2-} \rightarrow (ZnOH)_2 S\downarrow \quad (3)$$

$(ZnOH)^{+}$ ions are changed into low-dissociated combination and according to the reaction (1) $H)^{+}$ ions are accumulated in solution.

Undoubtedly the quantity of base zinc sulphide depends on zinc chloride pH value, as artificial

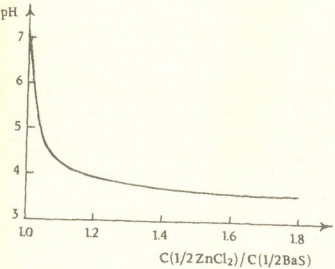

Fig.1. The dependence of ratio of initial reagents on suspension pH value.

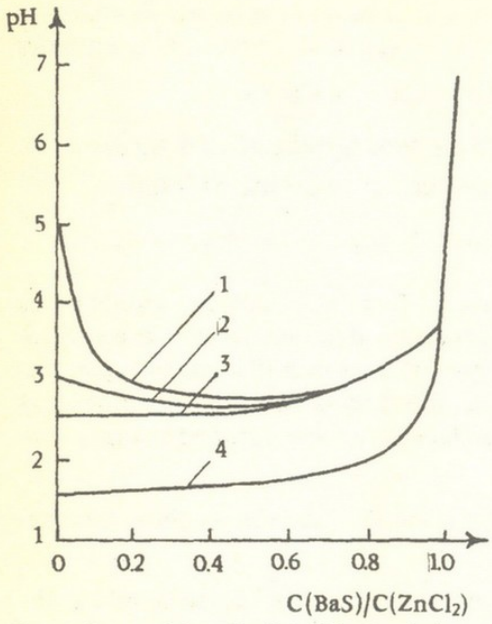

Fig.2. Influence of zinc chloride initial pH and zinc and barium ions ratio on synthesis pH

growth of acidity outweighs balance to the formation of zinc ions (1).

$$(ZnOH)^{+} + H^{+} \rightleftarrows Zn^{2+} + HOH,$$

which mainly causes the precipitation of mean zinc sulphide. Our conclusion is confirmed by experimental data, when beforehand acidified $ZnCl_2$ solution with pH-1.5 was used, and above-mentioned anomalous fall of synthesis pH had been disappeared. Analysis of the curve represented in Fig.2 shows that at pH ($ZnCl_2$)=2.5 – 3 hydrolysis of zinc ions is stopped. The curve 3 represents full precipitation of zinc sulphide. The obtaining of base zinc sulphide can be proved by following experiments. During synthesis, we pour out barium sulphide solution on zinc chloride solution, which are taken with equimolecular ratio. Bringing this zinc sulphide at 650^{0}C, we find 8.5k of zinc oxide there.

It is impossible to get such quantity of zinc oxide by oxidation of zinc sulphide.

During analogous synthesis we are charging both initial solutions simultaneously into reaction area.

So zinc sulphide that we have got, contains the trace of zinc oxide. We can suppose, that while pouring out barium sulphide on zinc chloride, we have surplus of zinc chloride, which causes the formation of base zinc sulphide. After heat treatment of zinc sulphide we can express decomposition of base zinc sulphide by the reaction:

$$(ZnOH)_2S \rightarrow 2ZnO + H_2S\uparrow.$$

In order to prove the presence of base zinc sulphide, we treated zinc hydroxide with barium sulphide solution. Chemical processes, happening during this time, can be expressed by the reaction:

$$Zn(OH)_2 + BaS \rightarrow ZnS + Ba(OH)_2$$

$$Zn(OH)_2 + BaS \rightarrow (ZnOH)_2S + Ba(OH)_2.$$

After that, we heated the sediment with concentrated sodium acid in order to except the presence of zinc hydroxide. Chemical analysis of the sediment exposed ZnS - 78%; $(ZnOH)_2S$ - 20.5%.

Fig.3 represents two sections of the curve. The first can be explained by the loss of humidity (the loss of the mass is up to 2 mg) and the second, where the loss of the mass is 15-16 mg. The second process proceeds at 510-730°C and is attended by exothermic effect. This effect is represented on DTA curve at 620 $^{\circ}$C in nitrogen area, by wide peak, but in the case of air - by two peaks at 580 $^{\circ}$C - 685 $^{\circ}$C.

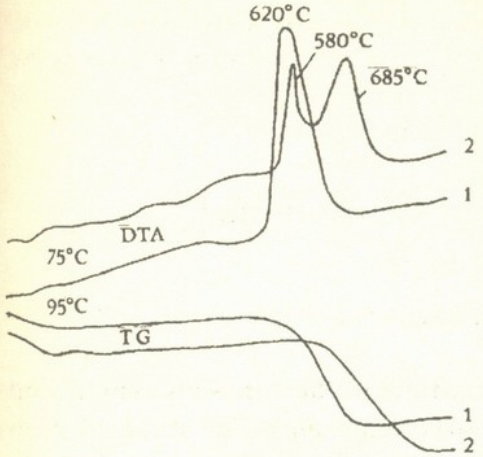

Fig.3. TGA of base zinc sulphide: 1) nitrogen; 2) air; weight 120 mg.

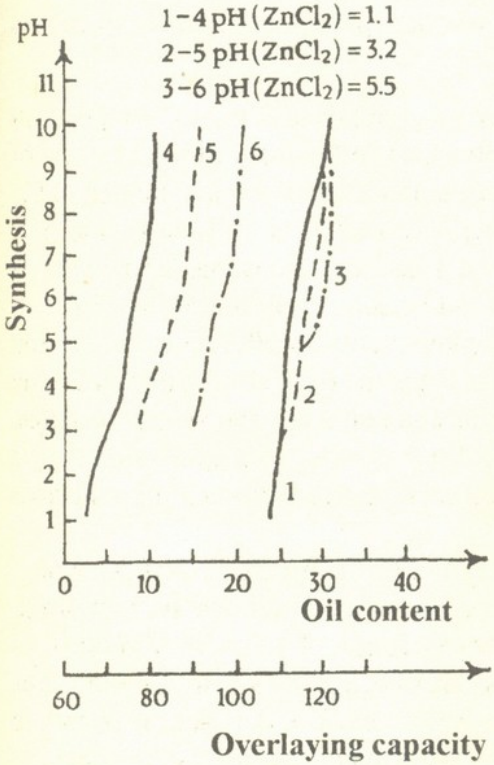

Fig.4. Influence of zinc chloride initial pH and zinc sulphide synthesis final pH on content of oil and overlaying capacity of zinc sulphide.

Chemical analysis of the product represents that it contains 20.5mg of base zinc sulphide and 70.5 mg of ZnS and according to the reaction (4), the loss of the mass (m_1) is equal to:

$$m_1 = 20,5x34/196 = 3,5 \text{ mg}$$

According to TGA, decomposition of base zinc sulphide is attended by oxidation of zinc sulphide, during which decrease of the loss (m_2) is occurred at 520 °C. So the loss of the mass will be (m_2):

$$m_2 = 70,5x16/97 = 11,6 \text{ mg}$$

The loss of the common mass is:

$$m_1 + m_2 = 3,5 + 11,6 = 15,13 \text{ mg}$$

These data agree with experimental data of TGA.

Initial pH of zinc chloride and synthesis pH of zinc sulphide affects pigmental characteristics of zinc sulphide (Fig.4).

Diminition of zinc chloride and synthesis pH up to 1-3 interval, changes and improves pigmented characteristics of zinc sulphide (content of oil and overlaying capacity accordingly 24-26 g/100 g and 65-78 g/m^2). We can explain this phenomenon by following: at low pH the opening of the smallest particles of ZnS occurs and we get more or less similar particles. At the same time, the formation of base zinc salts occurs and it has negative influence on qualitative indices.

So simultaneously pouring out zinc chloride and barium sulphide, and synthesis pH up to 1-3 interval, we get zinc sulphide and after thermal treatment of the product it has following pigmented characteristics: overlaying capacity 32-37 g/m^2; content of oil 18-19 g/100g; whiteness 94-95.

Georgian Academy of Sciences
Kutaisi Scientific Centre

REFERENCES

1. *E.F. Belenky, I.V. Riskin.* Khimiya i tekhnologiya pigmentov, L., 1974 (Russian).
2. *N.Z. Safin, G.A. Armonik.* Luminestsentnye materialy i osobo chistye veshchestva, 1975, No.13, 67-71 (Russian).

საქართველოს მეცნიერებათა აკადემიის მოამბე, 159, №3, 1999
BULLETIN OF THE GEORGIAN ACADEMY OF SCIENCES, 159, №3, 1999

Sh. Shatirishvili, Sh. Gigilashvili

Study of Biopolymers in Wines by Gas-Correlation Chromatography

Presented by Member of the Academy T. Andronikashvili, June 22, 1998

ABSTRACT. **Products of pyrolysis of the precipitates of the wines "Kakheti" and "Rkatsiteli" were investigated by gas-correlation chromatography. The obtained chromatograms enabled us to calculate not only the kinetics of the final products but also that of the process of decomposition.**

Key words: gas-correlation chromatography, kinetics, precipitates, wines, products of pyrolysis

While storing and ageing of any sort of wine, the precipitates of complex composition consist of aminoacids, carbohydrate, proteins or polymeric compounds formed by any of these components. Unfortunately compositions of wine precipitates are not studied sufficiently which probably is conditioned by two principal causes. First, generally, the precipitate is simply removed or it is not allowed to be formed and the wines are filtered at various stages of their making and storing. The second reason is that it is rather difficult to conduct such investigation due to the presence of components of different groups in the precipitate and various sources of their formation. At the same time investigation of wine precipitates is rather important for the study of the mechanisms of wine ageing, because those compounds and their mixtures represent the final product of a great number of chemical and biochemical processes going on at various stages of wine-making and storing.

A multiplet or correlation method of measuring is like "computer" method, where instead of measuring values of physical indices, their linear combinations are measured. To obtain the true values of physical magnitudes the resolution of a system of multiplets of linear equations is made. The advantage of random injection of a sample into chromatograph, availability of making analysis of non-linear effect and isolation from the linear one should be emphasized. In chromatography we often encounter the non-linearity, e.g., such a non-linearity of a detector is observed at the upper limit of the diapazone, or in capillar chromatography the dependence of distribution coefficient on the concentration in case of great number of samples. This position is the principle of correlation chromatography [1].

During the study of wine precipitates, original device was used which was equipped with impulse technique of sample delivery in short time intervals. Wine precipitate sample was placed in a pyrolyser heated rapidly up to 600^0C, while the portions of the produced prolysates were injected by impulses into a short (5 m) capillary column. Detection was performed by flame ionization detector. The sets of chromatograms were used for characterization not only of the products obtained on every separate stage, but also the kinetics

of the process of decomposition. Identification process of the pyrolysates is rather labour-consuming and we limited ourselves only to the qualitative data of the analysis, according to the method of "fingerprints".

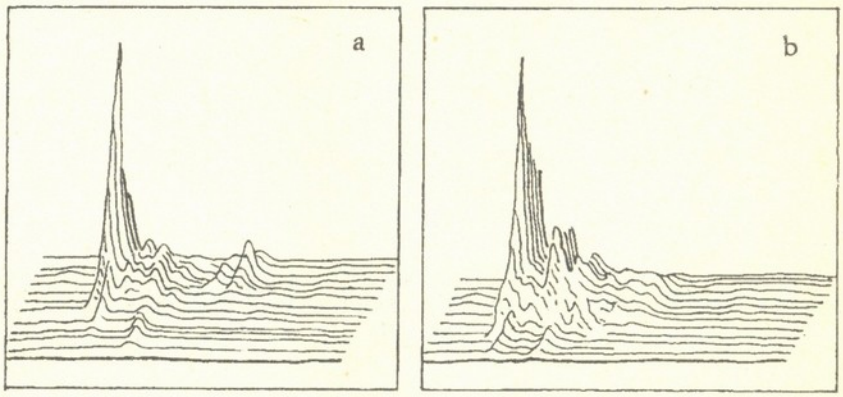

Fig. 1 Impulse thermochromatogram of wine precipitates: a-"Rkatsiteli"; b - "Kakheti"

We have analysed the precipitates of wines "Rkatsiteli" and "Kakheti" of two years ageing. Their typical complex chromatograms are given in Fig. 1. The obtained chromatograms prove the fact of the formation of polymer compounds of different structure and molecular mass in the process of ageing, which during pyrolysis yield gaseous products. Comparison of the presented chromatograms enable us to conclude that during general identification of the created products their concentrations for different wines are so different that we can achieve identfication of wine materials by means of sets of chromatograms using the method of "fingerprints"

For the creaton of reference system for identfication of the biopolymeric compositions according to the thermo-chromatographic data the peak intensity should be taken into consideration through parameters of the fixed value of their intensity with respect to their retention times. Thermograms to be used for the calculation of the distribution function may be presented as a multiple of phenomena:

$A = \prod_{i=1}^{n} A_i$, where A_i is a phenomenon, expressed by a peak of Si area. Time of setting of the phenomenon Ai is equal to t_{Ri} time of retention of i-peak. Probability of expressing of phenomenon, at the thermolysis of biopolymeric mass $P(A) = 1$ or

$P(A) = P(\prod_{i=1}^{n} A_i) = \sum_{i=1}^{n} (A_i) = 1$, where $P_i = P(A_i) - t_{Ri} / \sum_{n=1}^{n} t_{Ri}$; peak area is calculated

in relative units $S_i = S_i/S_\varepsilon$, where $S_\varepsilon = \sum_{i=1}^{n} S_i$. Let's use Si and Pi values and characterize the thermogram by the distribution function Si-P and calculate its parameters: a_1, a_2 - first and second starting moments and their ratios; $a_i = \sum_{i=1}^{n} (S_i \cdot P_i) = \sum_{i=1}^{n} (S_i \cdot t_{Ri}) / (S_\varepsilon \cdot t_z)$,

where n is a number of tracer peaks the areas of which are not less than some values of a proceeding from $\sum_{i=1}^{n} S_i$ (the sum of areas of all peaks on the pyrogram); $t_z = \sum_{i=1}^{n} S_i$ is total retention time

$$a_2 = \sum_{i=1}^{n} (S_i)^2 P_i = \sum_{i=1}^{n} (S_i^2 t_{Ri}) / (S_z^2 t_z)$$

$$a_1 / a_2 = S_z \sum_{i=1}^{n} (S_i^2 t_{Ri}) / \sum_{i=1}^{n} (S_i^2 t_{Ri})$$

Analysis of parameters has shown (their interval estimation by reliability probability is 95%) that for proper characterization of biopolymeric masses by the use of thermochromatographic data the a_1 and a_2 parameters, number of tracer peaks n and their total retention time t_z are sufficient.

Realization of such an approach enables us to chracterize a mixture of wine biopolymers by some quantity parameters the importance of which exceeds the reliability of identification of wines according to their precipitates.

Georgian State Agrarian University

REFERENCES

1. *E. Kullik et al.* I. Intern. Laboratory. Jan. /Feb. 1987, 72-81.

საქართველოს მეცნიერებათა აკადემიის მოამბე, 159, №3, 1999
BULLETIN OF THE GEORGIAN ACADEMY OF SCIENCES, 159, №3, 1999

PHYSICAL CHEMISTRY

D.Jishiashvili, I.Nakhutsrishvili, R.Dzhanelidze, M. Katsiashvili

Mechanism of the Germanium Oxynitride Film Formation

Presented by Member of the Academy K.Japaridze, April 13, 1998

ABSTRACT. **Surface reactions taking place at the Ge surface heated in the hydrazine vapour have been investigated in the temperature range of 300-973 K. GeO and Ge_3N_4 volatile molecules are formed onto the Ge surface. Their subsequent sublimation and condensation on the GaAs substrate results in the germanium oxynitride film formation. It was established, that at the different stages of a film deposition the film composition changes until it reaches $Ge_3N_{1.3}O_{1.2}$.**

Key words: germanium oxynitride, thin film, Auger spectroscopy, activation energy.

The germanium oxynitride film forms a high quality interface with semiconductors which have a different atomic and electronic structures of their surfaces [1]. Detailed investigation of the oxynitride film growth mechanism is needed to explain this nontrivial result. It is very important particularly in the case of GaAs because its surface passivation is still an unsolved problem [2]. The ion-plasma deposited germanium oxynitride film is of special interest particularly for its high radiation hardness. But the ion-plasma technologies can cause damage of the GaAs surface. For this reason the chemically enhanced "soft" deposition processes, such as pyrolisis, are the most suitable technologies for GaAs.

The purpose of this work was to analyze the reasons for a perfect interface formation between GaAs and the pyrolitic GeN_xO_y film. This was accomplished by investigating the chemical processes taking place at the germanium source surface during its heat treatment (300 - 973 K) in the hydrazine vapour and also by analysing the volatile products formed through this treatment and their condensation on the GaAs surface.

The oxynitride films were deposited in the evacuated quartz reactor, filled in with the hydrazine to its saturated vapour pressure (1.6x103 Pa) and containing two temperature zones. Ge was placed in the hot zone (T_{max} = 973 K) and it served as the source for the formation and subsequent sublimation of GeO and Ge_3N_4 molecules. These molecules were condensed onto the GaAs substrate which was placed in the cold zone (T_{max} = 573 K) at some distance above the Ge source.

To study the surface chemical reaction occurring on the Ge source, its mass change was continuously monitored by the built in microbalance with the sensitivity of 10^{-6} g.

The deposition process was starting at the room temperature. During the first 15 minutes the temperatures of the source and GaAs were raised up to 973 and 573 K respectively and then stabilized. Six fixed temperatures were selected in this range to study chemical reactions taking place at each deposition stage.

Kinetics of the Ge source mass change in the hydrazine vapour at different temperatures are illustrated in Fig.1. Up to 773 K the mass is increasing during the heat treatment, but it restores the initial value after evacuation at the same temperature (Fig.1,

curve 1). The activation energy for this process, calculated from the temperature dependence of the reaction rate constant, equals to 12.57 kj/mol [3] and proves that the physical adsorption of the hydrazine vapour occurs at this temperatures.

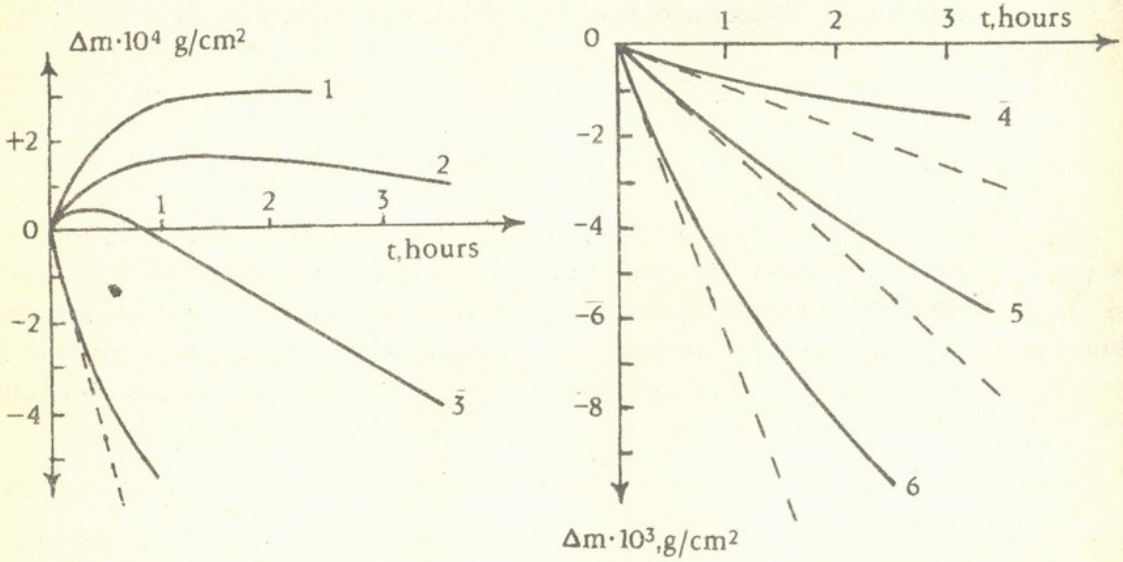

Fig.1. Kinetics of the Ge source mass change during its interaction with the hydrazine vapour at different temperatures : a) 1-748, 2-773, 3-823, 4-873 K; b) 4-873, 5-923, 6-973 K.

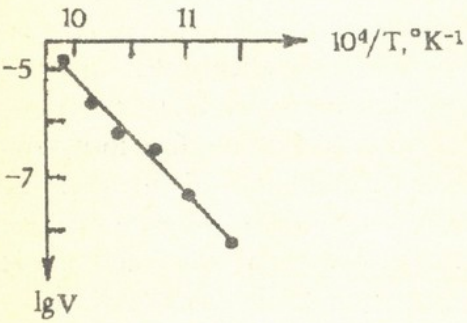

Fig.2. Dependence of the Ge source etch rate in the hydrazine vapour on the reaction temperature.

At 773 K and higher temperatures the adsorption related features are subsequently suppressed and the Ge source mass is decreasing. This is due to formation and sublimation of the volatile reaction products - GeO and Ge_3N_4. The formation heat (enthalpy) of Ge_3N_4 is greater than the same parameter for GeO (377.1 kj/mol versus 209.5 kj/mol). At lower temperatures GeO molecules are predominantly sublimating, followed by Ge_3N_4 sublimation at higher temperatures. The mass change rate was determined in the linear portion of the kinetic curves. The temperature dependence of a reaction rate (Fig.2) yields the activation energy value of 209.5 kj/mol, which coincides with the germanium monoxide enthalpy of vaporisation [4].

Calculations show that the most probable reactions for the volatile GeO molecule formation are:

$1/2Ge+H_2O=1/2GeO_2+H_2\uparrow$ $\quad \Delta H^\circ_{973}$=-16.34 kj/mol

$1/2Ge+1/2GeO_2=GeO\uparrow$ $\quad \Delta H^\circ_{973}$=-235.40 kj/mol

$Ge+H_2O=GeO-+H_2\uparrow$ $\quad \Delta H^\circ_{973}$=219.06 kj/mol

This last reaction is endothermic and its enthalpy equals to 219.06 kj/mol.

Deviation from linearity observed in the kinetic curves at 873 K and higher temperatures are caused by accumulation of the solid products of reaction which occurs together with GeO sublimation. According to X-ray analysis this product consists of the crystalline α- and β-Ge_3N_4 mixture (Fig.1, curves 4-6). A part of Ge_3N_4 produced, is simultaneously sublimating. If at the same temperature the reactor is filled in with the pure H_2O vapour, or with N_2H_4 containing 36 mas.% of H_2O, then Ge_3N_4 is not formed and kinetic dependencies are linear.

As it was established previously, due to its high activity the hydrazine vapour can etch the GaAs native oxide at temperatures very close to the room temperature. At 573-623 K the etch rate equals to 0.4 nm/s and this process is characterized by the low activation energy (20.11 kj/mol). At the initial stage of deposition GeO molecules appear on the *in situ* etched GaAs surface. They are interacting with the GaAs surface through the following reactions:

$$2GaAs + 6\,GeO = Ga_2O_3 + As_2O_3 + 6Ge \qquad \Delta H^{\circ}_{973}=-366.21\ kj/mol \qquad (1)$$

$$2GaAs + 3\,GeO = Ga_2O_3 + 2As + 3Ge \qquad \Delta H^{\circ}_{973}=-390.50\ kj/mol \qquad (2)$$

The enthalpy of the reaction (2) is smaller than that of (1) and thus the probability of the surface reaction (2) is higher. Due to these reactions the free Ge atoms are produced at the GaAs surface. This is in agreement with the results obtained during the thermal oxidation of GaAs in the presence of GeO_2 and GeO molecules [5]. In these experiments Ge was found at the oxide -GaAs interface and even in the bulk of GaAs.

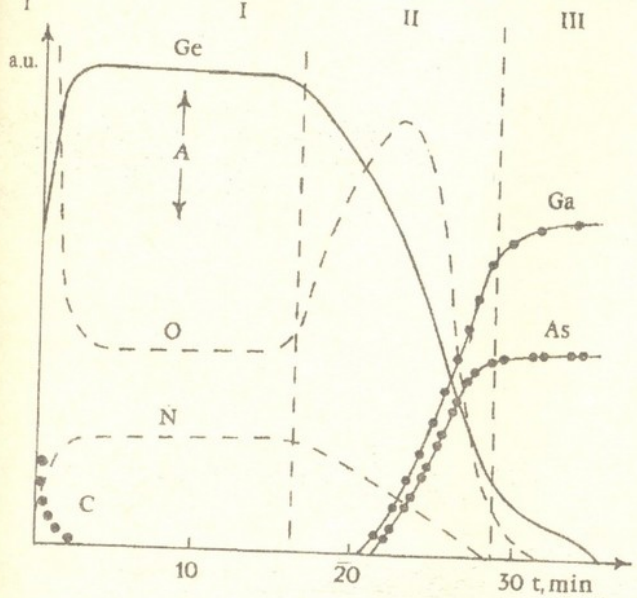

Fig.3. The depth profile of 70nm thick GeO_xN_y film deposited on GaAs.

Similar processes are taking place in our experiments. It was confirmed by the Auger profiling data. Fig.3 shows the Auger depth profiles of 70 nm thick pyrolitic oxynitride film deposited at 573 K. Ge pile up is observed adjacent to the GaAs surface. The thickness of the Ge film was estimated to be of 2-4 nm (region I). This film thickness prevents subsequent diffusion of GeO molecules through it and they are forming the oxide layer. Accordingly the Ge and O content gradually increase at some distance from the Ge - GaAs interface as is illustrated in Fig.3, region II.

As it was mentioned above, the deposition temperature is rising during the first 15 minutes and this is reflected on the depth profile. As the temperature of the Ge source is rising, the intensity of Ge_3N_4 formation and sublimation is increasing, causing the appearance and subsequent growth of the nitrogen signal in the region II. When the temperature

reaches its maximal value the amount of sublimated GeO and Ge_3N_4 molecules is also stabilized and the film with a uniform distribution of elements is deposited (region III).

At the point marked "A" calculated concentrations of elements are: Ge - 54 at.%, O - 22 at.%, N - 24 at.%. According to this data the Ge oxynitride composition can be described by the formula $Ge_3O_{0.2}N_{1.3}$. Comparing this result with the stoichiometric oxynitride formula ($Ge_3O_{1.5x}N_{4-x}$) we can conclude, that the film corresponds to the nonstoichiometric Ge oxynitride.

On the basis of the experimental results the following conclusions can be drawn:

- in the temperature range of 300-973 K interaction of Ge with the hydrazine vapour, containing 20 mas.% of H_2O leads to the formation of two volatile molecules - GeO and Ge_3N_4 ;
- GeO is sublimating at 773 K and higher temperatures, while Ge_3N_4 - at 873 K and higher;
- GeO molecules are reacting with the GaAs surface and forming the thin (2-4nm) Ge layer which determines the excellent surface passivation properties. This Ge layer is then covered by the insulating germanium oxynitride film with a uniform composition.

The authors would like to express their gratitude to M. Katsiashvili for manuscript preparation. A part of this work was supported by the grant of ISTC #G-059.

Georgian Academy of Sciences
Institute of Cybernetics

REFERENCES

1. *D.Jishiashvili, at al.* Key Interface,1, 1997, 14-16.
2. *A.Mills.* III-Vs Review, **10**, 4, 1997, 43-45.
3. Kratkaya khimicheskaya entsiklopediya. **1,** 1961 (Russian).
4. Davlenie i sostav para nad okislami khimicheskikh elementov. Edited by E.Kazenas and D.Chigikov. Moscow. 1976 (Russian).
5. *G.Bagratishvili at al.*Soobshch. AN GSSR, **130,** 2, 1988 (Russian).
6. *I.Mittova at al.*Neorganicheskie materiali,**26**,1,1990, 14-17 (Russian).

საქართველოს მეცნიერებათა აკადემიის მოამბე, 159, №3, 1999
BULLETIN OF THE GEORGIAN ACADEMY OF SCIENCES, 159, №3, 1999

PHYSICAL CHEMISTRY

S. Gedevanishvili, Z. A. Munir, Corr. Member of the Academy I. Baratashvili

The Use of an Electric Fields in the Combustion Synthesis of Ceramic Composite

Presented September 21, 1998

ABSTRACT. **Using field-activated combination synthesis (FACS), composites of (1 - x) $MoSi_2$-xSiC were prepared directly from elemental powders. Systems with $0 < x \leq 0.18$ can sustain a combustion wave but the product contained unreacted Si and C in addition to $MoSi_2$. Systems with $x > 0.18$ do not sustain a wave without the application of an external electric field. Composites of $MoSi_2$ and β-SiC can be synthesized for $0 \leq x \leq 1.0$ in the presence of fields above threshold field values. The threshold value decreased with increasing x value. Both combustion wave velocity and temperature increased nearly linearly with an increase in field above the threshold value for any given composition (x value). Effect of the magnitude of the field on the nature and microstructure of the product were also investigated.**

Key words: field activated combustion synthesis, composite, temperature.

The use of self-sustaining combustion synthesis is limited to those systems in which the exothermic reaction enthalpy is large. This limitation has been empirically related to the adiabatic combustion temperature, T_a, such that systems with T_a<2000K do not produce a self-sustaining wave [1]. For systems which are relatively less exothermic, the common approach has been the preheating of the reactants to effect an increase in T_a. However, the preheating of the reactants can alter the mechanism of the reaction, resulting in the formation of extraneous phases [2, 3].

A more recent method has been developed such that self-propagating combustion reactants can be initiated and sustained in less exothermic systems [4]. It involves the imposition of an electric field and an ignition source simultaneously. Under such a condition, a self-propagating combustion wave could be initiated in the synthesis of a variety of materials with low enthalpies of formation [5-8].

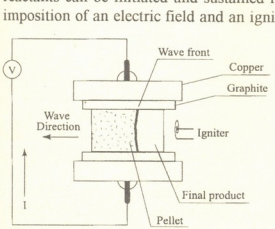

Fig. 1. Schematic diagram for the field-activated combustion process for $MoSi_2$/SiC.

Mixtures were prepared from powders of Mo, Si and C in a mechanical shaker for 60 min in proportions corresponding to compositions of (1-x) $MoSi_2$ + xSiC with $0 \leq x \leq 1.0$. The Mo powders were 99.9% pure and had a particle size range of 3-7 μm . Silicon and graphite powders were 99.5% and 99.0% pure respectively and had a sieve classification of -325 mesh. Green compacts were produced by

cold pressing to form cubic-shaped samples with an edge dimension of 1 cm. The specimens were placed between a pair of graphite electrodes across which a voltage was applied. A tungsten heating coil, placed near one edge of the sample was used to initiate the combustion. A schematic representation of this set-up is shown in Figure 1. The experiments were carried out inside a stainless steel pressure chamber under one atmosphere of argon.

In the absence of a field, a combustion wave can be propagated from one and of the sample to the other only for (1-x) $MoSi_2$ - xSiC compositions with $0 \le x \le 0.18$. For samples with $0.18 \le x \le 0.45$ a wave could be initiated without a field but it only propagated to approximately one fourth of the sample length before it stopped. For all of the above cases, x-ray analysis showed that the combusted part of the sample contained the compound $MoSi_2$ and the elements Si and C. Thus in the absence of the electric field, only Mo and Si react wholly or partially to produce $MoSi_2$; silicon and carbon do not react to form the second phase, SiC. In samples with $x > 0.45$, no self-sustaining wave could be initiated even for a limited distance without the application of a field.

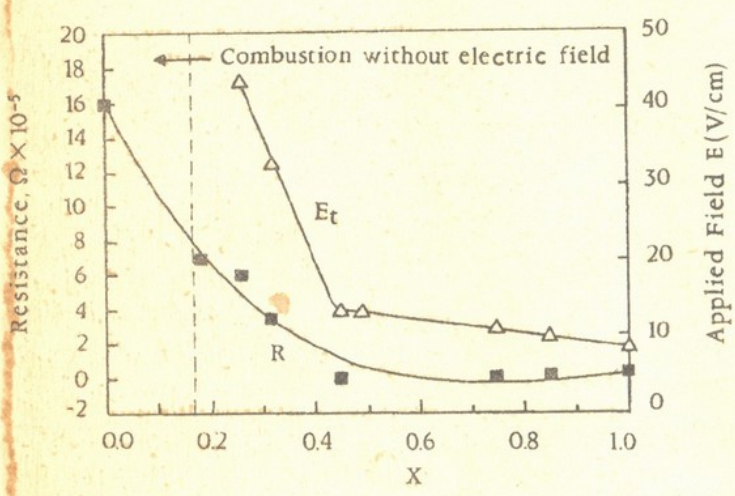

Fig. 2. Effect of (SiC nominal content) in the original mixture on the threshold field and resistance of the starting mixture.

In order to establish a self-sustaining wave, it was found that a minimum (threshold) field value is necessary. The dependence of the threshold field value, E_t, on x, shown in Figure 2, has the same trend as the dependence of the resistance of the initial reactants, R, on x. The probable reason for the decrease in the threshold field is the concomitant decrease in the resistance of the starting mixture. The mixture which has a resistance of more than 16 x $10^5\Omega$ needs a field higher than 45 Vcm^{-1} to become self-sustaining.

Figure 3 shows the effect of the applied field on the maximum combustion temperature, T_c, and wave velocity, U, for mixtures with $x = 0.45$. The velocity increased in a qualitatively similar way to the increase in temperature. In the interval between fields of 0 and 13 Vcm^{-1}, this mixture cannot support a self-sustaining combustion and when the field is about 35 Vcm^{-1} or higher, volume (simultaneous) combustion dominates. An increase in T_c of about 400^0C is observed as the applied field was increased from ~13 to 35 Vcm^{-1}.

To undestand the mechanism of conversion of the elemental powders in the fieldactivated process of composite formation, an experiment was performed in which the applied voltage (corresponding to $E = 15$ Vcm^{-1}) was interrupted during synthesis. In ich an experiment, when the voltage was reduced to zero, the wave continued to advance

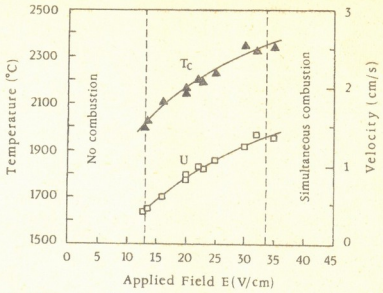

Fig. 3. Dependence of the combustion maximum temperature and wave velocity on the applied field. x=0

for a small increment (≈3mm) before it stopped completely. Visual observation of the sample showed the presence of three different regions. X-ray analyses of these regions showed the presence of $MoSi_2$ and β-SiC in the region behind the wave, $MoSi_2$, Si, and C in the region inside the wave, and an unreacted mixture of the Si, Mo, and C elements in the region ahead of the wave.

The above observations show that the field-activated formation of the $MoSi_2$/SiC composite is a two-step process. The first step is the formation of $MoSi_2$ and the second step is the reaction between Si and C to form β-SiC.

Typically the product of the field-activated combustion synthesis of $MoSi_2$/β-SiC composites is porous. However, when the applied field is>30Vcm^{-1}, the product is partially melted. Under a field of this magnitude the product contained small amounts of Mo_5Si_3. The Mo_5Si_3 was not observed in products synthesized under the influence of E < 30Vcm^{-1}.

Georgian Academy of Sciences
F. Tavadze Institute of Metallurgy

University of California, Davis, USA

REFERENCES

1. *Z. A Munir, U. Anslemi*-Tamburini. Mater. Sci. Rep. 3, 1989, 277.
2. *S. C. Deevi*. Mater. Sci. Eng. A 149, 1992, 241-251.
3. *D. C. Halverson, B. Y. Lum, Z. A. Munir*. ECS Proceedings, 88-85, 1988, 613.
4. *Z. A. Munir, W. Lai, K. Ewald*. U. S. Patent No. 5.380, 409, January 10, 1995.
5. *S. Gedevanishvili, Z. A. Munir*. J. Mater. Res. 10, 1995, 2642.
6. *S. Gedevanishvili, Z. A. Munir*. Mater. Sci. Eng. 211, 1, 1995.
7. *I. J. Shon, Z. A. Munir*. Mater. Sci. Eng. A202, 1995, 256.
8. *H. Xue, Z. A. Munir*. Metall. Mater. Trans. 27, 1995, 475.

საქართველოს მეცნიერებათა აკადემიის მოამბე, 159, №3, 1999
BULLETIN OF THE GEORGIAN ACADEMY OF SCIENCES, 159, №3, 1999

GEOLOGY

I. Kvantaliani

On the Lower Barremian of the Southern Limb of the Racha-Lechkhumi Syncline (Western Georgia)

Presented by Corr. Member of the Academy M. V. Topchishvili, April 13, 1998

ABSTRACT. **On the Southern limb of the Racha-Lechkhumi syncline, within the lower Barremian sediments, ammonites of Holcodiscidae family have been identified for the first time. An attempt of zonal subdivision of the Lower Barremian of the section in v. Nikortsminda outskirts in correlation with the Lower Barremian the Northern limb of the mentioned structure is made. Now on these grounds we can affirm that Holcodiscidae occurs not only on the Northern limb of the Racha-Lechkhumi syncline, as it was supposed earlier, but also in the section of Nikortsminda outskirts on the Southern limb, i. e. both in deepwater and shallow water parts of a neritic region of the sea. Recent data specify the spreading areal of "ammonitic facies of the Barremian".**

Key words: Barremian, biostratigraphic, Nikortsminda, ammonitic facies.

Barremian deposits of Georgia have been studied since long. Interesting information on diverse investigations of this stage are reflected in numerous publications [1-9]. The upper substage of the Barremian was studied thoroughly. As for the lower one, it became the subject of detailed investigations recently. In the end, new unified scheme of biostratigraphic subdivision was worked out for the Upper Barremian of Georgia [4, 5, 7, 8] as well as for the Lower Barremian [10, 11]. The latter should be investigated in detail not only in the Khidikari section, but also in other sections, especially on the Southern limb of the Racha-Lechkhumi syncline. One of such sections is fixed in the vicinity of v. Nikortsminda. Lateral changes of Lower Cretaceous sediment facies from Okriba towards the Racha-Lechkhumi syncline was first paid attention by A. Djanelidze [1]. He noted that the urgonian massive limestones with chamidae, spread in the vicinity of Kutaisi, northwards in Nikortsminda region (Southern limb of the Racha-Lechkhumi syncline) are substituted by similar massive limestones without chamidae, but with silicified nodular concretions in the upper part, and with the so-called transitive fauna in its uppermost horizons. In the Northern limb of the mentioned syncline (Khidikari section) the urgonian facies is utterly absent, here in the Barremian it is represented by laminated limestones with flinty concretions comprising rather abundant ammonitic fauna, according to which A. Djanelidze distinguished the "Barremian ammonitic fauna" . It is the "stratigraphic equivalent of the Okriba urgonian" [I, p.80]. Later this issue was broached repeatedly by many investigators [2-6, etc.]. Urgonian biosedimentary system of Georgia is studied very precisely by E. Kotetishvili [5]. At present, with appearance and storage of recent actual data, it is necessary to reconsider principles concerning the spreading and living condi-

tions of some populations of ammonitic family Holcodiscidae Spath, 1924 and presence or absence of "ammonite facies". While describing the section in the vicinity of Nikortsminda, we are speaking about the massive and laminated limestones of the Lower Barremian, occupying stratigraphic interval between the analogues of the Upper Barremian zone Ancyloceras vandenheckii and Upper Hauterivian limestones.

On the Southern limb of Racha-Lechkhumi syncline, North-Westwards of v. Nikortsminda, the authors of the paper (with the participation of M. V. Topchishvili and N. N. Kvakhadze), constructed the section on the road leading to v. Khonchiori, here the Hauterivian sediments with *Simbirskites* sp. [9] upwards are conformably followed by:

K_1h_2 1. Medium- and thick-bedded massive crystalline limestone with concretions of grey flints, where thick valved shells of amphidonts often occur 65m

$K_1br_1^I$ 2. Clayey-arenaceous medium-bedded limestones with abundant and diverse fauna in its lower part - amphidonts, brachiopods, bevalves, gastropods and ammonites - *Spitidiscus* cf. *seunesi* (Kil.), *S.* sp. *Barremites cassidoides* (Uhl.)., *Protetragonites crebrisulcatus* (Uhl.) ..... ~10m.

$K_1br_1^2$ 3. The same sediments, but more loose and without fauna ..... ~10m.

$K_1br_1^3$ 4. Compact grey limestones with breccia limestone parting (0.25-0.30m) in the uppermost part comprising sparce ammonitic fauna - *Holcodiscus* cf. *caillaudianus* (d'Orb.) ..... ~10m

$K_1br_2^I$ 5. Sandy marls without fauna 5m

$K_1br_2^2$ 6. Sandy marls, but more compact, wherein N. N. Kvakhadze [9] found ammonite species - *Heinzia ouachensis* (Coq.), *H. provincialis* (d'Orb.), *H. matura* **Hyatt**, *Barremites difficilis* (d'Orb.), *B. charrierianus* (d'Orb.), *B. rebouli* Kil., *Lytoceras subsequens* Kar., *L.* cf. *liebig*i Opp 2-3m

Stratigraphically higher follow marlaceous limestones with ammonites of Hemihoplites feraudianus zone.

In the described section transition from one layer to another is completely gradual. Band 1, by its stratigraphic position - interbedded between the layers with the Upper Hauterrivian *Simbirskites* sp. and Band 2 with Lower Barremian fauna, should correspond to the Upper Hauterivian zone Pseudothurmannia angulicostata auct. Band 2 comprises typical Lower Barremian ammonitic species - *Spitidiscus* cf.*seunesi* (Kil.), which to our data accompany the index species - *Spitidiscus hugii* of the lower zone of the Lower Barremian. In this interval of the section limestones from Band 3 are rather loose, due to it here was formed a ravine one of the Sharaula river heads. The greater part of the ravine is covered with recent sediments and vegetation disguishing the bedrocks but nevertheless here and there they crop out. True thickness of Band 3 is about 10m. By stratigraphic position, located between two faunistically well founded zones of the Lower Barremian, it corresponds with the Pulchellia compressissima zone, distinguished in the Northern limb of Racha-Lechkhumi syncline within the Khidikari section [10, II; see correlation scheme]. Ammonites from Band 4 represent index-species of the next, third zone of the Lower Barremian Holcodiscus caillaudianus. Though band 5 doesn't comprise fauna, its stratigraphic position can be identified faultlessly - it corresponds to the zone Ancyloceras vandenheckii (see Bands 4 and 6). And finally Band 6 - this is Heinzia sartousiana zone.

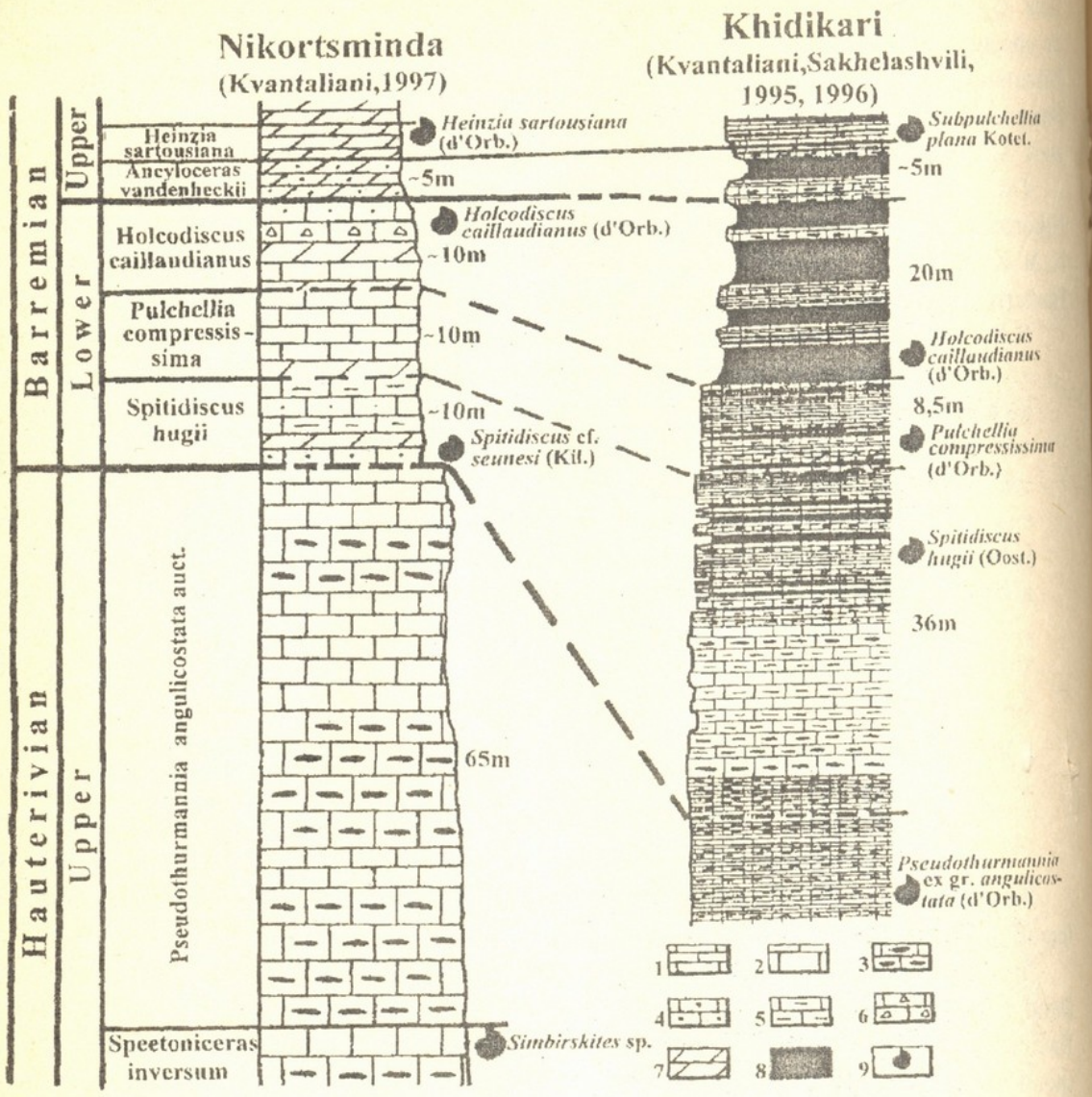

Fig. Correlation scheme of Lower Barremian sediments of the Northern (Khidikari river-gorge) and Southern (v. Nikortsminda) limbs of the Racha-Lechkhumi syncline (Western Georgia).

I - laminated limestones; 2 - thick-bedded limestones; 3 - limestones with flint concretions; 4 - arenaceous limestones; 5 - clayey limestones; 6 - breccia limestones; 7 - marls; 8 - clays, marls; 9 - stratigraphic level of fauna selection (ammonites predominantly).

Ammonites from this Band [9] defined as *Heinzia ouachensis, H. provincialis* and *H. matura* are regarded as synonymous with *Heinzia sartousiana* species. Therefore, we attribute Band 6 to Heinzia sartousiana zone. As for the rest of ammonites from this Band, their presence in the indicated list is not quite clear (N. N. Kvakhadze's oral information). Upwards follow other zones of the Upper Barremian-Hemihoplites feraudianus, etc.

Thus, we can come to quite a number of conclusions. In the Southern limb of the Racha-Lechkhumi syncline, in Nikortsminda section Lower Barremian ammonites - representatives of Holcodiscidae family have been fixed for the first time. Zonal subdivision

of the Lower Barremian on these grounds is also the first attempt. Available actual material enables us to apply the term "Barremian ammonitic facies" to some other sections of the Southern limb of the structure under consideration. Earlier, representatives of Holcodiscidae family were considered as deepwater inhabitants, widerspread on the Northern limb of Racha-Lechkhumi syncline, while on the Georgian Block they are entirely absent. These differences were explained by different geotectonic features, and presence of ammonites in the northern zone of the given syncline, towards the deep of the marine basin were considered as a common phenomenon [4,5]. On the contrary new actual material indicates that ammonites of Holcodiscidae family were the inhabitants of shallow water as well as of deepwater parts of the neritic sea. Further investigations will ascertain range of spreading of the "Lower Barremian ammonitic facies" in the Southern limb of Racha-Lechkhumi syncline.

Georgian Academy of Sciences
A. Janelidze Geological Institute

REFERENCES

1. *A. I. Djanelidze.* Geological observations in Okriba and Adjacent Parts of Racha and Lechkhumi. Tbilisi, 1940, 480 (Russian).
2. *M. S. Eristavi.* Trudy Geol. Inst. Acad. Nauk GSSR, geol. ser., monogr. YI(XI), Tbilisi, 1952, 132-220 (Russian).
3. *M. S. Eristavi.* Lower Gretaceous of the Caucasus and Grimea. Monograph. 10, Tbilisi, 1960, 150 (Russian).
4. *E. V. Kotetishvili.* Trudy Geol. Inst. Acad. Nauk GSSR, new ser., 25, Tbilisi, 1970, 117 (Russian).
5. *E. V. Kotetishvili.* Trudy Geol. Inst. Acad. Nauk GSSR, new ser., 91, Tbilisi, 1986, 1-160 (Russian).
6. *S. K. Gegutshadze.* Trudy Geol. Inst. Acad. Nauk. GSSR, new ser., 42, Tbilisi, 1873, 1-159 (Georgian).
7. *M. V. Kakabadze.* Bull. Acad. SCI. GSSR, 126(3), Tbilisi, 1987, 577-580 (Russian).
8. *M. V. Kakabadze.* Trudy Geol. Inst. Acad. Nauk GSSR, new ser., 71, Tbilisi, 1981, 1-197 (Russian).
9. *N. N. Kvakadze.* Bull. Acad. Sci. GSSR, 103(I), Tbilisi, 1981, 101-104 (Russian).
10. *I. V. Kvantaliani, L. Z. Sakhelashvili.* Bull. Georgian Acad. Sci., 151, 3, Tbilisi, 1995, 462-466 (Russian).
11. *I. V. Kvantaliani, L. Z. Sakhelashvili.* Geologica Carpathica, 47, 5, Bratislava, 1996, 285-288, (English).

საქართველოს მეცნიერებათა აკადემიის მოამბე, 159, №3, 1999
BULLETIN OF THE GEORGIAN ACADEMY OF SCIENCES, 159, №3, 1999

GEOLOGY

J.Meskhia

Geomorphology of Plains and Mountains: Interaction and Interrelation (on the Example of West Georgia)

Presented by Corr. Member of the Academy Z.Tatashidze, December 30, 1998

ABSTRACT. **Relief of West Georgia is considered in the united geomorphologic system: morphostructure -morphosculpture- correlated sediments, i.e. geologic-geomorphologic formation. The morphostructural analysis method with morphostructural and morphosculptural approach is worked out.**

Key words: mountain, plains, formation, interaction.

On the plenary session of RAS on geomorphology (Krasnodar, September, 1998), the problem of formation and dynamics of mountain systems, adjoining foothills and plains (interaction, interrelation) was presented. We assume that in order to solve this problem the following should be taken into consideration: modern relief of the Caucasus, concern to Late orogenic, i.e., geomorphic stage (neotectonic stage), therefore all of its elements should be considered to be the result of interaction of interrelated in time and space endo- and egzogenic geomorphogenesis factors. Thus process developed by such interaction is geomorphic, unified and the relief is a united geomorphic system: morphostructure-morphosculpture- correlated sediments. Neotectonic movements are conerosion. They are accompanied by development of morphosculpture and correlated consedimentation. Therefore, geomorphic system is totally a geologic-geomorphic formation. According to the above, we consider it to be necessary to join all geomorphic and geologic methods for solution of the problem.

We offer the worked out and tested on the example of West Georgia method of morphostructural analysis with morphostructural-morphosculptural approach. It's the complex of geomorphologic (morphologic, systemic-formation, structural-morphologic) and geologic (structural, stratigraphic, lithofacial, granulometric etc.) methods. Region of West Georgia is the most optimal geomorphic system for it. In Kolkhida intermont there is well studied geologic full stratigraphic section of Neogen—Quaternary molasse of the Black Sea basin correlated sediments of surrounding it mountain ranges of the Great Caucasus and Meskheti. Morphosculptures and structural forms of the basin are also well studied.

It's acknowledged that structural analysis of Neogen-Quaternary molasse of Kolkhida intermont [1] and lava covers of South Georgian highland [2] in neotectonic stage revealed the following orophases of late Alpine orogenic stage: Attic (upper Miocene, pre-Meotian), Rhodanian (middle Pliocene), Wallachian (upper Pliocene, pre-Chaudian) and Pasaden (inquaternary).

After inversion of geotectonic regime (upper Sarmatian) clayed material of Oli-

gocene and Miocene comes into Kolkhida molasse basin. In lower Pliocene coarse-grained conglomerates of Meotian-Pontian out of limestone rock of Cretaceous (Attic phase) begin to arrive, after them conglomerates out of porphyrite rock of Middle Jurassic and granitoids of Paleozoic (Rhodanian phase) follow. Preservation of conglomerate facies with changing their lithofacies composition denotes: 1) arch-block rising of the Greater Caucasus along the inherited faults (Attic orophase) and existence of high mountains in lower Pliocene; 2) migration of folding into the side of Kolkhida intermountain molasse depression and formation of brachymorphos folds at foothills of Meskheti and Caucasus ranges (Rhodanian phase). In lower Pliocene folding in the region of Meskheti (Adjara-Trialeti) range (Attic phase) finishes, but the range is still rising along the Rhodanian fault and on the boundary with Kolkhida-foothill the overbreaking Rhodanian brachymorphos folds and Rhodan-Wallachian flexure are developing. Coming out over the boundary of the investigated by us region, in the Caucasus in lower Pliocene lavas erupt (Attic phase), and in the Middle and upper Pliocene (Wallachian phase) they are covered with new lava flows deformed forming structural-formation stages.

Thus during the whole Middle and Lower Pliocene mountains continue to rise differentially and look like arch-block clevations which are transformed into straight and inversion structural (morphostructural) forms like high mountain ranges, foothills and intermountain depressions deformed according to the climate morphosculptures.

Considering the volume of Pliocene molasse of the intermont during Upper Pliocene the relief of the Greater Caucasus was lowered approximately by 2km and Meskheti range by 1 km [1]. We assume that together with sculptural forms of exogenic origin there were levelled roughnesses, made by Attic and Rhodanian faults together with Rhodanian folds of foothills. The change of lithofacies content of correlated sediments prove this opinion.

Deposition of the greatly weathered granite and porphyrite conglomerates of the Upper Pliocene [3] on the planation surface of foothills and low-mountain areas of the Greater Caucasus denotes the domination of warm and humid climate in the Upper Pliocene.

Geomorphic correlation of genetically different Pliocene-Quaternary formations shows the following: step-like growth of the height of erosion slopes, along the faults between the profile of Chaudian terraces and levelled surfaces of watersheds towards the main watershed of the Greater Caucasus and Meskheti ranges, shearing by the levelling surfaces of Attic (Greater Caucasus) and Rhodanian faults and folds faults show the rejuvenation of deep faults and differentially arch-block uplifting of ranges. The planation surfaces are younger than Rhodanian folds, which they cut and are more ancient than erosion slope of Upper Chaudian terraces, so the age of the slope is correlated with Wallachian uplifting. Step-like deformation of upper Chaudian terrace paralelly to the planation surfaces, the presence of fresh granite pebble, brought from the watershed of the high mountain part of the Greater Caucasus and glacial formations on them show the revival of differential upliftings during the Quaternary time and reaching the Chionosphere by the mountains. Erosion slopes, which are lower than Chaudian terraces are correlated with Pasadenan phase.

Glaciation is younger and it is correlated with ancient Euxine terraces of the Black Sea, that is with Mindel [4]. River terraces, correlated I (new Black Sea's) and II (new Karangat) Black Sea terraces in the river heads are developed lower of Würm throughs

and are consequently younger. The profiles of ancient Karangat and Uzunlar terraces towards the mountains are between Würm and Mindel throughs. They correspond to Russian glaciation [5].

Thus, Wallachian phase clearly differentiates Sarmatian-Pliocene relief from Quaternary. The first one according to structural morphologic analysis is worked out on inherited and neotectonic structures and is expressed by mountain systems and adjacent to them foothills. The second one with inherited depression is expressed in the present relief by Quaternary accumulative plain. All these units represent morphostructures of different class. Common for all of them are morphosculptures and correlated or Quaternary marine and illuvial sediments on the plain and in submarine conditions [6].

Tbilisi I.Javakhishvili State University

REFERENCES

1. *A.L.Tsagareli, S.I.Kuloshvili.* Tektonika i metalogenia Kavkaza. Tb., 1984 (Russian).
2. *N.I.Skhirtladze, K.Shirinian, S.I.Kuloshvili.* Trudy TGU, 322, seria geografia-geologia. Tb., 1997 (Russian).
3. *J.I.Meskhia.* Soobsh. AN GSSR, **82**, 2, 1976 (Russian).
4. *D.V.Tsereteli.* Pleistotsen Gruzii. Tb., 1966 (Russian).
5. *J.I.Meskhia.* Vsesoiuznoe soveshchanie po problemam geomorfologicheskoi korrelatsii. Mater. XVII plenuma geomorf. komisii AN SSSR (tezisy), Tb, 1986 (Russian).
6. *J.I.Meskhia.* XVII plenum geomorfologicheskoi komissii SSSR. V kn. Osnovnye problemy teoreticheskoi geomorfologii. Novosibirsk, 1985 (Russian).

საქართველოს მეცნიერებათა აკადემიის მოამბე, 159, №3, 1999
BULLETIN OF THE GEORGIAN ACADEMY OF SCIENCES, 159, №3, 1999

GEOGRAPHY

I. Bondirev, G. Khachapuridze, M. Bochoridze

The Spatial Differentiation of the Earth Crust's Energetic Parameters and Geography of Ancient Civilizations

Presented by Corr. Member of the Academy Z. Tatashidze, April 6, 1998

ABSTRACT. **The existence of definite correlation among the ancient civilizations and energetic knots, which are located in the Earth crust, is considered in the present article. The emphasis is done on the spontaneous character of these knots and the wide range of fluctuation of the energetic knots.**

Key words: ancient civilizations, energetic knots, spatial correlation, instability.

According to the modern notions the world ancient civilizations appeared first on the slopes and piedmonts. Gradually, with the development of agriculture, these sociums came down to plains. Later, the great civilizations of Egypt, Sudan, India, China, Peru, Mesopotamia, etc. have been formed.

The significance of the hypsometric levels' fluctuation in the whole process of Homo-sapiens' development has been already mentioned in the previous studies [1]. According to the map in the appendix, those regions, where the existence of ancient civilizations is stated, are characterized by the following complex of natural conditions:

1. The ancient civilizations are located in a definite diapason of geographical coordinates-between the latitudes-25 South and 38-42 North. This is caused by the helioenergetical factor.
2. This area is connected with two or more stripes of the junction of lithospheric plates.
3. There are (or, inevitably, were in past) one or more "hot points" close to these areas.
4. There are also global circular structures-nuclears nearby.
5. These areas are located in the zone of active earthquakes.
6. Magnetic fields are characterized by the sharp anomalies;
7. The mentioned areas are edged by the mountain systems, sharply dismembered massifs.

According to the map, all upmentioned conditions are related to the extent of ancient civilizations' area. But there is an exception an additional factor exists in the West part of North America. This is a net of multiple astroblem-sign of bombardment by meteorite streams. It is supposed that because of this factor ancient civilizations, besides several attempts, could not strike roots in this area [2,3].

It is supposed that all upmentioned conditions are based on the energetic factor [4]. Examined regions represent powerful energetic knots, which are located in the earth-crust and create distinctly defined energetic fields.

In addition, the evolution of the organic world can be represented as materialistic display of the intercorrelation of the fields having the opposite direction, which are in

Cosmos and inside the Earth (magnetic, gravitational, photonar, thermal, etc.). These fields create biophysical conditions for more intensive development (evolution) for whole populations and population groups, as well as for each single organism. They cause hierarchically wide and complicated levels inside the biocenoses and sociums.

What are characteristics of these energetic knots? As it is known, the stream of energy, which comes from the depth of the earth is 20 000 times weaker in a whole, then the stream of energy, which comes down from the sun to the earth surface. But the endogenetic energy flows unevenly and locally. As a result of it a powerful concentration of energetic conditions occurs on the small area of the earth surface.

For example, in placid plate regime (average capacity of the earth crust is 37 km) energetic stream is not more than 70 MWm ; altitude of the relief is 400 m above the sea level [5]. In California, which represents tectonically active region, thermal stream from the depth is fluctuating 73-106 MW [6]. At the extense of convective streams in the earth mantle, speed of space heating reaches $10x10^{-12}$ W/kg [7]. It should be mentioned that the most part of the earth crust's flexible energy reveal on the boundaries of the lithospheric plates. It reaches 1000 V here.

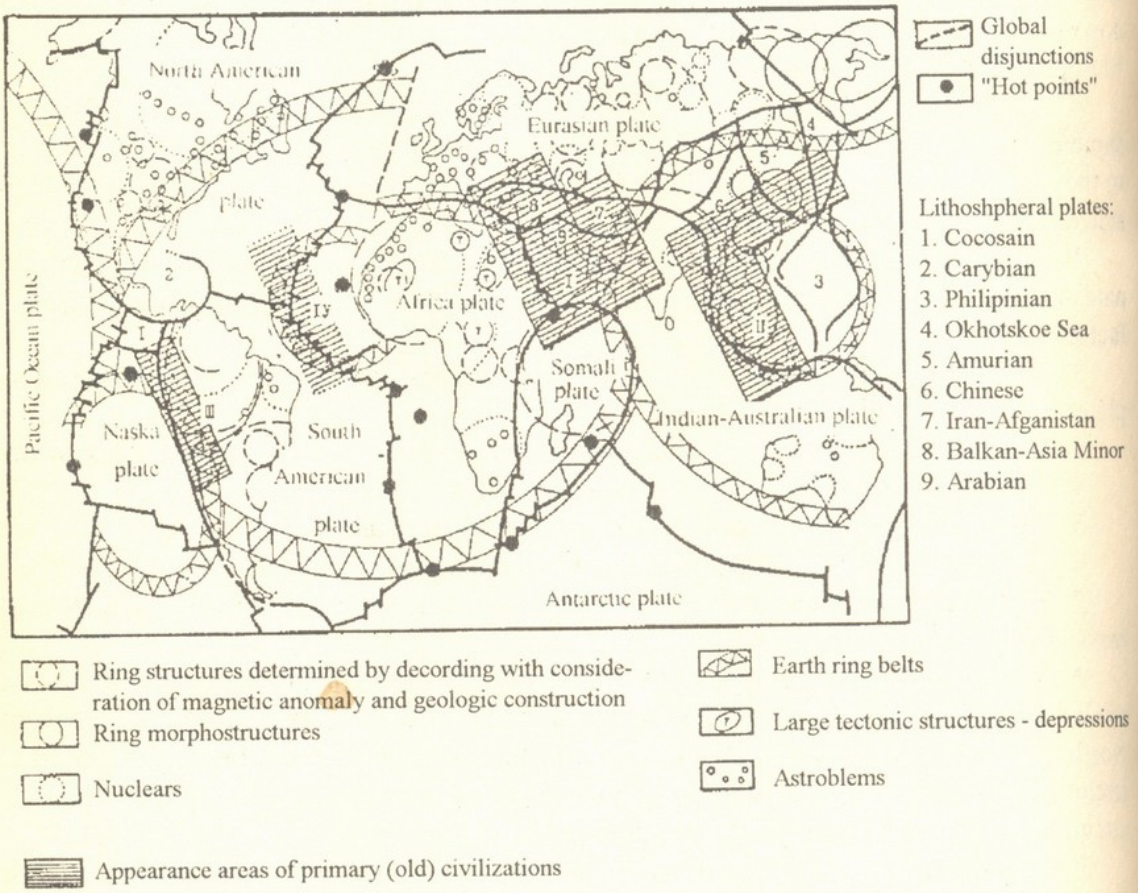

Fig.1. Litospheral plates, global disjunctions, basic ring structures and their correlation with apperance areas of primary (old) civilizations

The energopotential of geodynamic processes is given more detail in the following table.

Table

Some energetic characteristics of geodynamic processes

Parameter	Average data of energy potential		Boundaries of tectonic zones and lithospheric plates v/m^2	"Hot points" μ/calxcm^{2}xs	Earthquakes v/m^2
	Land v/m^2	Ocean v/m^2			
Energy concentrated in the Earth-crust	0.053	0.062	0.12-10x10^7	0.1-0.5	10^9-10^{22}

The unloading of energy in the earth crust often occurs like an explosion. Then comes a rather long period of its slow dispersion, which influences on the geological structures, as well as on the changes of the information and balance of energy on the area (landscapes) close to biosphere.

Proceeding from this, these parts of earth crust and their surface, are energetically unstable objects. These objects create a background, on which populations and sociums are compelled to develop faster and create a complicated system of adaptation-defensive reactions. The more the element of instability is, the more is intensity of natural selection in borders of particular ecosystems.

It should be mentioned, that these conditions may be considered from the other point of view. Cultures, which are related to the energetic knots, test eternal danger in case of powerful spontaneous discharge of energy, e.g. the civilization of Crete-Mikene perished from the explosion of the mighty volcano Santorin.

Georgian Academy of Sciences
V. Bagrationi Institute of Geography

REFERENCES

1. *I.V. Bondyrev.* Georg. Jour. Genetic Ecology. **1**, 2, 1995, 16-19.
2. *Cl. Wissler.* The relation of nature to man in aboriginal America. N-Y., 1926.
3. *C.W. Ceram.* Der Erste Amerikaner, Hamburg, 1972.
4. *I.V. Bondyrev.* Iv. Javakhishvili Georgian St. Univer. Sci. Sesion. Tbilisi, 1998 (Georgian).
5. *G.I. Reyner, D.I. Yoganson.* Boll. MOIP, sec. geol. **72**, 3, 1997, 5-13 (Russian).
6. *C.I. Williams.* US Geol. Surv. Bull., F1-F25, 1994.
7. *H.-P. Bunge, M.A. Richard.* Geoph. Res. Lett. **23**, 21, 1995, 2987-2990.

საქართველოს მეცნიერებათა აკადემიის მოამბე, 159, №3, 1999
BULLETIN OF THE GEORGIAN ACADEMY OF SCIENCES, 159, №3, 1999

HYDROLOGY

N. Bolashvili

Attempt of Flood Forecast on the Basis of the Theory of Recognition Images

Presented by Member of the Academy G. Svanidze, May 4, 1998

ABSTRACT. **The theory of images recognition and OP method is considered. Hypersurface was constructed giving the possibility to forecast water discharge increase with concrete values of the process causing factors.**

Key words: divisional surface, educational sequence, recognized controlling events.

Forecasting of some complicated natural processes (including flood) by means of determinative models is impossible nowadays. Computing methods of modern prognoses are based on statistical communications and regressive analysis. To get the satisfactory results by means of the above mentioned methods, it is obligatory to have the definite size empirical material. Although the use of these methods is limited. The so-called "rough" models help to solve the above problem. They have the ability to make small size empirical material with programme-algorithmical complexes.

Recently, the theory of image recognition has been spread in different branches of science, mostly in classificational and forecasting disciplines, and based on description of the Universe according to a man's perception.

The mathematical models of this theory are similar. An educational sequence is formed of the known situations and their corresponding types of researching process. The main task is to create the programme, by means of which educational sequence will produce (study) regulation and will make the same processional classification of unknown situations with receiving exactness.

The rule received by classification is estimated with examinational sequence that includes the known situations and their suitable classes in the same processes.

The theory of image recognition is described in many mathematical models [1]. Their majority bear field characteristics accounting some peculiarities of various fields.

A quite well known method OP [2,3], is rather effective and profitable in geographical science. "OP" represents the constructed method of the divisional surface - "Generalized Picture", which has a simple geometric interpretation: there is a hypersurface in space $\sum_{i=1}^{m} \lambda\varphi = 0$, which divides it into two subspaces. It is assumed, that if X vector is situated on one side of the flatness and the unequation $\sum_{i=1}^{m} \lambda\varphi \geq 0$ is carried out for it. Then it belongs to the first class, in other situations, it belongs to the second class.

The main attention is paid to the existed materials' quantity, the structure of researching process and the optimal expedients of approximately functioned complication.

The OP complex programs work in the space of the Binary qualities, which gives the possibility of quantitative and qualitative-logical description simultaneously. The main work runs automatically, but qualified interference of the specialist extremely improves the results.

The above mentioned method is claimed for classification of the regimes of the Kvirila (*h/p* Zestaphoni) and Tana (*h/p* Ateni) rivers.

We have selected two levels: the first one, when it was a speedy increase of water discharge (flood) and the other one, when the water level did not produce any effective changes (floodless). Both those processes have been described with the same forecasting factors: Air temperatures (medium and maximum) and deficit of humidity connected with the day of water flood and also a day before it, total volume of rainfall before flood, a day before it and water flood.

There was selected educational sequence of 20 events and 22 events of examinational trends on the river Kvirila (winter season). There were also selected the groups consisting of approximately 20 and 15 events on the river Tana.

The initial material has been presented in two classes. The factors' values were given to programme. These factors cause flood on the one hand and on the other hand they are not able to cause flood. The educational and examinational turns were already set, and the informational quality of each separate factor was approved. For optimization of all these factors, their gradual estimation was held, through which the most highly informational (0.64) factor was selected on the river Kvirila (medium temperature on the day of flood) and simultaneously classification was done. Just only this one factor was not enough to build divisional surface. For this purpose the following highly informational factor (maximum temperature before the day of water flood - 0.51) was added on the second stage. At the same time classification and divisional surface were constructed. The results of recognition are shown in Table 1.

Table 1

	A	B	A1	B1
flood	20	20	22	22
floodless	20	19	22	17

A is the initial number of educational sequence; A1- the initial number of controlling sequence; B - the number of recognized educational sequence; B1 - the number of recognized controlling sequence.

For improvement of the classification results the third highly informational factor (rainfall the day before flood, 0.36) was added, but the desirable effect was achieved by addition of the forth factor (rainfall the flood day, 0.26). Well-recognized cases increased to 20. The results did not change during the addition of the other factors (see Table 2).

Informatoinal quality of the factor was estimated for the river Tana, by similar types of calculation. The rainfalls on the day of water flood (0.39) carry the quality of the most

important informational factor. Not only the above mentioned factor, but also the other following highly informational factors (rainfall happening one day before flood, corresponds to 0.18) were not enough for construction of the divisional surface.

Table 2

	A	B	A1	B1
flood	20	20	22	22
floodless	20	20	22	20

Identification task was carried out and classification was established by using three changeable ones. We took the rainfall of previous periods (0.18) as a third changeable factor. So, we received the suitable result and by its means all events of flood were recognized. Then when there were no floods, from a lot of events just four ones were excepted by the programme and so divisional surface was built without them (see Table 3).

Table 3

	A	B	A1	B1
flood	20	20	15	15
floodless	20	20	15	11

Analyzing initial material we found that the excepted cases were created mainly by the factors, which differ from the educational sequences. It includes all those samples that programme avoided and could not learn.

At this stage of research classification has been carried out. Here is a rule made by our programme, which at the same time gives the possibility to fix process that may happen or not for the concrete significance of the factors. Perhaps next time we will try to search and analyze all complicated peculiarities of this problem. We will present already discussed events as gradations and subclasses, maybe after such presentation of events we will be able to pay attention to its intensive quality.

Georgian Academy of Sciences
V. Bagrationi Institute of Geography

REFERENCES

1. *N. Nilson.* Learning machines. Moscow, 1967 (Russian).
2. *V.N. Vapnik.* The alghoritms and programs of dependence restoration. Moscow, 1984 (Russian).
3. *V.A.Rumiantsev.* Possibility of using recognizaton systems for discharge forecasting. Works of SARNIGMI, 1972 (Russian).

საქართველოს მეცნიერებათა აკადემიის მოამბე, 159, №3, 1999
BULLETIN OF THE GEORGIAN ACADEMY OF SCIENCES, 159, №3, 1999

HEAT ENGINEERING

T. Magrakvelidze, N. Bantsadze, N. Lekveishvili

Similitude Equations for Calculating Heat Transfer Coefficient in Stirred Tanks

Presented by Corr. Member of the Academy P. Merabishvili, April 13, 1998

ABSTRACT. **Heat transfer from smooth and rough surfaces in stirred tank has been investigated experimentally. It was shown that two-dimensional artificial roughness increases heat transfer intensity for about two times. Equations for calculating heat transfer coefficient both for smooth and rough surfaces are obtained.**

Key words: heat, transfer, roughness, surface, turbulence.

Heat transfer intensification particularly in stirred tanks is of great practical interest. At the same time the intensification of heat transfer using the method of artificial roughness, when the liquid is turbulently mixed in a pool has not been investigated.

As it is known from [1], by means of artificial roughess heat transfer coefficient has been improved for about 1.6 times, when the mixer's paddles were situated at the same level as the heated surface was ($\Delta H = 0$). Later experimentally it was established that in case of different level replacement ($\Delta H = 30, 60, 90$ mm) heat transfer coefficient of rough surface is better than the smooth one for about 2 times.

The great number of experiments were done at different heights (h) and pitches (s) of the rough elements [2]. It was established, that the highest intensification of heat transfer appears when $5 \le s/h \le 10$. It was established also that increasing Prandtl number (Pr = 2 - 6.2) the degree of heat transfer intensification grows up. Particularly in case of smooth surface $Nu \sim Pr^{0.33}$ and in case of rough surface $Nu \sim Pr^{0.38}$.

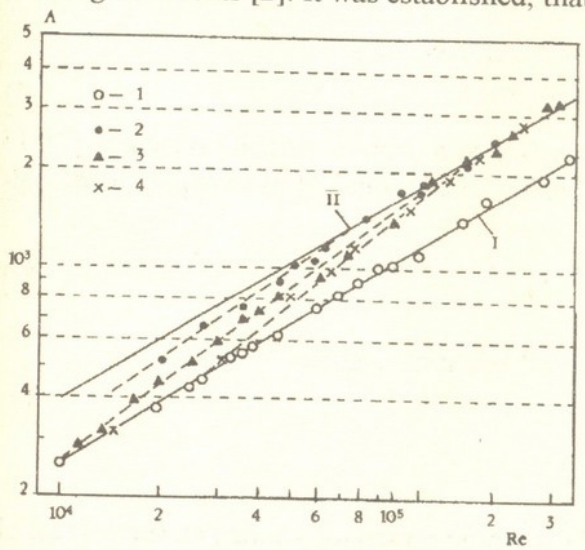

Fig.1. Relation between heat transfer intensity and Reynolds number in case of different height of roughness elements ($\Delta H = 0$). 1-smooth surface; rough surfaces, $s/h = 10$: 2 - h = 1.4mm. 3 - h = 0.5mm, 4 - h = 0.25mm. I-using equation (12), II-using equation (13).

In Fig. 1 experimental result are shown for smooth and rough surface as a relation $A = f(Re)$ when $\Delta H = 0$.

$$A = \frac{Nu}{Pr^m (D/d)^k (D/H)^{0.25}}, \qquad (1)$$

where $Nu = \alpha D/\lambda$ is Nusselt number, $Pr = \nu/a$- Prandtl number, $Re_c = nd^2/\nu$- Reynolds number, D is a diameter of the cylindrical tank, m; d is a diameter of the mixer, m; H is a level of the liquid in the tank, m; n is a rotational fre-

quency of the mixer, 1/sec; λ - thermal conductivity coefficient of the heated tube wall, w/k; a - thermal diffusivity of the liquid, m^2/sec; ν - kinematic viscosity of the liquid, m^2/sec; α - heat transfer coefficient, w/m^2k.

For smooth surfaces $m = 0.33$, $k = 0.35$; for rough surfaces $m = 0.38$, $k = 0.2$.

The data shown in Fig.1 were obtained when $\Delta H = 0$, $h = 0.25$. 0.5 and 1.4 mm.

From the diagrams (Fig.1) it can be seen three different regimes:

1. The range of Reynolds numbers where the artificial roughness has no influence on heat transfer intensification; 2. The range of Reynolds numbers where the effect of artificial roughness appears partially; 3. The range of Reynolds numbers where the effect of artificial roughness appears completely.

Here must be mentioned, that in apparatus with mixer the effect of artificial roughness is less, than in canals. Particularly in stirred tanks heat transfer intensification was about 60%, in canals - about 250%. The reason of such difference was explained by authors in investigation [1]. We offer analysis which is similar with [4] done for smooth surfaces.

As it is well-known in stirred tanks the liquid flow is three-dimensional. According to Konsetov in the first approximation it can be supposed, that the turbulence is isotropic [3]. Radial and axial streams are passing over the heated coil considered as a longitudinal.

$$Nu = (2Nu_{cr} + Nu_1)/3 \tag{2}$$

According to Zukauskas for cross flow in case of smooth surface [4]

$$Nu_{0cr} = \alpha_{0cr} d/\lambda = 0.25 Re^{0.6} Pr^{0.38} (Pr_f/Pr_w)^{0.25}. \tag{3}$$

For smooth surfaces in case of longitudinal flow can be used formula, offered by Mikheev [5]:

$$Nu_{0tan} = \alpha_{0tan} d/\lambda = 0.21 Re^{0.8} Pr^{0.43} (Pr_f/Pr_w)^{0.25}. \tag{4}$$

For longitudinal flow and rough surface by Gomelauri [6]

$$Nu_{tan} = \alpha_{tan} d/\lambda = 0.051 Re^{0.8} Pr^{0.47} (Pr_f/Pr_w)^{0.25}. \tag{5}$$

According to Levich $l = d/2$ can be considered as a characteristical dimension [7]. To determinate the average velocity of the turbulent fluctuations, let us examine power balance in apparatus:

$$N = K_N \rho n^3 d^5, \tag{6}$$

here K_N is a power criterion.

This power is equal to kinetic power of all streams together:

$$N = \Sigma N_i i. \tag{7}$$

The power of one stream is: $N_i = mu^2/2 = \rho u^3 l^2/2$.

here m is a mass of the stream.

The quantity of streams can be found by dividing apparatus volume on the volume of one stream: $i = \pi D^2 H/4l^3$. The total power

$$N = (\pi/8)\rho u^3 D^2 H/l \tag{8}$$

As far as $n = u_{tan}/\pi d$,

$$u = u_{tan}(8K_N/\pi^4)^{1/3}(d/D)^{2/3}(1/H)^{1/3}. \quad (9)$$

Using as a characteristical dimension the diameter of the vessel -D, taking into account, that $Re_c = nd^2/\nu = u_{tan}d/\pi\nu$, and substituting the meanings of u and l in equations (3) and (4), for smooth coil it can be written:

$$Nu_0 = (0.69Re^{0.6}Pr^{0.38}K_N^{0.2}(d/H)^{0.2}(D/d)^{0.6}(Pr_f/Pr_w)^{0.25}+$$

$$+0.026Re^{0.8}Pr^{0.43}K_N^{0.27}(d/H)^{0.27}(D/d)^{0.47}(Pr_f/Pr_w)^{0.25})/3. \quad (10)$$

For rough coil can be used equations (3) and (5):

$$Nu = (0.69Re^{0.6}Pr^{0.38}K_N^{0.2}(d/H)^{0.2}(D/d)^{0.6}(Pr_f/Pr_w)^{0.25}+$$

$$+0.063Re^{0.8}Pr^{0.47}K_N^{0.27}(d/H)^{0.27}(D/d)^{0.47}(Pr_f/Pr_w)^{0.25})/3. \quad (11)$$

In our case the calculations using equations (10) and (11) show that $Nu/Nu_0 = 1.3 - 1.5$. It's in a good agreement with experimental data.

The results published earlier and the data obtained in the present investigation can be generalized with the following equations which are more suitable for practical usage:

$$Nu_0 = C_0Re^{0.62}Pr^{0.33}(D/H)^{0.25}(D/d)^{k_0} \quad (12)$$

for smooth surface; and for rough surface:

$$Nu = C\,Re^{0.62}Pr^{0.38}(D/H)^{0.25}(D/d)^{k}. \quad (13)$$

Equations (12) and (13) are valid for two paddle mixers, $2 \le Pr \le 6.2$. When the heated coil and paddles are at the same level ($\Delta H = 0$), then $C_0 = 0.82$, $C = 1.27$, $k_0 = 0.35$, $k = 0.2$; and when $\Delta H \ge 30$mm, then $C_0 = 0.62$, $C = 1.16$, $k_0 = 0.25$, $k = 0$.

Equation (13) is valid for rough surface, when the roughness effect develops completely $5 \le s/h \le 10$.

From Fig.1 it can be seen, that experimental results are going in good agreement with equations (12) and (13).

Georgian Academy of Sciences
A. Eliashvili Institute of Control Systems

REFERENCES

1. *T. Maglakvelidze, N. Bantsadze, N. Lekveishvili.* Bull. Georg. Acad. Sci., 154, 3, 1996.
2. *Idem.* Proceed. A. Eliashvili Institute of Control Syst. Georg. Acad. Sci. , Tbilisi, 1997.
3. *V. V. Konsetov.* Journal of Engineering Physics. 10, 2, 1966.
4. *A.A. Zukauskas.* Convective Transfer in Heat-Exchangers. Moscow, 1982 (Russian).
5. *M. A. Mikheev.* Heat Transfer. Moscow, 1956.
6. *V. I. Gomelauri.* Proceed. Institute Phys. Georg. Acad. Sci. **9**, 1963.
7. *V. G. Levich.* Physical and Chemical Hydrodynamics, 1959.

საქართველოს მეცნიერებათა აკადემიის მოამბე, 159, №3, 1999
BULLETIN OF THE GEORGIAN ACADEMY OF SCIENCES, 159, №3, 1999

F. Shatberashvili , O. Sichinava, A. Siamashvili

Some Hydraulic and Hydromorphometric Regularities of Flow in Stable Beds

Presented by Member of the Academy O. Natishvili, February 3, 1999

ABSTRACT. **The approaches for determining soil bed parameters were studied. New dependence to calculate the permissible velocities for types of soils is proposed.**

Key words: hydraulics, irrigation, river, stable beds, velocities.

Selection of stable routes run across unlined soils, i. e. unprotected from the action of water is important for construction of hydraulic power, irrigation and reclamation engineering facilities, for rational use of water and preservation of environmental ecosystems [1-3]. It is actual to determine the optimal parameters and forms of river beds, in which the main hydraulic characteristics of the water flow and the physical and mechanical properties of the bed soils prove to be decisive.

To calculate the permissible velocities for types of soils according to the norms and instructions adopted at present the dependences proposed by Ts.Mirtskhoulava are used [2].

We considered the equilibrium conditions of an aggregate located on the slope of watercourses of water-saturated cohesive soils. The aggregates are assumed to be of spherical shape and linked by a cohesion force [3].

The limiting equilibrium conditions of the aggregate are estimated by the expression:

$$N\left(\frac{P_e}{M_s F}+\frac{P_f \delta_1 d}{M_b W}\right)-\frac{G_{WT}}{F}\le G_{ctr}+\frac{G_{WN}}{F}, \qquad (1)$$

where P_e, P_f, are the frontal and ejective forces, G_{WT} is the tangential component of the mass of the aggregate in water, G_{WN} the normal component of the aggregate mass, M_s and M_b are the respective coefficients for the strain and bend of the aggregate. It is assumed that $M_s = M_b = M$ [4], N is the overload coefficient, G_{ctr} is the minimum possible ground calculation resistance to tension, F the area of the resting part of the aggregate, G_e the weight of the aggregate in water, W the moment of the resting part resistance.

Introducing $P_f = P_e$, G_{WT}, G_{WN}, F, W values in expression (1) we obtain the following critical expression of velocity

$$V_0=\sqrt{\frac{2M}{\rho_0\left(\frac{4\lambda_x\delta_3}{\pi\delta_4^2}-\frac{\lambda_y\delta_1\delta_2}{0{,}098\delta_4^3}\right)}\left[\frac{2}{3\delta_4^2}(\rho_4-\rho_0)gd[\cos\alpha-\sin\alpha]+G_J^H\right]}. \qquad (2)$$

Taking into account the values of the λ_x, λ_y, δ_1, δ_2, δ_3, δ_4 coefficients [5] and the logarithmic distribution of velocity the values of washout velocity are determined for cohesion soils in beds of trapezoidal form

$$V_C = \left(\lg \frac{8.8h_{mean}}{d}\right)\sqrt{\frac{2M}{1.3\rho_0 n}[(\rho_4 - \rho_0)gd(\cos\alpha - \sin\alpha) + 1.25C_y^H \cdot K]}. \quad (3)$$

Taking into consideration the dependence between the eroding and non-eroding velocities $V_C = 1.4\ V_n$ (2), (3), we shall finally obtain the following values of the bottom and mean velocities permissible on the channel bed slope of trapezoidal cross-section

$$V_{H(bot)} = \left(\lg \frac{8.8h_{mean}}{d}\right)\sqrt{\frac{2M}{2.6\rho_0 N}[(\rho_4 - \rho_0)gd(\cos\alpha - \sin\alpha + 1.25C_y^H \cdot K]} \quad (4)$$

$$V_{\Delta H(bot)} = 1.25\sqrt{\frac{2M}{2.6\rho_0 N}[(\rho_4 - \rho_0)gd(\cos\alpha - \sin\alpha) + 1.25C_y^H \cdot K} \quad (5)$$

Experiments were conducted on special hydraulic installations for soils of various cohesion and conditions of trapezoidal sections of various forms, thereby defining the limits of application of the dependences obtained [4,5].

Morphometric regularities of dynamically stable beds are also proposed towards a perfect solution of the problem set in [6].

For the case of regulated water courses:

$$\frac{B}{H} = KQ^{x_1}(GI)^{-x_2}d^{-x_3}, \quad (6)$$

where B and H are the width and mean depth of the bed; Q is the calculated water discharge for 10% provision; d is the mean weighted thickness of the bed bottom layer deposit; I is the longitudinal gradient of the water surface; g is the free fail acceleration 9.81.

The deposit of the bed slopes and bottom in non-cohesion soils is formed of various (gravel) materials whose parameters have the following numerical values

$$k = 0.42,\ x_1 = 0.159,\ x_2 = 0.08,\ x_3 = 0.354.$$

As for the boundary value of the B/H parameter, the increase of which leads to the start of the breakdown of its stability in plan, it is determined by the condition:

$$\left(\frac{B}{H}\right)\sqrt{\lambda Fr} \le 0{,}45 \quad (7)$$

where λ is the hydraulic friction coefficient, while Fr is the Froude number for the mean depth of flow taking into consideration the expression $\lambda = 8g/C^2$, $F_z = V_0/gH$, the proposed criterion assumes the following form:

$$\frac{B}{H} = \frac{0.16C\sqrt{H}}{V_0}, \quad (8)$$

where C is the velocity coefficient, V_0 is the permissible non-eroding velocity.

The bed elements of cohesive soils may be calculated by the expression:

$$\frac{B}{H}=6.1\left(\frac{Q}{\sqrt{1+94.7C_y}}\right), \tag{9}$$

where C_y is the normative strength of the soil.

A comparison of the results obtained by the proposed method with the data of studies carried out by other authors in natural conditions has shown good agreement permitting the use of the approaches discussed above in assessing the limit state of the bed.

Georgian Academy of Sciences
Institute of Water Management and
Engeneering Ecology

REFERENCES

1. *V. C. Altunin.* Meliorativnye kanaly v zemlianykh ruslakh. 1989, 255 (Russian).
2. *Ts. E. Mirskhulava.* Razmyv rusel i metodika otsenki ikh ustoichivosti. 1967, 180 (Russian).
3. *V. N. Goncharov.* Dinamika ruslovykh potokov. L. 1968, 374 (Russian).
4. *O. A. Sichinava, A. A. Siamashvili.* In: Problemy ecologii i melioratsii. Tbilisi, 1990, 82-89.
5. *O. Sichinava, A.Siamashvili.* Soobchenie Academii nauk Gruzii, 124, 1, 1986 (Russian).
6. *F. A. Shatberashvili.* Materials of Intern. Seminar on flood prevention. Insburg, Avstria, 1971, 15.

საქართველოს მეცნიერებათა აკადემიის მოამბე, 159, №3, 1999
BULLETIN OF THE GEORGIAN ACADEMY OF SCIENCES, 159, №3, 1999

T.Gvelesiani, R.Danelia, G.Berdzenishvili

Mathematical Model of Nonstational Hydrodynamic Processes of Mobile Mud Flow on the Bottom of Reservoir

Presented by Member of the Academy O.Natishvili, April 10, 1999

ABSTRACT. **Wave process generated in reservoir as a result of constant thickness mud flow spreading on its bottom is regarded. Corresponding solution of flat boundary problem is obtained on the basis of the theory of small amplitude waves and assumption that liquid is ideal, but its movement is potential. The results of computer calculations are given for one of the examples: wave profiles for various moments of mud flow spreading on the bottom.**

Key words: mud flow, wave, reservoir.

The formation of mud flows followed by negative ecological effects on the environment and significant material losses is rather frequent in some mountain regions [1,2]. In order to provide secure functioning of flooding structures (dams, embankments etc.) it is necessary to make engineering prognostic calculations in respect to mud flow action on hydraulic structure. This implies not only determination of dynamic action of the mud flow directly on the structure [2], but also consideration of the action of those hydromechanical forces which originate (in the form of waves and hydrodynamic pressures) as a result of mud flow running into reservoir and spreading in it.

Due to the difficulty of the mentioned processes at present there is little known about the interaction of mud flow with water in the reservoir [3].

Particularly, maximum wave amplitude is determined immediately on the place of mud flow ertry into reservoir [3]. Beneath we regard more generalized mathematical model according to which in schematic reservoir (L length and H depth) at the initial moment ($t = 0$) wave process is originated from one of its sides as a result of stratified D_c thickness mud flow running and then its spreading on the bottom ($t > 0$) with velocity $U_c(x,t)$ during t_0 period (until its stopping) (Fig.1). It is meant that "excitation zone" of B_c length originates as a result of water driving out in front of mud flow where the movement of water flows is mainly directed vertically up (Fig.1). It is assumed that the velocity of this movement on the whole B_c section is uniform and equals W_c. Together with the mud flow movement dislocation of B_c excitation zone took place along X-axes during $0 < t < t_0$. When $t > t_0$ mud flow movement stopped and $U_c = 0$. Assume $U_c(x,t) = U_c = \text{const}$. At that time (Fig.1) transposition coordinate $S_c(t)$ of mud flow equals:

$$S_e(t) = \begin{cases} \int_0^t U_e(x,\tau)d\tau = U_e t, & \text{when} \quad 0 < t < t_0 \\ U_e t_0 = S_0, & \text{when} \quad t \geq t_0, \\ 0, & \text{when} \quad t \leq 0. \end{cases} \tag{1}$$

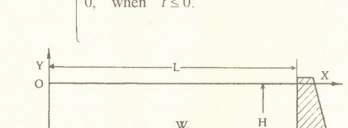

Fig.1. Calculation scheme of nonstational wave process originated as a result of mud flow movement on the bottom of reservoir

Formation of the above mentioned hydrodynamic problem is derived on the basis of small amplitude wave theory [4] assuming that the liquid is ideal in the reservoir and its motion is potential.

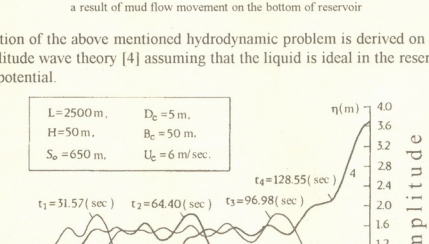

Fig.2. Wave profiles of mud flow spreading on the bottom of the reservoir in various moments (t_1,t_2,t_3,t_4) of different time (t_1,t_2,t_3,t_4)

In this case the solution of the problem is the solution of equation $\Delta\varphi = 0$ (where $\varphi(x,y,t$ for is velocity potential; $\Delta = \partial^2/\partial x^2 + \partial^2/\partial y^2$) for corresponding initial and boundary conditions. Particularly, boundary condition on the bottom of the reservoir can be written as:

$$\frac{\partial \varphi(x,y,t)}{\partial y} = \begin{cases} W_c, & \text{when} \quad S(t) \le x \le s(t) + B_c, \\ 0, & \text{when} \quad S(t) + B_c < x \le L, \\ 0, & \text{when} \quad t < 0, t > t_0. \end{cases} \tag{2}$$

where $W_c = D_c S_0 / B_c t_0$, because $S_o D_c = W_c t_0 B_c$.

To obtain the solution of the problem (or determination of j-function) method of integral transformation was used in relation to t and x variables [4]. For determination of wave amplitudes $\eta(x,t)$ generated by mud flow in reservoir, the mentioned solution can be written as:

$$\eta(x,t) = \frac{W_c B_c}{L} I_0(t) + \frac{2W_c}{L} \sum_{n=1}^{\infty} \frac{\cos a_n x}{a_n cha_n h} \cdot \frac{1}{\sigma_n^2 - y_n^2} \cdot I_n(t), \tag{3}$$

where $I_0(t) = \begin{cases} t, & \text{when} \quad o < t < t_0, \\ t_0, & \text{when} \quad t > t_o \end{cases}$ $\quad n = 1,2,3,...$

$$I_n(t) = C_n \sigma_n (\cos \gamma_n t - \cos \sigma_n t) + S_n (\sigma_n \sin \sigma_n t - \gamma_n \sin \gamma_n t), \quad 0 < t < t_0;$$

$$I_n(t) = C_n (\sigma_n \cos \gamma_n t + \gamma_n \sin \sigma_n t_0 \sin \gamma_n \Delta t - \sigma_n \cos \sigma_n t_0 \cos \gamma_n \Delta t) +$$

$$+ S_n (\sigma_n \sin \sigma_n t_0 \cos \gamma_n \Delta t + \gamma_n \cos \sigma_n t_0 \sin \gamma_n \Delta t - \gamma_n \sin \gamma_n t), \quad t > t_0;$$

$$a_n = \frac{n\pi}{L}; \Delta t = t - t_0; S_n = \sin \chi_n; C_n = \cos \chi_n - 1; \chi_n = n\pi (B_c / L);$$

$$\sigma_n = n\pi (U_c / L); \gamma_n = \sqrt{a_n g th a_n h};$$

g is accelaration of free-fall.

The results of carried calculations using formula (3) for one of the examples are given in Fig.2. Wave profiles are expressed in it (among them in case of maximum level raising at the embankment) for various moments of spreading of the mud flow on the bottom.

Georgian State Agrarian University

REFERENCES

1. *M.S.Gagoshidze.* Selevye yavlenia i bor'ba s nimi. Tbilisi, 1970 (Russian).
2. *O.Natishvili et al.* Intern. Seminar on antimud flow phenomena. Tbilisi, 1969.
3. *T.G.Voinich-Syanozhenski, E.S.Avaliani.* O volnakh generiruemykh v vodokhranilischakh vstupleniem selevykh potokov. Moscow, 1974 (Russian).
4. *F.Griado, T.Gvelesiani et al.* Appl. Math. and Informat. 2, Tbilisi, 1997.

საქართველოს მეცნიერებათა აკადემიის მოამბე, 159, №3, 1999
BULLETIN OF THE GEORGIAN ACADEMY OF SCIENCES, 159, №3, 1999

V. Mdzinarishvili

New Orthonormal Systems Based on Even Numbers

Presented by Member of the Academy V. Chichinadze, October 12, 1998

ABSTRACT. **New orthonormal systems based on even numbers are received. The new orthonormal system based on odd number is used. Illustrative example is given.**

Key words: orthonormal, even, approximation.

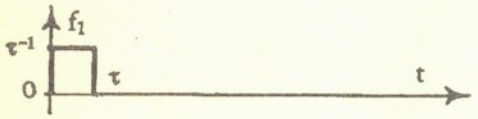

Fig. 1

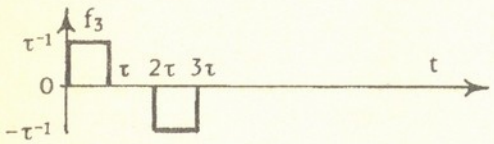

Fig. 2

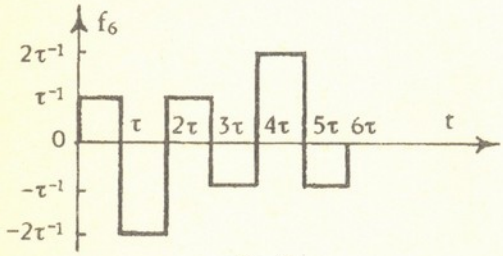

Fig. 3

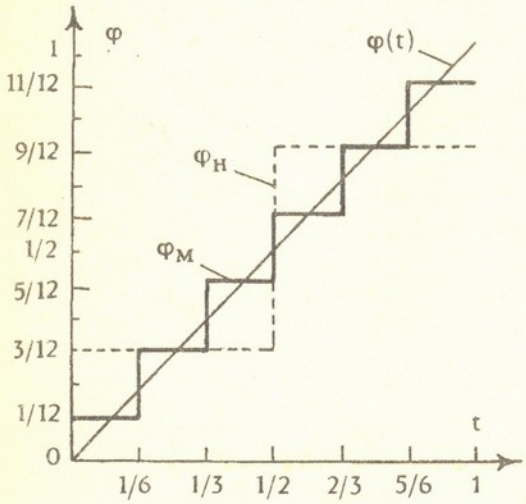

Fig. 4

Let's consider a sequence of functions $f_1(t)$, $f_3(t)$ and $f_6(t)$ shown in Figs. 1-3.

Laplace transform of this function is:

$$F_1(s)=\frac{1-e^{-\tau s}}{\tau s},\ F_3(s)=\frac{1-e^{-\tau s}}{\tau s}(1-e^{-2\tau s}),$$

$$F_6(s)=\frac{\left(1-e^{-\tau s}\right)^3}{\tau s}(1-e^{-3\tau s})$$

where $s=\sigma+j\omega$, and $j=\sqrt{-1}$

Instead of the function $f_6(t)$ arbitrary function $f'_6(t)$, which cross the axis Ot as many times as the function $f_6(t)$, can be used. As an example, let's take the function $f_6'(t)$, Laplace transform of which is

$$F'_6(s)=\frac{1}{\tau s}(1-e^{-\tau s})^6.$$

If the orthonormalized process [1] is used with respect to these functions we'll have the following system (collection) of orthonormal functions

$$M_1=1(t)\ t\in[0,1],\ M_3=\frac{\sqrt{3}}{\sqrt{2}}\begin{cases}1, & t\in\left[0,\frac{1}{3}\right)\\ 0, & t\in\left(\frac{1}{3},\frac{2}{3}\right),\\ -1, & t\in\left(\frac{2}{3},1\right]\end{cases}$$

$$M_6 = \frac{\sqrt{6}}{\sqrt{2}} \begin{cases} 1, & t \in \left[0, \frac{1}{6}\right) \\ -1, & t \in \left(\frac{1}{6}, \frac{1}{3}\right) \\ 1, & t \in \left(\frac{1}{3}, \frac{1}{2}\right) \\ -1, & t \in \left(\frac{1}{2}, \frac{2}{3}\right) \\ 1, & t \in \left(\frac{2}{3}, \frac{5}{6}\right) \\ -1, & t \in \left(\frac{5}{6}, 1\right] \end{cases}$$

Instead of vector-column M_6 vector-column M'_6 can be used:

$$M'_6 = \frac{\sqrt{6}}{\sqrt{2}} \begin{cases} 1/\sqrt{5}, & t \in \left[0, \frac{1}{6}\right) \\ -1, & t \in \left(\frac{1}{6}, \frac{1}{3}\right) \\ 1, & t \in \left(\frac{1}{3}, \frac{1}{2}\right) \\ -1, & t \in \left(\frac{1}{2}, \frac{2}{3}\right) \\ 1, & t \in \left(\frac{2}{3}, \frac{5}{6}\right) \\ -1/\sqrt{5}, & t \in \left(\frac{5}{6}, 1\right] \end{cases}$$

However, for orthonormal decomposition while estimating the coefficient the integrated interval is grouped as [1]:

$$\left\{\left[0, \frac{1}{6}\right), \left(\frac{5}{6}, 1\right]; \left(\frac{1}{6}, \frac{1}{3}\right), \left(\frac{2}{3}, \frac{5}{6}\right); \left(\frac{1}{3}, \frac{1}{2}\right), \left(\frac{1}{2}, \frac{2}{3}\right)\right\}.$$

Finite result of approximation will be the same for M_6 and M'_6.

We received the orthonormal system created on the basis of even numbers (with the exception of numbers 2^n, $n = 0, 1, 2, 3, \ldots$) in two steps:

1. First let's construct orthonormal system on the basis of odd numbers m [2]:

$M_1 = 1(t)\ t \in [0,1],$

$$M_{l,m} = \frac{m^{\frac{1}{2}}}{2}\begin{cases} 1, & t \in \left[0, \frac{2}{m}\right) \\ (\alpha_k - 1)\alpha_k^{-1}, & t \in \left(\frac{2}{m}, \frac{4}{m}\right) \\ (\alpha_k - 2)\alpha_k^{-1}, & t \in \left(\frac{4}{m}, \frac{6}{m}\right) \\ \vdots & \\ \alpha_k^{-1}, & t \in \left(\frac{k-2}{m}, \frac{k}{m}\right) \\ 0, & t \in \left(\frac{k}{m}, \frac{k+1}{m}\right) \\ -\alpha_k^{-1}, & t \in \left(\frac{k+1}{m}, \frac{k+3}{m}\right) \\ \vdots & \\ -(\alpha_k - 2)\alpha_k^{-1}, & t \in \left(\frac{m-6}{m}, \frac{m-4}{m}\right) \\ -(\alpha_k - 1)\alpha_k^{-1}, & t \in \left(\frac{m-4}{m}, \frac{m-2}{m}\right) \\ -1, & t \in \left(\frac{m-2}{m}, 1\right] \end{cases}, \quad M_m = \left(\frac{m}{2}\right)^{\frac{1}{2}}\begin{cases} 1, & t \in \left[0, \frac{1}{m}\right) \\ -1, & t \in \left(\frac{1}{m}, \frac{2}{m}\right) \\ 1, & t \in \left(\frac{2}{m}, \frac{3}{m}\right) \\ \vdots & \\ 1, & t \in \left(\frac{k-1}{m}, \frac{k}{m}\right) \\ 0, & t \in \left(\frac{k}{m}, \frac{k+1}{m}\right) \\ 1, & t \in \left(\frac{k+1}{m}, \frac{k+2}{m}\right) \\ \vdots & \\ -1, & t \in \left(\frac{m-3}{m}, \frac{m-2}{m}\right) \\ 1, & t \in \left(\frac{m-2}{m}, \frac{m-1}{m}\right) \\ -1, & t \in \left(\frac{m-1}{m}, 1\right] \end{cases} \tag{2}$$

where $k = 2, 3, 4, \ldots$, $l = k+1$, $m = 2k+1$, $\alpha_k = [0.5k+1] - 1$, $[\alpha]$ is the whole part of α numbers; the case, when $k = 1$, is given in expression (1).

2. Then we make doubling of the appropriate vector-column M_m norm, again doubling etc.:

$$M_{2m} = m^{\frac{1}{2}}\begin{cases} 1, & t \in \left[0, \frac{1}{2m}\right) \\ \vdots & \\ -1, & t \in \left(\frac{k}{2m}, \frac{k+1}{2m}\right) \\ 1, & t \in \left(\frac{k+1}{2m}, \frac{k+2}{2m}\right) \\ \vdots & \\ -1, & t \in \left(\frac{2m}{m}, 1\right] \end{cases}, \quad M_{4m} = (2m)^{\frac{1}{2}}\begin{cases} 1, & t \in \left[0, \frac{1}{4m}\right) \\ \vdots & \\ -1, & t \in \left(\frac{k}{4m}, \frac{k+1}{4m}\right) \\ 1, & t \in \left(\frac{k+1}{4m}, \frac{k+2}{4m}\right) \\ \vdots & \\ -1, & t \in \left(\frac{4m-1}{4m}, 1\right] \end{cases} \tag{3}$$

Collection (3) is a continuation of orthonormal system (2).

In general case, when we have even number $q = bm$ ($b = 2^{\nu}$, $\nu = 1, 2, 3, \ldots$) let's write down the sequence of orthonormal functions:

$$M_1, M_{1,m}, M_m, M_{2m}, M_{4m}, \ldots, M_{q/2}, M_q \tag{4}$$

where each element of vector-column Mq belongs to the intervals $\left(\frac{k^*-1}{q}, \frac{k^*}{q}\right)$ $k^* = 1, 2, \ldots, q$.

By means of change of parameter ν and m we can receive any dimension of vector-column M.

For example: M_{36} and M_{216} can be received with the following sequence by double number

$$M_9 \to M_{18} \to M_{36}; \quad M_{27} \to M_{54} \to M_{108} \to M_{216}.$$

If we create orthonormal system (4) by module q, which equals to arbitrary even number 6, 10, 12, 14,.... then the following theorem is valid.

Theorem. *If q is even number for which the orthonormal system is constructed, then boundary relation*

$$\lim_{(bm)_n \to \infty} \int_0^1 \left[\varphi(x) - \sum_{i=0}^{(bm)_n} (\varphi M_i) M_i(x) \right]^q d\mu \to 0, \tag{5}$$

where $(bm)_n q^0, q^1, q^2, \ldots, q^n$, q=const, $n = 0, 1, 2, \ldots, \infty$, *is executed by Lebegian measure* $d\mu$ *and is valid for each function* $\varphi(x)$ *belonging to* L^q *class, i. e.* $\varphi(x) \in L^q$.

Example. The function $\varphi(t) = t$, $t \in [0,1]$ is given. It is necessary according to (5) to find the approximating function $\varphi_M = \sum (\varphi M_i) M_i$. In Fig. 4 the approximation curve φ_M is shown when $q = 6$ and $n = 0, 1$ (1). It is seen that convergence of function φ_M like Haar's function φ_H is uniform. But in case of function φ_M approximation error is smaller than

$$\varphi_H = \sum_{i=0}^{2^n} (\varphi H_i) H_i .$$

In case, when $m = 1$, vector-columns $M_{1,m}$ and M_m change into zero and orthonormal function system (4) change into Haar's system.

Gori Economic-Humanitarian Institute

REFERENCES

1. *V. Mdzinarishvili*. Bull. Georg. Acad. Sci, **159**, 1, 1999, 121-125.
2. *V. Mdzinarishvili*. Bull. Georg. Acad. Sci, **159**, 2, 1999, 296-299.

საქართველოს მეცნიერებათა აკადემიის მოამბე, 159, №3, 1999
BULLETIN OF THE GEORGIAN ACADEMY OF SCIENCES, 159, №3, 1999

BOTANY

Sh. Shetekauri

Biotopes of Petrophytic Flora of the High Mountain Caucasus

Presented by Corr. Member of the Academy G. Nakhutsrishvili, May 25, 1998

ABSTRACT. **High mountain florocoenotic community of the Central and Eastern Caucasus and their biotopes are studied. The rich variety of biotopes is revealed in different vertical belts. The lithological location is declared as the centre of speciation.**

Key words: petrophyte, lapischistophyton, glareophyton, endemics, lithological locations.

The Central and Eastern Caucasus has specific features in its flora and the unique geologo-geographical history reaching far back in time. It is distinguished by the variety of ecotype spectrum of floristic areas influenced by physico -geographic peculiarities of vertical belts, composition of slopes, air humidity, moisture-holding capacity, etc. Under the term "mountain flora" the unity of floristic composition of the upper borders of the woods is understood [1,2] relatively coinciding with the levels where the mean July isotherm is ranging from 10 to 11^0C.

The petrophytes of Central and Eastern parts of the Caucasus (1800-3600) m ASL (Svaneti, Racha-Lechkhumi etc., Tusheti, Khevsureti, mountain regions of Kakheti) have been investigated. Petrophylous flora in comparison with other high mountain florocoenotic communities is the richest in amount of endemic species [3,4]. The wealth of endemics in mountain floras is explained not only by their geological age, but also by climatic contrasts. Mountain plants are far better resistant to the weather conditions than lowland plants. That's why the amount of endemic species increases in high mountain despite the dwindling of the plant coverage. It should be marked that petrophylous florocoenotic communities are distributed in various lithological locations of Central and Eastern parts of the Caucasus: rock streams, moraines etc., and rarely in high mountain meadows and alpine mats and contain all types of species of the landscape and vertical belts: the woodbelts, subalpine, alpine and subnival belts. In wooding subalpine and alpine belts cenosiums of petrophytic flora, layers, competition and cooperation, etc. are marked. We can not say the same about the upper alpine, subnival belts, where petrophylous flora makes small coenosiums, aggregations or subaggregations [5] of fragments of phytocoenosiums.

Inspite the richness of existing lithophylous locations in floristic species they still create only small communities, and coenotic alliances (especially on the first stage of succesion) are undeveloped. This is proved by small coverage and layering. The list of distinguished main biotope groups and their combinations is given beneath (Table).

1. Shaley, granitic, porphyritic rocks covered by obligatory chasmophytes: *Omphalodes loikae* Somm. et. Lev., *Saxifraga ruprechtiana* Manden., *Silene linearifolia* Otth., *Draba*

bryoides DC, *Campanula kryophyla* Rupr., *C. argunensis* Rupr., *Hypericum nummularioides* Trautv., *Scrophularia lateriflora* Trautv., *Jurinea filicifolia* Boiss., *Senecio lapsanoides* Dc., *Minuartaia bieberschteinii* (Rupr.) Schischk.

2. Chalk-stone rocks are covered by obligatory chasmophytes: *Campanula dzaaku* Albov., *C. fonderwisii* Albov., *C. rathensis* Charadze, *C. anomala* Fom., *Draba mingrelica* Schischk.

3. Shaley, granitic, porphiritic rock streams, moraines, pebbles, covered by obligatory lapischistophyton, morainophyton, glareophyton: *Cerastium multiflorum* C. A. Mey., *Coluteicarpus vesicaria* (L.) Holmoboe, *Silene caucasica* (Bunge) Boiss., *S. humilis* C. A. Mey., *Pseudovesicaraia digitata* (C.A. Mey.) Rupr., *Ranunculus tebulossicus* Prima, *Delphinium caucasicum* C. A. Mey., *Cerastium kazbek* Parrot., *Noccaea pumila* (Stev.) Steud.

Table

The variety of Central and Eastern Caucasus high-mountain petrophytic flora

	Ecobiomorphs	Main biotops	Vertical belts
1.	Obligatory chasmophyton	shaley, granitic porphyritic rocks	woods, subalpine, alpine, subnival
2.	Obligatory chasmophyton	chalk-stone rocks	woods, subalpine
3.	Obligatory laphishistophyton, morainophyton, glareophyton	shaley, granitic, porphyritic rock streams	woods, subalpine, alpine, subnival
4.	Obligatory lapishistophyton	chalk-stone rock streams	woods, subalpine
biotops combination			
1.	Facultative lapishistophyton, morainophyton, glareophyton	rock streams, moraines, pebbles	woods, subalpine, alpine, subnival
2.	Facultative chasmophyton, lapishistophyton, morainophyton, glareophyton	rocks rock streams, moraines, pebbles	woods, subalpine, alpine, subnival
3.	Facultative chasmophyton, lapishistophyton, glareophyton	rocks, rock streams, pebbles	woods, subalpine, alpine, subnival
4.	Facultative chasmophyton, lapishistophyton	chalk-stone rocks, chalk-stone rock streams	woods, subalpine

4. Chalk-stone rock streams and moraines are covered by obligatory glareophyton, lapischistophyton, morainophyton: *Psephellus colchicus* Sosn., *Gentiana oschtenica* (Kusn.) Woron., *Scutellaria helenae* Albov., *Ranunculus abchasicus* Freyn.

Chalk-stone biotopes in Central and Eastern Caucasus are rare (Khvamli; Chalk-stone ridge in Racha) and are mainly located in woods and subalpine belts. We have not investigated morainophyton as a separate biotope for unstable floristic composition of moraines.

The floristic species located on moraines could be found in the petrophylous communites as well as in florocoenotic complexes of alpine meadows and alpine mats [6].

Alongside with main biotopes we distinguished various combinations of biotopes.

Those biotopes are occupied by species with relatively widespread location – so called facultative lapischistophyton, chasmophyton, morainophyton, glareophyton. Some of them are: *Aetheopappus caucasicus* Sosn., *Thymus caucasicus* Willd.ex. Ronn., *Myosotis alpestris* L., *Oberna lacera* (Stev.) Sims., *Sedum caucasicum* (Grossh.) A. Bor., *Cerastium polymorphum* Rupr., *Veronica gentianoides* Vahl., *Poa alpina* I., *Colpodium versicolor* (Stev.) Schmalh.

The variety of ecotype spectrum existing in high-mountain belts is the result of destruction under pressure after freezing of water [4]. Narrow, middle destructions, cabbles, immobile, mobile and hard mobile destructions, moraines, cracks etc.) are the special locations where endemic species of the Caucasus are concentrated [7]. Those biotopes differ according to distribution of floristic species. Narrow, mobile and unstable biotopes are occupied by single floristic species, whereas dense floristic community is found on stable, immobile biotopes of upper alpine belts.

The investigation of Central and Eastern Caucasus high-mountain flora has shown that the majority of endemic and rare species are found in petrophylous flora. All endemic genera found in the Caucasus, and also *Trygonocarium* Trautv., *Pseudovesicaria* (Boiss.) Rupr., *Symphyoloma* C. A. Mey., *Pseudobetckea* (Hoeck) Lincz., *Sobolevskya* Bieb., *Mandeovia* Alava, etc. are connected with the above mentioned biotopes.

The investigation proves that Central and Eastern Caucasus owns its profusion of endemic species to climate diversity and location and creates exceptionally favourable conditions for arising of numerous local endemics [8]. The lithological location is the centre of speciation.

Georgian Academy of Sciences
N. Ketskhoveli Institute of Botany

REFERENCES

1. *A. Doluchanov, M. Sachokia, A. Kharadze.* Trudy Tbil. Bot. Inst. 8, 1942, 113-132 (Russian).
2. *R. Gagnidze, Sh. Shetekauri* In: Rastitelnyi mir visokogornykh ekosystem. Vladivostok, 1988, 202-226 (Russian).
3. *Sh. Shetekauri.* Bull. AN GSSR, **119**, 3, 1985, 592-595 (Russian).
4. *Sh. Shetekauri.* Ser. Biol. **20**, 1-6, 1994, 117-123 (Russian).
5. *B. Norin, L. Kitcing, O. Michailova.* Bot. zhurnal. **67**, 12, 1982, 1609-1617 (Russian).
6. *John R. Spence, Richard J. Shaw.* Creat Basin Natur. **41**, 2, 1981, 232-242.
7. *A. Magakian.* Etapy razvitia visokogornikh lugov Zakavkaziya, Erevan, 1947, 189 (Russian).
8. *A. Kolakowskii, S. Adzinba.* Bull. Georg. Acad. Sci. **140**, 3, 1990, 577-580 (Russian).

საქართველოს მეცნიერებათა აკადემიის მოამბე, 159, №3, 1999
BULLETIN OF THE GEORGIAN ACADEMY OF SCIENCES, 159, №3, 1999

PLANT PHYSIOLOGY

E. Chkhubianishvili, L. Kobakhidze, Sh. Chanishvili

UV-Radiation Effect on Content of Total Protein and Productivity of some Vegetable Cultures

Presented by Member of the Academy G. Sanadze, April 13, 1998

ABSTRACT. **Influence of additional ultraviolet (UV) radiation in field conditions (using DRT-400 lamp) was studied on experimental plants of carrot (*Daucus sativus* L.), radish (*Raphanus sativus* L. var. radicula D. C.) and beet (*Beta vulgaris* L.). In studied plants the highest content of total protein was found in the middle period of vegetation. The following intensities of radiation; 60-133 "C" section, 1000-1400 "A" section and 9500-20400 J. $m^{-2}.min^{-1}$ PhAR seemed to be the most favorable for plant productivity. It is supposed, that in field conditions photoreactivation of negative effect of short wave UV-radiation takes place.**

Key words: root vegetable, UV-radiation, total protein, productivity.

During the last years UV-radiation is considered as a significant regulative factor of biochemical processes of plant. Its effect is associated with the changing of ozone screen stability. Even the little changes in stratospheric ozone amount may induce relatively high biological effect of UV-radiation. It is known, that short wave UV-radiation (280-320 nm), taken separately, negatively affects the accumulation of dry and fresh substances, inhibits the growth of seedlings, but slightly influences on the protein content [1,2].

It is shown also, that the negative effect of UV-radiation is connected with the plant species specificity and ability to synthesise UV-radiation absorbing substances (anthocyanes and others) [3-6]. At the same time, there are data on the stimulative effect of UV-radiation on protein accumulation in leaves of maize, kidney-bean and radish [7-9]. As a matter of this, the purpose of our investigation was to study the additional UV-radiation influence on the content of total protein and plant productivity in root vegetables carrot (*Daucus sativus* Hoffm.) beet (*Beta vulgaris* L.) and radish (*Raphanus sativus* L. var. radicula D. C.) in field conditions.

In different stages of vegetation the weight of the above-and underground parts of plants was measured. The content of total protein in leaves was studied after Lowry [10].

The bulb DRT-400 was used as a source of radiation. The intensity of radiation was measured by dosimeter DAU-81, which made possible to estimate the intensity of photosynthetically active radiation PhAR, "C" and "A" sections. The experimental variants differed in distance from the source of radiation i. e. in amount of received intensity of radiation (Table 1). In control variants the amount of total proteins in leaves varies with the age of plant. The content of protein in leaves reaches its maximum in the middle of vegetation. Then the content decreases. It is cleared, that selected plants have different content of total protein: it is more in radish and less in beet and carrot leaves (Table 2).

The additional UV-radiation affected the content of total proteins.

Table 1

Intensity of additional UV- radiation /J.m^{-2}.min^{-1}/

Section	Variants					
	1	2	3	4	5	Background
"C"	186	133	60	40	20	-
"A"	2200	1400	1000	601	204	-
"PhAR"	41600	20400	9500	3700	1900	1100

Among the plants of the first variant, where the intensity of radiation was the highest, at the beginning of vegetation influence of additional radiation was less observed and the experimental plants hardly differed from control ones. In further stages of vegetation the content of protein in irradiated leaves clearly decreased.

Table 2.

UV-radiation effect on the content of total protein in leaves (mg.g^{-1} of fresh weight)

Plant	Period of vegetation	Control	Variants				
			1	2	3	4	5
Radish	Beginning	7.6	6.5	8.4	16.7	6.7	7.1
	Middle	9.2	8.3	13.0	18.1	13.0	10.0
	End	3.5	1.8	10.1	10.0	7.1	2.8
Beet	Beginning	3.6	3.8	4.1	9.0	3.5	3.0
	Middle	5.8	3.8	5.0	8.4	4.9	5.0
	End	2.1	1.9	3.0	6.1	3.1	2.5
Carrot	Beginning	3.5	4.1	8.3	8.9	5.0	3.8
	Middle	5.1	3.0	10.5	10.3	5.7	4.1
	End	3.0	2.1	8.1	8.8	2.9	3.0

In the fourth and fifth variants of experimental plants the content of proteins either approaches or exceeds the control.

Especially the second and third variants of experiments must be mentioned, where the additional UV-radiation induced considerable effect. From the beginning of vegetation the content of total protein in leaves of irradiated plants exceeded the control. These plants maintained high content of protein up to the end of vegetation, wich reached its maximum at the middle of development. The obtained data are associated with the weight of the above and underground parts of plants. The influence of radiation on the amount of fresh weight is given (Table 3).

In the one pair of leaf phase the above- and underground parts of the first, second, third and fourth variants of irradiated radish do not differ in weight. The weight of control and fifth variant plants is relatively low. In the two and three pair leaves phase the most effective were the second and the third variants of experiment. UV-radiation has considerably increased the weight of the above and underground parts (Table 3).

We may conclude, that the intensity of radiation, which corresponds to 60-133 of "C" section, to 1000-14000 of "A" section and 9500-20400 J.m^{-2}.min^{-1} of PhAR, has positively affected the productivity of plants and protein accumulation in leaves.

It is known, from the literature, that first of all, the short wave UV-rays affect the structural and functional state of the photosystem II. Reactionary centres and the sections of water breaking and oxygen isolation serve as targets for the damagable action of these rays [11,12]. A. Kolin and N. Gorbatchevich studied the effect of different dozes of UV-radiation on potato tuber. It was revealed, that the UV-rays promoted leaf number and area increase, activated photosynthesis and biochemical processes in plants [13]. Similar data are obtained for tomato [14], cucumber [15] and carrot [16].

Table 3

UV-radiation effect on the fresh weight of the above and underground parts of radish (g.)

Variant	One pair leaf phase		Two pair leaf phase		Three pair leaf phase	
	aboveground	underground	aboveground	underground	aboveground	underground
Control	1.94	0.20	4.72	0.38	13.17	1.03
1	2.90	0.35	5.07	0.64	29.96	1.51
2	2.21	0.36	11.50	0.86	62.11	4.09
3	2.33	0.36	11.45	0.83	93.89	8.13
4	2.26	0.37	5.73	0.48	15.21	1.85
5	1.87	0.28	4.66	0.43	12.92	0.85

There are some data, after which the negative action of short-wave UV-radiation on plants is declined by the additional long wave radiation [17].

In our experiments UV-radiation was used only in sunny days, as addition to a day light spectrum, while "C", "A" and "B" sections were not isolated. Therefore, it may be supposed, that photoreactivation of the negative effect of short wave UV-radiation takes place. This is reflected through the positive influence of UV-radiation on plants of the second and the third variants.

Georgian Academy of Sciences
N. Ketskhoveli Institute of Sciences

REFERENCES

1. *C. V. Vu, L. H. Allen, A. Garrald.* Environ. and Exp. Bot., **28**, 34, 1982, 465-473.
2. *T. Juschi, A. Megumi, Sh. Hideyaki et al.* Physiol Plant, **76**, 3, 1989, 425-430.
3. *M. Tevini, A. H. Teramura.* Photochem. and Photobiol., **50**, 4, 1989, 479-487.
4. *F. Borman.* Photochem. and Photobiol., **8**, 3, 1991, 337-347.
5. *C. F. Musil, S. J. E. Wand.* Plant, Cell and Environ, **17**, 3, 1994, 245-255.
6. *W. Rou, H. Hofmann.* Wetter and Leben, **45**, 4, 1993, 5-16.
7. *L. A. Khodarenko, A. E. Barai.* In: Optimisation of the Photosynthetical Apparatus by the Action of Several Factors. Minsk, 1976, 32-39 (Russian).
8. *M. Teoni, W. Jwanzi, V. Thema.* Planta, **153**, 4, 1981, 388-394.
9. *A. F. Tibuseio, M. T. Pinol, M. Serano.* Environ. and Exp. Bot., **25**, 3, 1985, 203-210.
10. *O. H. Lowry.* Methods of Enzimology, II, 1956, 448-450.
11. *J. F. Borman.* Photochem. and Photobiol., **4**, 2, 1989, 145-158.
12. *J. Panagopoulos, G. F. Borman, L. O. Byorn.* Photochem. and Photobiol. **8**, 1, 1990, 73-87.
13. *A. R. Colin, N. A. Gorbatchevich.* In: Problems of Photoenergy of Plants and Arise of Photoproductivity . Lvov, 1984, 143-144 (Russian).
14. Techno Jap., 22, 7, 1989, 144.
15. *S. J. Britz, P. Adams.* Photochem. and Photobiol., **60**, 7, 1994, 116-119.
16. *A. S. Sultanbaev.* Proc. Acad. Sci. Kirgizstan, **17**, 12, 1991 (Russian).
17. *K. Odilbekov, G. Shamansurov.* Proc. Acad. Sci. Tajik. SSR. 1, 1987, 83-85.

საქართველოს მეცნიერებათა აკადემიის მოამბე, 159, №3, 1999
BULLETIN OF THE GEORGIAN ACADEMY OF SCIENCES, 159, №3, 1999

PLANT PHYSIOLOGY

N.Kacharava, L.Gamkrelidze, N.Datiashvili, Sh.Chanishvili

Effect of UV-Radiation on some Root Plants Productivity

Presented by Member of the Academy G. Sanadze, April 14, 1998

ABSTRACT. **The influence of additional UV-radiation on the photosynthetic intensity, content of plastid pigments and productivity of root plants: beet (*Beta vulgaris* L. ssp. esculenta), carrot (*Daucus sativus*, Hoffm.) and radish (*Raphanus sativus* L.) was studied. It was revealed, that the additional UV-radiation has increased all the studied characteristics. Stimulative effect was different for studied species following the developmental phases and dozes of radiation. Differences in chloroph./carot. ratio between experimental plants was revealed. In carrot and radish increase of carotenoides synthesis may be conditioned by protective function of these pigments. It is supposed, that the influence of additional UV-radiation on experimental plants is expressed in photoreactivation.**

Key words: UV-radiation, plastid pigments, productivity, root plants.

One of the important problems of recent photobiology is to study the effect of ultraviolet(UV) rays in the forming of morphophysiological chracteristics and adaptive mechanisms of plant, correspondingly to unfavourable conditions. The purpose becomes more important in respect to destrucive changes of ozone screen, which are responsible for increase of UV-radiation on the Earth. In such conditions plant vegetation decrease, decline of biological productivity and competative ability between species may be expected [1-4]. There are some opposite suppositions, according to which photobiological reactivation and inductive processes may occur in plant as an adaptation to the changed radiation regime to decrease its harmful effect [5-8].

The purpose of our investigation was to study the influence of additional UV-radiation on the photosynthetic apparatus of plant and to reveal how the changed radiation regime affects plant productivity.

For experiments the root plants: beet (*Beta vulgarus* L. ssp. esculenta), carrot (*Daucus sativus* Hoffm.), and radish (*Raphanus sativus* L.) were selected. Experiments were done after [9, 10].

In our studies the bulb DRT-400 served as a source of artificial radiation with short wave "C" section. To make different radiation regime, plants were divided into five variants. The distance between them was 10 m. The last fifth variant was in 40-50 m from the source. The intensity of radiation of DRT-400 bulb in "C" section for the first variant was about 0.06 $W.cm^{-2}$ and for the fifth variant -0.02 $W.cm^{-2}$.

The additional radiation was given during the whole vegetation only in sunny days (5, 6 hours a day). Plants were collected during the three calendar periods: I - the beginning, II - the middle and III - the end of vegetation.

The intensity of photosynthesis was measured radiometrically [11]. The content of

plastid pigments was studied after [12]. For studying the biological productivity 10 plants from every variant were weighed. Experiment was repeated 3-fold.

In our experiments affecting with UV-radiation "C" section (so-called F-regime) not only declined the unfavourable influence of UV-radiation on photosynthesis, but intensified the process (Table 1).

The stimulative effect is different in species, phases of vegetation and radiation dozes. In beet and radish the maximum of photosynthesis is mentioned in the third variant, while for carrot the most suitable were the weak dozes of the 5th variant plants. Recently obtained results are in agreement with our early investigations [8, 13].

Following our data F-regime had increased pigments synthesis (Table 2), which is especially clearly expressed at the end of vegetation. The difference in chl./carot. ratio of the experimental plants should be mentioned.

Table 1

Effect of UV-radiation on photosynthetic intensity (imp·min^{-1}·10^{-3}·g^{-1} dry weight)

Variant	Period of vegetation					
	Middle			End		
	Beet	Carrot	Radish	Beet	Carrot	Radish
Contr.	575	218	185	329	185	142
I	776	281	212	348	191	190
II	832	397	291	422	245	220
III	915	346	484	455	268	267
IV	786	411	327	421	231	212
V	701	494	317	415	217	220

By this index there is no difference between the control and experimental variants in beet, while in carrot and radish the additional radiation has decreased this ratio on the account of carotenoids synthesis enhancement.

Table 2

Effect of UV-radiation on plastid pigments content (mg · g^{-1} fresh weight) at the end of vegetation

Variant	Chlor.	Carot.	Chlor./Carot.	Chlor.	Carot.	Chlor./Carot.	Chlor.	Carot.	Chlor./Carot.
Contr.	2.12	1.00	2.0	1.67	0.64	2.6	1.93	1.20	1.6
I	2.24	1.07	2.0	1.74	0.79	2.2	2.10	1.47	1.4
II	2.33	1.13	2.0	1.80	0.81	2.2	2.10	1.50	1.4
III	2.45	1.16	2.1	1.81	0.81	2.2	2.16	1.54	1.4
IV	2.42	1.15	2.1	1.92	0.87	2.2	2.04	1.45	1.4
V	2.40	1.13	2.1	2.01	0.91	2.2	2.04	1.43	1.4

Following the data from literature it is possible, that the increase of carotenoids synthesis in radish and carrot is conditioned by the protective functions of these pigments, while in beet such role of defencive screen may have anthocyanes of phlavonoid

nature [1, 5, 6]. This shows the difference in adaptive mechanisms to F-regime.

Increase of photosynthesis under the influence of radiation is expressed in plant productivity (Table 3). At the end of vegetation the weight of experimental roots was 2 - 2.5 fold higher than that of control ones. In beet and radish the highest index of root weight and green mass was mentioned in the third variant of experimental plants, in carrot - in the 5th variant.

Table 3

Productivity of root plants at the end of vegetation (average of 10 plants)

Variant	Beet		Carrot		Radish	
	aboveground	underground	aboveground	underground	aboveground	underground
Control	-	850	-	400	120	280
I	-	900	-	500	350	450
II	-	1500	-	400	520	600
III	-	1850	-	450	650	622
IV	-	1300	-	500	380	540
V	-	1600	-	900	300	500

Following our data the positive influence of UV-radiation on experimental plants was expressed in the intensification of photosynthesis, in plastid pigments synthesis and productivity increase which may be explained by the photoreactivation phenomenon.

According to recent suppositions [1,14], photoreactivation proceeds by the acting of high sensitive enzyme photolyase, which is activated by means of long UV wave (λ = 360, 390 nm) rays and serves as a source of electrons for reconstruction of damaged structures.

It may be supposed, that described molecular mechanism may serve for F-regime effect explanation.

Georgian Academy of Sciences
N.Ketskhoveli Institute of Botany

REFERENCES

1. *G. I. Fraikin.* Fiziologiya rastenii, **34**, 4, 1987 (Russian).
2. *W. B. Sisson, M. M. Caldwell.* Expt. Bot., **28**, 4, 1977.
3. *F. M. Fox, M. M. Caldwell.* Oecologia, **36**, 2, 1978.
4. *P. D. Usmanov, I. G. Mednik et al.* Fiziologiya rastenii, **34**, 4, 1987 (Russian).
5. *M. Tevini, W. Ivanzik, V. Thoma.* "Role Solar Ultraviolet Radiat. Mar. Ecosystem Proc. NATO Conf. Copenhagen, 28 -31 July, 1980", 1982.
6. *J. F. Borman.* Photochem. and Photobiol. **8**, 3, 1991.
7. *I. P. Sokolov.* Priroda, 2, 1977 (Russian).
8. *N. T. Kacharava, M. N. Chrelashvili.* Mtsenare da ultraisperi skhivebi, Tb., 1978 (Georgian).
9. *A. S. Sultanbaev, L. P. Sokolov.* Priroda, **12**, 1982 (Russian).
10. *O. A. Aknazarov.* Dr. Sci. Thesis, Dushanbe (Russian) 1991.
11. *V. L. Voznesenski et al.* Metody issl. fotosinteza i dikhania rast. M., 1965 (Russian).
12. *V. F. Gavrilenko et al.* Bolshoi practikum fiziologii rastenii, M., 1975 (Russian).
13. *Sh. Chanishvili, N. Kacharava, L. Gamkrelidze, L. Kobakhidze.* Proc. Acad. Sci. Georgia, **22**, 1-6, 1996 (Georgian).
14. *G. B. Sanear, A. Sanear.* Trends in Biochemical Sciences /TIBS/ **12**, 7, 1987.

საქართველოს მეცნიერებათა აკადემიის მოამბე, 159, №3, 1999
BULLETIN OF THE GEORGIAN ACADEMY OF SCIENCES, 159, №3, 1999

PLANT PHYSIOLOGY

T. Barblishvili, Sh. Chanishvili, E. Giorgobiani, M. Dolidze, G. Badridze

Influence of Source-Sink System on Starch Content in Grapevine Leaves

Presented by Member of the Academy G. Sanadze, November 17, 1998

ABSTRACT. **The effect of source-sink relations on starch accumulation in grapevine leaves (*Vitis vinifera* L., var. "Rkatsiteli") was studied. Exporting capacity of leaf was artificially altered by means of partial defoliation, stem ringing and exogenous growth regulators. Partial defoliation (30%) enhanced starch accumulation in leaves. Stem ringing caused the high level of starch and changed its diurnal dynamics. Leaf treatment with growth regulators slightly increased starch content. In case of cluster treatment starch content was decreased probably due to enhancement of sink demand.**

Key words: starch, source-sink system, defoliation, stem ringing, growth regulators, grapevine.

Regulatory function of starch is a peculiar problem of endogenous regulation of photosynthesis. When supply of assimilates for trophic and energetical needs of growth is limited or active photosynthesis exceeds epigenetic demands of plant, temporal depositions of assimilates are originated. The "extra" assimilates accumulate in reserve structures of plant. While changing external conditions starch is found to be the most variable carbon fraction of a plant [1-4].

The diurnal periodicity of starch content has been established for grapevine leaves [5].

We studied the influence of source-sink relations on starch accumulation intensity of grapevine leaves. Source-sink relations were changed by defoliation, stem ringing and application of growth regulators.

The diurnal course of starch accumulation in different zone leaves of field-grown grapevine (*Vitis vinifera* L., var. "Rkatsiteli") was investigated. Starch content in leaves was determined colorimetrically according to [6]. Indices presented in tables are mean values of three replicates. Partial defoliation and stem ringing were performed two days before the analysis. Leaf or cluster were twice, per minute, treated with solutions of growth regulators: ABA (abscisic acid) - 40 ppm, IAA (indoleacetic acid)-50 ppm, BAP (benzylaminopurine)-100 ppm. Starch content was determined on the third day after treatment with growth regulators.

It was established that incompletely expanded leaves of the upper-zone with the source function didn't accumulate the detectable amount of starch. It implied that photoassimilates were almost fully utilized for growth processes (Table 1).

Table 1

Diurnal dynamics of starch content in different zone leaves in berry intensive growth phase (% in dry weight)

Time, h / Leaf zone	7	10	14	18	20	21	22
Upper	0	0	0	0	0	0	0
Middle	0.18	0	3.63	4.80	4.98	4.56	4.26
Lower	1.42	1.30	4.00	4.50	5.50	7.00	6.15

The middle-zone leaves accumulated about 5% of starch, while in lower-zone leaves maximum content of starch reached 7%. Maximum of starch content was gained for 21h. Then it decreased due to starch hydrolysis, utilization of hydrolysis products for growth processes and their translocation towards the reserve organs. In the morning hours in the middle-zone leaves the trace of starch was found, but in lower-zone leaves its content was higher - 1.42%. As it seems, the export of assimilates from the middle-zone leaves is more intensive, than that from the older lower-zone leaves. Middle-zone leaves might utilize more assimilates for growth, while lower-zone older leaves are characterized with lower metabolism due to which starch reserve isn't fully utilized. Starch content indices are in accordance with data obtained for the same variety "Rkatsiteli" [5].

As the middle zone leaves of "Rkatsiteli" are characterized with maximum intensity of photosynthesis and high source activity, the effect of partial defoliation and stem ringing on starch accumulation was examined in these leaves.

Defoliation is an artificial mean affecting exporting capacity of donor leaf. In a number of plant species partial removing of leaves causes activation of assimilates export from the remained leaves and decrease of starch content [1, 7, 8].

Contrary to the above data after partial defoliation significant rise of starch content was marked in middle-zone leaves (Table 2)

Particularly, maximum content of starch was twice as large as in control plant leaves. Possible explanation of this fact is considerable intensification of photosynthesis after defoliation. Although according to some literature data defoliation causes stimulation of photosynthesis or its inhibition [1].

Table 2

Effect of defoliation and ringing on starch content in middle-zone leaves (Diurnal dynamics) (% in dry weight)

Time,h / Variant	7	10	14	18	20	21	22
Control	0.15	0	3.23	4.96	4.98	4.94	4.70
Defoliation	2.20	1.50	2.83	5.80	8.72	7.95	7.73
Ringing	12.75	9.95	15.20	11.65	11.50	10.20	10.15

In the case of stem ringing, when due to phloem cutting export of assimilates from leaf was ceased, great amount of starch accumulated in leaf. As it seems, such high content of starch disturbs normal course of photosynthesis and dynamics of starch deposition [2]. Starch level in leaves reached its maximum value - 15.20% for the midday.

During the rest period of the day the accumulated starch was partly decomposed and in the evening its content was nearly the same as in the morning.

As photosynthesis and transport of assimilates undergo the hormonal control [2], we studied the effect of exogenous growth regulators on starch content of leaf (Table 3).

Table 3

Effect of growth regulators on starch content in leaves (% in dry weight)

Phase	Leaf treatment				Cluster treatment			
	Contr.	+ABA	+BAP	+IAA	Contr.	+ABA	+BAP	+IAA
Berry set	1.60	1.90	2.15	1.85	1.70	1.78	1.82	1.80
Berry intensive growth								
Upper-zone leaves	0.42	0.53	0.79	0.60	0.50	0.42	0.46	0.44
Lower-zone leaves	0.46	0.57	0.61	0.55	0.48	0.26	0.26	0.30

In berry set phase starch content of leaves treated with growth regulators was higher than of control ones. In the case of cluster treatment practically no effect occurs. Enhancement of starch in treated leaves may be explained by the stimulative effect of growth regulators on photosynthesis [9, 10].

In the following, berry intensive growth phase, starch content in lower zone leaves decreased because of the active supply of assimilates for growing cluster. In upper-zone young leaves in the case of leaf treatment this index slightly increased, but in the case of cluster treatment it reduced in both zone leaves and especially in lower-zone leaves. This result may be explained by the strengthened sink activity caused by growth regulators and by the nearness of lower-zone leaves to the cluster.

Thus, after partial defoliation starch content in grapevine leaves increases which might be caused by the intensification of photosynthesis in the remained leaves. Diurnal dynamics of starch accumulation is similar to the control. In the case of stem ringing high level of starch accumulation is observed during the whole day time.

Starch content in upper-zone young leaves treated with growth regulators increases, possibly due to intensified photosynthesis. In berry intensive growth phase when cluster is a strong sink, starch accumulation in treated leaves slightly increases. When growth regulators are applied to the cluster, starch accumulation decreases, especially in lower-zone leaves. This may be caused by the activation of assimilates export from the leaf.

Georgian Academy of Sciences
N. Ketskhoveli Institute of Botany

REFERENCES

1. *V. I. Chikov*. Fotosintez i transport assimilyatov. M., 1987, 186 (Russian).
2. *A. T. Mokronosov*. Fotosinteticheskaya funktsiya i tselostnost rastitel'nogo organizma. M., 1983, 63 (Russian).
3. *M. V. Turkina, O. A. Pavlinova*. Fiziologiya rastenii, **28**, 1, 1981, 184-205 (Russian).
4. *D. R. Geiger*. Can. J. Bot. **54**, 1976, 2337-2345.
5. *Sh. Sh. Chanishvili*. Peredvizhenie assimilyatov v vinogradnoi loze. Tbilisi, 1964, 102 (Russian).
6. *H. N. Pochinok*. Metody biokhimicheskogo analiza rastenii. Kiev, 1976, 134-138 (Russian).
7. *A. T. Mokronosov, R. A. Borzenkova*. Peredvizhenie veshchestv i metabolizm rastenii. Gorkii, 1972, 49-55 (Russian).
8. *T. F. Wareing, M. M. Khalifa, K. G. Treharne*. Nature, **220**, 5, 1968, 453-457.
9. *T. Barblishvili, M. Dolidze, Sh. Chanishvili*. Bull. Georg. Acad. Sci. **157**, 1, 1998, 103-106.
10. *T. Barblishvili, M. Dolidze, Sh. Chanishvili, G. Badridze*. Bull. Georg. Acad. Sci. **158**, 3, 1998, 485-487.

საქართველოს მეცნიერებათა აკადემიის მოამბე, 159, №3, 1999
BULLETIN OF THE GEORGIAN ACADEMY OF SCIENCES, 159, №3, 1999

PLANT GROWING

G. Agladze, A. Korakhashvili, G. Jimsheladze, A. Zubiashvili

The Actions for Improvement of the Georgian Arid Pastures

Presented by Corr. Member of the Academy T. Urushadze, May 4, 1998

ABSTRACT. **The arid pastures of Georgia are concentrated in the country and within watersheds of Mtkvari, Iori and Alazani rivers. They are presented by various associations, characteristic of semideserts and dry steppes and are located at the altitude of 90-900 m ASL , occupying the area of more than 300 thousand ha in lowland and under-mountainous zones and partially in the foothilly regions of eastern Georgia. These lands are used as seasonal pastures in winter and partially in spring and autumn for pasturing, cattle-breading and mainly for sheep breeding.**

Key words: arid pastures, semi-desert, dry steppes vegetation.

The climate in the zone of arid pastures is mostly dry, subtropical. The high location of some massifs and different degree of penetration of continental air currents from Aral-Caspian semi-deserts and deserts within their limits has considerable influence on the diversity of the climate. The average annual temperature varies from -12.0 to +14.2^0 C. The average monthly temperatures of the coldest months (January, February, December) vary from +0.3 to +2.5^{0}C and the average minimal temperature of these months is -1.8, 3.8^{0}C below zero. The average monthly temperature of the hottest months (July, August) reaches 22.8-25.7^{0}C. The average duration of frost-free period varies from 216 to 252 days.

The average annual precipitation varies from 200-250 (Samoukhi semi-desert) to 390-430 mm (Shiraki, Udabno, Kara-Douz massifs). Very unequal distribution of precipitation monthwise is a characteristic feature. The largest amount of precipitation comes in spring in the form of heavy shower and there are much less rains in winter and autumn [1].

The wind regime is characterised basically by northern and north-east point winds, most strong and frequent within western and north-west parts of the region.

The topsoil of the arid pastures of Georgia is greatly diversified. In flood lands and riverside terraces we find alluvial and also brown soils. In many massifs considerable areas are occupied by saline soils and salt-marshes. The plains and gentle slopes of table-lands are occupied by black earth and partially by dark chestnut soils and in case of more steep slopes we have brown forest soil. Along with denudative erosive and accumulative processes, the evaporation of moisture in summer stipulating enrichment of top horizons of the soil with salts over considerable areas, has a significant impact on the environment [2].

The vegetation is not less diversified. In the semi-desert zone various associations of wormwood pastures prevail whose edificator is Hansen's wormwood *Artemisia fragrans.* The considerable areas occupied by grasslands are represented by various wormwood groups of halophilous plants: *Salsola nodulosa, Salsola dendroides, Salsola ericoides*; ephemeral grasses: *Poa bulbosa, Agropyron pectinifolium, Bromopsis japonicus,*

Brachypodium distachyum, Hordeum leporinum, Medicago minima, Veronica polita etc.

The semi disert vegetation has been used as winter pasture for pairing sheepbreeding from time immemorial. This can be explained mainly by the climate, soil conditions and biological peculiarities of the basic plants of these pastures. Dry summer, very little precipitation, saline soils creating no possibility for agriculture without preliminary land-improvement and existence of fodder grass and plants determined these lands to be used as pastures. The character of precipitation distribution determining development of ephemeretum and eating of the main fodder plant Hanzen's wormwood by sheep only after the first autumn frost and a number of other reasons conditioned their use as pastures just in winter.

The vegetation of dry steppes is used as winter and transition (in spring and autumn) pastures, and in some more rainy years for laying in the hay as well. The following plants make the grassland of these pastures: *Koeleria gracilis, Phleum phleoides, Colpodium humile, Carex bordzizilowski, Medicago coeruela, Falcaria vulgaris, Lolium verum.*

The productivity of semi-desert pastures greatly varies depending on climatic conditions of a year and mainly on the amount of autumn and spring precipitation. The analyses of the data accumulated through many years of study of crop capacity and dynamics of wormwood and Russian pastures show that there are two maxima of crop capacity in autumn and spring. It should be noted that the autumn harvest almost always (for the exception of very dry spring) is better than the spring one. In the beginning of a winter pasturing season (the end of November) the crop capacity of grass of these pastures averages 0.8-0.9 t/ha of the green edible mass. From December to April the crop capacity of the green edible mass is correspondingly 0.48-0.74%. In the beginning of March - 0.42%; from the second half of March the crop capacity begins to increase reaching 0.5t/ha and in the first half of April, by the end of the winter pasturing season it makes 1.0-1.2 t/ha [3].

The harvest of beard grass lands in the middle of November is in average 1.6-2.2 t/ha of the green mass, with that approximately 0.9-1.4 t/ha is edible and it can hardly be called "green" as almost 90% of it consists of dried stems and leaves of beard grass with 16-20% total water content. During winter the grass harvest of beard grass pastures falls rather more sharply than in semidesert pastures. The dynamics of crop capacity from November to May averages monthwise correspondingly to 1.12; 1.05; 0.87; 0.65; 0.51; and in April to 0.76 t/ha of green edible mass. In May as the beard grass, which is the main grass, starts its vegetation rather late, the crop capacity doesn't exceed 1.0-1.3 t/ha of the green mass in average.

The nutritious value of edificators and basic fodder plants of the arid pastures of Georgia is quite high.

The present economic state of semi-desert and dry steppe pastures in Georgia is characterized by development of erosive processes, destruction of turf. The coverage density is decreasing and the pastures are full of stones and weeds. Most widely distributed weeds in semi-desert areas are various species of thistle, bristlethistle etc. The weeds found in beard grass pastures are the following: sandy everlasting, blue-cap; common centeurea, common and plummet thistle and, etc. In areas near water sources or around sheep-folds weeds form thickets. As they are unused ungrazed ballast, their formation suffers great losses as they cause significant loss of wool among sheep.

One of the peculiarities of the natural fodder base for pasturing sheep breeding in Georgia is that the area under summer pastures greatly exceeds the one which is under winter ones (correspondingly 1.3 mln ha against 320 thousand ha). Taking into consideration long duration of the winter pasturing season and higher crop capacity and nutritiousness of the summer pastures grass and rising difference between the productivity of the winter and the summer pastures it becomes absolutely clear that the task is to increase significantly fodder for the winter by improving the winter pastures and laying in more supply of fodder on plugged fields and also through converting some part of the summer pastures into hayfields [4].

The most radical way of improving the situation is to carry out land improving works on plain and slightly steep slopes of arid pastures (irrigation and in some cases of need desalination) and create planted, irrigated fodder fields by planting cereals, leguminous crops and perennial herbs like alfalfa, orchard grass, meadow fescow, owuless bromegrass [5].

The calculations show that bained- improving works and creation of planted fields can be done over the area of 200-220 thousand ha. 25% of this area is enough for the total number of sheep with all necessary types of fodder for winter. Execution of these projects is impossible at present without major investment. Taking some measures for superficial improvement seems more realistic. These measures include weed control, elimination of shrubs in places where they have no antierosion value. The studies show that elimination of weeds through mechanical or chemical methods by 15-30% increases useful pasturing area and sharply improves condition of wool among sheep. In the years with normal autumn and spring precipitation it is effective to introduce organic and mineral fertilizers, especially for ephemeretum. The experiments carried out for several five year periods show that in average introduction of N_{30} P_{40} increased the dry mass harvest of ephemery wormwood group of grass by 1.4 t/ha or 131.2% in the spring [6].

Georgian Agrarian State University

REFERENCES

1. *G. D. Agladze.* Sakartvelos satibebis da sadzovrebis ganoqiereba , Tbilisi, 1980, 153.
2. *A. Korakhashvili, U. D. Bolkvadze,.* Tipologicheskaja klassifikatsia estestvennykh kormovykh ugodii Gruzii, Tbilisi, 1988, 149 (Russian).
3. *G. D. Agladze.* Sakartvelos mtis sadzovrebi da satibebi. Tbilisi, 1987, 163 (Georgian).
4. *A. Korakhashvili.* Sakvebis xarisxis shepasebis tanamedrove metodebi, Tbilisi, 1991, 48 (Georgian).
5. *G. Agladze , A. N. Zotov.* Gornye pastbishcha i senokosy Kavkaza, Tbilisi, 1987, 463 (Rusiian).
6. *G. Agladze, A. Korakhashvili.* Arid pastures of Georgia, Syria Allepo, 1998.

საქართველოს მეცნიერებათა აკადემიის მოამბე, 159, №3, 1999
BULLETIN OF THE GEORGIAN ACADEMY OF SCIENCES, 159, №3, 1999

GENETICS AND SELECTION

J. Kapanadze, G. Kapanadze, I. Guledani

Mutations in the Taxons of *Aurantioideae* Subfamily

Presented by Corr. Member of the Academy D. Jokhadze, November 11, 1998

ABSTRACT. **In the process of aforesting the taxons of *Aurantioideae* subfamily produce negative mutants. Such mutants are: *acormose, procumbent, coil-coiled, odorata, cauliflorya, colocynthis, nonacidum, nonspinosum, buxifolia*, etc. These mutants are characterized by normal meiosis and development.**

Key words: aforesting, negative mutation, autothinning.

Experiments were carried out on neotenic monoembryonal forms with normal meiosis [1]. The seeds were sown in open spaces of *alnus* forests. The following samples were studied: *C. jambiri* (3617), *C. iuzu* (3511), *C. wilsonii* (3600), *C. ichangensis* (3009) from citrus genus, *F. japonica* (4115) *F. meiva* (4109) from *Fortunella* genus, and two variations from *Poncirius* genus: *P. trifoliata var, spinosa* (5001), *P. trifoliata var. nonspinosa* (5119).

Organic fertilizers were used in open spaces of the forest (40 kg / 10m^2). After that the ground was dug at 30 cm depth. The ground surface was totally covered with seeds, and then the seeds were covered with humus on 4 cm thickness. In the first and second years *Alnus* tree seedlings were removed from the sowings, but in the third year they were left in 1.5 x 1.5 distance. Selection of mutant forms started in the forth year. Out of each sample 50 000 seeds were sown. Experiments were carried out on the banks of the Bibisira big lake in 1987-1992 (borough of Achigvara, Gali, Georgia). In our case the natural loss of seedlings was 70% even in case of thinning. Frost-resistance of the selected seedlings was tested in a climate chamber .

Data on the types and number of mutants obtained are given in the Table.

C. jambiri (rough lemon). Even in the forth year of thinning 24 900 seedlings were left. Among the mutants there were *acormose*, *nonspinosum*, *nonacidum*, *procumbent*, *cauliflorya*, *odorata*, *colocynthis*, *erythrocarpous*, *esculent* and *frost-resistant* seedlings. From the practical point of view those frostresistant forms are of interest, whose frost-resistance has reached –13^{0}C, while the frost-resistance of the mother genotype is not more than –5^{0}C. Tolerance of the frost-resistant mutants against frost is limited by the fact that at the end of September they stop growing and start transition into pre-winter rest period [2]. As to the generation of *nonacidum* forms of this species of lemon, similar facts are observed and fixed in other species of *citrus genus*, such as oranges, lime, bergamot [3].

C. iuzu (Georgian variation). After thinning 10 920 seedlings were left. Among the mutants there were: *acormose* (bush), *nonspinosum*, *procumbent*, *cauliflorya*, *odorata*, *apyrene* and *nonacidum* forms.

C. wilsonii (A. A. Gogiberidze's form). After autothinning 15 100 seedlings were left. Among the mutants there were: *acormose*, *nonspinosum*, *procumbent*, *cauliflorya*,

Aurantioideae mutant generation in the process of their afforesting

Objects	Number													
	seedlings	*acor-mose*	*procum-bent*	*coil-coiled*	*odo-rata*	*cauly-floria*	*colocyn-this*	*nonaci-dum*	*nonspi-nosum*	*escu-lent*	*buxi-folia*	*frost-resis-tent*	apyrene	mutants
C. jambiri	24 900	3	5	3	7	3	9	20	11	13		7		81
C. iuzu	10 920	2	5	2		1		3	10				2	25
C. wilsonii	15 100	5	11	1	3	2	9		3				7	41
C. ichan-	13 990	3	5			6	21		3					
gensis			3						5		2		7	38
F. japonica	13 115	6		2		5	11		11				13	23
F meiva	18 219	7				3	29		7				4	49
P. trifoliata	19 060	13		5		6	30			3				56
P. trifoliata	17 900	5												44

coil-coiled, frost-resistant (*C. wilsonii* genotypes resist -11^0C, while their mutants are frozen at -7^0C), *leukocarpous, odorata* and *colocynthis*.

C. ichangensis (M. T. Bgazhba's form).In the fourth year of selection in the result of autothinning 11 990 seedlings were left.Among the mutants there were: bushes, nonspinosum, procumbent, oligofrost-resistant (*C. ichani* resists -17^0C and its mutants -8^0C), *cauliflorya*, *colocynthis* and *esculent* (the genotypes of this plant bear nonesculent fruit).

F. japonica (*macrocarpous*). After autothinining 13 115 seedlings were left. Among the mutants there are: *acormose*, *nonspinosum*, *procumbent* (in Georgian subtropics genotypes of this variation of *Fortunella* resist -12^0C, while their mutants freeze at -7^0C), *apyrene*, *erythrocarpous buxifolia*, high frost-resistant (these mutants can resist -18^0C), i. e. in this case retrospective (archaic) mutants are obtained. Genetic mechanism of *buxifolia* mutants is very interesting: on starting of freezing the plasmolysis of cells begins at -1-5^0C. Isolated liquid accumulates in intercellular spaces . Along with the dehydration of cells the lower epidermis comes off its mesophyll and finally there appears a vacancy in the leaves where the water isolated from the cell accumulates. On further temperature decrease the afore mentioned water freezes, and on getting warm the ice thaws and the water is absorbed by dehydrated cells. Morphologically buxifolia mutants are identical to the *Severinia buxifolia* (*poir.*) Tenore. The motherland of this genus is the tropical part of the earth [4]. It must be noted that the above described genetic mechanism has not yet been noticed in buxfolia.

F. meiva (Achigvara variation). After autothinning there were left 18 219 seedlings . Among the mutants there were: *acormose*, *coiled*, *caulyfloria*, *colocynthis*, *nonspinosum* and *apyrene* mutants.

P. trifoliata (*spinosum* form). After autothinning there were left 19600 seedlings. Among the mutants there were: *acormose*, *caulyfloria*, *colocynthis, nonspinosum* formsand apynene.

P. trifoliata (*nonspinosum* form). After autothinning there were left 17 900 seedlings. Among the mutants there were: *acormose*, *colocynthis*, *caulyfloria* and *esculent* forms. Fitness of the mutant fruit for eating is determined by vanishing the acrid oils and gum in the vesicles [5,6]. This type of mutation must have been formed due to the peculiar state of *nonspinosum trifoliata*. These types of mutation are also observed in other objects of living organisms [7].

As shown by the given data the taxons of the *Aurantiodeae* subfamily generate homological orders of the mutants in the forests, namely, in *alnus* forests. Most of these mutants can exist in the forests as well as in cultures at the Black Sea coast in the Caucasus. Their adaptation to subtropical climate is defined by appearing a new genetic mechanism such as reduction of the vegetation period and dehydration at the beginning of frosts.

Sokhumi Branch of Tbilisi
I. Javakhishvili State University

Academy of Sciences of Russian Federation
Institute of Gene Biology

REFERENCES

1. *J. S. Kapanadze, B. I. Kapanadze*. Onthogenesis, **27**, 6, 1996, 413-418 (Russian).
2. *J. S. Kapanadze et al.* Subtropicheskie kultury, N3, 1990, 91-92 (Russian).
3. *R. W. Hodgson*. The Citrus industry. Univ. of California, **1**, 1967, 464.
4. *W. T. Swingle*. The Citrus industry. Univ. of California, **1**, 1967, 284.
5. *J. S. Kapanadze*. Bull. Acad. Sci. GSSR, **133**, 3, 1989, 617-619. (Russian).
6. *J. S. Kapanadze*. Bull. Vir. **68**, 1977, 59-64 (Russian).
7. *N. P. Dubinin*. Nekotorye problemy sovremennoi genetiki, M., 1994, 75 (Russian).
8. "მოამბე", ტ. 159, №3, 1999

საქართველოს მეცნიერებათა აკადემიის მოამბე, 159, №3, 1999
BULLETIN OF THE GEORGIAN ACADEMY OF SCIENCES, 159, №3, 1999

BIOPHYSICS

A. Chogoshvili, M. Chochua, B. Lomsadze

Low-temperature Stress and Dehydration Effect on the Induction Curves of Delayed Fluorescence in Leaves

Presented by Corr. Member of the Academy D. Ugrekhelidze, April 27, 1999

ABSTRACT. **The induction curves of delayed fluorescence in the young leaves of lemon show drastic but reversible reduction of thylakoid membrane photoenergization at chilling stress. The transmembrane proton gradient maximum is drastically decreased. Long effect of freezing stress causes irreversible reduction of fluorescence due to the cryodamage of the membrane, while the transient freezing causes strong increase of induction maximums due to the stimulation of photoenergization process after warming. All the above said should be the result of structural changes induced by the temperature decrease and dehydration in thylakoid membrane which is reflected in permeability of membrane and delayed fluorescence.**

Key words: fluorescence, thylakoid, frost-resistance.

Delayed fluorescence is the result of recombination of the primary stabilized charged couple P_{680} and Q_A formed after the absorbtion of light energy by photosystem II, which makes the induction curves on the recording apparatus [1-3]. The mentioned curves clearly show the process of thylakoid membrane photoenergization. The detected signal depends on the membrane potential, proton gradient, phosphorylation degree, permeability, the membrane ingredients and conformation of its components, i. e. on such properties that are sensitive to stress factors [4,5]. The advantage of the method is proved by the fact that it permits to carry out quick analysis of membrane processes immediately registering the fluorescence in the intact leaf. It is especially convenient and effective for quick analysis of different stress-resistant species without fractionation of the tissue.

The goal of our study was to analyse the action of freezing, chilling and water deficite stresses and their concomitant factors on the process of thylakoid membrane photoenergization by means of registering the induction curves of the delayed fluorescence in leaves.

Delayed fluorescence was registered by means of a dual disk phosphoroscope with the rotation constant 0.33 m.p.s. The apparatus consisted of a photoprinter (PEU-79), intensifier and rectifier blocks. On the paper of the fast acting recorder an induction curve was recorded. The leaf was placed between the disks in a dark chamber. Exitation was made with strong illuminator, light saturation was tested by constructing the curve of light. The possibility of change and fixation of the leaf temperature was taken into consideration. The objects - citrous plants, triticale and others were grown either under laboratory conditions or were obtained from the specialized agricultural farm.

The effect of chilling or the low, non-freezing temperature on the induction curves of delayed fluorescence in leaves of a young, 20-day Georgian lemon is shown in Fig. 1. Before the action of chilling stress (Fig. 1, A), when the plant temperature is close to the

physiological optimum (25^{0}C), both maximums of the leaf induction are well expressed. But during the chilling stress, when the plant temperature is 5^{0}C, the height of the I maximum increases and the II maximum is drastically reduced (Fig. 1, B). Besides, the comparison of the Figs. 1, A and 1, B shows that at low temperature the time interval *t*, which is the time from the moment of switching on the light (↑) up to the highest point of the II maximum, increases evidently. If we take into account that the I maximum of the induction curve is considered to be the difference between the electric potentials of thylakoid membrane during illumination and the II maximum is considered to be the indicator of transmembrane proton gradient [6,7], then we can consider the ratio of the height of the II maximum and the time (h/t) to be the speed of photoenergization process. Only the fluorescence method used in this work is not enough to define the limiting reason of photoenergization reduction at low temperature and it is not the goal of the present work either. But, it should be noted that, one of the possible reasons is the reduction of thylakoid membrane permeability or the decrease of plastoquinone diffusion rate in the hydrophobic part of the membrane due to the proceeding structural transitions in the lipids at temperature reduction.

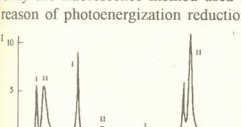

Fig. 1. The action of chilling stress (A, B) and freezing and warming effect (C, D) on the delayed fluorescence in lemon leaves. The ordinate I - fluorescence intensity. The abscissa - time of registration (min)

Chilling stress doesn't cause the irreversible damage of plasmatic or subcellular membranes of lemon. Placing the plants again at 25^{0}C the curves shown in Fig. 1, A regenerate.

At decreasing the temperature up to -5^{0}C, which is the temperature limit of lemon leaf freezing damage, marked damage is noticed only in that case if at this temperature the frozen plant is exposed for no less than 2.5-3h. After warming the induction maximums are not marked (Fig. 1, C). But if the plant is exposed at -5^{0}C for the shorter period -, no more than 30-40 min, then instead of depression the stimulation is marked (Fig. 1.D), which is shown by the increase of the height of the maximums and the value of h/t compared with the control one (Fig. 1,A). Such stimulation may be caused by a number of reasons: water freezing outside the cell and due to it partial dehydration of the cell, redistribution of ions among compartments, generation of transmembrane pores, etc. The reason of such stimulation may also be the deterioration of photosynthesis dynamic regulation mechanism during the stress.

Tbilisi I. Javakhishvili State University

REFERENCES

1. *J. Amesz, H. van Gorkom.* Ann. Rev. Plant Physiol, **29**, 1978, 47.
2. *P. A. Jursinic.* Light Emission by Plant and Bacteria, Orlando, 1986, 291.
3. *Yu. Fedulov.* Cereal Research Communications, Hungary, **24**, 4, 1996, 425.
4. *P. Chelidze, A. Chogoshvili, D. Oniani.* Trudy I resp. konf. po "Biologii Kletki", Tbilisi, 1984, 75 (Russian).
5. *P. Chelidze, A. Chogoshvili.* Proceedings of Tbilisi State University. 1984, 75 (Russian).
6. *V. Gold, N. Glevskii.* Teoret. osnovy i metody izuch. fluores. khlorofilla. Krasnoiarsk, 1984, 60 (Russian).
7. *S. Malkin.* Delayed Luminescence. Primary Processes of Photosynthesis, Amsterdam, 1977, 349.

საქართველოს მეცნიერებათა აკადემიის მოამბე, 159, №3, 1999
BULLETIN OF THE GEORGIAN ACADEMY OF SCIENCES, 159, №3, 1999

BIOCHEMISTRY

N.Gabashvili, M.Tsartsidze, A.Gujabidze, E.Tsartsidze

Polyethylene Degradation with Mould *Cladosporium herbarum*

Presented by Corr. Member of the Academy N. Aleksidze, March 16, 1998

ABSTRACT. **Polyethylene aging in humid atmospheric conditions of subtropics (Colkhis Research Center of Climatic Testing - v. Shekvetily, Ozurgety region, Georgia) and its degradation in laboratory conditions (mould *Cladosporium herbarum*) was observed. The aging estimation with infrared spectroscopy revealed CH_2-groups amount decrease and terminal carboxyl groups formation in the polyethylene molecules. The mechanism of polyethylene degradation is proposed.**

Key words: mould, biodegradation, hydrogen peroxide.

As we have mentioned earlier, along with organic acids [1] and ferment systems [2], oxidation process plays significant part in biodegradation of synthetic polymers [3,4]. Simultaneously, the study of microorganisms density on synthetic polymers show that they are mainly associated with *Cl. herbarum* [5]. For this reason the purpose of the given

Table 1

Weight loss changes of polyethylene under the influence of various substances 30 days after cultivating initiation of *Cl. herbarum*

Substance	Polyethylene weight loss	
	mg	%
Polyethylene (PE)	37.00 ± 0.10	-
PE with added mould	31.45 ± 0.07	15.00
PE with added mould and ascorbic acid	31.24 ± 0,13	7.41
PE with added mould and propylgalate	34.66 ± 0.09	6.34
PE with added mould and mannitol	34,72 ± 0.06	6.18
PE with added mould and subjected to light source	30.90 ± 0.08	16.49
PE with added mould and NAD-H	30.10 ± 0.05	18.65
PE with added mould and Cr (VI)	30.62 ± 0.03	17.25
PE with added mould and Fe (III)	30.73 ± 0.04	16.95

work is to investigate the biodegradation possibilities of polyethylene through *Cl. herbarum* mould as well as to study oxidation processes taking place in cultural medium infected by the mentioned fungus.

Cl. herbarum mould was used in the experiments. The rate of degradation was measured by weighing. The amount of hydrogen peroxide and catalase activity in feeding medium infected by mould were determined in accordance with [6,7], while the mass of protein according to Lowry [8]. Six days after initiation of cultivation, the inhibitors of oxidation processes were added to the feeding medium: ascorbic acid ($12.5.10^{-3}$M) and propylgalat ($12.5.10^{-4}$M), as well as specific inhibitor of hydroxyl radical-mannitol ($12.5.10^{-4}$).

The aging and biodegradation of polyethylene have been effected both in the humid atmospheric conditions of subtropics (Colkhis Reseach Center of Climatic Testing-v. Shekvetily, Ozurgety region, Georgia) and in the laboratory environment, according to the procedures described in [9]. The infrared spectra of polyethylene were made on Specord M-80 spectrophotometer. The in-depth study of the polyethylene degradation dynamics by *Cl. herbarum* mould has revealed that reduction of polymer was observed 6 days after infecting the feeding medium by micromycet, and after 30 days the polymer had degraded further down to 15% (Table 1).

While assessing the polyethylene aging under humid atmospheric conditions of subtropics, the infrared spectra of polyethylene have been made (Table 2). By application of infrared spectroscopy only those areas of polyethylene have been studied where the fungus density was evaluated per 3 and 5 point scale [10]. For control checking the intact film was used. As it is seen from the table, polyethylene remains undamaged within 1700 cm^{-1} spectrum field (zero absorption on undamaged film). But, at the initial stage of mould introduction, the maximum absorption becomes observed within 1712cm^{-1} field (corresponding to C = O carboxyl group), and its intensity increases with enhancement of damage rate of polymer. Thus, the break down of C-C bonds is observed and the terminal carboxyl groups emerge.

Table 2

Intensity changes on fields of strips of polyethylene infrared spectrum, when damaged under humid atmospheric conditions of subtropics

Substances	Rate of damage, points of scale	Absorption intensity strip (D, cm^{-1})	
		D_{1712}	D_{720}
Polyethylene	0	0	2.15 ±0.06
	3	0.35 ± 0.04	1.95 ± 0.09
	5	0.57 ± 0.07	1.72 ± 0.05

In order to determine the role of oxidation processes in polyethylene degradation, the influence of antioxidants (ascorbic acid, propylgalat) on the said process has been studied. It was found that both antioxidants significantly inhibit biodegradation process of polymer (the polymer weight loss made 7.41% and 6.34% correspondingly). Thus, along with fermenting, the oxidation processes play significant part in biodegradation of synthetic polymers, and namely, polyethylene (Table 1).

Investigation of the influence of hydroxyl radical specific inhibitor-mannitol on the polyethylene biodegradation process has shown that mannitol inhibits this process (polymer weight, loss makes 6.18% - see Table 1). These data, in addition to our published papers [3,4] point out to an essential role of hydroxyl radical in oxidation process of polyethylene degradation. The data obtained in case with *Cl. herbarum* mould, confirm as well that the hydroxyl radical together with hydrogen peroxide may participate in degradation of synthetic polymers, while hydrogen peroxide could be considered as one of the hydroxyl radical sources.

For this reason, the study of hydrogen peroxide generation ability of *Cl. herbarum* mould is of particular interest. The hydrogen peroxide generation dynamics has been studied in the process of fungus cultivation. It appeared that at the initial stage of cultivation (up to 6 days), the traces of peroxide have observed in cultural liquid, then 9 days after cultivation significant production of peroxide was noted, with further gradual reduction of peroxide amount (Table 3).

Table 3

Dynamic changes of catalase activity, amounts of NAD-H and H_2O_2 to cultural of NAD-H (2.10^{-7}M), infected by *Cl. herbarum*

Substances	Days of cultivating						
	6	9	12	15	18	24	30
NAD-H	2 ± 0.1	8 ± 0.4	17 ± 0.6	34 ± 0.9	27 ± 0.7	24 ± 0.3	16 ± 0.5
Catalase	-	25 ± 2.0	-	150 ± 4.2	-	85 ± 1.6	60 ± 3.1
H_2O_2	-	40 ± 3.7	80 ± 1.5	200 ± 5.7	150 ± 4.8	99 ± 2.5	90 ± 4.1
H_2O_2 after adding NAD-H	-	-	-	250 ± 6.3	120 ± 2.7	83 ± 3.9	62 ± 2.5

In relation to the said role of hydrogen peroxide in polyethylene degradation by *Cl. herbarum* mould, the analysis of catalase, ferment responsible for hydrogen peroxide degradation, has been made.

Determination of catalase activity in cultural liquid reveals that it starts 9 days after the cultivation initiation of fungus, and reaches its maximum on the 15th day; the said activity reduces on 20th day after beginning of cultivation (Table 3). It is suggested that catalase diffusion into cultural medium 15-20 days since the cultivation initiation of the fungus, is necessary for the detoxication of large concentrations of hydrogen peroxide which is accumulated in cultural medium.

According to one of the ways of H_2O_2 out-of-the-cell formation, the simultaneous effect of light and NAD-H upon the resulted hematoporphyrine is the reason of generating superoxide and peroxide of hydrogen [11]. In our experiments, while treating degrading polymer with the light of 500 W bulb, the rate of polymer degradation increases (Table 1). It is suggested that the light activity causes generation of H_2O_2 in cultural medium of fungus, which is an additional generation source of OH; and that stipulates the enhancement of polymer degradation rate.

Similar results have been obtained from our next experiments. Namely, single addition of metals with transit valency [Cr(VI) and Fe(III)] (2.10^{-7}M concentration) stipulates the growth rate of polyethylene degradation (weight loss 17.25% and 16.95% correspond-

ingly - see Table 1). It seems that effect is determined by interacting of H_2O_2 present in cultural medium, with metals having transit valency. As the result of such interaction OH• is generated, which is the reason of enhancement of polymer degradation rate.

The experiments investigated influence of NAD-H on out-of-the-cell formation of hydrogen peroxide and efficiency of polyethylene film degradation were of interest as well. It was found that single addition of NAD-H (2.10^{-7}M concentration) causes 25% increase of degradation rate (18.65% weight loss - see Table 1). The study of quantitative changes of H_2O_2 after NaD-H addition (on the 15th day from cultivation start) first indicated to its significant increasing, and then to similar decreasing (Table 3).

With application of the above-mentioned experiments the degradation procedure of polyethylene by *Cl. herbarum* mould will be as the following: when polyethylene is infected by mould, NAD-H is being accumulated in cultural medium (Table 3), and that combined with out-of-the-cell monooxigenases [in *Cl. herbarum* these ferments are localized both within the mould and in cultural medium [11]] generates H_2O_2. Interaction of out-of- the-cell hydrogen peroxide with metal of transit valency induces hydroxyl radical, which is one of the reasons of polyethylene degradation.

Tbilisi I. Javakhishvili State University

REFERENCES

1. *A. A. Anisimov et al.* In: Actualnye voprosy biopovrezhdeniya, M., 1983, 77-86 (Ruassian).
2. *M. Tien, T. K. Kirk.* Science, **221**, 4511, 1983, 651-655.
3. *M.A Tsartsidze.* Papers of Transcaucasian Conference of microbiologists. 1988, Tbilisi, 112-127 (Russian).
4. *M. I. Koshoridze.* Candidate thesis, Tbilisi, 1991 (Russian).
5. *N. Y. Gabashvili, M. A. Tsartsidze, A. O. Gujabidze.* Bull. Georg. Acad. Sci. **154**, 2, 1996, 289-292.
6. *R. K. Root, I. Metcalf, N. Odino, S. Change.* J. Clin. Invest., **55**, 1975, 945-950.
7. *H. B. Aebi.* Verlag Chemie, **3**, 1983, 273-284.
8. *O. U. Lowry, N. I. Rosenbrough, A. L. Farr, R. I. Randoll.* J. Biol. Chem., **193**, 1951, 265-272.
9. *A. O. Gujabidze, M. I. Koshoridze, V. N. Rusieshvili, M. A. Tsartsidze.* Bull. Acad. Sci., GSSR **133**, 2, 1989, 393-396 (Russian).
10. Testing methods for microbiol. stability. Standard GOST 9.048-80 (Russian).
11. *F. S. Sariaslani.* CRC Crit. Rev. Biotechnol., **9**, 3, 1989, 171-176.

საქართველოს მეცნიერებათა აკადემიის მოამბე, 159, №3, 1999
BULLETIN OF THE GEORGIAN ACADEMY OF SCIENCES, 159, №3, 1999

BIOCHEMISTRY

N. Butskhrikidze, M. Lashkhia, A. Shkolni, A. Tsereteli

Purification and some Properties of α-Galactosidase Obtained from the Strain *Penicillium canescens sopp 20171*

Presented by Member of the Academy G. Kvesitadze, March 3, 1998

ABSTRACT. **From the strain *Penicillium canescens sopp. 20171* the enzyme α-galactosidase has been separated and purified to homogenic state. It has also been chosen the optimum growing medium, where vine trimmings and aminoacid hydrolisate served as carbon source. Precipitation was carried out by one volume of spirit alcohol.**

Three-fold purification of the enzyme was carried out on CM-TOYPEARL column. The homogeneity was determined by SDS-electrophoresis. Some properties of the purified preparation have been studied.

Key words: enzyme α-galactosidase.

The α- galactosidase catalyses hydrolisis of α-galactoside containing preparations. The enzyme is widely spread in nature and could be successfully applied both in biotechnology (sugar production), and in medicine [1-3].

The aim of our work was to study α-galactosidase obtained from fungus *Penicillium canescens sopp. 20171.*

Penicillium canescens sopp. 20171 was grown in 750 ml flascs at 28^0C during 72 hours on 200-250 r/min. shaker 1.44 mg O_2/Lh under airation.

To deretmine α-galactosidase activity para-nitrophenyl -α-D galactopyranoside [2] has been used as a substrate. The medium contained 0.1 ml of substrate (0.004 M), 0.3 ml of acetate buffer (0.05 M, pH 4.3) and 0.1 ml of enzyme solution. The reaction was carried out at 37^0C during 10 min, and was interrupted by addition of 3 ml 1 M Na_2CO_3 solution. The amount of separated para-nitrophenol was determined colorimetrically on 405 nm.

The β - galactosidase activity was determined by Kuby and Lardy [4], and that of invertase by Somogyi [5] methods. Xylanase activity was determined through the application of xylane as a substrate [6]. The amount of the enzyme that in given conditions catalysed the transformation of 1 mk mole substrate in a minute was considered as the unit of enzyme activity.

Protein concentration was determined either by Lowry or spectrophotometrically on 280 nm.

Disk-electrophoresis was carried out by Davis [7]. To determine protein molecular weight in Tris-glycine buffer, 7.5% gel, p.H 8.3, the electrophoresis by Na-dodecylsulphate (SDS) in 8% gel was applied, where the markers were bovine serum albumin-68000, peroxidase - 44000, lysozyme - 14000.

The isoelectric point of the enzyme was determined by isoelectric focusing according

to Vestberg [8].

In order to optimize and cheapen *Penicillium canescens sopp. 20171* growing medium various industrial and agricultural materials: vine trimmings, tea production wastes, citric wastes, sugar-beet extract and melase, together with low vitamin complex or aminoacid hydrolysate were tested as the carbon source.

Owing to the maximum activity (6u/ml), the following medium was chosen: vine trimmings, and aminoacid hydrolisate (both concentrations were 3-3%). For protein precipitation from cultural solution 1,2 and 4 volumes of spirit alcohol were used. As the results turned out to be similar, priority was given to precipitation by 1 volume of spirit.

Obtained enzyme preparation was three-fold purified on CM-TOYOPEARL column (Firm "Toyosoda" - Japan, size - 1.6x35) (Table 1). Homogeneity was determined by disc-electrophoresis by Davis. According to electrophoresis data it could be said, that enzyme doesn't consist of sub-units. According to the above mentioned method its molecular weight was determined and it equals to 60000.

Table 1

Stages of α-galactosidase purification from *Pen. canescens sopp. 20171* culture solution

Stages of purification	α-galactosidase total activity units	Yield %	Protein Mg	Specific activity un/mg	Degree of purification
1. Filtrate	3000	100	1800	1.6	1
2. Precipitation by spirit	2730	91	391.3	6.8	4.3
3. Chromatography on CM-TOYOPEARL (NaCl grad.)	2070	69	110.8	18.7	11.7
4. Chromatography on CM-TOYOPEARL (pH grad.)	1800	60	52	34.6	21.6
5.Chromatography on CM-TOYOPEARL (NaCl grad.)	1530	61	30.5	50.2	31.4

Some properties of purified α-galactosidase were studied. The pH optimum of the enzyme operation turned out to be 4.2-4.6. As a result of PNFG application as the substrate at pH 3 during 30 min it maintained 30% of the activity, but at pH 7.0 almost entire loss of activity was observed.

The α-galactosidase thermo- stability and temperature effect on the enzyme activity were also studied. The enzyme revealed its maximum activity during 10 min incubation at 50^0C, but after 90 min it maintained only 30% of total activity. 70% of activity was lost after first 30 min at 55^0C at 45^0C after 90 min it maintained 50% of the initial activity. At 37^0C the enzyme preparation almost for 2h maintained the initial activity. The data prove rather high thermostability of *Penicillium canescens sopp. 20171* α-galactosidase.

The effect of metals (with 10^{-3} M concentration) and that of organic compound (with EDTA 0.2 10^{-3} concentration) on α-galactosidase activity was studied.

The species were beforehand dialyzed against 10^{-2} EDTA and distilled water. As it is shown in Table 2, EDTA doesn't affect its activity, Cu^{2+} and Mn^{2+} cause significant but Co^{2+} and Fe^{2+} slight increase of α-galactosidase activity.

The activity of above mentioned enzyme is insignificantly inhibited by Ba^{2+} ion and it demonstrates no changes while being influenced by other metal ions.

It has also been determined the isoelectric point of the enzymatic preparation of *Penicillium canescens sopp. 20171*, which was equal to 4.5.

Table 2

Influence of metal ions on *Pen. canescens sopp. 20171* α-galactosidase

List of metal ions	Activity un/ml	Activity increase (+) Activity decrease (-) in %
$CuSO_4$	43.2	(+)85
$MnCl_2.4H_2O$	64.7	(+) 176.5
$CoCl_2.6H_2O$	25.2	(+)7.7
$NiCl_2.6H_2O$	23.4	-
$BaCl_2.2H_2O$	21.6	(-) 7.7
$FeSO_4.7H_2O$	35.6	(+) 52.1
$Ca(OH)_2$	23.4	-
Na_2SO_4	23.4	-
$HgSO_4$	22.8	-
EDTA (SERVA)	23.4	-
Control	23.4	100

Thus, the preparation of *Penicillium canescens sopp. 20171* can be stored for a long period. It's possible to purify it to homogeneous state. It's quite thermo- and acidstable. Its highly purified preparations could be used in various fields of national economy, medicine and biochemical analysis.

Georgian Academy of Sciences
S. Durmishidze Institute of Plant Biochemistry

REFERENCES

1. *I. Ulezlo, O. Zaprometova.* Prikladnaya biokhimia i microbiologiya, **18**, 9, 1982, 3-15.
2. *O. Zaprometova.* Candidate Thesis, 1986.
3. *A. Bezborodov, I. Ulezlo, O. Zaprometova et al.* Doklady AN SSSR. **285**, 2, 1985, 475-479.
4. *S. A. Kuby, N. A. Lardy.* J. Amer. Chem. Soc., **75**, 1, 1953, 890-896.
5. *M. Somogyi.* J. Biol. Chem. **195**, 1, 1952, 19-23.
6. *M. J. Bailey, K. Poutanen.* Appl. Microbiol. Biotechnol. **30**, 1989, 5-10.
7. *B. Y. Davis.* Ann. N. Y. Acad. Sci. **521**, 1, 1964, 404-427.
8. *O. Vestberg.* Sci. Tools, **16**, 1969, 24-27.

საქართველოს მეცნიერებათა აკადემიის მოამბე, 159, №3, 1999
BULLETIN OF THE GEORGIAN ACADEMY OF SCIENCES, 159, №3, 1999

BIOCHEMISTRY

G. Pipia, G. Grigorashvili, P. Machavariani

Investigation of Biological Effect of Preparation Produced from the Vine Ridge Nutritious Fibres

Presented by Corr. Member of the Academy G. Ugrekhelidze, March 30, 1998

ABSTRACT. **Biological effect of preparation produced of the vine ridge nutritious fibres on white rats was studied. It is determined that the preparation has no toxic effect on the animals. While studying the embryotoxic characteristics of the preparation it was revealed that there were no anomalies in the embryos of experimental animals. The effect of cholesterol lowering action of nutritious fibres preparation was obtained in specific experiments. The investigations show that the nutritious fibres preparations are safe.**

Key words: nutritious fibres, white rats, biological effect, embryotoxic characteristics, cholesterol lowering action.

One of the risk-factors in the so-called "civilized diseases" pathogenesis is poor consumption of nutritious fibres [1, 2]. Thus massive production of products, enriched with nutritious fibres became essential [3-7].

According to the literary sources [8, 9] remainders of industrial processing of grapes, particularly grape ridge, have high content of nutritious fibres. Elaborated wasteless technology makes possible getting of nutritious fibres preparation and promoter for alcohol drinks production from grape ridge [10]. However, the use of this preparation in nutritious purposes must be argued by comprehensive medico-biological investigations.

The present study aims to investigate the biological effect of nutritious fibres, produced from vine ridge. Isolation of nutritious fibres preparation from vine ridge was carried out in semi-industrial conditions in Sagarejo distillery. Its chemical composition was determined by generally accepted methods [11].

Study of biological effect of nutritious fibres was carried out on 40 common white rats. Their initial body weight was 110g (two groups of animals: experimental and control, 20 rats in each group). Animals of an experimental group took 18% of casein and 10% of nutritious fibres preparation together with nutrition. The experiment lasted for 90 days.

We assess the state of animals by integral indicators - body weight, viability, nutrition consumption, general state, changes in morphological composition of peripheral blood [12], and by the biochemical indicators - composition of protein in general and protein fractions [13]. Rates of organs (liver, kidney, spleen, heart) were determined at the end of the experiment and pathomorphologic investigation of these organs was carried out as well.

To reveal the possible effect of nutritious fibres on reproductive function of animals

BIOCHEMISTRY

G. Pipia, G. Grigorashvili, P. Machavariani

Investigation of Biological Effect of Preparation Produced from the Vine Ridge Nutritious Fibres

Presented by Corr. Member of the Academy G. Ugrekhelidze, March 30, 1998

ABSTRACT. **Biological effect of preparation produced of the vine ridge nutritious fibres on white rats was studied. It is determined that the preparation has no toxic effect on the animals. While studying the embryotoxic characteristics of the preparation it was revealed that there were no anomalies in the embryos of experimental animals. The effect of cholesterol lowering action of nutritious fibres preparation was obtained in specific experiments. The investigations show that the nutritious fibres preparations are safe.**

Key words: nutritious fibres, white rats, biological effect, embryotoxic characteristics, cholesterol lowering action.

One of the risk-factors in the so-called "civilized diseases" pathogenesis is poor consumption of nutritious fibres [1, 2]. Thus massive production of products, enriched with nutritious fibres became essential [3-7].

According to the literary sources [8, 9] remainders of industrial processing of grapes, particularly grape ridge, have high content of nutritious fibres. Elaborated wasteless technology makes possible getting of nutritious fibres preparation and promoter for alcohol drinks production from grape ridge [10]. However, the use of this preparation in nutritious purposes must be argued by comprehensive medico-biological investigations.

The present study aims to investigate the biological effect of nutritious fibres, produced from vine ridge. Isolation of nutritious fibres preparation from vine ridge was carried out in semi-industrial conditions in Sagarejo distillery. Its chemical composition was determined by generally accepted methods [11].

Study of biological effect of nutritious fibres was carried out on 40 common white rats. Their initial body weight was 110g (two groups of animals: experimental and control, 20 rats in each group). Animals of an experimental group took 18% of casein and 10% of nutritious fibres preparation together with nutrition. The experiment lasted for 90 days.

We assess the state of animals by integral indicators - body weight, viability, nutrition consumption, general state, changes in morphological composition of peripheral blood [12], and by the biochemical indicators - composition of protein in general and protein fractions [13]. Rates of organs (liver, kidney, spleen, heart) were determined at the end of the experiment and pathomorphologic investigation of these organs was carried out as well.

To reveal the possible effect of nutritious fibres on reproductive function of animals

number of experiments were carried out on 40 female rats. They were divided into two groups. During the whole period of pregnancy experimental rats were given 18% of casein. On the 20th day of pregnancy the rats were killed and investigated. Number of yellow bodies, implantation and resorbtion places, alive embryos, body weight, existence of internal and external anomalies were determined. General embryonic mortality rate was calculated as well [14].

To reveal the cholesterol lowering effect of the preparation the experiment was carried out on 40 rats with average body weight of 120g (animals were divided into two groups, 20 rats in each). Animals of control group were given 18% of casein and 2% of cholesterol preparation in composition of their nutrition and experimental group animals were given the same nutrition with addition of 10% of nutritious fibres preparation. The experiment lasted for 30 days. The indicators, studied at the end of the experiment are as follows: total amount of cholesterol in blood [15], morphological composition of peripheral blood [12], total content of protein fractions in blood serum [13].

Determination of chemical composition of nutritions fibres preparation showed that the content of nutritious fibres in the preparation is 90.1% (cellulose - 62.5%, hemicellulose - 20.8%, pectin - 6.8%), total protein - 1.3%, total lipids - 0.3%, monosaccharides - 0.3%, ash - 1.8%, and humidity - 5.0%.

Experimental investigations showed that consumption of nutritious fibres preparation caused reduction of the body weight increase in comparison with control group rats, but these differences were not statistically reliable. Determination of blood morphological composition and some biochemical indicators didn't reveal the statistically reliable differences between the animals of experimental and control groups.

Application of nutritious fibres preparation didn't show any pathomorphologic and ultrastructural changes in liver, kidney, spleen and heart parenchymata and stromata. The study of the embriotoxic characteristics of the preparation showed that no anomalies were found in 20 days embryos of rats (Table 1).

Table 1

Indicators of white embryonic development

Indicators	Experimental group	Control group
Number of pregnant rats	20	20
Number of yellow bodies	172	188
Average number of yellow bodies	8.6±0.5	9.4±0.4
Number of implantation places	172	184
Number of alive embryos	140	154
Number of dead (resorbed) embryos	32	30
Mortality, %		
Pre-implantation	0.0	0.0
Post-implantation	18.6±0.9	16.3±0.8
Total mortality	18.6±0.9	16.3±0.8
Embryo weight, gr	2.45±0.10	2.71±0.15

Table 2

Some indicators of experimental animals state, taking the preparation of nutritious fibres

Indicators	Experimental group	Control group
Total cholesterol, mmole/l	5.87±0.06	6.55±0.06
Total protein, g/l	59.8±2.9	66.0±1.3
Albumines, %	37.0±4.6	37.8±2.6
Globulines, %	63.0±4.6	62.2±2.6
Correlation Al/Cl	0.57±0.08	0.57±0.06
Hemoglobine, g/l	154.0±3.3	162.0±6.5
Erythrocytes, 10^{12}/l	6.35±0.68	6.6±0.19
Leicocytes, 10^{9}/l	9.38±0.71	9.6±0.81

Experiments, aimed on revealing of cholesterol lowering effect of nutritious fibres preparation showed that inclusion of this preparation in rats nutrition significantly (11.2%) reduces the level of total cholesterol content in blood.

Determination of blood morphological composition and some biochemical indicators didn't give statistically reliable differences between the animals of experimental and control groups. Thus, the results of the experiment indicate cholesterol lowering effect of the nutritious fibres preparation. It is in conformity with the data of other authors [16]. The results of the investigation confirm the safety of nutritious fibres preparation isolated from the vine ridge. Further investigations will make possible to outline the optimal ways of the use of the preparation.

Georgian State Agrarian University

Scientific -Research Institute of Sanitary and Hygiene

REFERENCES

1. *M. Nesterin, V. Konyshev.* Fiziologiya cheloveka, 3, 1980, 531-542.(Russian).
2. *Y. Rigo.* Voprosy pitaniya, 4, 1982, 26-30 (Russian).
3. *A. Artemov, V. Vankhanen, A. Kovalenko.* Voprosy pitaniya. 3, 1984, 35-38 (Russian).
4. *M. Brentz, I. Slavogorodskaya, N. Kalinina.* Voprosy pitaniya. 6, 1986, 59-62 .(Russian).
5. *P. Darmanian, D. Sorogan.* Izv. Vysshei Shkoly. Pishchevaya Tekhnologiya. 3, 1986, 42-46.(Russian) .
6. *F. Meizer, P. Suckow.* Aktuelle Ernahrungsmed. 10, 3, 1983, 96-101.
7. *S. Miche, F. Lilichkis* . Ernahr. Umzhau. 11, 1986, 343-346.
8. *N. Razuvaev.* Kompleksnaya pererabotka vtorichnykh produktov vinodeliya. M., 1975. (Russian).
9. Netradıtsionnye korma v ratsionakh selskokhozyastvennykh zhivotnykh. M., 1988. (Russian).
10. *G. Grigorashvili, I. Moniava, G. Machavariani.* Patent Certificate N35, Republic of Georgia, 1982.
11. *L. Burshtein.* Metody issledovaniya pishchevykh produktov. Kiev, 1973. (Russian).
12. *O. Elizarova, L. Zhidkova, G. Kochetkova.* Posobiye po toksikologii dlya laborantov. M., 1976. (Russian).
13. *V. Ronin, G. Starobinets*, I. Uttevsky. Rukovodstvo k prakticheskim zanyatiyam po metodam klinicheskikh laboratornykh issledovanii. M., 1976. (Russian).
14. *I. Sanotsky, V. Fomenko.* Otdalennye posledstviya vliyaniya khimicheskikh soedinenii na organizm. M., 1979 (Russian).
15. *V. G. Kolb, V. S. Kamishnikov.* Spravochnik po klinicheskoy khimii. - Minsk, 1982. (Russian).
16. *S. Vainshtein, A. Masik.* Pishchevye volokna. Kolos, Kiev, 1987. (Russian).

საქართველოს მეცნიერებათა აკადემიის მოამბე, 159, №3, 1999
BULLETIN OF THE GEORGIAN ACADEMY OF SCIENCES, 159, №3, 1999

BIOCHEMISTRY

R. Goguadze, M. Chipashvili, E. Zaalishvili, N. Gogesashvili,
Corr. Member of the Academy N. Aleksidze

Influence of some Neurotransmitters on Rat Brain Glial Cells Actomyosin-Like Protein Ca^{2+}-, Mg^{2+}- ATP-ase Activity

Presented March 30, 1998

ABSTRACT. **Actomyosin-like protein (AMLP) was isolated from the rat brain glial cells. AMLP Ca^{2+}-, Mg^{2+} – ATP-ase activity was investigated. It became clear that the AMLP enzyme activity depends on KCl concentration. The influence of some neurotransmitters, such as serotonin, acetylcholine and GABA (10^{-6}, 10^{-5}, 10^{-4}, 10^{-3} M) on the ATP-ase activity was investigated. It is concluded that neurotransmitters modulate AMLP ATP-ase activity, glial cells' pulsation and their trophic function.**

Key words: brain actomyosin-like protein, Ca^{2+}-, Mg^{2+}-ATP-ase activity, neurotransmitters.

There is information in literature about glial cells pulsation [1, 4], which is conditioned by actomyosin-like protein. Actomyosin-like nonmuscular contractile proteins, neurostenines, were isolated from nervous system and glial cells [6-8]. It seems that they play an important role in numerous movements, where ATP is an energy source.

Nowadays it is well known that glial cells are chracterized by trophic function, expressed in active transport, uptake of different neuromediators and in their inactivation. That is how the normalization of neurodynamic processes is achieved. Neurotransmitters and ions on their side take active part in formation of neuron-neuroglial system and ensure inverse metabolic relationship between them [1,11].

Proceeding from the above mentioned, we aimed to study the influence of acetylcholine, serotonin and GABA on Ca^{2+}- and Mg^{2+}- ATP-ase activity of actomyosin-like protein isolated from the enriched fraction of glial cells according to the method [7,8]. Ca^{2+}-, Mg^{2+}-ATP-ase activity was studied as high (0.6 M KCl) and low (0.1 M KCl) ionic strength.

Ca^{2+}–, Mg^{2+} – ATP-ase activity was determined by the amount of inorganic phosphate released after ATP-ase hydrolysis [9,10]. At the incubation media contained ATP-Na_2 -3, $MgCl_2$ (or $CaCl_2$)-5, Tris-HCl (pH-7,4)-30, KCl-125 or 600, protein 300-400 მg.

In the first series of experiments we studied the influence of different concentrations of serotonin (10^{-3}, 10^{-4}, 10^{-5}, 10^{-6} M) on actomyosin-like protein Ca^{2+}- and Mg^{2+}-ATP-ase activity.

First of all it was shown that Mg^{2+}- and Ca^{2+}-ATP-ase activity of actomyosin-like protein quantitatively changes depending on serotonin concentration and ionic strength of incubation media (Fig.1).

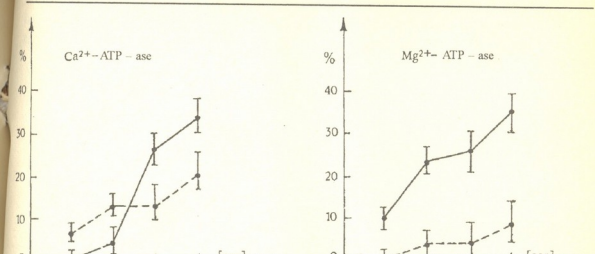

Fig.1. The influence of serotonin (10^{-3}, 10^{-4}, 10^{-5}, 10^{-6} M) on rat brain cells actomyosin-like protein Ca^{2+}-, Mg^{2+} -ATP-ase activity.
(—) ATP-ase activity in 0,6 M KCl conditions
(...) ATP-ase activity in 0,125 M KCl conditions.

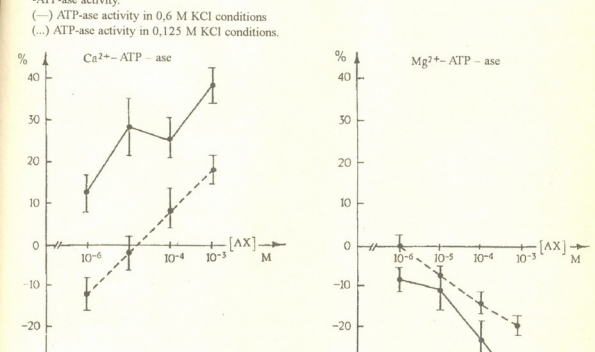

Fig. 2. The influence of acetylcholine (10^{-3}, 10^{-4}, 10^{-5}, 10^{-6} M) on rat brain cells actomyosin-like protein Ca^{2+}-, Mg^{2+} -ATP-ase activity.
(—) ATP-ase activity in 0,6 M KCl conditions
(...) ATP-ase activity in 0,125 M KCl conditions.

At high ionic strength (0.6 M KCl) of incubation mixture serotonin (10^{-5} M) stimulates Ca^{2+}-ATP-ase activity and it makes 30% against control. At low ionic strength and

10^{-3}M serotonin concentration this index is by 15% less. Analogical results were revealed in experiments with Mg^{2+} – ATP-ase too. So, in general, serotonin stimulates Ca^{2+}–, as well as Mg^{2+} – ATP-ase activity.

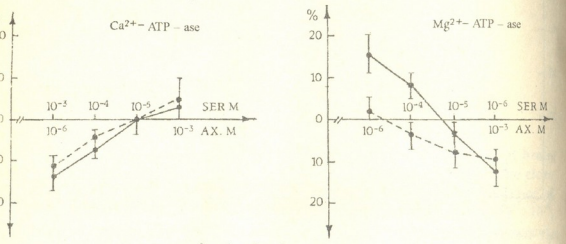

Fig. 3. The influence of acetylcholine (10^{-3}, 10^{-4}, 10^{-5}, 10^{-6} M) and serotonin (10^{-6}, 10^{-5},10^{-4}, 10^{-3} M) quantitative correlation on ATP-ase activity of actomyosin-like protein isolated from rat brain glial cells
(—) ATP-ase activity in 0,6 M KCl conditions
(..) ATP-ase activity in 0,125 M KCl conditions.

In further experiments we studied the influence of acetylcholine (10^{-6}, 10^{-5}, 10^{-4}, 10^{-3}M) on actomyosin-like protein Ca^{2+} - and Mg^{2+} -ATP-ase activity.

It is known, that acetylcholine as a neurotransmitter plays the main role in muscle contraction. Under the influence of acetilcholine the simultaneous releasing of Ca^{2+} ions from endoplasmic reticulum is denoted.

It was confirmed that like the serotonin the effect of acetylcholine depends on ionic strength of incubation media. Fig. 2 shows that the effect of acetylcholine is reciprocally dependent on Ca^{2+}- and Mg^{2+}- ions concentration. In the presence of Ca^{2+} acetylcholine stimulates enzyme activity, but in the presence of Mg^{2+} ions, on the contrary, acetylcholine inhibits ATP-ase activity. This effect is clear at high ionic strength (0.6 M KCl). The decrease of ATP-ase activity correlates with the increase of acetylcholine concentration. (Fig. 2).

Because of the different influence of serotonin and acetylcholine on Ca^{2+}-, Mg^{2+}- -ATP-ase, we considered necessary to study the result of their simulataneous actions. It was confirmed that during the simultaneous actions of serotonin and acetylcholine actomyosin ATP-ase activity becomes average. At high acetylcholine (10^{-3} M) and serotonin low (10^{-6} M) concentration in comparison with norm ATP-ase activity was increased. In case of 10^{-4} M acetylcholine and 10^{-5} M serotonin concentrations in the presence of Ca^{2+} ions ATP-ase activity returns to its usual norm again at low, as well as at high ionic strength.

An interesting result was received during the research of GABA – the specific inhibitory neurotransmitter of Central Nervous System [11]. Its inhibitory action is revealed in polarization of neuronal cells membrane.

From literature it is known that glutamine and GABA are specifically uptaken by glial cells [2].

It was confirmed that in existence of low (0.125 M KCL), as well as high (0.6 M KCl) ionic strength at various concentrations of GABA actomyosin-like protein Ca^{2+}-, Mg^{2+}- -

ATP-ase activity decreases in comparison with norm. This effect was clearly expressed in case of Mg^{2+} - ATP-ase at high ionic strength-enzyme activity was inhibited by 70% (Fig.4).

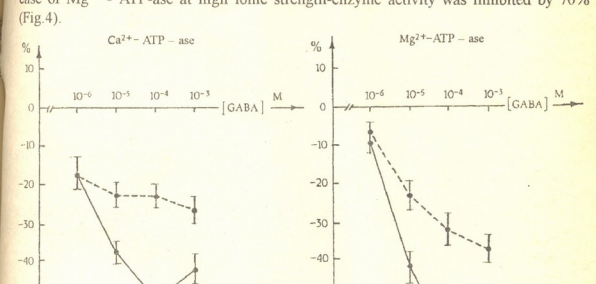

Fig.4. The influence of GABA (10^{-3}, 10^{-4}, 10^{-5}, 10^{-6} M) on rat brain cells actomyosin-like protein Ca^{2+}-, Mg^{2+} - ATP-ase activity.
(—) ATP-ase activity in 0,6 M KCl conditions
(...) ATP-ase activity in 0,125 M KCl conditions.

According to the given information it's once more proved, that neurotransmitters, as triggers, take an active part in membrane metabolism and secure the formation of unique metabolic systems.

Tbilisi I. Javakhishvili State University

REFERENCES

1. *N. Aleksidze.* Molekulyarnye i kletochnye mekhanizmy integrativnoi deyatel'nosti golovnogo mozga. Tbilisi, 1988 (Russian).
2. *N. Aleksidze, N. Maisov, M. Chipashvili, K. Raevsky.* In: Funktsii neiroglii, Tbilisi, 1979, 270-275 (Russian).
3. *T. Bakhanashvili, N. Maisov, N. Aleksidze.* "Izvestia Georg. Acad. Sci.", 1980, 273 (Russian).
4. *R. Glebov.* Itogi nauki i tekhniki ser. Biologicheskaya khimiya. M., 17, 1982, 147-275.
5. *I. Ivanov, B. Korovskin, G. Pinaev.* Biokhimiya myshts, M., 1977, 67 (Russian).
6. *I. Krasnovskaia.* Sravnitel'naya neirofiziologiya i neirokhimiya, 1976, 175 (Russian).
7. *D. Sandalov, M. Chipashvili, R. Beletskaia et al.* Bulletin of Experimental Biology and Medicine, 3, 1977, 280.
8. *S. Pusckin, S. Berl.* Science, 161, 3837, 1968, 170.
9. *B. Beucini, L. Wild.* Analytical Biochemistry, 1983, 254-258.
10. *D. Mikeladze, D. Kacharava.* Proc. Acad. Sci., G. SSR, Biol. series 1979, 40-47.
11. *L. Pevzner.* In: Funktsii neiroglii. Tbilisi, 1979, 251-261.

9. "მოამბე", ტ. 159, №3, 1999

საქართველოს მეცნიერებათა აკადემიის მოამბე, 159, №3, 1999
BULLETIN OF THE GEORGIAN ACADEMY OF SCIENCES, 159, №3, 1999

BIOCHEMISTRY

M. Chipashvili, E. Davitashvili, K. Menabde, Corr. Member of the Academy
N. Aleksidze

The Glycoprotein Nature of Rat Brain Actomyosin-Like Protein

Presented March 30, 1998

ABSTRACT. **The Ca^{2+} - ATPase activity of actomyosin-like protein, isolated from rat brain homogenate, has been stimulated by various concentrations of galactoso- and glucoso-specific (CS-Gal and CS-Glu) lectins. The glycoprotein nature of actomyosin-like protein was established by means of different monosaccharide-specific lectins used as sound. In actomyosin-like protein complex D-glucose and D-mannose have predominated among the galactose/N-acety/-D-galactosamine terminal monosaccharides.**

Key words: brain actomyosin-like protein (AMLP), lectin, Ca^{2+}-ATPase activity.

At present a lot of findings on localization, function and physico-chemical properties of contractile proteins from the nervous system have been accumulated but their structural organization in the membrane is not elucidated so far [1-4].

In our opinion the modification of membrane-bound enzymes activity is induced by lectines [5]. The relations between the rat's brain actomyosin-like protein (AMLP) and lectins, and the influence of some of them on AML protein Ca^{2+}-ATPase activity have been studied. The commercial lectins such as Concanavalin A(Con A, "Sigma"), WGA ("Sigma"), PNA ("Biotest"), LBA ("Biotest") and D-galactose -(CS-Gal) and D-glucose-specific (CS- GLU) lectins, isolated from *Coriandrum sativum* in our laboratory [6] , have been tested.

Actomyosin-like protein was isolated from rat's brain homogenate according to the method described by us in [7].

The hemagglutination activity of lectins was determined in 2% trypsinized rabbit erythrocytes suspension by serial 2-fold dilution of extract on microtiter -U-plates [8].

The relation between actomyosin-like protein and lectins has been investigated in hemagglutination medium by hapten-inhibitory technique [8].

Ca^{2+}-ATPase activity was estimated according to the released inorganic phosphate quantity in consequence of ATP hydrolysis [9, 10]. Ca-dependent ATP hydrolysis was calculated by subtracting the "basal" activity (in the absence of Ca^{2+}) from "total" activity (in the presence of Ca^{2+}). Ca^{2+}-ATPase activity was calculated as mkM phosphate/1 mg protein/1 min. Reaction medium (2.5 ml) included: Ca^{2+}-ions (50 mkM), Mg^{2+}-ions (3 mM), AML protein (100 mkg), ATP (1 mM) and different concentration of lectins. Protein concentration was measured by method of Lowry.

It has been established, that CS-Gal, CS-Glu and Con A stimulates Ca^{2+}-ATP-ase activity of AML protein (Fig 1, A, B, C). Unlike CS-Gal and CS-Glu lectins, high concen-

tration (35 mkg/ml) of Con A decreased enzyme activity, though its level exceeded the control level.

Table

Sounding of actomyosin-like protein monosaccharide determinants by plant lectins

Lectins mkg/50 mkl	Titrators wells number												Lectin protein/ glycoconjug. protein
	1	2	3	4	5	6	7	8	9	10	11	12	
WGA 0.06	+	+	+	+	+	+	+	+	+	+	+	+	
Con A 1.22	-	-	-	-	+	+	+	+	+	+	+	+	1:20
CS-Glu 0.4	-	-	-	-	-	-	+	+	+	+	+	+	1:26
CS-Gal 0.2	-	-	-	-	-	-	-	+	+	+	+	+	1:9
LBA 0.2	-	-	-	-	-	-	+	+	+	+	+	+	1:26
PNA 0.7	-	-	-	-	-	-	+	+	+	+	+	+	1:3

Actomyosin-like protein titers (basal concentration 170 mkg/100 mkl), added lectin with constant concentration: 1. WGA (N-acetyl-D-glucosamine-specific); 2. Con A (D-mannose-spec.); 3. CS-Glu 9D-glucose-spec.); 4. CS-Gal (D-galactose, N-acetyl-D-galactosamine spec.); 5. LBA (N-acetyl D-galactosamine-spec.); 6. PNA 9-galactose spec.).

"+"-hemagglutination, "-" -hemagglutination is absent.

Based on experiments carried out at the early stages and the received results, we have concluded that influence on Ca^{2+}-ATPase activity is caused by interaction of lectin with AML protein's terminal monosacharides (D-galactose for CS-Gal, G-glucose for CS-Glu and D-mannose for Con A). To postulate this assumption we investigated the influence of AML protein on lectin hemmagglutination activity. First of all it was demonstrated that AML protein does not agglutinate the 2% trypsinized rabbit erythrocytes suspension, but significantly blocked lectin activity after their co-incubation at the room temperature for 20 min. The monosaccharide determinant of AML protein was defined by hapten-inhibitory technique. Briefly, serial 2-fold dilutions of 100 mkl sample (AML) in all microtiter-U-plates wells over mode, the constant concentration of lectin was added, mixed and left at the room temperature. After the incubation 2% trypsinized rabbit erytrocytes suspension was added. The titer was defined as reciprocal of the highest dilutions still giving a visible agglutination. The results are summarized in Table. It was shown (Table) that at the beginning of titer, when AML protein concentration was high, lectin hemagglutination activity has not been displayed (Table 2-6) as a result of their binding with glycoconjugate AML protein. This effect has been revealed when the relation of lectin to lectin-binding protein (AML)

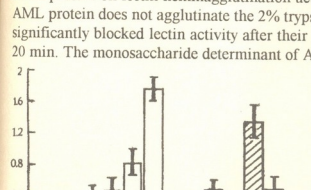

Fig.1. The lectins influence on rat brain actomyosin-like protein Ca^{2+}-ATPase activity.
Control-actomyosin-like protein Ca^{2+}-ATPase; A-influence of CS-Gal lectin; B-influence of CG-Glu; C-influence o Con A.
Ca^{2+}-ATPase activity expressed in mkM phosphate/1 mg/ 1 min.
Lectin concentrations: 1- 0.004 mkg/ml; 2-0.4 mkg/ml; 3-1.0 mkg/ml; 4-5 mkg/ml; 6-35 mkg/ml

concentration was 1:9 for CS-Gal lectin, 1:7 - for PNA, 1:20 for Con A, 1:13 for CS-Glu and 1:26 for LBA.

The obtained results indicate that AML protein is of glycoprotein nature with monosaccharide determinants specific for the used lectins (D-galactose-N4, N6; N-acetyl-D-galactosamine-N5; D-mannose-N2; D-glucose N3). AML protein was nonspecific to N-acetyl-D-glucosamine (N1).

In our opinion the monosaccharide presence in AML protein might be the result of glycoprotein nature enzymes absorbtion, although, by the electrophoretic and histochemical investigations the synaptic membrane actin-like protein had been identified as glycoprotein [4, 11].

Tbilisi I. Javakhishvili State University

REFERENCES

1. *K. Kath, G. Langford, K. Hammar, P. Smith.* Biological Bulletin. 1997 (Oct.), 219-220.
2. *M. Chipashvili, R. Gogouadze, E. Zaalishvili.* International symposium. The Physical-chemical basis of the Organization and Function of Biological systems. Tbilisi, 1996.
3. *C. Lin, E. Espreafico, M. Mooseker, P. Forscher.* Biological Bulletin, 1992 (Feb), 183-183.
4. *R. Glebov.* In: Itogi nauki i tekhniki, ser. Biol. Chem. **17**, 1982, 147-275 (Russian).
5. *M. Lutsik, E. Panasjuk, A. Lutsik.* The Lectins. Lvov, 1981.
6. *E. Davitashvili, K. Menabde, G. Alexidze, N. Aleksidze.* Bull. Georg. Acad. Sci. **153,** 1996, 105-108.
7. *Yu. Sandalov, M. Chipashvili et al.* Bull. exper. biol. and medic. Moscow, 3, 1977, 280.
8. *M. Lutsik, E. Panasjuk.* Method. recomend. Lvov, 1983.
9. *D. Beucini, I. Wild.* Analyt. Biochem. 132, 1983, 254-258.
10. *D. Mikeladze, D. Kacharava.* Proceed. Acad. Sci., Georg. SSR. Biol. Series. **5**, 19790, 40-47.
11. *M. Caron et al.* Lectins: Biology, Biochemistry, Clinical Biochemistry. **10**, 1994, 227-233.

საქართველოს მეცნიერებათა აკადემიის მოამბე, 159, №3, 1999
BULLETIN OF THE GEORGIAN ACADEMY OF SCIENCES, 159, №3, 1999

BIOCHEMISTRY

R.Akhalkatsi, T.Bolotashvili, Corr.Member of the Academy N. Aleksidze

The Identification of Lectin-Like Proteins from the Rat Brain Isolated Nuclei

Presented June 15, 1998

ABSTRACT. **The conditions for extraction of lectin-like proteins with hemagglutination activity have been elaborated, which confirm the evidence of their localization in the inner nuclear membrane.**

Key words: rat brain, nuclear lectine-like proteins

The study of brain lectins is rather limited due to their small content in the nervous tissue and low lectin activity. It particularly concerns nuclear lectins whose existence was established 10-15 years ago [1,2]. The use of affinity chromatography made it considerably easy to study lectins from nervous tissue. However, in spite of this the preparation of the initial material remains critical. The data found in literature point to the fact that the brain lectins are mainly presented in a bound form, and a special methodic approach is necessary for their isolation [3,4].

Proceeding from the above mentioned we carried out a research studying the conditions of extracting proteins with lectin- like activity from the rat brain isolated cellular nuclei.

White rats of both sexes weighing 100-120 g were used as experimental objects. Rat brain cellular nuclei were isolated by the method of Shauveau [5] . The purity of nuclear fractions was controlled by means of a microscope. The lectin activity was measured by the hemagglutination reaction of rabbit trypsinized erythrocytes by microtitration on U - plates by the method of Takatshi in the hemagglutination mixture (40 mM K^+ -phosphate buffer (pH 7,4), 0,9 % NaCL). Lectin activity was measured at the protein minimal concentration, which caused a clear expression of rabbit trypsinized erythrocytes agglutination [6]. The proteins were measured by the method of Lowry et al.[7].

For the purpose of extracting of the lectin-like proteins from rat brain isolated cellular nuclei we employed next buffer solutions 1. 0.9% NaCl solution prepared on K^+-phosphate buffer (pH 5.0); 2. The agglutination buffer (0.9% NaCl, 40 mM K^+-phosphate buffer, pH 7.4); 3. 0.1% Triton X-100, 0.9% NaCl and 20 mM K^+ - phosphate buffer (pH 7.4); 4. 0.05 M glycine-HCl buffer (pH 3.0); 5. 0.5% Triton X-100 solution prepared on 0.9% NaCl and K^+-phosphate buffer (pH 4.3).

For the selection of buffer solutions, we considered the fact, that the endogenous lectins in the nucleus must be bound with glycoconjugates and this connection must be broken to isolate the lectins and this process only takes plase in acidic area [6]. For this purpose we have selected such buffer solutions, whose pH was mostly inclined towards the acidic area.

We carried out the extraction of rat brain isolated cellular nuclei with the above mentioned solution (homogenization with homogenization mixture at the ratio of 1:3 (w/v), centrifugation at 16000 g/20 min; the dialysis of the supernatant against the agglutination buffer). The hemagglutination activity of extractable proteins was checked.

Table 1

The hemagglutination activity of protein extracts received from rat brain isolated cellular nuclei by various buffer solutions

N	Extractable buffer solution	Hemagglutination activity
1	0.9% NaCl + 20 mM potassium phosphate buffer (pH 5.0)	-
2	0.9% NaCl, 40 mM potassium phosphate buffer (pH 7.4)	-
3	0. 1% Triton X-100, 0.9% NaCl, 20 mM potassium phosphate buffer (pH 7.4)	The trace of agglutination
4	0.5 M Glycine - HCl (pH 3.0)	-
5	5% Triton X-100, 0.9% NaCl, 20 mM potassium phosphate buffer (pH 4.3)	+++

Table 1 shows, that the use of acidic extraction buffers is not sufficient for isolating the protein with hemagglutination activity from rat brain isolated cellular nuclei. The nuclear extracts with 1 and 4 solutions display no hemagglutination activity. The lectin-like protein is not extracted from the nuclei by the extraction with the agglutination buffer (solution N2). As to solution N3 only the trace of agglutination was noticed. The received results point, that lectins must be firmly bound with glycoconjugates in the nucleus. The glycoconjugates are probably localized in the inner membrane of the nucleus. It was proved by the experiments in which the extraction of nuclei with solution 0,1% Triton X-100 displayes only a trace of agglutination.

In the next series of experiments we carried out the stepwise fractionation of proteins from rat brain isolated cellular nuclei to receive the inner membrane fraction of the nucleus. After the removal from the isolated cellular nuclei of the proteins soluble in phosphate buffer (solution N2) and extractable in 0.1% Triton X-100 (solution N3) [8], the remaining pellet (membrane fraction) was treated by 0.05 M glycine-HCl buffer pH 3.0. The supernatant was dialyzed against the agglutination buffer and then it was tested on agglutination activity of the dialyzate. No hemagglutination activity was revealed in this protein fraction. Then we solubilized rat brain cellular nuclear membrane fraction in solution 0.5% Triton X-100, 20 mM K^+-phosphate buffer pH 4.3, 0.5 mM phenylmethyl sulfonyl fluoride, 1.5 mM ditiotreitol, by the ratio 1:2 (w/v). We carried out the extraction of the nuclear membrane fraction by the hand homogenizer at $+4^0$ C, 1h and centrifuged at 16000 g/20 min. The supernatant was dialyzed against the agglutination buffer, centrifuged at 16000 g/10 min and the supernatant's hemagglutination activity was measured (Tables 1, 2). As Table 2 indicates there is lysis in the first four wells of plates, in the fifth well there is no agglutination because the glycoconjugate is probably extracted with lectin extraction, and its dilution did not take place. In wells N6-N8 the agglutination of rabbits trypsinized erythrocytes is marked. Rats isolated cellular nuclear lectin-like protein has a

high hemagglutination activity. Its titre is equal to T^{-1} =256, and the specific activity-to SA = 104.4 (Table 3).

Table 2

The hemagglutination activity of lectin-like proteins of rat brain isolated cellular nuclei

	No.of plates wells											
	1	2	3	4	5	6	7	8	9	10	11	12
1	-	-	-	-	-	-	-	-	-	-	-	-
2	x	x	x	x	•	+	+	+	-	-	-	-

1. Control-100 ml of agglutination buffer (0.9% NaCl, 20 mM K^+ phosphate buffer pH 7.4) +50ml of 2% rabbit trypsinized erythrocytes.

2. Rat brain isolated cellular nuclei membrane fraction received from the solution 0.5% Triton X-100, + 0.9% NaCl, 20 mM K^+ -potassium phosphate buffer pH 4.3 is titred (245 mkg/100ml of agglutination buffer) + 50 ml of 2 % rabbit trypsinized erythtocytes.

"X"-lysis, "+" -agglutination, "-" -agglutination is absent.

Table 3

The hemagglutination activity of lectin-like protein from rat brain isolated cellular nuclei membrane fraction

Protein fraction	Volume V ml	Protein concentration C mg/ml	Titre T^{-1}	Specific activity SA	Total activity TA
Lectin-like protein of isolated cellular nuclei membrane fractions	2.56	2.45	256	104.4	327.68

$SA=T^{-1}\cdot C^{-1}$, $TA=T^{-1}\cdot V$

Tbilisi I. Javakhishvili State University

REFERENCES

1. *E. C. Bayer, S. H. Barondes,* J. Supramol. Struct. **13,** 1980, 219-227.
2. *R. A. Childs, T. Feizi.* Cell Biol. Int. Rep. **4**, 1980, 775.
3. *J. P. Zanetta, M. Dontenwill, A. Meyer, G. Roussel.* Dev. Brain Res., **17**, 1985, 233-243.
4. *M. Caron, R. Hubert, D. Bladier.* Biochem. et. Biophys. Acta. **925**, 1987, 290-296.
5. *I. Shauveau, J. Moule, Ch. Rouiller.* Exptl. Cell Res., II 1956, 317-321.
6. *M. D. Lutsyk, E. N. Panasjuk, A. D. Lutsyk.* The Lectins, Lvov, 1981.
7. *O. H. Lowry et al.* J. Biol. Chem. **193,** 1961, 265-275.
8. *R. Akhalkatsi, T. Bolotashvili, G. Alexidze, N. Aleksidze,* Bull. Georg. Acad. Sci. **153,** 2, 1996, 277-279.

საქართველოს მეცნიერებათა აკადემიის მოამბე, 159, №3, 1999
BULLETIN OF THE GEORGIAN ACADEMY OF SCIENCES, 159, №3, 1999

BIOCHEMISTRY

R. Gakhokidze, L. Beriashvili, T. Chigvinadze

Conversion of Succinic Acid in Plants

Presented by Corr. Member of the Academy N. Nutsubidze, March 9, 1998

ABSTRACT. **It has been shown that radioactive carbons of 1,4^{14}C and 2,3^{14}C - succinic acids in seedlings of kidney bean (*Phaseolus vulgaris*) - C_3 plant and maize (*Zea mays*) - C_4 plant participate in biosynthesis of organic acids, amino acids and sugars with different intensity.**

Key words: succinic acid, conversion, kidney bean, maize.

In comparison with other Krebs' cycle acids, the participation of carbon atoms of succinic acid in biosynthesis of other compounds is less studied.

The goal of the present work was to study the participation of radioactive carbons of 1,4^{14}C - and 2,3^{14}C -succinic acids in biosynthesis of organic acids, free amino acids and

Table 1

Distribution of radioactive carbons of 1,4^{14}C - and 2,3^{14}C -succinic acids in fractions of compounds of kidney bean and maize seedlings (in per cent of total radioactivity of the fractions), exposure 8 h.

Variant of experiment	Plant organ	Organic acids	Amino acids	Sugars	CO_2
1,4^{14}C -succinic acid Kidney bean					
Light	roots	72.3	24.6	3.1	-
	leaves	66.4	12.9	8.4	12.3
Dark	roots	74.6	23.4	2.0	-
	leaves	63.7	15.6	5.1	15.6
Maize					
Light	roots	62.8	34.3	2.9	-
	leaves	64.6	15.5	9.7	10.2
Dark	roots	69.7	28.5	1.8	-
	leaves	58.2	26.0	3.9	11.9
2,3^{14}C -succinic acid Kidney bean					
Light	roots	81.2	17.1	1.7	-
	leaves	65.3	28.7	4.2	1.8
Dark	roots	79.7	19.4	0.9	-
	leaves	70.6	25.3	2.1	2.0
Maize					
Light	roots	78.2	19.3	2.5	-
	leaves	69.4	25.6	3.9	1.1
Dark	roots	82.0	16.9	1.1	-
	leaves	75.6	16.6	4.2	1.6

sugars. The experiments were carried out on the seedlings of kidney bean (*Phaseolus vulgaris*) - C_3 plant and maize (*Zea mays*) - C_4 plant. 1,4-^{14}C - and 2,3-^{14}C -succinic acids with identical weight and specific radioactivity were injected through roots. Experiments were carried out on the light and in the dark at 26-29°C. The $^{14}CO_2$, emitted by conversion of 1,4-^{14}C - and 2,3-^{14}C -succinic acids, was bound with 20% KOH, radioactivity of which was determined as $Ba^{14}CO_3$. The fixation of samples was carried out with the boiling 90% - and the extraction - with 80% ethanol. Organic acids, free amino acids and sugars fractions were isolated by chromatographic method [1]. Individual components were identified by chromatography and radioautography [2-4].

Table 2

Distribution of radioactive carbons of 1,4-^{14}C - and 2,3-^{14}C -succinic acids in individual compounds of kidney bean and maize seedlings leaves (in per cent of total radioactivity of the fractions), exposure 8 h., dark

Compound	1,4-^{14}C -succinic acid		2,3-^{14}C -succinic acid	
	Kidney bean	Maize	Kidney bean	Maize
Total radioactivity of organic acids 1000 cpm/g	9045	8206	11578	12852
Malic acid	18.7	24.2	18.4	19.6
Citric acid	5.6	6.7	6.3	5.2
Succinic acid	46.2	42.3	61.9	62.1
Fumaric acid	17.4	20.4	12.4	14.4
Glycolic acid	8.9	3.2	5.7	6.9
Other organic acids	3.2	0.2	5.3	1.8
Total radioactivity of amino acids 1000 cpm/g	2215	3666	4149	2822
Glycine	16.6	26.2	21.4	14.7
Alanine	12.8	12.4	15.7	16.7
Aspatric acid	29.2	23.2	32.4	28.8
Glutamic acid	25.0	25.4	14.3	19.4
Other amino acids	16.4	12.8	16.2	20.4
Total radioactivity of sugars 1000cpm/g	724	549	344	714
Glucose	41.2	51.6	42.8	50.3
Fructose	39.4	26.0	36.0	26.9
Sucrose	19.4	22.4	21.2	22.8

The results of experiments showed that radioactive carbons of carboxyls and second and third carbons of succinic acid, assimilated by roots of kidney bean and maize seedlings differently participate in biosynthesis of organic acids, free amino acids and sugars. Definite part of radioactive carbons from leaves of investigated plants was emitted as CO_2, especially by conversion of 1,4-^{14}C -succinic acid (Table 1). Among formed products with high radioactivity fraction of organic acids was marked. In leaves and roots of both plants among organic acids after succinic acid the fumaric and malic acids displayed high radioactivity. Also, the citric acid had the label. By conversion of 1,4-^{14}C -succinic acid in

strawberries among organic acids also the malic acid had high radioactivity [5].

The data presented in Table 2 showed that by conversion of 2,3^{14}C -succinic acid the radioactivity of succinic acid was much higher, than that by conversion of 1,4^{14}C -succinic acid. On the one hand, it may be the result of an active decarboxylation of succinic acid and on the other hand it is not excepted, that by the action of isocitratliase on isocitric acid, formed after succinic acid incorporation in Krebs' cycle, the glyoxilic acid is produced and from cycle succinic acid goes out remaning the label in second and third carbon atoms. In favour of this conversion indicate also the experiments on different plants with 1,4^{14}C -succinic acid [6-8].

Among amino acids with high radioactivity are characterizied aspartic and glutamic acids. The results showed that in investigated plants oxaloacetic and α-ketoglutaric acids formed by the conversion of succinic acid in Krebs' cycle are activity aminated.

Georgian Academy of Sciences *Tbilisi I. Javakhishvili State University*
S. Durmishidze Institute of Plant Biochemistry

REFERENCES

1. *R. Shkolnik, N. Doman, V. Kostilev.* Biochimia, **26**, 4, 1961 (Russian).
2. *Zh. Uspenskaia, V. Kretovich.* Metodika kolichestvennoi bumazhnoi chromatografii sakharov, organicheskikh kislot i aminokislot u rastenii, M., 1962 (Russian).
3. Chromatografia na bumage, Pod red. I. Khaisa i K. Matseka, M., 1962 (Russian).
4. *S. Aronov.* Isotopnye metody v biokhimii, ILM, 1959 (Russian).
5. *H. Metchthild.* Gartenbauwissenschaft, 27, 4, 1963, 453.
6. *T. V. Beriashvili.* Biochimia rastenii, M., Tbilisi, 1973, 124-137 (Russian).
7. *A. Zemlyanukhin, A. Igamberdiev, A. T. Eprintsev.* A. A. Los. Fiziol. rast., **34**, 5, 1987 (Russian).
8. *A. I. Igamberdiev, B. V. Ivanov, M. I. Rodionova.* Fiziol rast. **37**, 3, 1990 (Russian).

საქართველოს მეცნიერებათა აკადემიის მოამბე, 159, №3, 1999
BULLETIN OF THE GEORGIAN ACADEMY OF SCIENCES, 159, №3, 1999

BIOCHEMISTRY

A.Gujabidze, T.Macharashvili, N.Gabashvili, M.Tsartsidze

Determination of the Coefficient of Aging for Polymer Materials Damaged with the Mould Fungi in the Conditions of Humid Subtropics

Presented by Corr. Member of the Academy N. Aleksidze, April 5, 1999

ABSTRACT. **On the basis of recent investigations and the analysis of UV and IR spectra of polymers injured in the conditions of humid subtropics we have offered factors of aging for every polymer in the above-stated conditions, enabling us to determine maximum life length of every material for production of the articles which should work in the conditions approximated to the considered ones.**

Key words: subtropics, mould fungi

In the conditions of humid subtropics mould fungi are rather quickly developed. It is conditioned by high humidity (over 80%), constant positive temperature, capacity to form a condensate and abundance of organic dust containing spores in great quantity [1].

The analysis of fungi formed on the materials has revealed the differentiation of species according to the type of material. The rate of their development on the surface of polymers is also different, which in its turn determines the speed of their structural change [2]. The above stated results in the changes in physical and chemical indices, the form and size, exhaustion of the surface, enhancement of the process of water penetration into the material depth, aging of the material and its becoming unfit for exploiting [3]. In order to define the guarantee period, great significance has been attributed to the determination of destruction rate to be measured by the methods of spectral analysis [4]. Destruction rate shows that every polymer has its own, inherent only to it, maximum of the specter of difference, the intensity of which is used for determination of bio-injury level.

We have carried out experiments enabling us to study the changes in optical density of polymers, in the process of growing of mould fungi on the surface of the material. In such a case the area occupied by the fungi on the surface of the polymer, that is the degree of growth, suffers changes. We have used aromatic polyimide. Polyimide films of 37x18 mm size were sterilized with ethyl alcohol and washed down with distillate (approximately 200 films). Then we sprayed polyimide films with suspensions of different fungi: *Trichoderma lignorum* (Tode) Harz (Tc), *Cladosporium herbarum* (Pers) Link et Gray, *Acrodontium crateriforme* (Ac.), which were isolated from the same aromatic polyimide in the process of climatic experiments. The films without suspensions of fungus were also used in the experiments. All samples were kept in a thermostat at 27^0C. Every five days we selected samples with approximately equal coating, we washed them with distilled water and took differential specter in 400-500 nm length wave area by a spectrophotometer with respect to the control. The results are given in Table 1.

Table 1.

Intensity changes of differential spectrum in the process of bio-damage of aromatic polyimides

Incubation time (24hr)	Intensity of absorption maximum 430 nm		
	Trichoderma	*Cladosporium*	*Acrodontium*
0	0	0	0
5	-7.0+1.4	-5.1+1.2	-3.8+1.0
10	-12.2+1.5	-10.3+1.4	-7.4+1.2
20	-24.0+1.5	-21.0+1.6	-15.0+1.4
30	-46.0+1.8	-32.0+1.9	-29.0+1.5

The analysis has shown that optical density suffers changes proportionally with the time and linearly with respect to coating, that is the incidence of the angle formed by drawing the line on the maximums of optical densities with respect to the start of coordinate does not alter. Tangents of incidence of this angle varies for different species of fungus and we can get it as a coefficient of aging: $tg\alpha=K$; $K_{fc}=46\%$ optical density / 30 day=–1.53; $K_{cl}=32\%/30=-1.07$ and $K_{ac}=29\%/30=-0.96$. We can calculate time, needed for destruction of all functional groups which are absorbed at this maximum. For this, it is necessary to divide the whole number (1.0) of functional groups on the aging coefficients, enabling us to determine life-length of a polymer in the conditions of humid subtropics.

Table 2

Changes of optical density of aromatic polyimide at 430 nm wave length area during its aging in natural conditions

Exposure time, month	Changes of optical density at 430 nm	Factor of aging $tg\alpha$
0	0	0
3	0.08+0.01	0.026
6	0.15+0.02	0.026
9	0.25+0.01	0.025
12	0.33+0.01	0.026
15	0.46+0.01	0.031
18	0.60+0.01	0.033

In natural conditions, during 18 month experiments, the analysis was conducted in every three months, and the aging coefficient had different indices compared with those in laboratory conditions (comparatively small value). Within 1-12 months $tg\alpha=0.026$, while by the 15 month the aging coefficient increased and amounted to 0.031, and by the

18th month it equaled to 0.033 (Table 2). Such a difference is conditioned by the fact that during the laboratory experiments we had the fungus which really is grown on the given polymer. At the same time due to constant optimal temperature of growth, the growth of biomass proceeded almost equally. In natural conditions during the experiments certain time passes till the spore of this fungus being able to develop falls upon the surface of the material. At the same time ambient temperature change does not enable the fungus to develope homogeneously on the surface. Here external chemical and physical factors exert their influence, which during their action favour the development of other fungi. It is possible that the effect of their influence strengthens each other. Therefore the maximum value of the aging coefficient is to be used.

While studying the IR spectra of the polymers it was shown that we obtained absorption maximums at 1800-1600 cm area, which is connected with the formation of COOH-groups. This fact may be used for determining the aging coefficient [5] (Table 3).

Table 3

Values of aging factor of polymer materials is natural conditions for subtropics (results of 18 months experiments)

Material	IR spectrum area, cm	Increase of optical density	tg, per month	Life-length, month
1. Aromatic polyimide	1645	0.102	0.006	150
2. Polytetrafluoro-ethylene	1712	0.187	0.01	100
3. Polyethylene	1712	0.571	0.034	294
4. Vinylidene fluoride with hexafluoropropylene	1708	0.241	0.018	77
5. Celulose	1718	0.76	0.042	24

The obtained results enable us to suppose that in the conditions of humid subtropics all functional groups of aromatic polyimide may suffer destruction within 1.0:0.006/month=150 months, those of poly-tetrafluoro ethylene within 1.0:0.01=100 months, etc. The values brought here are the maximum life-lengths of these materials, which are to be taken into account while manufacturing certain articles which must work in the conditions close to the considered ones.

Tbilisi I. Javakhishvili State University
Scientific-Research Center of Climatic
Investigation of Colkhida

REFERENCES

1. *I. A. Dudka, V. N. Rusieshvili et al.* Ukrainski Botanicheski Zhurnal **45**, 1, 1988, 46-49 (Russian).
2. *D. A. Svanidze et al.* Mat. All-Uni. Sci. Tech. Conf. "Automat. of Means of Metrologic Provision of National Ecology", Tbilisi, 1989, 644-647 (Russian).
3. *B. K. Frolov.* Problemy biologicheskikh povrezhdenii i obrastanii, 1972, 3-8 (Russian).
4. *A. O. Gujabidze et al.* Bull. Acad. Sci. Georgian SSR, **133**, 2, 1989, 394-396;
5. *N. Y. Gabashvili, A. O. Gujabidze, M. A. Tsartsidze.* Bull. Georg. Acad. Sci. **154**, 2, 1996, 289-293.

საქართველოს მეცნიერებათა აკადემიის მოამბე, 159, №3, 1999
BULLETIN OF THE GEORGIAN ACADEMY OF SCIENCES, 159, №3, 1999

ZOOLOGY

R. Zosidze

Investigation of the Hydrofauna of Charnalistskali River, a Tributary of Chorokhi River

Presented by Corr. Member of the Academy B. Kurashvili, December 30, 1998

ABSTRACT. **As a result of hydrobiological investigation of Charnali river 61 species of the benthofauna and 7 species of the fresh-water fish were recorded. It was found that the majority of the benthofauna comprises the insect larvae, mostly presented by *Diptera, Ephemeroptera, Trichoptera,* and *Plecoptera.* The species diversity, organisms' density and biomass volume were most significant in the middle stream of the river.**

Key words: fresh-water benthofauna, insects, fish, insect larvae, food chains.

The Adjarian rivers-Chorokhi, Acharistskali, Kintrishi, Choloki, and some of their major tributaries, are poorly investigated from the hydrobiological standpoint. The hydrobiology of the main rivers was investigated more or less exhaustingly [1-5], but the smaller tributaries never have been the subject of special study so far. The goal of the present study was investigation of the hydrobiont species of Charnali (Charnalistskali) river, their distribution according to their specificity and number, their ecological overview, and establishment of means for increase of the fish resources.

Investigation of the river was carried out from January till November. Collection of the material was made separately in the upper-, middle-, and lower streams of the river. The hydrological and hydrochemical tests were made as well. The qualitative and quantitative specimens of the benthos were collected by means of Sadowsky benthometer [6], the area of which was 0.09m^2.

Along with the benthos invertebrates, the fish species of the river were examined as well. Total of 7 species (100 fish altogether) were collected and examined along the upper-, middle-, and lower streams.

Table 1

The seasonal hydrological indices of the Charnali river

Hydrological elements	Spring	Summer	Autumn	Winter
1. Water level	53.3	47	50	53.6
2. Water debit, m^3/s	1.1	0.9	1.3	1.32
3. Water temperature, ^{0}C				
a) Upper stream	9.2	13.5	11.0	5.9
b) Middle stream	10.1	14.6	11.1	6.1
c) Lower stream	10.5	15.4	11.5	6.2

The Charnali river is a typical mountain river with narrow bed, abundant boulders and stones, and fast water-flow. The main hydrological indices of the river are presented in Table 1.

Investigations have shown that the benthos organisms include 61 species (Table 2). The river fauna consists mainly of 4 groups: minor *Annelidae, Mollusca, Crustacea,* and *Insecta* (larvae). The insect larvae are especially abundant, which cover about 74% of the whole benthofauna. Out of 61 species of the benthofauna 45 species comprise insects. The most abundant are *Diptera* (13 species), *Ephemeroptera* (12 species), *Trichoptera* (11 species), and Plecoptera (9 species).

Table 2

The number and biomass of the Charnali river benthofauna (the mean number per $1m^2$ and biomass in mg/m^2)

Organisms	Upper stream		Middle stream		Lower stream	
	Number	Biomass	Number	Biomass	Number	Biomass
Annelidae	20	40	116	186	364	928
Mollusca	12	100	8	82	-	-
Crustacea	3	12	4	16	-	-
Ephemeroptera	585	2153	1321	5709	1026	2673
Plecoptera	59	577	143	2300	44	320
Trichoptera	87	630	423	3125	470	2714
Diptera	306	970	466	1185	590	269

As it is obvious from Table 2 various groups of the benthfauna are distributed unevenly along the river stream. Although, in all the three parts of the river *Diptera*, and *Truchoptera* are most densely distributed *Ephemeroptera*,. The seasonal dynamics of the benthofauna density and biomass are presented in Table 3.

Table 3

The seasonal dynamics of the benthofauna (number per m^2 and biomass g/m^2)

The river region	Spring	Summer	Autumn	Winter
Upper stream	2100	1800	750	650
	7.5	6.2	3.5	1.8
Middle stream	4300	3500	2200	1800
	16.5	14.8	9.8	7.5
Lower stream	3550	2750	1850	1560
	9.3	8.2	6.1	5.2

The fish population of the Charnali river is not diverse and abundant. Total of 7 species were recorded. 1) *Salmo trutta labrase* Pall. m. L; 2) *Leuciscus cephalus orientalis* Nordm; 3) *Chondrostoma colchicus* (kessi.) Deriugini; 4) *Gobigobio lepidoloemus* K. n. caucasicus Kam; 5) *Varicorhinus tinca* Hesk.; 6) *Barbus tauricus eschrichi* Stend.; 7) *Alburnoides bipunctatus fasciatus* Nordm.

At upper- and middle streams of the river only three fish species were found. The dominant species in this region is *Salmo trutta labrase*. The latter fact is in conformity with ecological conditions – clear and cold oxigen-rich water – of the above-mentioned parts of the river. However, the Charnali river is poor in both fish species diversity and population of each of the species. On the other hand, the invertebrate benthofauna pro-

vides enough food for fish. As was shown above, the middle stream of the river is highly populated with the insects' larvae and other invertebrates. Thus, the low density of fish population should be attributed to the anthropogenic factor (e. g. poaching and other illegal activities). That is why the main conclusion is pointed at protection of the river basin and, as a tentative proposal, to establish the National Park in the region.

Considering the ecological properties of the Charnali river it could be proposed as well to introduce and acclimatize here other subspecies of *Varicorhinus tinca*, which may well reproduce and even flourish in the river, providing hence an additional source of biomass.

Batumi Sh. Rustaveli State University

REFERENCES

1. *J. Meskhidze*. Proc. Batumi Pedagogical Institute, 9, 1962 (Georgian).
2. *J. Meskhidze*. Proc. Batumi Pedagogical Institute, 9, 1964 (Georgian).
3. *J. Meskhidze*. Proc. Batumi Pedagogical Institute, 9, 1965 (Georgian).
4. *R. Zosidze*. Proc. Batumi Pedagogical Institute, 16, 1973 (Georgian)
5. *R. Zosidze*. Bull. Acad. Sci. Georgian SSR, 68, 1972 (Russian).
6. *A. Sadowsky*. Bull. Acad. Sci. Georgian SSR, 9, 1948 (Russian).

საქართველოს მეცნიერებათა აკადემიის მოამბე, 159, №3, 1999
BULLETIN OF THE GEORGIAN ACADEMY OF SCIENCES, 159, №3, 1999

ZOOLOGY

A.Diasamidze, R.Zosidze

Hydrofauna of Uchambistskali and Chirukhistskali Rivers

Presented by Corr. Member of the Academy B.Kurashvili, November 3, 19 98

ABSTRACT. **The invertebrate animals of the two Adjarian rivers (Uchambistskali and Chirukhistskali) were investigated according to their distribution along the river length at their upper, middle, and lower streams. The number of individual species and their biomass have been evaluated. Investigated invertebrates' feeding value is discussed in relation to the fish-breeding.**

Key words: Adjarian rivers, trichoptera, ephemeroptera, plecoptera, chiromonidae, biomass.

The hydrobiological indices of the two Adjarian rivers (Uchambistskali and Chirukhistskali) haven't been investigated yet. One of the rare studies [1] was concerned only with the lower tributary part of Chirukhistskali river. The aim of the present investigation was evaluation of the invertebrates along the upper-, middle, and lower streams of the two rivers. The material collection was carried out by the generally adopted methods. The specimens under study were assessed by seasons.

Chirukhistskali river is a left tributary of Acharistskali river. The former is a typical mountain river, the source of which is in the Chirukhi mountains. The length of the river is about 40-50 km. The river bed is strongly inclined and rich with the boulders and stones. Along the whole stream of the river a large number of waterfalls and whirlpools are presented. The water is clear all the year round; the temperature varies between 2° and 17°C.

Uchambistskali river is a left tributary of Chirukhistskali. It is relatively shallow river, the length of which is about 15-20 km. The hydrological regime is essentially the same.

Investigations have shown that the water fauna of Uchambistskali and Chirukhistskali is fairly diverse. In Uchambistskali river total of 45 species of the benthos animals were recorded, while in Chirukhistskali - 78 species. The earlier investigations [1, 2] have shown lesser number of species than in the present one. According to the present investigation the faunistic content of the rivers is somewhat different in the upper-, middle, and lower streams.

The following invertebrates were found in the fast-flow stony regions of the rivers: total of 16 species of *Trichoptera* (including *Phyacophila cupresorum* Mart., *Rh. nubila* Zett., *Rh. Obliterata Mcl., et al.*), 9 species of *Ephemeroptera* (including *Baetis alninus* Pict., *B.pumilus Burm., Epeorus torrentium* Epton., *Ecdionurus fleuminum* Pict., *et al.*),

5 species of *Plecoptera* (*Perlodes microcephala* Pict., *Perla marginata* Panz., *P.caucasica* Guer., et al.), 7 species of *Chironomidae* (*Tanitarsus ex gr. labatifrons* Kieff., *Cricotopus ex gr. bicinetus* Mg., *Polipedilum ex gr. pedesta* Mg., et al.), 2 species of *Blepharoceridae* - *Dioptopsis luryfrons* Bisch., *Yoponeura sp.* , 1 species of *Simulidae* - *Odagmia voriegata vernalis* Rubz.

In the afore-mentioned benthos animals of Chirukhistskali the dominants are *Diptera* and *Ephemeroptera*. The *Diptera* are mostly presented by the dominant species *Odagmia variegata vernalis* Rubz. (*Simulidae*), the density of which is about 1000-1500 /m^2, and the biomass - 2-3 g/m^2; out of *Blepharoceridae* the *Dioptopsis eurifrons* Bisch. is abundant as well - 600-800/m^2, biomass - 0.8-1.2 g/m^2, while out of *Ephemeroptera* the most abundant is *Epeorus torrentium Eoton,* the density of which is 500-600/m^2 and biomass - 4-5 g/m^2.

In the Chirukhistskali river, at the middle stream, 56 species were found, which could be distributed as follows: 21 species of *Trichoptera*, 11 species of *Ephemeroptera*, 6 species of *Plecoptera*, 10 species of *Chironomidae*, and 8 species of other *Diptera*.

Thus, at the mentioned region of the river the most abundant organisms are presented by *Trichoptera* and *Diptera*, which are characterized by the high population density and biomass indices.

At the lower stream of the river the species diversity is presented mostly by *Diptera*, 32 species of which were recorded. Especially abundant were *Chironomidae* (21 species). Similarly, abundant were *Trichoptera* (13 species) and *Ephemeroptera* (13 species). One of the Ephemeroptera (*Oligoneuriella tskohomelidzei sp.n.*) was first described in co-operation with our Polish colleague Dr.R.Sowa [3]. One of the *Chironomidae* species - *Parametriocnemus stylatus adzharicus sp.n.*, was also first described in co-authorship with Polish colleague Dr.A. Kownacky [4, 5].

The summary of the benthos fauna distribution in the two Adjarian rivers is presented in Table 1. Distribution of the benthos fauna of the two Adjarian rivers by seasons is presented in Table 2.

Table 1.

Density (per m^2) and biomass (g/m^2) of the benthos fauna - average yearly indices.

Organisms	Chirukhistskali river						Uchambistskali river			
	Upper stream		Middle stream		Lower stream		Upper stream		Lower stream	
	n	mass	n	mass	n	mass	n	mass	n	mass
Ephemeropt.	1000	6.3	1200	7.1	800	4.3	650	3.4	840	4.5
Plecoptera	120	1.2	160	1.4	100	1.2	70	0.3	115	1.2
Trichoptera	150	1.4	400	3.5	350	3.1	200	2.1	360	3.2
Chironomid.	180	0.5	200	0.6	2000	2.8	115	0.2	300	0.3
Blepharocer.	700	1.1	600	1.1	150	0.3	650	1.1	200	0.4
Simulidae	1200	2.5	1500	2.5	250	0.6	1050	2.2	300	0.7
Varia	30	0.6	50	1.2	70	1.4	15	0.2	25	0.3

Table 2

The benthos fauna numerical value dynamics by seasons

Rivers		Spring		Summer		Autumn		Winter		Mean	
		n/m^2	mass, g/m^2	n/m^2	mass, g/m^2	n/m^2	mass, g/m^2	n/m^2	mass, g/m^2	n/m^2	mass, g/m^2
Chirukhi -stskali	Upper stream	750	5.6	1800	0.5	1200	6.4	890	3.8	1160	8.3
	Middle stream	1300	7.4	3100	12.5	2200	7.5	1250	6.5	1962	8.4
	Lower stream	1490	8.2	3220	15.4	1130	5.6	4170	16.9	2500	11.4
Uchambi -stskali	Upper stream	800	5.8	1600	7.2	1150	5.3	750	3.5	1075	5.4
	Lower stream	1500	8.3	3100	14.2	1250	6.2	950	4.1	1700	8.2

In both rivers there was found not only the high diversity of the benthos animals, but fairly high biomass of these organisms (Table 2).

In the investigated rivers 5 species of fishes were recorded as well (including the river trout). However these are very scarce in the mentioned rivers, which is due to the intense unauthorized fishing (poaching). The mass elimination of the fishes is frequent. The upper streams of the rivers are more protected and the number of the river trout is preserved on a more or less high level.

It should be mentioned that natural food for the fish reproduction in the two Adjarian rivers is satisfactory (see above) and thus the poaching and water pollution should be controlled strictly to increase the volume of valuable ichthyofauna.

Batumi Sh.Rustaveli State University

REFERENCES

1. *R.Sh.Zosidze.* Thesis of Ph.D. Diss., 1971 (Russian).
2. *R.Sh.Zosidze.* Proc. Batumi Pedagogical Institute, v.16, 1973 (Georgian).
3. *R.Sowa, R.Zosidze.* Bull. Pol. Acad. Sci., Biol. Ser., v.21, 1973.
4. *A.Kownacky, R.Zosidze.* Acta Hydrobiol., 22, 1980.
5. *A.Kownacky, R.Zosidze.* Bull. Pol. Acad. Sci., Biol. Ser., 21, 1973.

საქართველოს მეცნიერებათა აკადემიის მოამბე, 159, №3, 1999
BULLETIN OF THE GEORGIAN ACADEMY OF SCIENCES, 159, №3, 1999

ZOOLOGY

V. Yasnosh, G. Japoshvili

Parasitoids of the Genus *Psyllaephagus* Ashmead (*Hymenoptera: Chalcidoidea: Encyrtidae*) in Georgia with the Description of *P. georgicus sp. nov.*

Presented by Corr. Member of the Academy I. Eliava, December 25, 1998

ABSTRACT. **Six species of the encyrtid genus *Psyllaephagus* Ashmead are now recognized in Georgia, four of them for the first time, one of which is new for science: *P. georgicus*. The information of hosts and distribution of all species are given.**

Key words: *Chalcidoidea, Encyrtidae, Psyllidae, Psyllaephagus georgicus,* new species.

Encyrtids of the genus *Psyllaephagus* Ashmead (*Hymenoptera*: *Chalcidoidea*) are known as parasitoids of psyllids (*Hemiptera*: *Psylloidea*), among them many pest insects of plant are known. In the Palaearctic 57 species of *Psyllaephagus* are known, predominantly from southern regions[1]. 10 species were registered in the Caucasus, including two of the species from Georgia: *P. procerus* (Mercet) and *P. badchysi* Myartseva. In the present paper six species recorded in Georgia are listed. Four of them are registered for the first time, including one new species for science *P. georgicus,* parasitoid of *Trioza magnisetosa* Loginova on the *Elaeagnus angustifolia*.

The information of all species and the description of new species are presented.

Terminology generally follows to Trjapitzin[1] and Noyes and Wooley[2].

Genus *Psyllaephagus* Ashmead, 1900

***P. badchysi* Myartseva**

Parasitoids of psyllids.

Distribution: East Georgia and Turkmenistan.

This species was earlier recorded in Georgia, but without any data [1].

***P. bachardenicus* Myartseva**

Tbilisi, canyon Vera, 30.V. 1997 ex *Trioza magnisetosa* on *Elaeagnus angustifolia* 3♀, 4♂; Tbilisi, Plato Nutzubidze, 6.VI. 1998 ex *Psylla ramnicola* on *Rhamnus sp.* 2♀ (G. Japloshvili).

Parasitoid of *T. magnisetosa* and *P. ramnicola*.

Distribution: Georgia and Turkmenistan.

Parasitoid in Georgia and the hosts are recognized for the first time. The species was described from Turkmenistan [3], but the hosts were unknown.

***P. procerus* (Mercet)**

Parasitoid of different species of *Psylloidea*.

Distribution: Georgia, Armenia, Russia, Ukraine, Moldavia, Hungary, Italy, Spain and Mongolia.

The species was registrated in Georgia, but without any data [1].

***P. tokgaevi* Myartseva**

Tbilisi, canyon Gldamula, 28.VI.1998 ex *Crastina tamaricina* on the *Tamarix* 1♀, 1♂ (G. Japoshvili).

Parasitoid of *Crastina tamaricina*.

Distribution: Georgia and Turkmenistan.

Parasitoid in Georgia is registered for the first time. This species was earlier described in Turkmenistan [1,4].

***P. sp. aff. rubriscutellatus* Myartseva**

Tbilisi, canyon Vere, 30.V. 1997 ex *Trioza magnisetosa* on the *Elaeagnus angustifolia* 3♀, 3♂ (G. Japoshvili).

Parasitoid of *Trioza magnisetosa*. Distribution: Georgia.

This species is near *P. rubriscutellatus* Myartseva [4], but the type material of *P. rubriscutelatus* is unknown for us for comparison.

***P. georgicus* Jasnosh et Japoshvili, sp. n.**

Tbilisi, canyon Vere and park Mziuri ex *Trioza magnisetosa* on the *Elaeagnus angustifolia* 7♀, 17♂. Holotype 1♀ is among them (G. Japoshvili).

Parasitoid of *T. magnisetosa*.

Distribution: Georgia.

This is a new species for science and description is given below.

***Psyllophagus georgicus* Jasnosh et Japoshvili, sp. n.**

Holotype: ♀ Georgia, Tbilisi, Vere canyon, 25.VII. 1994 ex *Trioza magnisetosa* on the *Elaeagnus angustifolia* (G. Japoshvili).

Paratypes: 6♀ and 17♂ were reared in laboratory during 21,29.VII.1994, 9.VII,10.VII.1997 from the same collected hosts as holotype.

The holotype and paratypes of the new species are preserved in the collection of the Institute of Zoology, Tbilisi, Georgia.

Description. **Female**. Body dark with metallic lustre. Frontovertex colour with rather green-silver-violet lustre, cheeks with violet lustre, face above fossae antenales with green-silver lustre, the other parts of head dark lustre.

Antennal scape and pedicel brownish-yellow with yellow-brownish tops; funicle and club yellow-brownish, the last segment of club blackish. Palpi yellow-brownish.

Pronotum violet-dark with lustre; mesonotum and scutellum black-goldish(silver) with goldish-green lustre on apices; axillae black-goldish; mesopleura with violet-silver lustre; propodeum with violet-goldish lustre. Fore wings without coloration, light. Legs yellow-brown, all coxae femora, hind tibiae, dark and dark brown coloration on the tops of front tibiae. Gaster dark, the basal tergites(or tergites+sternites) with green-goldish lustre.

Sculpturing. Frontovertex, mesonotum and scutellum with not deep sculpture and minute dense punctation, the top of scutellum with two long setae.

Funicle of antennae with long setae, on club the setae are shorter.

Head. Minimum width of vertex about 0.25 of maximum width of head. Apical angle of occelar triangle somewhat less than 90°. Distance from posterior ocelli to ocular margins less than diameter of one ocellus; distance to vertex margin somewhat more. Anten-

nal toruli at ocelli hind border. Distance between antennal toruli twice more than distance from them to occelli margin. Scape 6 times as long as wide, a little widening to apex. Pedicel about twice as long as wide, some widening to apex, from 4th to 6th funicle segments widening. 6th funicular segment 1.3 wider than length; 2nd and 3rd funicular segments about quadrate. Club a little wider than the 6th funicular segment, about 2.35 times as long as wide and as long as 3rd-6th funicle segments, broad rounding on apex. Fig. 1.

Mesosoma. Pronotum is short, its length measured along its middle less than its width. Mesonotum wider than length (13:9), scutellum slightly shorter than mesonotum.

Fore wings well developed, 2.5 times as long as wide, venation on Fig 2.

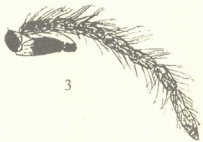

Fig. Psyllaephagus georgicus sp.nov. 1. antennae of ♀; 2. vennation of ♀, pant; 3. antennae of ♂.

Mesotibial spur a little longer than middle basitarsus. Metasoma almost as broad as mesosoma. Propodeum wider than length, in the middle more than twice shorter than scutellum. Abdomen shorter than torax. Ovipositor a little exerted.

Body length 1.1-1.3 mm.

Male similar to female, differs from female by antennae and cheeks coloration. Cheeks green-silver-lustre.

Antennal scape 2.7 times as long as wide and more wider in the middle, basal part dark-brown; pedicel shorter, etwas longer than wide, dark brown. Funicular segments as long as wide, twice longer than wide; club about two times as long as two last funicular

segments. Antennae yellow-brownish with many long setae (Fig. 3).

Body length 1.0 mm.

New species is close to *P. nartschukae* Trjapitzin described from Kirghyzstan [5]. Females differ by characters of antennae, venation of wings and body coloration. The male of this species and the host are unknown.

New species is also near to *P. bachardenicus* Myartseva described from Turkmenistan [3]. The male and host of this species was unknown too.

Etimology. The species is named for the name of the country Georgia.

Comments. On the transliteration of the first author's name. Earlier all her publications were under the name Jasnosh, but Yasnosh is more correct. Rosen and De Bach [6] suggested to adopt the following policy for the Russian name.

The authors are very thankful to professor V. Trjapitzin from Zoological Institute in S. -Petersburg for the consultation.

Georgian Academy of Agricultural Sciences
L. Kanchaveli Research
Institute of Plant Protection

Georgian Academy of Sciences
Institute of Zoology

REFERENCES

1. *V.Trjapitzin.* Parasitic Hymenoptera of the fam. *Encyrtidae* of Palaearctics. Leningrad,1989, 3-488 (Russian).
2. *Noyes J.S. Wooley J.B. North.* Journal of Natural History, 28, 1994, 1327-1401.
3. *S. Myartseva.* Izvestia of AN TSSR, 1, 1980, 47-54 (Russian).
4. *S. Myartseva.* Parasitic Hymenoptera of the fam. *Encyrtidae* of Turkmenistan and definite regions of Central Asia. Ashkhabad, 1984, 3-304 (Russian).
5. *V. Trjapitzin.* New palaearctics species of the genus *Psyllaephagus* Ashmead (*Hymenoptera, Encyrtidae*). Transactions of Institute of Zoology AN USSR, 159, 1986, 57-63 (Russian).
6. *Rosen D., De Bach P.* Species of *Aphytis* of the world (*Hymenoptera: Aphelinidae*), Jerusalem, 1979, 3-801.

საქართველოს მეცნიერებათა აკადემიის მოამბე, 159, №3, 1999
BULLETIN OF THE GEORGIAN ACADEMY OF SCIENCES, 159, №3, 1999

ENTOMOLOGY

M. Chkoidze, B. Tavadze, T. Chapidze, M. Tvaradze, A. Supatashvili, G. Kapanadze, M. Shonia

Influence of Microorganisms on Hemocyte Structure and Quantitative Composition of *Ocneria dispar* L.

Presented by Member of the Academy G. Gigauri, September 14, 1998

ABSTRACT. **Pathological changes caused by the action of different entomopathogenic microorganisms and parasites are studied in hemolymph cells of *Ocneria dispar L.***

Key words: hemolymph, hemocytes, hemogram, entomopathogenic microorganisms.

The earlier diagnostics of insect-pests epidemic diseases is considered to be important both for forecasting mass breeding and developing the methods of fighting against them [1-2].

In 1995-1997 hematological investigation of *Ocneria dispar* larvae of different ages (III-IV-V) was carried out. We aimed to study diseases and the character of microorganisms causing these diseases in the forests of Mtskheta, Didgori and Saguramo State reserve.

Microscopic analysis of fixed and Gymza-Romanovski stained hemolymph preparations was conducted by Sirotina's method [3].

The hematological investigation began with hemolymph analysis of healthy insect to study pathological changes caused by different diseases and unfavourable environment factors.

By the microscopic analysis in hemolymph of *Ocneria dispar L.* seven types of formed elements (hemocytes) were detected: proleukocytes, macronucleocytes, micronucleocytes, phagocytes, eosinophils, enocitoides and dead cells.

By comparing the hemograms, leukocytic formula was made from healthy larvae hemolymph of different ages (Table 1).

Table

Hemograms of *Ocneria dispar* larvae of different instars in norm and pathology

Instar of larvae	Percentage of Hemocytes							
	Proleucocytes	Macronucleocytes	Micronucleocytes	Phagocytes		Eosinophils	Enocitoides	Dead and pathologic cells
				spindle-shaped	non spindle-shaped			
III instar larvae								
healthy	11.5	27.1	35.1	5.3	8.9	7.1	3.2	2.8
infected	6.1	13.2	15.2	17.1	5.1	1.3	1.1	40.9
IV instar larvae								
healthy	9.1	25.8	37.8	6.1	9.2	7.4	3.5	1.1
infected	5.2	10.1	15.3	18.0	7.5	4.5	2.3	36.1
V instar larvae								
healthy	5.2	19.3	46.2	7.1	10.1	8.5	4.1	0.5
infected	2.3	12.1	16.2	20.2	8.1	5.1	1.2	31.5

As shown from the Table limited number of formed elements of blood is characteristic of each instar larvae.

Reconnoitring investigation revealed that natural mortality of *Ocneria dispar L.* spread at Mtskheta and Didgori Forestries was 30-40% whereas at Saguramo State Reserve 70-80%. The samples from those three sites showed that natural mortality was mainly caused by virus type disease, as well as by microorganizms of different types, natural enemies and unfavourable environment factors.

The data obtained from Saguramo State reserve indicate to the epizootic disease of virus type, but in populations from Mtskheta and Didgori forestries formation of expected epizooty was marked.

In alive larvae of *Ocneria dispar L.* viral, fungous, bacterial, protozoal type diseases and different species of parasites were revealed. The most pathogenic was polyhedric typed viral disease which was expressed by deep pathological changes in hemolymph. According to the degree of disease quantitative, morphological and structural changes of hemolymph cells took place in larvae of different pests. The hemograms of quantitative and pathological changes of infected larvae hemocytes are given in the Table.

As shown from the Table inserts of virus origin caused deep pathological changes in hemolymph, where as compared to norm the quantity of dead and pathological cells was increased twenty times, but those of cells with protective functions – spindle-shaped phagocytes – three times.

The quantity of the rest type of cells has considerably decreased.

In insect hemolymph infected by microorganisms along with quantitative changes of the formed elements hemocytes morphologic and structural changes took place by the following pathology: deformation of cell membrane, decentralization of nucleus to the periphery, formation of virus polyhedral contours in nucleus light places, transformation of destroyed nucleus into polyhedrons, pycnosis of different type cell nuclei, destruction of cytoplasm structure; vacuolization of enocitoides, macronucleocytes, eosinophils, micronucleocytes, phagocytes and cells degeneration.

Deep pathological changes caused by the toxins of microorganisms in hemocytes of *Ocneria dispar L.* results in insect septicemia.

According to the hemocytes quantitative, morphologic and structural changes it is possible to determine the insects physiological state, their fertility and thus make forecast of expected depression.

In conclusion we can say that the pest outbreak of the mentioned populations in the nearest future is not expected.

Georgian Academy of Sciences
V. Gulisashvili Institute of Mountain Forestry

REFERENCES

1. *N. V. Lappa.* Zaschita rastenii 4, 4, 1991 (Russian).
2. *M. Chkoidze.* Bull. Acad. Sci. GSSR, 129, 3, 1988.
3. *M. I. Sirotina.* In: Nadzor, uchet i prognoz massovykh razmnozhenii khvoi i listogryzuschikh nasekomykh. M. 1965 (Russian).
4. *M. Chkoidze.* Thesis of reports. Sovremennye dostizhenia mikrobiologii i virusologii v selskom khozyai stve. Tbilisi, 1986.
5. *M. A. Barracco, G. A. Netto.* Rev. Bras Genet., 7, 3, 1991.

საქართველოს მეცნიერებათა აკადემიის მოამბე, 159, №3, 1999
BULLETIN OF THE GEORGIAN ACADEMY OF SCIENCES, 159, №3, 1999

EXPERIMENTAL MEDICINE

Kh. Kaladze, B. Mosidze, Z.Kakabadze

The Influence of the Splenectomy on the Immunological Status of the Patients, Operated on Malignant Cancer of Stomach

Presented by Corr. Member of the Academy T. Dekanosidze, February 22, 1999

ABSTRACT. **We studied the dynamics of cellular and humoral immunity. The changes of phagocytic activity of lymphocytes, immune complexes circulating in the blood serum, T and B lymphocytes were investigated. The levels of IgG, IgA, IgM and immune complexes circulating in the blood, activity of C_{3c} complement were defined. Investigation showed the depression of patients' immunity with splenectomy. The amount of immunoglobulins in the blood serum was reduced and plagocytosis was suppressed. Investigations, conducted by us confirmed, that splenectomy may cause the decrease of resistance of the organism against infection and increase the risk of septic state development.**

Key words: splenectomy, immunological status, lymphocytes, immunoglobulins of blood serum, phagocytosis, circulating immune complexes.

With the purpose of the operative treatment of patients with stomach cancer gastrectomy or proximal resection is frequently applied. In most cases it is necessary to perform the splenectomy. According to the author [1] among the total number of operations, the frequency of splenectomy ranges from 50% to 92%.

In case of stomach cancer, the indications of splenectomy are the following: growth of malignant tumour in the pancreas tail, metastasis in the lymphatic nodes along the spleen arteries, disruption of the integrity of spleen during mobilization of stomach and small sizes of short gastric arteries ("technical" splenectomies), infiltration of stomach body and of the third part of the big curve (splenectomy by oncological reasons).[1,2]

It's known, that spleen plays important role in immunological status of organism. Resection of spleen reduces the resistance of organism against infections and may cause the development of septic condition during the postoperational period. After the splenectomy "post splenectomy syndrome "develops and results in decreasing immunologic resistance, dangerous consequence of which might be "immediate sepsis" [3-5].

With the purpose of full estimation of the results of splenectomy on the human's immunological status, we continued the investigations of oncological patients. Observations were conducted on the patients infected by malignant cancer of stomach and esophagus. The clinico-immunological state of these patients was observed before and after operation.

Our purpose was to investigate the immunological status of these patients subjected to the splenectomy and those who did not need splenectomy. Twenty two patients were observed and divided into two groups. The first group of 10 patients with gastrectomy or

proximal resection along with splenectomy. The second group consisted of 12 patients with the same type of operations, but with unresected spleen. Investigations were conducted before operation and on the 5th, 14th, 30th days after the operation.

We studied the cellular and humoral immunity indices: T and B lymphocytes, circulating immune complexes in the blood serum, changes of phagocytic activity of lymphocytes, activity of complement C_{3c} and the level of IgG, IgA, IgM in the blood serum.

The humoral immunity condition was discussed according to the circulating immune complexes (CIC) in the blood. The absorbing phase of phagocytosis was determined by phagocytic index (PI) and phagocytic activity index (PAI).

Our researches showed that amount of T lymphocytes before operation and on the 5th day after operation was almost adequate in both groups, but it was significantly decreased in comparison with normal indices. On the 14th-30th days after the operation in the first group of the patients the level of the cells was significantly decreased, but in the second group the level of the same cells reached the normal level (Table 1).

The amount of T-active (T_{act}) cells before operation was normal in both groups. On the 5th day after operation, it was noted the tendency to diminishing of T_{act} cells and such condition lasted till 14th-30th days in the first group. In the second group the amount of T_{act} cells was increased in the same interval of time.

In the first group the amount of T-helpers (T_H) was significantly reduced during the postoperational period. But, in the second group, T_H number was increased and reached the normal level. On the 5th-14th days after the operation, number of T suppressors (T_s) decreased in the first group of patients. The second group did not show the significant fluctuation of cells.

In the first group of patients the proportion of T_H/T_s was increased on the5th-14th days after operation, but on 30th day it returned to the initial level, due to reducing the amount of T_H and T_s cells.

In the second group, the mentioned proportion gradually increased, that was caused by relative growth of T_H cells' amount.

In both groups, the number of B lymphocytes before operation was the same and at the normal level.

On the 5th-14th days after the operation it was noted the tendency to their decreasing,

Table 1

Distribution of the indices of immune system in the blood serum of patients according to the different groups, before and after the operation

Indices	I group (n=10)				II group (n=12)			
	A	B	C	D	A	B	C	D
T total (%)	35.8±2.8	27.6±2.7	17.9±1.8	19.2±2.2	36.3±2.2	31.6±2.1	37.3±2.1	42.6±0.9
Tact (%)	16.4±2.6	9.9±1.1	5.4±0.8	8.4±2.0	17.8±1.4	13.0±1.1	18.2±0.7	20.9±0.9
Th(%)	31.3±3.4	19.4±1.0	13.7±0.6	17.8±2.8	31.7±2.4	23.3±1.9	29.6±1.3	36.4±1.5
Ts(%)	13.6±1.5	7.0±0.7	4.1±0.4	8.3±6.3	12.9±1.7	8.9±1.0	10.9±0.9	12.1±1.0
Th/Ts	2.3	2.8	3.3	2.1	2.4	2.6	2.7	3.0
B total (%)	12.3±1.3	8.6±0.8	5.9±0.5	6.8±0.7	13.3±1.3	11.2±1.0	12.1±0.7	13.7±0.7
CIC	0.04±0.008	0.04±0.007	0.06±0.001	0.06±0.008	0.04±0.006	0.05±0.006	0.05±0.006	0.05±0.006
Complement C_{3c} mg/ml	0.68±0.131	0.40±0.034	0.36±0.044	0.37±0.046	0.67±0.20	0.58±0.18	0.63±0.18	0.67±0.18

A-before the operation, B, C, D - on the 5th, 14th, 30th days after the operation; $p \leq 0.05$

but on the 30th day, their number slightly increased. However, in comparison with initial number of B lymphocytes, their level was far low.

On the 5th, 14th, 30th days after the operation, the number of B lymphocytes almost did not change.

Before operation the number of CIC remained normal in both groups and increased in the first group after the operation.

Table 2

Distribution of the concentration of immunoglobulins in the blood serum of patients before and after the operation according to the different groups

Indices / Group	IgG(M±m) (g/l)				IgA(M±m)(g/l)				IgM(M±=m)(g/l)			
	A	B	C	D	A	B	C	D	A	B	C	D
I(n=10)	13.07±2.03	8.52±1.56	6.96±1.44	5.89±0.11	1.05±0.11	0.71±0.18	0.69±0.11	0.98±0.2	0.94±0.22	0.6±0.08	0.49±0.08	0.39±0.07
II(n=12)	11.17±1.20	9.6±1.63	10.83±1.92	11.6±2.02	1.05±0.2	1.04±0.17	1.11±0.20	1.25±0.25	1.02±0.31	0.84±0.28	0.99±0.38	1.03±0.31

The amount of CIC in the second group remained on the upper limit of the normal level.

Before operation, in both groups the level of C_{3C} complement fluctuated within normal limits.

On the 5th day after the operation the level of C_{3C} decreased and continued decreasing till 14th-30th days after the operation.

The second group showed the normal content of C_{3C} even after the postoperational period.

Splenectomy affected the content of immunoglobulins in the blood serum (Table 2).

Before the operation the amount of IgG in both groups remained at normal level. On the 5th days after the operation the number of IgG was slightly reduced in both groups. On the 14th-30th days after the operation the level of IgG was significantly reduced in the first group, but in the second group their level gradually increased. The number of IgA in both groups before the operation was nearly the same. After the operation the level of IgA in the first group was significantly decreased in the blood serum and was bellow the lower limit, but in the second group their amount did not fluctuate significantly.

Before the operation the number of IgM was at normal level in both groups. On the 5th day after the operation both groups showed the tendency to diminishing the number of IgM. In the first group it continued till 14th-30th days after the operation. In the second group the number of IgM increased and reached the initial (before operation) level on the 14th-30th after the operation.

On the background of such dynamics the immune status alteration, the decrease of PM and PAI was noticeable in the first group of the patients. (Table 3)

Table 3

Indices of the phagocytal activity in the I and II groups of patients before and after the operation

Indices	I group (n=10)				II group (n=12)			
	A	B	C	D	A	B	C	D
Phagocytic indices (%)	63.6±1.6	55.4±0.8	53.8±1.1	52.5±0.4	65.4±2.4	57.3±1.0	62.7±1.0	63.6±1.3
Phagocytal activity index	10.8±0.8	7.8±0.6	6.7±0.5	7.3±0.6	11.2±1.0	8.7±0.8	10.4±0.6	12.1±0.7

On the 5th day the second group showed the reducing of the number of PI and PAI as compared with initial and normal levels and on 14th-30th after the operation.

The number of PM and PAI returned to the initial (prior to operation) level.

The above mentioned indices evidenced that the first group showed the depression of the immune system, when the second group did not show any important changes.

So, the splenectomy leads to the important disruption of the immunological status: immunoregulative subpopulation (TS) decreases along with the violation of proportion of different subpopulations of lymphocytes. The amount of IgG, IgA, IgM in blood serum diminishes. Phagocytosis function is suppressed, that might result in reducing resistance and increasing the risk of the development of septic state.

So, it is necessary to spare the spleen if possible. In the cases when splenectomy is inevitable we must try to keep the function of spleen somehow. It may be possible by introducing cells and substances, which are produced by spleen in the organism.

Tbilisi Medical Academy for Post Diploma Education of Physicians

K. Eristavi Research Institute of Surgery

REFERENCES

1. *A. Klimenkov, Z. Kadagidze et al.* Voprosi onkologii, 1989, 7, 822-826 (Russian).
2. *R. E. Hermann.* Surgery. 113, 4, 1993, 361-364.
3. *I. P. Pavlovski, S. N. Chulkin.* Khirurgiya, 6, 1986, 136-140 (Russian).
4. *F. A. Moore, E. E. Moore et al.* Surgery, 113, 4, 1993, 462-465.
5. *W. T. Peter, M. D. Pister et al.* Ann. Surg. 219, 1994, 225-249.

საქართველოს მეცნიერებათა აკადემიის მოამბე, 159, №3, 1999
BULLETIN OF THE GEORGIAN ACADEMY OF SCIENCES, 159, №3, 1999

EXPERIMENTAL MEDICINE

R. Jashi

The State of Cardiovascular System in the Children of Mothers Treated for Infertility of Endocrine Genesis

Presented by Corr. Member of the Academy V. Mosidze, February 19, 1998

ABSTRACT. **76 children of the mothers surgically treated for Stein-Leventhlal syndrome – primary polycystosis(I group) and 77 children of healthy mothers (II group) were studied. Cardiovascular system investigations of I group revealed that in children of mothers with PCOS in comparison with those of healthy mothers on the background of high frequency of chronic tonsillitis and vegetodystonia disregulation of cardiovascular system of both cardial (functional cardiopathies) and vascular type(arterial dystonias) have been expressed.**

Key words: infertility, Stein-Leventhal syndrome, children, mothers.

The most frequent and particularly heavy form of human sterility is the form of endocrine genesis. The cases of this disease among the other forms of women infertility amount 37.7-45% [1-4]. According to the data of Zhordania Institute of Human Reproduction in Georgia in the endocrine infertility structure of women, one of the polycystosis form – the primary (PCOS)-Stein-Leventhal syndrome has got the leading rate amounting 35%. Its surgical treatment in most cases leads to normalization of menstrual (91.9%) and birth functions (64.6%) [5]. There are several cases of investigations carried out on the healthy state of the children delivered after surgical treatment of OPS. Basically new-borns [6] and girls of pubertal period were studied. The authors point out the high rate of reproductive function disorder in these girls [7-10].

The state of cardiovascular system in the children of mothers treated for infertility of endocrine genesis is not studied. For the first time we've studied functional state of various systems of children delivered after surgical treatment of OPS, nosologic structure and frequency of this disease including their sex and age. The problem of infertility treatment will be considered finally solved when it results in delivering healthy, mentally and physically perfect generation.

As many as, 153 children were studied. The information was ranked according to the age and sex. In the main group there were 42 girls and 34 boys, and in the control group 37 and 51 respectively. All the patients were investigated according to the same program. The children were examined together with the specialists (neuropathologist,ophtalmologist, otolaringologist, endocrinologist, iridologist) of the consultation polyclinics of Pediatric Scientific-Research Institute.

The functional state of different systems(cardiovascular, respiratory, gastroenterologic, CNS and VNS) were studied. In case of need to specify the diagnosis, hormone determination and echoscanning of small pelvis cavity organs and adrenal gland(ultrasonic in-

vestigation) were carried out at Zhordania Institute of Human Reproduction.

Functional investigations were carried out at the Functional Diagnostic Department of the Pediatric Scientific–Research Institute. To evaluate cardiovascular system there were used ECG and PCG investigations by German polyparametric cardiograph. ECG-registration was carried out in 12 inclinations on the cardiograph "4-NEK-6" and PCG on the phonocardiograph (Mirgograf-34) from the following points: summit, the fifth point, lung artery, aorta, t, m_1, m_2 and h rate. For evalution of vegetative nervous system and functional state of the organism method of cardiointervalography was used.

Analysis of obtained information revealed tonsils enlargment in the I group children, within 12-months of age, unlike the control group. The frequency of this pathology grew in accordance with the age of children. The cases of chronic tonsillitis were 1.5 times and the cases of adenoidal vegetation –2 times more frequent in the I group than in the II one, more in girls than in boys, that should be caused by change of the organism's reactivity due to inefficiency of the adaptation-compensatory mechanisms and can be explained by congenital disfunction of vegetative regulation in these children.

The analysis of the clinical data showed that from the cardial rhythm disorders there prevail cases of bradycardia(28.6%-9.1%) and sinus arrhythmia (19%-9.1%) in children of mothers with (PCOS) under 7 years in accordance with the control group, but in 8-16-year children tachycardia (30.8%-14.3%) and bradycardia(29.1%-14.3%) were mostly expressed. Moderately expressed heart tone deafness was shown with equal frequency in both groups. In half of the main group of children under 7 years systolic murmur was revealed. It was mostly tender and rarely of moderate intensity. In 8-16-year children murmur was expressed in two third of cases.

In both age groups children of mothers with ovary polycystosis different from the children of healthy mothers the rise of maximal arterial hypertension was marked, but as to pulse hypertension it was increased in 3-7 and decreased in 12-16-year children that shows presence of vegetative vascular dystonia in this category of children.

Study of cardiac bioelectric processes showed that in the main group more often automatism and excitation and lesser conductibility function disorders were shown. Disorder of metabolic processes in myocardium was revealed by electric systole extension, its phase structure disorder, voltage reduction, prolongation of systolic indices, morphologic changes of T and P waves and by repolarization disorder. All of these, in accordance with tonsillogenic intoxication may be conditioned by neuro-vegetative regulation disorders.

Analysis of phonocardiogram data revealed that in the children under 7 years of mothers with OPS, disorder in tones correlation in the projective area of the summit and V point was sharply expressed in both age groups, 92.3%-90.5% accordingly. Systolic murmur in early age children was revealed in 56.9% and in 23.1% by lower moderate amplitude. In 8-16-year children systolic murmur was expressed less frequently (48.65%). It was mostly of low or of moderate amplitude.

Length of murmur was expressed alike in both age groups, mostly it was 1/3 of systole and rarely 1/2 of it . Systolic murmur was revealed with equal frequency on the summit, V point, lung artery and on some points at the same time 12.5%, that is nearly identical for both age groups. But on the aortus murmur was revealed 2 times less frequently than in early age children.

While working on the material according to the sex it was revealed that changes of bioelectric activity in the early age are equally shown in both sex children, but in pre and pubertal period mostly in girls. On the background of variation analysis of cardial rhythm in most children (60%)of mothers treated after SLS there were shown vagotonic directed vegetative disbalance and decrease of organism functional state (81.8%) and adaptation reserves (72.6%) by which early reveal and high rate of polylymphoadenopathies (tonsillitis, adenoidites) can be explained in these children. The results obtained response to the literature data according to which electrocardiographic changes were revealed while studying patients with vegetative disorders [11].

Investigators think that the genesis of the obtained results is in connection with inefficiency of neuro-vegetative control of cardiac electric activity while being increased the effect of parasympathetic system. Systolic murmur in the main group children must have been conditioned by functional deficiency of mitral valve apparatus that may be caused by falling of myocardium contractility function, from the other hand by inclusion of VNS in this process. According to N. Belokon's data the changes developed in cardiovascular system during chronic tonsillitis may be caused by inclusion of VNS in the process and by reflex effect from pathologically changed tonsils [12].

Thus, in children of mothers with PCOS in comparison with the children of healthy mothers, disregulation of cardiovascular system both of cardial (functional cardiopathies) and vascular type (arterial dystonies) was more revealed that was confirmed by the data of clinical and instrumental (ECG, PCG) investigations and may be explained by high frequency of tonsillogenic intoxication and vegetovascular dystonia.

Complex therapy of these children is advisable by the individually chosen scheme according to the data of functional diagnostic investigations.The obtained results should be taken into consideration while working out the preventive measures for children of the above-mentioned category.

Scientific Research Institute of Pediatrics

REFERENCES

1. *B.M.Sidelnikova.* Nevynashivanie beremennosti. M.,1986, 20-23 (Russian).
2. *C.I. Kheifets.* Besplodie endokrinnogo proiskhozhdeniya y zhenschin. M., 1970, 191 (Russian).
3. *W. Bickenbach, G. Pozing.* Die sterilität der Frau. Stuttgart, 1967.
4. *H. Staemmler.* Der gyna Kologischen Endocrinologie. Stutgart, 1969.
5. *E.G. Veinberg, O.C. Markarova, N.I. Bablidze.* Akush. I Ginek, N10, 1982,19-22.
6. *C.I. Kheifets, M.B. Igitova.* Akysh. I ginek. N4, 1991, 52-54.
7. *C.I. Kheifets, E. Markova.* Tezisi dokladov vtoroi vsesous. konf. po ginekologii detei i podrostkov. 1990, 135.
8. *I. B. Kuznetsova.*Candidate Thesis. Moskva, 1991, 17.
9. *M. Ushikishvili et al.* XI World congress pediatric and adolescent gynaecology, Singapore, 1995, 124.
10. V. Dramusic. XI World congress pediatric and adolescent gynaecology, Singapore, 1995 p.38.
12. *B.I. Makolkin, C.A. Abbakymova.* Neirocirkylyatorn. distoniya v terapevt. praktike. M., 1985, 192 (Russian).
13. *I.A. Belokon, M.B. Kyberger.* Bolezni serdtsa i sosydov u detei M.,1987, 480 (Russian).

საქართველოს მეცნიერებათა აკადემიის მოამბე, 159, №3, 1999
BULLETIN OF THE GEORGIAN ACADEMY OF SCIENCES, 159, №3, 1999

ECOLOGY

D. Tskipurishvili, N. Chikvaidze

Ecodynamics Prognosis Problem in the Case of *Microtus socialis Pallas* Population

Presented by Corr. Member of the Academy I. Eliava, August 3, 1998

ABSTRACT. **The method of the prognosis of the population dynamics taking into account the biological and climatic data is worked out.**

Key words: population dynamics, statistical-probabilistic model.

This paper follows the purpose to work out the vole (M. soc. Pall.) reproduction prognosis on the base of scientifically established facts and regularities. This gives us an opportunity to carry out effectively the measures of the struggle against the voles in order to avoid the outbreaks in voles, when they greatly damage the agriculture and make serious danger to human's health.

The statistical-probabilistic model of the vole population dynamics given in [1] makes it possible to calculate the number of voles in any time interval (the least in a two-month interval) if the vole's biological characteristics are known.

The annual development cycle t of voles is considered and divided into two-month intervals Δt_i (i = 1,...6) taking together January and February (Δt_1), March and April (Δt_2), etc. For a quantitative evaluation of the influence of the environment on the reproduction process the reproduction coefficient γ is taken, which represents the product of the sex ratio, the average number of embryons per pregnant female and the average percent of females taking part in reproduction. The mortality is evaluated by means of the life span τ, since the probability of mortality for time interval Δt is given by formula $\pi(\Delta t)=1-\exp(-\alpha*\Delta t)$, where $\alpha = 1/\tau$.

The investigations [2-4] have shown that in Shiraky steppes, which is the main and typical part of vole's area in Georgia, γ is varied from one two-month interval to another (seasonal variations) as well as within each interval according to the optimum (j_i=1), middle (j_i = 2) and minimum (j_i = 3) life conditions. To j_i = 1 correspond the high values of γ and τ, to j_i = 2 - the middle values and to j_i = 3 - low values of γ and τ. Thus, the influence of the environment on the birth process is described by 18 parameters (γ_{ij}, j_i=1,2,3; i=1,...,6) and the influence on the death process by 3 parameters (τ_{j_i}; j_i=1, 2, 3). Let us describe the year by the environmental changes marking by "a" the optimum (j_i=1), by "b" the middle (j_i=2) and "c" the minimum (j_i=3) life conditions, we shall get 3^6=729 different "structures", as $a_1a_2a_3a_4a_5a_6$, *aaaaab*,...., *cccccc*.

Let us introduce a coefficient Γ which shows how many times the number of voles increases during a year if mortality is taken into account ($N_6 = N_0*\Gamma$, where N_0 is an initial number of voles). We shall call it the coefficient of the yearly increase in number

and define it by the following: $\Gamma_{j_1,\ldots,j_6} = \prod_{i=1}^{6}(1+\gamma_{j_i i})\varepsilon_{j_i i}$, where $\varepsilon_{j_i i}=\varepsilon_{j_i}=\exp(-\Delta t_i/\tau_{j_i})$

shows the fraction of surviving voles in Δt_i time interval.

Thus, the model gives us an opportunity to calculate the number of voles at the end of the year, or at the end of any two-month interval Δt_i, if the "structure" of the year, for example "abbcaa" and γ and τ corresponding to this structure are known. The determination of the structure of the year is connected with the prognosis of those factors which define the optimum, middle and minimum life conditions for the voles.

The model [1] was checked up by Shiraky steppes' data, where there were the curve of the voles population dynamics with 6 peaks within 23 years, the voles' biological characteristics in each two-month interval corresponding to the life conditions and the data of the following factors: the precipitation (x_1), temperature (x_2), vegetable cover (x_3), sun-sports (R. Wolf's numbers-x_4) and etc.

Using the methods of the regression analysis the relationship between the environmental factors and the average number of embryons (Z) and the yearly reproduction coefficient (Γ) are received. Moreover, Z depends on x_1 and x_2, but Γ depends on four factors. The variation limits of the factors in the given time inretval (two months for Z and an year for Γ) correspond to the minimum and maximum values of the factors within 23 years.

The linear regression equations for the average number of embryons (in code designations) are:

$$Z_{(I\text{-}II)} = 4.845 + 1.92x_1 + 0.88x_2 - 0.045x_1x_2, \quad (1)$$

$$Z_{(III\text{-}IV)} = 7.055 + 0.42x_1 - 0.575x_2 - 0.05x_1x_2, \quad (2)$$

$$Z_{(V\text{-}VI)} = 6.7 + 0.9x_1 - 0.675x_2 + 0.275x_1x_2, \quad (3)$$

$$Z_{(VII\text{-}VIII)} = 4.2 + 0.825x_1 - 0.45x_2 - 0.325x_1x_2, \quad (4)$$

$$Z_{(IX\text{-}X)} = 5.375 - 0.375x_1 + 0.875x_2 + 0.625x_1x_2, \quad (5)$$

$$Z_{(XI\text{-}XII)} = 4.875 + 0.675x_1 + 0.875x_2 - 0.325x_1x_2, \quad (6)$$

The linear regression equation for the yearly reproduction coefficient Γ is:

$$Y_\Gamma = 6 + 3.062x_1 - 2.937x_2 + 3.5x_3 - 0.687x_4 - 2.375x_1x_2 + 2.862x_1x_3 - 0.675x_1x_4 - 2.637x_2x_3 - 0.075x_2x_4 - 0.637x_3x_4 \quad (7)$$

On the basis of the equations (1),..., (6) we may conclude that: the influence of the temperature and the precipitation on the average number of embryons is different in the various intervals of time. The increase of the temperature in cold months promotes the increase of Z (equat. (1), (5), (6)), but high temperature in hot months reduces the number of embryons (equat. (2), (3), (4)). The abundance of precipitation (more than normal) (mean for many years) plays the main part in each two-month interval except the IX and X months, where the interaction effect of two variables x_1 and x_2 is much more important than the effect of the precipitation taken separately. The main role of the precipitation is quite clear, as it is closely connected with the amount and variety of the vegetable cover in Shiraky steppes (the correlation coefficient equals to 0.757).

According to the equation (7) the yearly reproduction coefficient Γ is mainly influenced by the vegetable cover, the precipitation, the temperature and the combinations of

these factors. The sun-sports' influence is much less.

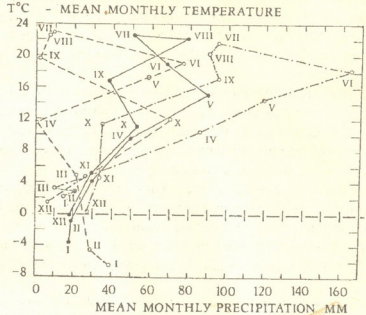

Fig. 1. Graph showing the mean monthly temperature and precipitation within the year in Shiraky steppes. — • — normal (mean for many years), — — ○ — — and — · — ○ — · — correspond to the years when min. and max. number of voles vere observed.

At the same time the analysis of the temperature and the precipitation for 23 years shows that in the years of the population peaks the temperature in Shiraky steppes in January was 2-6^{0}C higher than normal, in February it is 1-3^{0}C higher and the XI and XII months before the peak years the temperature is 1-3.5^{0}C higher. As to the annual mean precipitation in peak years it is much higher than normal (493 mm). The mean monthly precipitation is especially higher in the IV-IX months.

In Fig. 1 the graphs showing the mean monthly temperature and precipitation are given. One of them corresponds to the normal (mean for many years) values of the temperature and precipitation the rest correspond to the years, when the low and the peak number of voles were observed.

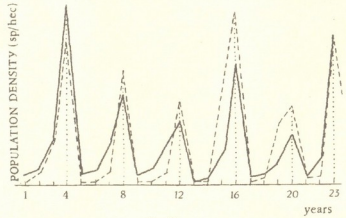

Fig. 2.

On the basis of the received results and the correlation coefficients between factors, which make possible to consider the temperature and precipitation as independent factors (correlation coefficient equals to -0.18), the optimum, middle and minimum life conditions for each two-month's period for 23 years were determined and according to the model [1] the number of voles was calculated. The results may be also checked up by [6,7], where paper [1] is used.

In Fig.2 the theoretical (obtained by calculation) and real (based on observations) curves of the vole population dynamics for 23 years are given. We can see clearly that the results of the calculation agree with the observed data. The theoretical curve reflects all the basic peculiarities of the vole population dynamics and coincides completely with the real curve based on observations in Shiraky steppes.

So, for the prognosis the number of voles in any period of time according to the given statistical-probabilistic model [1], it is necessary: on the basis of the prognosis of the precipitation and the temperature of each two-month's period to determine the optimum (a), middle (b) and minimum (c) life conditions for voles and according to the γ and τ corresponding to these conditions to calculate the expected number of voles.

Georgian Academy of Sciences
Institute of Zoology

Tbilisi I. Javakhishvili State University

REFERENCES

1. *D. G. Tskipurishvili.* The statistical-probabilistic simulation of the ecological system. Extract from 6th International Congress on Cybernetics, Namur (Belgique), 1972.
2. *S. S. Kokhia.* Sazogadoebrivi memindvria (Microtus socialis Pallas) Sakartveloshi. Tbilisi, 1968, (Georgian).
3. *V. I. Kankava.* Sazogadoebrivi memindvriis embrionebis sksta tanapardoba sezonebis mikhedvit. Tskhovelta ontogenezuri ganvitareba. Tbilisi, 1965 (Georgian).
4. *T. A. Otskhelli.* Masalebi sazogadoebrivi memindvriis nakopierebis dinamikis shestsavlisatvis Shirakis velis pirobebshi. Tskhovelta ontogenezuri ganvitareba. Tbilisi, 1965 (Georgian).
5. *N. L. Johnson, F. C. Leone.* Statistics and experimental design in the engineering and physical sciences, New York, 1977.
6. *V. V. Chavchanidze.* Bull. Acad. Sci. GSSR, 67, 1, 1972. dep. VINITI, N 4921-72. Tbilisi, 1972 (Russian).
7. *D. G. Tskipurishvili, V. V. Chavchanidze, N. P. Naumov, V. S. Lobachov.* Proc. Acad. Sci. Georg. Biolog. series, 5, 2, 1979 (Russian).

საქართველოს მეცნიერებათა აკადემიის მოამბე, 159, №3, 1999
BULLETIN OF THE GEORGIAN ACADEMY OF SCIENCES, 159, №3, 1999

LINGUISTICS

L.Gamsakhoordia

Phonetic Means of Expressing Modality

Presented by Member of the Academy T.Gamkrelidze, February 12, 1998

ABSTRACT. **Subjective or textual modality is perceived on the level of integral poetic text (PT). Relatively autosemantic segments of PT united into an integral dynamic system can have aesthetic influence upon the reader. Sound orchestration as an inseparable part of PT conveys a poetic message imbued with emotional and attitudinal evaluations.**

Key words: modality, poetic text

Modality as a textual category being a dynamically extended system is connected with the generative mechanism of text. In poetic text (PT) the expression of modality is based on particular arrangement of speech units and their communicative purport. Presented in a written from PT is a message imbued with emotional and attitudinal overtones and designed to be spoken. The spoken means can express modal content and represent a complex unity of verbal, segmental and suprasegmental features. The interrelation between informative and modal structures is very complex and cannot be detected in a single utterance. Textual modality, which is subjective in its essence [1], constitutes part of the poet's pragmatism and needs a textual space to be revealed. Segments of PT are characterized by relative independence. Purposeful arrangement of lexical images in PT, their horisontal and vertical interrelationship create a lexical net which is made into one whole by its unified theme and sentiment. The character of syntactical units, their prosodic patterning, the metrical scheme modified to suit the natural rhythm of a language, and sound orchestration form integral PT capable of expressing subjective, i. e. textual modality. Hence relatively autosemantic segments of PT can have an aesthetic impact upon the reader when they are united into a unique dynamic system. Consequently the isolation of speech units is artificial and serves only to facilitate linguistic analysis.

In PT, for convenience, the performer's and the author's means [2] can be singled out. The author's means constitute the verbal side of PT, its sound orchestration, punctuation, division into lines and stanzas, end-pauses which are graphically indicated. As far as the performer's means are concerned (tone direction, pitch, tempo, loudness, internal pauses, etc.), they are revealed during performance and depend on an interpretation of PT. This paper deals with the author's means of expressing the poetic message - sound orchestration. Under this term is meant assonance, alliteration, euphony, onomatopoeia, paronomasia, sound images, rhythmic and rhyme systems.

Adgar Allan Poe's poetry shows how artistic arrangement of sounds brings to light pragmatic intent and attitudinal relations of the poet. One of his poems "Eulalie" is a good illustration of this.

" Eulalie" is a poem of three stanzas having a peculiar rhythmic and rhyme pattern-ing: the first stanza is shorter than the rest. The lines within each stanza are irregular: the first and second lines have four and five syllables respectively. The third line has eight or nine syllables. The two final lines of each stanza contain fifteen syllables with the exception of the last line in the second stanza which is made up of seventeen syllables.

Neither stress distribution is regular in the poem: the short lines have two or three accented syllables and in the long lines six syllables are given prominance by stress. The same can be said about the metrical scheme which is modified within the limits of each stanza: the four-syllable lines have iambic metre, in a five-syllable line the iambic foot is followed by the amphibrachic or anapaestic foot. Longer lines usually contain amphibrachic or anapaestic feet. The final three-syllabled segments of the long lines cannot be placed within the frame of the recognized English metrical pattern, e. g. blushing bride (- ∪ -). In accordance with linear succession, these words are epithets: stagnant tide, radiant girl, unregarded curl, careless curl, matron eye, violet eye. Horisontally these line-ending words are rhymed: tide - bride; girl - pearl - curl; sigh - sky - eye. These epithets used by the poet to characterise his sweetheart are emphasized by internal rhyme, euphony, heavy accents and end-pauses.

Ah, less - less bright
The stars of the night
Than the eyes of the radiant girl!
And never a flake
That the vapor can make
With the moon-tints of purple and pearl,
Can vie with the modest Eulalie's most unregarded curl -
Can compare with the bright-eyed Eulalie's most humble and careless curl.

Rhyme and rhythmic patterns are repeated in each stanza (aabccbbb) with the exception of the first shorter stanza (aabbb). Each seemingly asymmetric stanza turns out to be extremely symmetrical within the limits of the whole poem. The stanza as the largest segment is in dichotomous relation with the whole poetic text: the asymmetry of each stanza is removed by the symmetry of the poem considered as integral PT.

Irregularity of small and large poetic segments, lingering final lines, divided by caesuras, quicker tempo of shorter lines create an impression of a shift in the rhythm of the poem.

Full external and internal rhyme patterns enrich the poem with sweet melody. It seems that only through verbal means the poet failed to give a perfect artistic image of the fantastic world in which Astarte, the Phoenician goddess of beauty and violet-eyed Eulalie coexist.

Now Doubt - now Pain
Come never again,
For her soul gives me sigh for sigh,
And all day long
Shines bright and strong,
Astarte within the sky,
While ever to her dear Eulalie upturns her matron eye -

While ever to her young Eulalie upturns her violet eye.

This poetic idea is strengthened by alliteration (l m n t d j s) and assonance (ou ei ai etc.) which are moderatelly distributed throughout the poem. The sound l, in this comparatively short poem, recurs thirty-seven times and forms euphonic pairs: gentle Eulalie, yellow-haired Eulalie, purple and pearl, careless curl, etc.

The phonic effects employed by the poet seems to be in harmony with the transcendent world created by him. Some shift in the meaning of words thanks to their euphonic features is not an unusual phenomenon in E. A. Poe's poetry.

In "Eulalie" we have some examples of paranomasia which support this suggestion. The words "purple and pearl" partially losing their dictionary meaning in the context suggest some fantastically beautiful shades of colour with which the moon can tint the cloud. The connotation is based on the fact that these adjacent words are euphonic. In vertical section the euphony of the words is made more masked by distant and close alliteration, assonance, and by full rhymes.

Equally interesting seems to be the alliterated words of the third stanza -" For her soul gives me sigh for sigh." The word" sigh" is not used with its usual referential meaning (deep breath indicating sadness, tiredness, relief), here it denotes spiritual harmony existing between the lovers. This connotation is supported by the previous lines in which the poet assures us that pain and doubt are never to come again" For her soul gives me sigh for sigh".

Recurrent sounds, euphony, original rhythmical arrangement, the changing metrical scheme are supposed to help the poet express spiritual uplift and belief in a celestial world of beauty where his lover dwells. E. A. Poe's poetry abounds in sound images; onomatopoeia and rhythmical shifts are often employed to express emotion (e.g. The Raven, The Bells, Eldorado and others). Sound orchestration, in the lesser degree, is also used in prose and drama. Shakespeare, for instance, in" Romeo and Juliet" by purposeful distribution of sibilants and close vowels makes Juliet (act III, scene V) express her negative attitude to dawn which threatens the lovers with separation. However, Shakespeare, as any other poet, uses larger sequences of PT to express attitudinal relationship. Reference of a single sound to meaning or emotion is arbitrary and subjective. Textual modality is perceived on the level of integral PT where all speech units are united by one pragmatic purport. E. A. Poe is well aware of this, his poetic idea is expressed through metaphor incarnated in verbal and sound images.

Sound orchestration in PT consisting of interrelated segments convey meaning and modality. Passing through the inner world of a poet, it emerges as a poetic message coloured with emotional overtones and attitudinal evaluations.

Tbilisi I. Javakhishvili State University

REFERENCES

1. *J. K. Galperin.* Tekst kak obiekt lingvisticheskogo issledovaniya. M., 1981 (Russian).
2. *I. V Arnold.* Stilistika sovremennogo angliiskogo yazyka. L., 1981 (Russian).

საქართველოს მეცნიერებათა აკადემიის მოამბე, 159, №3, 1999
BULLETIN OF THE GEORGIAN ACADEMY OF SCIENCES, 159, №3, 1999

LINGUISTICS

M. Khachiashvili

Distinctive Category of Creative Text

Presented by Member of the Academy M. Andronikashvili, December 30, 1998

ABSTRACT. **The article presents the investigation on the text of creative literature. A new category of the text characteristic in the opposition "creative - non creative-text" has been proposed.**

Key words: text, creative literature.

Text theory is considered to be an independent discipline, though the investigators have not yet come to common ground as to the definitions of the text and its categories: integration, cohesion, retrospection and other categories which are considered to be inherent in any text generally. To our mind they do not completely cover all the texts, namely, the text of creative literature. Both texts (prosaic and poetic) are characterised by two unique distinctive features, one of which is well-known to poetics, but is scarcely mentioned in the text linguistics. One of the features principally differentiates pieces of art from "synonymous genres", e. g., paintry from photography, creative literature from non-creative literature: a portrait created by an artist from a photo, a creative text from non-creative text. This feature shows the existence of two types of information in a piece of art (information expressed by explicitly on the surface level and on the underlying level) and since as a result the possibility of multifold decoding of a literary work compared with other types of texts. This feature has already been known to poetics.

The second distinctive feature of the creative text is to our mind the category which can be called the category of "deep symmetry". We think that this category of "deep symmetry" means distinctive feature, which differentiates a literary text from a non-literary one, a poetry from a simple verse. We could have called this the category of esthetics, but we do not. This would be just a mere general, abstract characteristics. We propose that it lies in the fact of creating the above-mentioned symmetry. That is why we call it "deep symmetry". In other words it is the category which turns a verse to prose.

Here is an example of a verse:

Sweet porridge hot,
Sweet porridge cold,
Sweet porridge in the pot
Nine days old
    Some like it hot
    Some like it cold,
    Some like it in the pot
    Nine days old.

This is a verse but not a poetry. It does not contain "deep symmetry". To put it in

other words, there is no "symmetric" kind of interrelation (coincidence) between different phenomena of the Universe, being more precise, between a human being (including the reader) and the mankind, between laws of human life and those of the life of the Universe.

The same can be expressed in different way. One of the main functions of art, including verbal art is to turn personal and individual into the fact of the general culture. An artist is able to find the "cause-result" relations between the phenomena of the world. He generalizes them up to the point of common, generally human, universal laws.

Thus, we propose a new category of the text, the category of "deep symmetry" and consider it to be an essential, distinctive characteristics in the opposition: "creative - non-creative text".

REFERENCES

1. *R. Bart.* Novoe v zarybezhnoi lingvistice, VIII, M., 1978, 1-442 (Russian).
2. *V. Dresler.* Novoe v zarybezhnoi lingvistike, VIII, M., 11-138 (Russian).
3. *S. M. Gindin.* AKD, M., 1972.
4. *G. V. Kolshanskii.* Lingvistica teksta, materialy nauch. konf. MGPIIA im. Morisa Toresa, I, M., 1974, 48 (Russian).
5. *M. Natadze, G. Natadze.* Dasavlet evropis literatura, Tbilisi, 1988, 194-260 (Georgian).

LINGUISTICS

V. Akhalaya

Interrogative Particles as Means of Subordination in Zan

Presented by Corr.Member of the Academy G.Topuria, February 15, 1999

ABSTRACT. **There are two interrogative particles in Zan: -o (Megrelian) and -i (Chan), which sometimes serve as subordinative suffix.**

Key words: particle, Zan.

In special literature it is indicated that "...on early stage a complex sentence was conjunctionless or asyndetic, where interrelations were expressed only by intonation". ([1], p.7). On the following stage the intonation became marked. It is so in Zan where two interrogative particles -o (Megrelian), -i (Chan) sometimes appear as subordinative suffix. The particle -o in (Megrelian) sometimes serves as a conjunction -ni [-rom] (that) . In such cases subordinate clause anticipates principal clause and the verb of a subordinate clause stands before predicate which borders a principal clause, ending in interrogative particle -o ([2], p.18). The same phenomenon is observed in Chan.

First let's regard examples from Megrelian.

a) **A subordinate clause is followed by principal clause**: kars mioǯinu-o, mudgareni kimkočaru (Khub,3_{11}) "kars šexeda-a (=that looked), rayac micerili akvs." Bošik ešeʔdo gioǯinu-o, kičinu ǯɣabi (Khub, 34_{24}) "biči avida da šexeda-a (=rom šexeda), icno gogo". [The boy climbed and when looked, recognized a girl]. Ešmakemk gogonu-o, kalam tik agičkar (Megr., I, p.102) "ešmakebma štagagones-a (=rom štagagones) kalami iman agičkara" [the devils inspired you to take the pen]. Tina vardu-o, ma voɒvilapen? (Megr., II, p.130)". Is ar iqo-a (=ar iqo rom), me movakvlevine? [Wasn't he that I made kill].

It seems -o particle form is found in another position with above-mentioned function:

b) **A subordinate clause is preceded by the principal clause**. Eper muk acgaǯiru, čkimda kisxune-o tina? (Megr., I, p.91) "Iseti ra mogečvena, čems tavs arčie-a (=rom arčie is. [What have you seen that you prefer it than me]. Dia, koγo, demetxii, gvalo arto včkomunk-o? (Megr., I, p.195) "bičos, koγo, damexsen, sul mtlad mčam-a [rom mčamo]? (=that you eat me)?" [Oh, leave me alone, the mosqito, you are eating me]. Mu ore, baba, koči xolo orkun-o? (Megr., II, p.74) "ra aris, baba, kaci kidev aklia-a (=rom aklia)?" [What is it, father, that we are still short of a man]. E bošik ucuu: - kibe kuuyunia-a-v-o (Megr., II, p.14) "am bičma utxra: - kibe tu akvso" [This boy asked if he had a ladder]. Mu reni, koičkun-o, ale-v-a? (Megr., II, p.138) "ra aris, tu ici, aleo?" [Aleo, what is the matter, if you know?].

Particle -o from Megrelian corresponds to Old Georgian interrogative -a marker ([3,4], p.187) which is also found in Svan e.g. marexi-a? [Are you a man?]. ([5, 256]) This marker is not used in Modern Georgian, [6] but it is found in Khevsurian, Tushian, Pshavian and is also marked by A.Shanidze as far back as in 1915 [8].

As to Gurian and Acharian, according to K.Lomtatidze ([7], p.337-345) the final

vowel of the subordinate clause in final word is lengthened (Gurian *rom dabrundebă...* Acharian *rom daacvenĕn...*). Analogue is found in Ingiloan (which historically must have been so) where -a vowel which "...can't be separated in this place as the lengthening of final vowel in Gurian-Acharian" ([7], p.340) e.g. rom mobrunda-a... rum misulan-a, etc.

Thus, a conclusion is made that "in Gurian and Acharian -a must have been lost and on its basis the final vowel is lengthened. It seems as if -a represents affirmative-interrogative "ara" particle, or the part of the auxiliary verb "ara" in the function of determination ([7], p.342). More reliable seems the supposition by which this -a is an interrogative particle, and in the mentioned dialects the lengthening of the final vowel expresses interrogation by intonation. "Such obstacle indicates to old tradition when simple sentences coexisted side by side and one of them i.e. the bearer of interrogation later transformed into independent sentence, a connection was elaborated in it, a note of interrogation was omitted and two sentences were joined by grammatical means - the process of subordination was finished" ([9], p.448).

In Megrelian dialect of Zan along with oden-o forms of interrogative particle other subordinative particles are used, after which the function of -o together with interrogative to express subordination disappeared and in such case it only expresses interrogation e.g. natrik koc̣geurta-ni, mutun cingis vačarun-o, (Megr., I, p.39) "natvra rom kacs auxda, aravitar cignši ar ceria-a?"... vešilcben-o tik xolo memidinas-ni (Megr., II, p.162) "gana ar šeizleba-a, rom isic damekargos?" [Isn't it possible, that he might be lost too?]. čkimi va mobaγ̣ du-o, šxvaši va mibǯiniko-ni (Kipsh., 115_{17-18}) "čemi ar meqoboda-a, rom sxvisi ar mimemategina?" [Wasn't it enough for myself not to add the others?], iša va gisxunano, dudi va diγorati-ni? (Kipsh., 116_{3-4}) "is ar girčevniat-a tavi rom ar moitquilot?" [Isn't it better for you not to deceive yourself?].

Thus the lengthening of the above mentioned vowel in Gurian and Acharian, preservation of interrogative particle -a in Ingiloan, and reveal of this vowel corresponding to -o in the Megrelian dialect of Zan appear as reflection of a united syntaxic phenomena i.e. a united oldest means of expressing subordinate clause. Functionally such forms as rom [that], tu [if] are represented as predecessors of subordinate clause with conjunction.

Let's regard Chan dialect of Zan. In Chan interrogative is formed by means of -i particle if interrogative sentence doesn't contain interrogative word ([4], p.187). E.g. xoǯa, tokis pkveri kogipinen-i? (Chik., II, 9_{27-28}) "xoǯa, tokze pkvilis gapena šeiǯleba-a?"[Khoja, can the flour be hanged on the rope?] Axmedi, mskveri doqvil-i-ma? (Chik., I, 96_{23}) "axmed, iremi mokali-a-metki? [Akhmed, did you kill the deer?] ...oxoršа ham čima lazuti amčešen-i? (Chik., II, 105_{21}) "cols šeuzlia-a am cvimaši siminds udaraǯos (damcqemsos)?" [can the wife keep watch of corn in such a rain?] si xandγa čumani bazariše va idi-i (Chik., II, 53_{14}) "šen dγes dilas bazarši ar caxvedi-a?" [Didn't you go to the market this morning?].

In interrogative words and other particles of Chan verbal forms side by side with -i-(j)-a endings –i-i(j)a can be found too, where -i standing between interrogative -i- and particle of the other word -(j)a appears as emphatic vowel ([10], p.93): moxtes-i-a||moxtes-i-i-a? "Have they come" ...ičinit-i-a||ičinit-i-i-a? [Did you recognize?]

Interrogative particle -i in Chan, analogous to Megrelian -o, derives subordinate clause by "tu" (if), "rom" (that) conjunctions which can be transmitted into Georgian.

A principle clause is followed by subordinate clause, and sometimes is preceeded

by it: imuq̇a rtus mextartu-i? (N.Marr, p.83) "gaemgzavrebi, rac ar unda moxdes-a?" [Will you start all the same?]; ma qali memoč̣kira gintur-i-a?! (Chik., 1, 15_{26}) "čemtvis qeli gamogečra, gindoda-a-o" (=rom gindodao) [Did you want to cut my throat?]; ɣeas mu boɣodi, kogičkin-i-a? (Chik., II, 33); "imas ra uqavi, ici-a (i.e. "tu icio?") [what have you done with it if you know?]. ɣonas goc̣kenan "K?extu-i va ?extu-i? (Chik., II, 50_6) "qanas atvalierebeп: 'amovida-a, ar amovida-a" (i.e. "tu amovida, tu ar amovida") [They are watching the corn field if it grows or not].

Here again similar to interrogative form of -o particle in Megrelian, when in the words formed by -i particle appear other subordinate particles, -i particle expresses a kind of interrogation: si-a, ma-na gicume, va ognami-i-a? (Chik., II, 37_{15}) "šeno, me rom geubnebi, ar gesmis-a-o?! [Didn't you hear when I'm speaking to you]; guguli nena var ogna-ša, mendulun-i?! (Chik., II, 127_{9-10}) "gugulis daʒaxils ("sitqvas") sanam ar gaigonebs, çava-a?! [Before you hear the nightingale call, will it go?!]; mažura kočis ucu-ki komoxtu-i-a? (Chik., II, 33_8) "meore kacs rom utxra movida-a-o? [When he told the another man, if he came?].

According to the illustrative material mentioned above the behavior of the interrogative particle -o in Megrelian and in Chan is very similar. Both of them are able to build the construction equivalent to subordinative conjunctions "rom" [that] and "tu" [if].

But if -o naturally corresponds to interrogative -a particle in Georgian, and to -i in Chan such correspondence isn't observed in Georgian, although there is a functional correspondence between them ([4]. p.187).

Tskhinvali State Pedagogical Institute

REFERENCES

1. *V.Topuria.* Kartuli enis da literaturis sc̣avlebis sakitxebi skolaši. Tbilisi, 1960 (Georgian).
2. *N.Abesadze.* Collective works of TSU, 114, Tbilisi, 1965 (Georgian).
3. *I.Kipshidze.* Gramatika mingrelskogo (iverskogo) yazyka. St.Petersburg, 1914 (Russian).
4. *A.Chikobava.* čanuris gramatikuli analizi. Tbilisi, 1936 (Georgian).
5. *A.Chikobava.* Introduction to Linguistics. Tbilisi, 1952.
6. *B.Jorbenadze.* The Kartvelian Languages and Dialects. Tbilisi, 1988.
7. *K.Lomtatidze.* Iberian Caucasian Linguistics. Tbilisi, 1, 1946.
8. *A.Shanidze.* Kartuli enis strukturisa da enis sakitxebi. I, Tbilisi, 1957.
9. *Sh.Dzidziguri.* Kavširebi kartul enaši. Tbilisi, 1973.
10. *G.Kartozia.* Theses of Xth scientific session on dialectology. Tbilisi, 1988 (Georgian).

ABBREVIATIONS:

Megr.I - Kartuli xalxuri sitqviereba. megrulis tekstebi, I, poezia, Tbilisi, 1975.
Megr.II - Idem, v.II, Tbilisi, 1991.
Khub. - M.Khubua. Megruli tekstebi, Tbilisi, 1937.
Kipsh. - I.Kipshidze. Gramatika mingrelskogo (iverskogo) yazyka. St.Petersburg, 1914 (Russian).
Marr. - N.Marr. Gramatika chanskogo (lazskogo) yazyka. St.Petersburg, 1910 (Russian).
Chik. - A.Chikobava. čanuri tekstebi, xopuri kilo. Tiflis, 1928 (Georgian)
Chik. - A.Chikobava. čanuris gramatikuli analizi. Tiflis, 1936 (Georgian).

საქართველოს მეცნიერებათა აკადემიის მოამბე, 159, №3, 1999
BULLETIN OF THE GEORGIAN ACADEMY OF SCIENCES, 159, №3, 1999

LAW

L.-G. Kutalia

Death Penalty in Modern Criminal Law

Presented by Corr. Member of the Academy G. Intskirveli, July 20, 1998

ABSTRACT. **The modern criminal law has not definitively solved the problem of the abolition of death penalty. But chiefly it stands for the substitution of life imprisonment for the capital punishment which is theoretically unacceptable because in both cases the doctrinal role of the special prevention in the concept of criminal punishment is equally disregarded. As a result the problem of the abolition of death penalty must be resolved within the frame of temporary imprisonment.**

Key words: death penalty.

Death penalty is a century-old tradition and to convince the society of the necessity of its abolition presents a quite delicate task for the modern criminal lawyers. Although the Georgian legislator has already abolished this kind of criminal punishment, its debatableness does not decrease in our dogmatics. But Georgia is not the only country where the abolition of the death penalty has become one of the most acute criminal problems; global importance of this question is beyond all doubt.

In our opinion the main directions in which the research is to be conducted are:

1. **The relationship between death penalty and general principles of the criminal punishment.**

a) Preventive element — Death penalty and crime prevention. Does the death penalty make a terror to evil doers? Of course, it does. But does not the imprisonment, which is often called "a living death", create the same terror? It is obvious that the capital punishment cannot be regarded as the unique effective measure of crime prevention. No punishment in the system of criminal punishments could be devoid of effectiveness in this regard, i.e. the preventive nature of punishment results from the punishment as such and not from its form (imprisonment or death penalty). Moreover, "when a person commits a crime, as a rule he hopes to escape it (the punishment)" [1] and its limit or mode makes again no difference. Finally, an act committed in the heat of passion demonstrates once more that the death penalty cannot always determine the crime prevention because in such a case the person does not think at all of legal consequences of his act [2].Therefore, it is not quite correct to speak in this context of the particular effectiveness of death penalty.

b) Repressive element — Death penalty as a retaliatory measure. Right to life is a right of initial, all-embracing kind. To deprive a person of it means to deprive him of all other legal rights and freedoms-not temporarily, but forever. On the other hand, "commission of any unlawful act covers only a part, only a certain side of the delinquents' personality and not the whole of it since each act is just an episode of the individuals' life" [3].

Hence it follows that the death penalty cannot be justified as a retaliation even for the most heinous crime.

c) Reformatory element — Death penalty as a reformation of the delinquent (!!). Here we arrive at the following syllogism:

Every criminal punishment is a reformation of the delinquent.
Every death penalty is not a reformation of the delinquent.
Every death penalty is not a criminal punishment.

2. **Death penalty and error of justice.** As distinct from other rights the right to life cannot be restored. And for modern criminal law it could not be admissable that even a single innocent person erroneously to become deprived of this "unrestorable right". *Ipso facto* each precedent of the error of justice in such cases is a convincing proof of the practical groundlessness of the death penalty.

3. **Ethical aspect of the death penalty.**

a) Death penalty as a corporal punishment. Death penalty is to be defined as the highest degree of corporal punishment [4]; since the latter is absolutely unacceptable from the ethical point of view, the death penalty can be considered the most unethical kind of punishment ever given in criminal law.

b) Death penalty as "moral killing" of executioner. In modern society killing cannot be a profession, i. e. a permanent duty. When a person executes a sentence of death, it always has an incorrigible negative influence on his psychology. Thus, death penalty is not only a physical killing of convict, but also a "moral killing" of executioner.

4. **Death penalty — no ultima ratio against the terrorism**. Terrorism is an ever increasing danger to the whole world and to eradicate it ought to be the top priority task. But we do not agree with those criminalists who claim that the abolition of the death penalty would paralyse the fight against this crime. When the state kills a menacing terrorist, this action arises from the right to self-defence and not to death penalty. Right to self-defence and right to death penalty are not the same criminal terms.

5. **Solution of the problem.**

a) In theory. Although life sentence costs much more for the state than the death penalty, this circumstance is of no importance: life cannot be measured by anything because it is itself the measure of all things and phenomena. The very fact that a criminal can be rendered harmless without deprivation of right to life proves sufficiently the advantage of the life imprisonment over the death penalty. Nevertheless imprisonment for life could not be an optimum substitute for the capital punishment since here too the special prevention is completely sacrificed to the aims of the general prevention, which is theoretically inadmissible [5]. Consequently, the most reasonable solution of this problem in theory could be found within the frame of temporary imprisonment.

b) In practice. Most of the developing countries are not prepared to accept the abolition of the death penalty for the time being, although there is a strong trend in abolishing the capital punishment which indicates that this form of criminal punishment earlier or

later will be totally banned. In this respect good examples have been shown by universal and regional international organisations dealing with the protection of human rights[6]. So that the acceleration of this process will be a firm guarantee of the positive practical solution of the problem concerned.

Tbilisi I. Javakhishvili State University

REFERENCES

1. *J. Gunn.* Psychiatric Aspects of Imprisonment. London, New York, San Francisco, 1978. 256.
2. Art. Kaufmann, Um die Todesstrafe. In: Schuld und Strafe, Köln, Berlin, Bonn, München, 1966, 17.
3. *B.V. Khornabujeli.* Psikhologicheskaia storona viny. Tbilisi, 1981, 10 (Russian).
4. *E. Tyan.* Institutions du Droit Public Musulman. Paris, 1954. 414.
5. *G.T. Tkesheliadze.* Sudebnaia praktika i ugolovnyi zakon, Tbilisi, 1975, 98 (Russian).
6. Compendium of U. Nat. Stand. and Norms in Crime Prevention and Criminal Justice. New York 1992, 219.

Subscription Information

Bulletin of the Georgian Academy of Sciences
is published bimonthly

Correspondence regarding subscriptions, back issues should be sent to:

Georgian Academy of Sciences,
52, Rustaveli Avenue, Tbilisi, 380008, Georgia
Phone : + 995-32 99-75-93;
Fax/Phone : + 995-32 99-88-23
E-mail : BULLETIN@PRESID.ACNET.GE

Annual subscription rate for 1999 is US $ 400

გადაეცა წარმოებას 20.05.1998. ხელმოწერილია დასაბეჭდად 30.06.1999.
ფორმატი 70×108 1/16. აწყობილია კომპიუტერზე. ოფსეტური ბეჭდვა.
პირობითი ნაბ. თ. 11. საღრიცხვო-საგამომცემლო თაბახი 11.
ტირაჟი 250. შეკვ. 188 ფასი სახელშეკრულებო.

რედაქციის მისამართი: 380008, თბილისი–8, რუსთაველის პრ. 52, ტელ. 99-75-93.
საქართველოს მეცნიერებათა აკადემიის საწარმოო-საგამომცემლო გაერთიანება „მეცნიერება",
380060, თბილისი, დ. გამრეკელის ქ. 19, ტელ. 37-22-97.